

**Interactions between
Bacteria and Solid Surfaces
in Relation to
Bacterial Transport in Porous Media**

CENTRALE LANDBOUWCATALOGUS



0000 0576 8607

Promotoren: Dr. A. J. B. Zehnder, hoogleraar in de microbiologie
Dr. J. Lyklema, hoogleraar in de fysische chemie, met
bijzondere aandacht voor de grensvlak en kolloïdchemie

Co-promotor: Dr. Ir. W. Norde, universitair hoofddocent bij de vakgroep
Fysische en Kolloïdchemie

87110280001, 1778

H.H.M. Rijnaarts

Interactions between Bacteria and Solid Surfaces
in Relation to Bacterial Transport in Porous Media

Ontvangen

25 MEI 1994

UB-CARDEX

Proefschrift

ter verkrijging van de graad van
doctor in de landbouw- en milieuwetenschappen
op gezag van de rector magnificus,
Dr. C. M. Karssen,
in het openbaar te verdedigen
op woensdag 25 mei 1994
des namiddags te vier uur in de Aula
van de Landbouwuniversiteit te Wageningen

1511530697

40951

This research was funded by grant C6-1/8939 from The Netherlands Integrated Soil Research Programme and by the EAWAG, Dübendorf, Switzerland. It was carried out at the Department of Microbiology and at the Department of Physical and Colloid Chemistry of the Wageningen Agricultural University, Wageningen, The Netherlands.

**BIBLIOTHEEK
LANDBOUWUNIVERSITEIT
WAGENINGEN**

CIP-DATA KONINKLIJKE BIBLIOTHEEK, DEN HAAG

Rijnaarts, Huub

Interactions between bacteria and solid surfaces in relation to bacterial transport in porous media/ Huub

Rijnaarts. -[S.1. : s.n.]

Thesis Wageningen. - With summary in Dutch.

ISBN 90-5485-252-6

Subjects headings: bacterial adhesion / colloid stability
/ porous media

Stellingen behorend bij het proefschrift "Interactions between Bacteria and Solid surfaces in Relation to Bacterial Transport in Porous Media". Huub. H. M. Rijnaarts, 25 mei, 1994.

1. Een onderzoeker heeft in zijn directe werk-omgeving op zijn minst één collega nodig die sterk verwant onderzoek doet om de kans op fouten of vertraging aanvaardbaar laag te houden. Hiermee wordt nog te weinig rekening gehouden bij het indienen en honoreren van wetenschappelijke onderzoeksprojecten.

2. De hydrofobiciteit van de gehydrateerde buitenkant van bacteriën kan niet worden gemeten.

Dit proefschrift.

3. Het onderzoek naar het mechanisme van hechting van microorganismen wordt sterk belemmerd door het overdreven belang dat aan onmeetbare grootheden als hydrofobiciteit (Rosenberg and Doyle) en de grensvlakspanning van een vaste stof (Absolom et al., Van Oss) wordt toegeschreven.

Absolom, D. R., F. V. Lamberti, Z. Policova, W. Zingg, C. J. Van Oss, and A. J. Neumann, 1983, *Appl. Environ. Microbiol.* 46:474-486.

Doyle, R. J. and M. Rosenberg, 1990, *Microbial Cell Surface Hydrophobicity*. American Society for Microbiology, Washington D.C.

Van Oss, C.J., 1991, *Biofouling* 4:25-35.

Dit proefschrift.

4. De vaak waargenomen discrepantie tussen DLVO-theorie en het depositiegedrag van polystyreen latex deeltjes bij lage ionsterktes (bijv. Elimelech and O'Melia) doet vermoeden dat deze net zo "behaard" zijn als bacteriën.

M. Elimelech and C. R. O'Melia, 1990, *Environ. Sci. Technol.* 24:1528-1536.

Dit proefschrift.

5. Het gebruik van de term "biologische beschikbaarheid" is alleen verantwoord wanneer het systeem, het organisme en de factor tijd gespecificeerd zijn.

6. Ongecontroleerde hydrodynamica levert beroerde resultaten.

7. De wetenschap zou een stuk sneller vooruit gaan als eens wat vaker achterom gekeken werd. Zo had de griekse wijsgeer Herakleitos (ca. 500 BC) al een survival-of-the-fittest concept, een oerknal-theorie, en wist ook al dat veel processen in de natuur niet in evenwicht zijn en daarom alleen met kinetische modellen beschreven kunnen worden. Dit laatste moet door veel milieu-wetenschappers nog steeds ontdekt worden.

8. Falsifieerbaarheid, zoals voorgesteld door K. R. Popper, is nog steeds het enig afdoende criterium om de kwaliteit van (natuur)wetenschappelijk onderzoek te karakteriseren.

K. R. Popper, 1934, *Logic der Forschung*.

9. Het motto "iets meer rekenen is beter dan verkeerde conclusies trekken" is niet voor alle wetenschappers even vanzelfsprekend.
10. De wetenschap is het klooster van de moderne tijd.
11. Wetenschap populariseren zonder te vervallen in populaire wetenschap is een kunst die iedere onderzoeker tegenwoordig moet beheersen.
Atwood-Gailey, E. and S. M. Day, 1993, ASM news 59: 544-545.
12. De maatregel die het wachtgeld van nieuwbakken maar werkeloze doctors voor rekening van de universiteiten laat komen is een eerste positieve stap om de gestage groei van deze groep te beteugelen en de universiteiten tot een beter promovendi/post-doc beleid te bewegen.
13. Het feit dat kinderen voornamelijk door vrouwen worden verzorgd is geen biologisch automatisme maar een gevolg van sociale factoren.
14. Extremisme is de uitslag van een zieke politiek.
15. Promoveren in verkiezingstijd is niet ongunstig: er zijn dan tenminste een stuk of twintig vacatures.
16. Beleidsvoerders en wetenschappers die vinden dat "Wonen op gif" acceptabel moet worden (zie bijv. R. Diddé), zouden zelf het goede voorbeeld moeten geven.
Diddé, R. Intermediair, 11 juni 1993: 39.

Handwritten text, possibly a signature or name, located in the center of the page.

voor Nora, Timon en Iris

Voorwoord

Toen ik in het voorjaar van 1988 aan de landbouwhogeschool afstudeerde als milieuhygiënicus koos ik voor het matig betaalde promotie-avontuur; ik voelde me geroepen tot de wetenschap. Mijn afstudeer-werk was al goed voor het eerste hoofdstuk van mijn proefschrift dat over "afbraak van geadsorbeerde verbindingen door bodembacteriën" zou moeten gaan. Het proefschrift dat nu voor U ligt gaat echter ergens anders over. In het onderstaande wil ik uitleggen hoe dat zo gekomen is.

Het onderzoek waar ik aan begon was behoorlijk complex. Ik moest achterhalen hoe bacteriën vastgeplakte (geadsorbeerde) stoffen (verbindingen) opeten. Daarvoor is het nodig dat je de wisselwerkingen tussen de bacterie, het vaste oppervlak en de verbindingen kent. Na het kiezen van de juiste oppervlakken, bacteriën en verbindingen begon ik met de bestudering van de afzonderlijke wisselwerkingen: verbinding-oppervlak, verbinding-bacterie en bacterie-oppervlak. Ik besteedde flink wat tijd aan de eerste twee interacties. Ook begon ik aan de bestudering van de laatste wisselwerking, de hechting van bacteriën op oppervlakken. Hierbij kon ik voortbouwen op het werk van mijn voorganger, Marc van Loosdrecht. De meeste van mijn bacteriën bleken anders te hechten dan verwacht. Er werd besloten om de oorzaak hiervan op te sporen. Dit nam veel extra tijd in beslag wat natuurlijk ten koste ging van het andere werk. Aan het einde van mijn aanstellingstijd had ik veel meer resultaten over hechting van bacteriën dan over afbraak van geadsorbeerde verbindingen. Ik besloot daarom het onderwerp van mijn proefschrift te veranderen. Door deze gang van zaken had ik aan het begin van het laatste jaar van mijn aanstellingsperiode nog geen enkel artikel/hoofdstuk voor mijn proefschrift geschreven, hetgeen zeer ongebruikelijk is. Ik begon daarom met spoed met schrijven. Halverwege het derde hoofdstuk ontdekte ik echter een fout in de theorie die onze onderzoeksgroep tot dan bij interpretatie van hechting van bacteriën had gebruikt. Door het bijstellen van de theorie kwamen mijn resultaten in een heel ander licht te staan. Het opnieuw interpreteren en herzien van de al geschreven hoofdstukken heeft daarom nog flink wat extra tijd gekost. Zo kon het dus gebeuren dat ik, in plaats van na vijf jaar, na zes jaar mijn proefschrift gereed kreeg en dat het onderwerp anders was dan oorspronkelijk gepland. Het niet opgenomen werk over "afbraak van geadsorbeerde verbindingen door bodembacteriën" zal nog in enkele afzonderlijke artikelen gepubliceerd worden.

Table of contents

1. Introduction	1
2. Bacterial Adhesion under Static and Dynamic Conditions	15
3. Reversibility and Mechanism of Bacterial Adhesion	27
4. The Isoelectric Point of Bacteria as an Indicator for the Presence of Cell Surface Polymers that Inhibit Adhesion	57
5. DLVO and Steric Contributions to Bacterial Deposition in Different Ionic Strength Environments	71
6. Bacterial Deposition in Porous Media Related to the Clean Bed Collision Efficiency and to Substratum-Blocking by Attached Cells	99
7. Bacterial Deposition in Porous Media: Effects of Cell-Coating, Substratum Hydrophobicity, and Electrolyte Concentration	123
Summary and Concluding Remarks	145
Samenvatting: hechting van bacteriën in poreuze media; een basis voor de toepassing van bacteriën in de biologische reiniging van bodem en water	155
Dankwoord	164
Curriculum Vitae	166

Chapter 1

Introduction

The primary aim of this research project is to provide a systematic analysis of bacterium-solid interactions and their effects on bacterial transport in porous media. This knowledge is required for the application of bacteria in the bioremediation of contaminated soils, sediments and groundwaters. It is also important for the treatment of industrial waste streams in fixed bed biofilm reactors. The fundamental and systematic approach makes this study also valuable for bacterial adhesion research and microbial ecology in general.

Ecological aspects of bacterial adhesion.

Interfaces occur abundantly in nature, either as the surfaces of suspended particles in oceans, lakes and rivers or of solid grains of soils and sediments. Microorganisms living in these ecosystems interact with these surfaces in different ways. Many microorganisms tend to accumulate at the solid-liquid interface. This is demonstrated by the fact that all surfaces in aquatic ecosystems are covered with microbial layers (biofilms), and newly introduced surfaces become rapidly colonized (11, 63). In soils, sediments and natural streams most active bacteria are bound to solid particles (26, 31, 52). However, sometimes microbes do not attach and, as a consequence, spend their lives in the aqueous phase (26, 31).

Advantages of adhesion. The ubiquity of bacterial adhesion in natural waters must imply that the attachment is beneficial. Upon reviewing the literature, Van Loosdrecht et al. (59) found no evidence for changes in the intrinsic activity of bacteria upon adhesion. This was confirmed by recent studies in our laboratory (28, 45, 59). Hence, the often observed increase in activity upon adhesion (59) must have another origin. Most probably, this is caused by the fact that nutrient and substrate fluxes are often greater for attached bacteria than for suspended cells. This may occur for two reasons

(59): (i) Organic compounds and non-organic chemicals generally accumulate at solid-liquid interfaces. These serve as a source of nutrients and substrates for microorganisms. Uptake by the organisms creates concentration gradients. Attached organisms are situated within the diffusion layer and much closer to the adsorption site than suspended cells. Hence, the gradients between cell and solid are generally steeper and diffusion rates are generally greater for attached cells than for suspended bacteria (44, 59). (ii) In non-turbulent flowing aqueous media, the transfer of nutrients and substrates from bulk liquid may be different for attached and suspended cells. The liquid phase moves generally faster than solid particles with attached cells. As a consequence, these cells are supplied with nutrients and substrates by convection and diffusion (28, 45). In contrast, suspended cells tend to follow the flowpath of the fluid phase. Hence, they remain in the same liquid element and are mainly supplied by diffusion (28, 59).

Attachment can also be advantageous for reasons not related to substrate and nutrient supply. For example, adhered microorganisms are less susceptible to predation (43, 61). In biofilms, attached bacteria are embedded in a macromolecular matrix. Toxic chemicals and antibiotics bind to these macromolecules and are therefore much less effective (14). Furthermore, attached microbial communities create a micro-habitat in which different species work together in degrading compounds which they are not able to digest on their own. Examples of such symbioses are the inter-species hydrogen transfer in aggregates of fatty acid degrading anaerobic consortia (32) and the coupled anaerobic and aerobic bioconversion steps in the biomineralization of chlorinated aromatic compounds (23).

Relevance for environmental biotechnology.

Microbial communities play a central role in the degradation and detoxification of natural and anthropogenic compounds. This ability of bacteria is exploited in environmental biotechnology which generally employs immobilized microorganisms.

Wastewater and wastegas treatment. The implementation of domestic

and industrial wastewater technology has significantly reduced the pollution of natural waters during the last three decades. Currently, bioreactors to treat industrial wastewater and wastegas streams are further being developed (2, 17, 29). In these reactors, the active biomass is immobilized on a solid phase. Hence, the improvement of the performance of such reactors demand an understanding of bacteria-solid interactions and biofilm formation.

Bioremediation of soils, aquifers and sediments. Thousands of sites with contaminated soil or sediment have been identified during the last 15 years, and many more are still likely to be found. These sites form a potential hazard for ecosystems and human health. Many of them cannot be remediated with current physical-chemical cleaning procedures for economical and/or technological reasons. On site and *in situ* bioremediation techniques employing indigenous microorganisms that degrade the harmful chemicals offer new potentialities (4, 5, 35). Chemicals that cannot be degraded by natural communities may be treated by introducing specialized (possibly genetically engineered) bacteria.

Successful and safe techniques for bioremediation of soils, sediments and groundwaters rely on a control of the dispersal of the microbes in these systems, which, in turn, requires insight into the interactions between bacteria and solid surfaces. For example, the adhesion of indigenous or intentionally added bacteria in a contaminated aquifer should not clog the pores between the aquifer grains which would prevent any further treatment. On the other hand, the microorganisms should be retained at the contaminated site for optimum performance. An uncontrolled increase in number and migration of bacteria in groundwater may also have undesired effects. It may reduce the microbial quality of groundwater (38, 39) or lead to spreading of chemicals by colloid-facilitated transport (39).

Additional interests.

Microbial adhesion and biofilm formation have a great economic impact (10): biofilms on ship-hulls and the inner walls of pipes in water-supply systems

increase fluid friction and therefore cause energy loss. On heat exchangers in electric power plants they reduce the efficiency of heat transfer and promote corrosion of the exchanger surface. Adhesion of microbes on fermentor walls in food industry requires costly cleaning measures (54). Adhesion can also be beneficially applied, for instance, in the mining industry to enhance metal leaching from ore (6), and in the oil industry to improve oil recovery from the subsurface (33).

Bacterial adhesion is also important for medical reasons; it plays a role in dental diseases, in microbial infections introduced via prosthetic devices, and in pathogenic infections of the urinal and intestinal tract (8, 14, 27). Protection of drinking water resources from microbial contamination requires the removal of pathogenic microbes from waste water during passage through sand filters (40) and from groundwater flowing to aquifers (38, 39). Finally, the mobility and adhesion behaviour of genetically engineered microorganisms in the natural environment should be considered in the assessment of their risks and applicability (50).

Bacterial adhesion is a widely spread phenomenon with a large technological, economic, and medical impact. Therefore, an insight into generally occurring adhesion mechanisms is very important.

Mechanisms of bacterial deposition.

Deposition of bacteria onto solid supports includes two steps: transport and adhesion (Fig. 1). Transport is hydrodynamically determined whereas the adhesion step is controlled by cell-substratum interactions. After deposition, the attached cells may excrete polymers and start multiplying: this leads to surface-attached microcolonies or even to thick continuous biofilms. This thesis focuses on the transport and adhesion step.

Transport. In static systems, diffusion controls (bacterial) particle transport from bulk liquid to substratum. Diffusion results from random displacements which is called Brownian motion. Under dynamic (flowing) conditions, transfer of cells occurs by convection and diffusion. The following

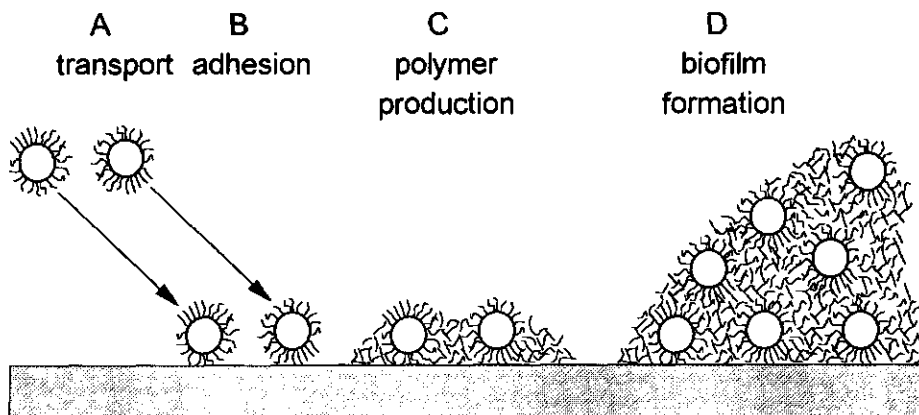


FIG. 1. The succeeding steps in microbial deposition and biofilm formation on solid surfaces.

dynamic systems are often used to study the deposition of bacteria and particles under defined transport conditions: the rotating disk (37, 46), the impinging jet (62), the flat plate flow cell (49), and the porous medium column packed with spherical collectors (18, 36). Transport in the static and the dynamic porous medium system are illustrated in Fig. 2A. Sedimentation may also contribute to transport.

Interactions in adhesion. Cell-substratum interactions govern the adhesion step in deposition. In general, these interactions are expressed in terms of the Gibbs energy which is a function of the separation h between cell and surface (57) (Fig. 2B). Three models are available in the literature to describe the interactions between solid surfaces and bacteria. These apply to different h -ranges as explained below and in Fig. 2C.

(i) The DLVO (Derjaguin, Landau, Verwey and Overbeek) theory of colloid stability (47, 55, 57, 58) accounts for long range Van der Waals and electrostatic interactions as a function of cell-solid separation h . For bacteria,

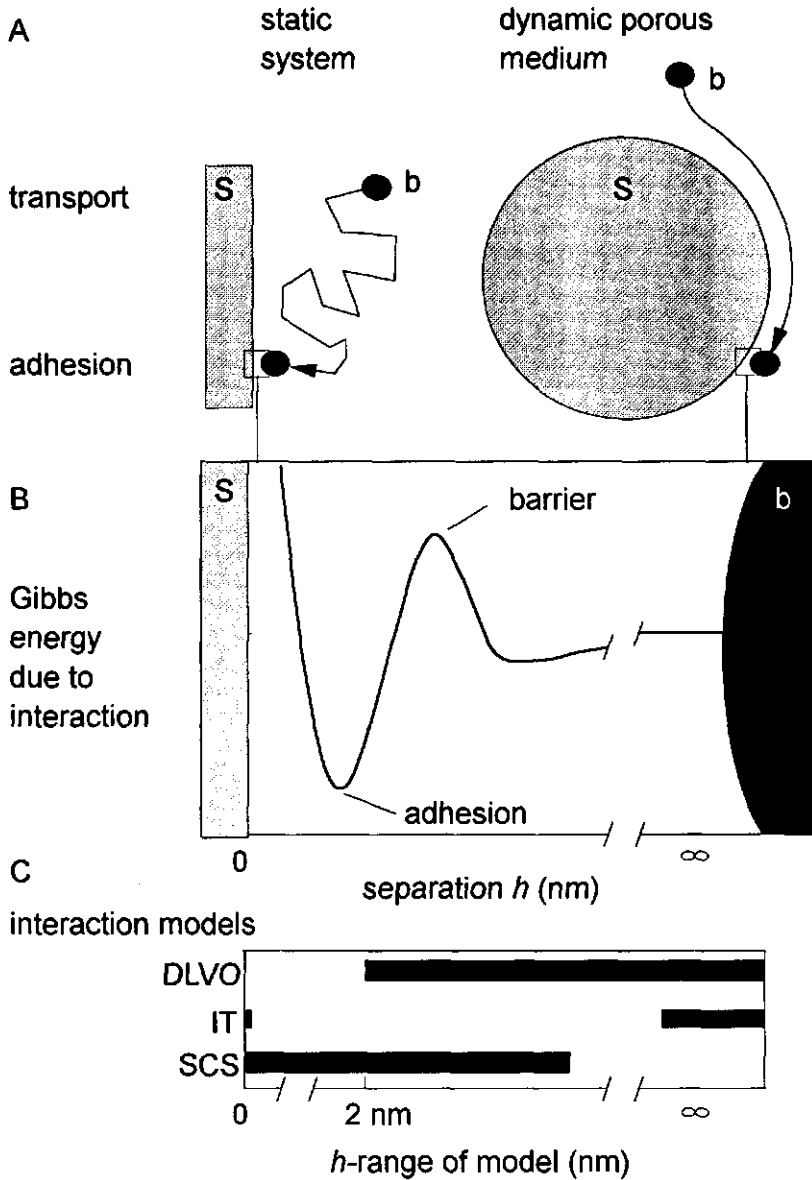


FIG. 2. A. Deposition in static systems (transport primarily by diffusion) and in dynamic porous media (transport primarily by convection): S stands for Substratum, b for bacterium. B. The Gibbs energy due to interaction as a function of cell-solid separation h . C. Interaction models for assessing the Gibbs energy of interaction and the separation ranges to which these apply. For model abbreviations, see text.

the model does not apply to very short range interactions.

(ii) The interfacial tension (IT) method (1, 9, 60) is based on the concept of formation and destruction of interfaces, i.e., it only considers the situations before ($h = \infty$) and after adhesion. The model only accounts for short range interactions, since it assumes adhesion to occur at $h = 0$.

(iii) Steric colloid stability (SCS) theory comprises the interactions resulting from macromolecules at the bacterium-water and solid-water interfaces (19). Steric interactions are functions of h .

Relevance of interaction models to bacterial adhesion. Electrostatic interactions affect bacterial adhesion (16, 22, 24, 25, 58). Hence, the DLVO theory, which includes these interactions, can at least be used to assess a part of the microbial attachment. Non-DLVO interactions related to the hydrophobicities of cells and solids have been reported to also contribute to adhesion (1, 7, 8, 9, 20, 21, 27, 41, 53, 55, 56, 58). These non-DLVO interactions may be accounted for by either the IT or the SCS theory.

The IT method is often used to assess the non-DLVO interactions in adhesion. However, this model has the following shortcomings (42, 56): (i) it ignores the distance dependence of the non-DLVO interactions. (ii) The Gibbs energy of adhesion is determined from interfacial tensions, which, in turn, are derived from measured contact angles and an empirical additional relation between interfacial tensions. (iii) The implicit assumption that a new cell-substratum interface is formed is not necessarily valid: cells may adhere by long range interactions without making substratum contact (55) or by cell surface structures that contact substrata only locally (7, 42, 58). (iv) Adhesion is often reported to be irreversible (8, 41, 49, 62). Assessment of irreversible adhesion requires a kinetic approach by accounting for Gibbs energy barriers that inhibit adhesion (Fig. 2B). The IT approach is an equilibrium-model, i.e., it only considers the Gibbs energy difference between the adhered and the non-adhered state (Figs. 2B and 2C) and therefore does not allow for a kinetic interpretation of adhesion. Hence, the non-DLVO interactions in adhesion cannot be appropriately assessed with the IT model.

The SCS model can in principle account for the contribution of non-DLVO interactions. It allows for a kinetic interpretation of (bacterial) particle deposition and is complementary to the DLVO theory (19). Together, these two theories cover the interactions for the total h -range (Fig. 2C).

Knowledge gaps

Generally speaking, the understanding and prediction of adhesion and transport of bacteria in porous media is hampered by a lack of knowledge on two main subjects: (i) the fundamentals of the adhesion process and (ii) the application of particle deposition theory to microbial transport in porous media.

Fundamentals of adhesion. Some bacteria almost behave like ideal colloidal particles whereas others may have very complex surface structures (3, 51) which may affect adhesion differently under different conditions. Furthermore, the transport step significantly influences the adhesion results in any method. In many bacterial adhesion studies, including those formerly used in our laboratory (55, 56, 57), methods were used in which the methodical and/or transport effects were not properly accounted for. Hence, the development of better procedures to obtain method-independent data is an important first step in the analysis of the mechanism and the reversibility of adhesion of bacteria.

The DLVO theory and the SCS model are the appropriate tools to analyze bacterial adhesion. The parameters required for a determination of the DLVO interaction can in principle be obtained relatively easily. In contrast, the determination of steric interaction parameters is very difficult. This is demonstrated by the fact that, although the importance of steric interactions in bacterial adhesion has already been recognized in 1980 by Pethica (42) and others (47, 48), up to date no quantitative determination of such interaction has been reported. Hence, the relative contribution of DLVO and non-DLVO interactions is a major knowledge gap in bacterial adhesion research.

Bacterial transport in porous media. The great diversity in bacterium-solid

interactions that is known to exist among different bacterial species is not considered in most studies on bacterial transport in porous media (12, 13, 30, 34, 36). Hence, assessing the effect of bacterium-solid interactions on bacterial transport in porous media is an other important research goal (36). Furthermore, the performance of the deposition process during a prolonged application of bacterial suspensions to porous media, i.e., the occurrence or absence of pore clogging, is of great practical interest (15).

Aim and Outline of this thesis.

The purpose of the research presented in this thesis is to systematically analyze the interactions between bacteria and solid surfaces and their effects on microbial transport in porous media. This can only be appropriately performed with defined model systems in which the transport step and the interactions can be quantified.

The model systems chosen include static batch systems, dynamic porous media, various bacteria, and glass and teflon surfaces. Their characterization is described in chapter 2. Procedures to better distinguish between hydrodynamic and other system dependent influences and method independent physicochemical interactions are also described in this chapter. The reversibility and mechanism of adhesion are analyzed in chapter 3. A major contribution of non-DLVO interactions was observed which required a further characterization of the macromolecular composition of bacterial cell surfaces (chapter 4). The relative contributions of DLVO and non-DLVO interactions under static conditions are assessed in chapter 5. In that work, non-DLVO (steric) interaction parameters are defined and quantified. A quantitative expression for bacterial transport in porous media based on particle deposition theory is presented and experimentally verified in chapter 6. Finally (chapter 7), the effect of DLVO and non-DLVO interactions on bacterial transport in porous media is evaluated by analyzing experimental column results in terms of the concepts established in the previous chapters.

References

1. Absolom, D. R., F. V. Lamberti, Z. Policova, W. Zingg, C. J. Van Oss and A. W. Neumann. 1983. Surface thermodynamics of bacterial adhesion. *Appl. Environ. Microbiol.* **46**:90-97.
2. Bendinger, B. 1992. Microbiology of biofilters for the treatment of animal-rendering plant emissions: occurrence, identification and properties of isolated coryneform bacteria. Ph. D. Thesis, University of Osnabrück, Osnabrück, Germany.
3. Beveridge, T. J. and L. L. Graham. 1991. Surface layers of bacteria. *Microbiol. Rev.* **55**:684-705.
4. Bouwer, E. J. 1992. Bioremediation of organic contaminants in the subsurface, p. 287-318. *In* *New concepts in environmental microbiology*, John Wiley & Sons, New York.
5. Bouwer, E. J. and A. J. B. Zehnder. 1993. Bioremediation of organic compounds- putting microbial metabolism to work. *Trends in Biotechnology* **11**:360-367.
6. Briery, C. L. 1982. Microbial mining. *Sci. Am.* **247**:42-51.
7. Busscher, H. J., M. H. M. J. C. Uyen, A. J. W. Pelt, H. J. Busscher and A. H. Weerkamp. 1987. Specific and non-specific interactions in bacterial adhesion to solid substrata. *FEMS Microbiol. Rev.* **46**:165-173.
8. Busscher, H. J., M. H. M. J. C. Uyen, A. J. W. Pelt, A. H. Weerkamp and J. Arends. 1986. Kinetics of adhesion of the oral bacterium *Streptococcus sanguis* CH3 to polymers with different surface free energies. *Appl. Environ. Microbiol.* **51**:910-914.
9. Busscher, H. J., A. H. Weerkamp, H. C. van der Mei, A. J. W. Pelt, H. P. de Jong and J. Arends. 1984. Measurement of the surface free energy of bacterial cell surfaces and its relevance for adhesion. *Appl. Environ. Microbiol.* **48**:980-983.
10. Characklis, W. G. 1990. Biofilms: a basis for an interdisciplinary approach, p. 3-15. *In* W. G. Characklis and K. C. Marshall (ed.), *Biofilms*, John Wiley and Sons, Inc., New York.
11. Characklis, W. G., G. A. McFeters and K. C. Marshall. 1990. Physiological ecology in biofilm systems, p. 341-394. *In* W. G. Characklis and K. C. Marshall (ed.), *Biofilms*, John Wiley and Sons, Inc., New York.
12. Corapcioglu, M. Y. and A. Haridas. 1984. Transport and fate of microorganisms in porous media: a theoretical investigation. *J. Hydrology* **72**:149-169.
13. Corapcioglu, M. Y. and A. Haridas. 1985. Microbial Transport in porous media: a numerical model. *Adv. Water Res.* **8**:188-200.
14. Costerton, J. W., K. J. Cheng, T. I. Geesey, T. I. Ladd, J. C. Nickel, M. K. Dasgupta and T. J. Marrie. 1987. Bacterial biofilms in nature and disease. *Ann. Rev. Microbiol.* **41**:435-464.
15. Cunningham, A. B., E. J. Bouwer and W. G. Characklis. 1990. Biofilms in porous media, p. 697-732. *In* W. G. Characklis and K. C. Marshall (ed.), *Biofilms*, John Wiley & Sons Inc., New York.
16. Dickson, J. R. and K. Koochmaria. 1989. Cell surface charge characteristics and their relationship to bacterial attachment to meat surfaces. *Appl. Environ. Microbiol.* **55**:832-836.
17. Diks, R. M. M. and S. P. Ottengraf. 1991. Verification studies of a simplified model for the removal of dichloromethane from waste gases using a biological trickling filter. *Bioprocess Eng.* **6**:93-99.
18. Elimelech, M. and C. R. O'Melia. 1990. Kinetics of deposition of colloidal particles in porous media. *Environ. Sci. Technol.* **24**:1528-1536.

19. Fleeer, G. J. and J. M. H. M. Scheutjens. 1993. Modeling Polymer adsorption, steric stabilization and flocculation, p. 209-263. *In* B. Dobias (ed.), Coagulation and flocculation, Marcel Dekker Inc., New York.
20. Fletcher, M. 1977. The effects of culture concentration and age, time and temperature on the bacterial attachment to polystyrene. *Can. J. Microbiol.* **23**:1-6.
21. Fletcher, M. and G. L. Loeb. 1979. Influence of substratum characteristics on the attachment of a marine pseudomonad to solid surfaces. *Appl. Environ. Microbiol.* **37**:67-72.
22. Gannon, J., Y. Tan, p. Baveye and M. Alexander. 1991. Effect of sodium chloride on transport of bacteria in saturated aquifer material. *Appl. Environ. Microbiol.* **57**:2497-2501.
23. Gerritse, J. 1993. Growth of bacteria at low oxygen concentrations. Ph. D. Thesis, University of Groningen, Groningen, The Netherlands.
24. Gilbert, P., D. J. Evans, E. Evans and I. G. Duguid. 1991. Surface characteristics and adhesion of *Escherichia coli* and *Staphylococcus epidermidis*. *J. Appl. Bacteriol.* **71**:72-77.
25. Gordon, A. S. and F. Millero. 1984. Electrolyte effects on attachment of an estuarine bacterium. *Appl. Environ. Microbiol.* **47**:495-499.
26. Gouldner, R. 1977. Attached and free bacteria in an estuary with abundant suspended solids. *J. Appl. Bacteriol.* **43**:399-405.
27. Harkes, G. 1991. Interaction of *Escherichia coli* with solid surfaces; adhesion, growth and migration. Ph. D. Thesis, Twente Technical University, Enschede, The Netherlands.
28. Harms, H. and A. J. B. Zehnder. Influence of substrate diffusion on degradation of dibenzofuran and 3-chlorodibenzofuran by attached and suspended bacteria. *Appl. Environ. Microbiol.*: submitted for publication.
29. Hartmans, S. and J. Tramper. 1991. Dichloromethane removal from waste gases with a trickle-bed bioreactor. *Bioprocess Eng.* **6**:82-93.
30. Harvey, R. W. 1991. Parameters involved in modeling movement of bacteria in groundwater, *In* C. J. Hurst (ed.), Modelling the Environmental Fate of Microorganisms, American Society for Microbiology, Washington D. C.
31. Harvey, R. W. and L. Y. Young. 1980. Enumeration of particle bound and unattached respiring bacteria in salt marsh environment. *Appl. Environ. Microbiol.* **40**:156-160.
32. Houwen, F. P., C. Dijkema, C. H. H. Schoenmakers, A. J. M. Stams and A. J. B. Zehnder. 1987. ¹³C-NMR study of propionate degradation by a methanogenic coculture. *FEMS Microbiol. Lett.* **41**:269-274.
33. Jang, L. K., P. W. Chang, J. E. Findley and T. F. Yen. 1983. Selection of bacteria with favourable transport properties through porous rock for application of microbial enhanced oil recovery. *Appl. Environ. Microbiol.* **46**:1066-1072.
34. Lindqvist, R. and C. G. Enfield. 1992. Cell density and non-equilibrium sorption effects on bacterial dispersal in groundwater microcosms. *Microb. Ecol.* **24**:25-41.
35. MacDonald, J. A. and B. E. Rittmann. 1993. Performance standards for *in situ* bioremediation. *Environ. Sci. Technol.* **27**:1975-1979.
36. Martin, R. E., E. J. Bouwer and L. M. Hanna. 1992. Application of clean-bed filtration theory to bacterial deposition in porous media. *Environ. Sci. Technol.* **26**:1053-1058.
37. Martin, R. E., L. M. Hanna and E. J. Bouwer. 1991. Determination of bacterial collision efficiencies in a rotating disk system. *Environ. Sci. Technol.* **25**:2075-2082.
38. Matthess, G., A. Pekdeger and J. Schroeter. 1988. Persistence and transport of bacteria

- and viruses in groundwater- a conceptual evaluation. *J. Contam. Hydrol.* 2:171-188.
39. McDowell-Boyer, L. M., J. R. Hunt and N. Sitar. 1986. Particle transport through porous media. *Water Resources Research* 22:1901-1921.
 40. Moran, D. C., M. C. Moran, R. S. Cushing and D. F. Lawler. 1993. Particle behaviour in deep-bed filtration: part 1-Ripening and Breakthrough. *J. Am. Water Works Assoc.* 85:69-93.
 41. Pelt, A. W. J., A. H. Weerkamp, M. H. M. J. C. Uyen, H. J. Busscher, H. P. de Jong and J. Arends. 1985. Adhesion of *Streptococcus sanguis* CH3 to polymers with different surface free energies. *Appl. Environ. Microbiol.* 49:1270-1275.
 42. Pethica, B. A. 1980. Microbial and cell adhesion, p. 19-45. *In* J. M. Berkeley, J. M. Lynch, J. Melling, P. R. Rutter and B. Vincent (ed.), *Microbial adhesion to surfaces*, Ellis Horwood Lim., Chisester, England.
 43. Postma, J., C. H. Hok-A-Hin and J. A. van Veen. 1990. Role of microniches in protecting introduced *Rhizobium leguminosarum* biovar *trifolii* introduced into soil. .
 44. Rijnaarts, H. H. M., A. Bachmann, J. C. Jumelet and A. J. B. Zehnder. 1990. Effect of Desorption and intraparticle mass transfer on the aerobic biomineralization of α -hexachlorocyclohexane in a contaminated calcareous soil. *Environ. Sci. Technol.* 24:1349-1354.
 45. Rijnaarts, H. H. M., W. Norde, J. Lyklema and A. J. B. Zehnder. Effect of substrate adsorption and bacterial adhesion on microbial activity. : in preparation.
 46. Rutter, P. R. and A. Abbott. 1978. A study of the interaction between oral streptococci and hard surfaces. *J. Gen. Microbiol.* 105:219-226.
 47. Rutter, P. R. and B. Vincent. 1984. Physicochemical interactions of the substratum, microorganisms, and the fluid phase, *In* K. C. Marshall (ed.), *Microbial adhesion and aggregation*, Springer-verlag, Berlin.
 48. Rutter, P. R. and B. Vincent. 1988. Attachment mechanisms in the surface growth of microorganisms, p. 87-107. *In* J. I. Bazin and J. M. Prosser (ed.), *CRC Series in Mathematical models for microbiology*, CRC Press, Inc., Boca Raton, Florida.
 49. Sjollem, J., H. J. Weerkamp and A. H. Busscher. 1990. Deposition of oral streptococci and polystyrene latices onto glass in a parallel plate flow cell. *Biofouling* 1:101-112.
 50. Smit, E., J. D. van Elsas and J. D. van Veen. 1992. Risks associated with the application of genetically modified microorganisms in terrestrial ecosystems. *FEMS Microbiol. Rev.* 88:263-278.
 51. Stenström, T. A. and S. Kjelleberg. 1985. Fimbriae mediated non-specific adhesion of *Salmonella typhimurium* to mineral particles. *Arch. Microbiol.* 143:6-10.
 52. Stotzky, G. 1972. Activity, ecology and population dynamics of microorganisms in soil. *Crit. Rev. Microbiol.* 2:59-126.
 53. Uyen, H. M., H. C. van der Mei, A. H. Weerkamp and H. J. Busscher. 1988. Comparison between the adhesion to solid substrata of *Streptococcus mitis* and that of polystyrene particles. *Appl. Environ. Microbiol.* 54:837-838.
 54. Van de Mei, H. C., J. De Vries and H. J. Busscher. 1993. Hydrophobic and electrostatic cell surface properties of thermophilic dairy streptococci. *Appl. Environ. Microbiol.* 59:4305-4312.
 55. Van Loosdrecht, M. C. M., J. Lyklema, W. Norde, G. Schraa and A. J. B. Zehnder. 1987. Electrophoretic mobility and hydrophobicity as a measure to predict the initial steps of

- bacterial adhesion. *Appl. Environ. Microbiol.* **53**:1898-1901.
56. Van Loosdrecht, M. C. M., J. Lyklema, W. Norde, G. Schraa and A. J. B. Zehnder. 1987. The role of bacterial cell wall hydrophobicity in adhesion. *Appl. Environ. Microbiol.* **53**:1893-1897.
 57. Van Loosdrecht, M. C. M., J. Lyklema, W. Norde and A. J. B. Zehnder. 1989. Bacterial adhesion: a physicochemical approach. *Microb. Ecol.* **17**:1-15.
 58. Van Loosdrecht, M. C. M., W. Norde, J. Lyklema and A. J. B. Zehnder. 1990. Hydrophobic and electrostatic parameters in bacterial adhesion. *Aquat. Sci.* **52**:103-114.
 59. Van Loosdrecht, M. C. M., W. Norde, J. Lyklema and A. J. B. Zehnder. 1990. The influences of interfaces on microbial activity. *Microbiol. Rev.* **54**:75-87.
 60. Van Oss, C. J. 1991. The forces involved in bioadhesion to flat surfaces and particles-their determination and relative roles. *Biofouling* **4**:25-35.
 61. Vargas, R. and T. Hattori. 1986. Protozoan predation of bacterial cells in soil aggregates. *FEMS Microbiol. Ecol.* **38**:233-242.
 62. Xia, Z., L. Woo and T. G. M. Van de Ven. 1989. Microrheological aspects of adhesion of *Escherichia coli* on glass. *Biorheology* **26**:359-375.
 63. Zobell, C. E. 1943. The effect of solid surfaces upon bacterial activity. *J. Bacteriol.* **46**:39-56.

Chapter 2

Bacterial Adhesion under Static and Dynamic Conditions

Huub H.M. Rijnaarts, Willem Norde, Edward J. Bouwer, Johannes Lyklema and
Alexander J.B. Zehnder

Applied and Environmental Microbiology 59 (1993):3255-3265

Bacterial Adhesion under Static and Dynamic Conditions

HUUB H. M. RIJNAARTS,^{1*} WILLEM NORDE,² EDWARD J. BOUWER,[†] JOHANNES LYKLEMA,²
AND ALEXANDER J. B. ZEHNDER[‡]

Department of Microbiology, Wageningen Agricultural University, Hesselink van Suchtelenweg 4, 6703 CT Wageningen,¹ and Department of Physical and Colloid Chemistry, Wageningen Agricultural University, Dreijenplein 6, 6703 HB Wageningen,² The Netherlands

Received 11 March 1993/Accepted 21 July 1993

The deposition of various pseudomonads and coryneform bacteria with different hydrophobicities (water contact angles) and negative cell surface charges on negatively charged Teflon and glass surfaces was investigated. The levels of deposition varied between 5.0×10^4 and 1.6×10^7 cells cm^{-2} and between 5.0×10^4 and 3.6×10^7 cells cm^{-2} for dynamic column and static batch systems, respectively, indicating that there was a wide variation in physicochemical interactions. Batch and column results were compared in order to better distinguish between hydrodynamic and other system-dependent influences and method-independent physicochemical interactions. Despite the shorter suspension-solid contact time in columns (1 h) than in batch systems (4 h), the level of deposition (expressed as the number of cells that adhered) divided by the applied ambient cell concentration was 4.12 ± 1.63 times higher in columns than in batch systems for 15 of 22 strain-surface combinations studied. This demonstrates that transport of microbial particles from bulk liquid to surfaces is more efficient in dynamic columns (transport dominated by convection and diffusion) than in static batch systems (transport by diffusion only). The relative constancy of this ratio for the 15 combinations shows that physicochemical interactions affect adhesion similarly in the two systems. The deviating deposition behavior of the other seven strain-surface combinations could be attributed to method-dependent effects resulting from specific cell characteristics (e.g., to the presence of capsular polymers, to an ability to aggregate, to large cell sizes, or to a tendency to desorb after passage through an air-liquid interface).

A better understanding and control of bacterial adhesion are needed for application of microorganisms in fixed-bed bioreactors (5) and in microbiological techniques used for bioremediating contaminated aquifers and soils (12), for improving the recovery of oil from the subsurface (16), for assessing the movement of pathogens or genetically engineered organisms in groundwater systems (38, 39), and for preventing bacterial colonization and biofilm formation on human teeth (27), prosthetic and other medical devices (28), and the inner walls of pipes in water supply and industrial systems (8).

The deposition of micron size particles, such as bacteria, on solid surfaces can be regarded as a two-step process: (i) the particles are transported close to the adhesive surface, and (ii) adhesion takes place under the control of physicochemical interactions and shear forces (41).

Transport of bacteria from bulk liquid to surfaces strongly depends on the hydrodynamics of the system studied. Some authors have investigated adhesion under defined particle flux and fluid shear conditions by using a rotating disk (19), a flat plate flow cell (35), or an impinging jet system (48). With the latter two methods, adhesion can be measured *in situ*, which avoids uncontrolled effects of transfer of substrata through the air-liquid interface (34).

In addition to these advanced techniques, there is a need for quick, inexpensive, and reliable procedures to measure bacterial adhesion. One problem often encountered when data from investigators who use such simple systems (1, 7,

22, 42, 43) are compared is that seemingly insignificant differences in methods lead to substantially different results. This is especially true when the hydrodynamics of deposition are not properly controlled or when the effects of transfer of substrata through the air-liquid interface are not taken into account. Also, with methods used in our laboratory (42, 43) erratic results have been obtained occasionally. To better distinguish between transport and other effects of methods on deposition and the actual physical chemistry of adhesion, we compared batch and column methods for a limited number of bacterium-substratum combinations. In this paper we focus on the transport effects and effects of methods; the physicochemical mechanisms involved in bacterial adhesion have been thoroughly analyzed in another study (29).

Greater hydrophobicity of cells and substrata results in greater attractive forces and higher levels of adhesion (29, 42), whereas smaller (more negative) electrokinetic potentials of cells and solids and lower levels of ionic strength (*I*) result in greater repulsive electrostatic interactions and lower levels of adhesion (29, 43, 44). We selected hydrophobic Teflon and hydrophilic glass, both of which are negatively charged, as the model surfaces. Various gram-negative pseudomonads and gram-positive coryneform bacteria with different cell surface hydrophobicities and negative electrophoretic mobilities (*u*) were used. Adhesion on submerged flat pieces of surfaces was studied in static batch systems. Dynamic column systems were used to study adhesion from suspensions percolated over water-saturated packed beds of substratum granules. Transport of cells from bulk liquid to surfaces is controlled by diffusion under static conditions (17, 18) and is governed by convection and diffusion in dynamic columns (10, 41). In this study, we also investigated adhesion and detachment during the transfer of substrata through the air-liquid interface or as a result of

* Corresponding author.

† Present address: Department of Geography and Environmental Engineering, The Johns Hopkins University, Baltimore, MD 21218.

‡ Present address: EAWAG/ETH, CH 8600, Dübendorf, Switzerland.

shear during washing procedures. Possible contamination of the solid surfaces by compounds excreted by the cells during the adhesion assays which may have affected attachment (23) was also studied.

MATERIALS AND METHODS

Aqueous media. The aqueous media used for all experiments were made with deionized (MilliQ-treated) water (Nanopure System D4700 apparatus; Barnstead/Thermolyne Co., Dubuque, Iowa). Phosphate-buffered saline (PBS) solutions having various I values were used (PBS having an I of 0.1 M contained 84.4 mmol of NaCl per liter, 2.1 mmol of KH_2PO_4 per liter, and 6.8 mmol of K_2HPO_4 per liter in deionized water and had a pH of 7.2). PBS degassed by decompression (-3.3 kPa for 10 min) was used to prevent air bubble formation on the Teflon supports.

Bacteria. The strains used are listed in Table 1. These strains were selected on the basis of their cell surface properties (2, 4), their environmental relevance (ability to degrade xenobiotic compounds) (9, 30, 46), and their potential applications in biotechnology (32, 47).

Bacterial cultivation and preparation. Rhodococcus strains C3 and C4 and all of the pseudomonad strains except P2 were cultivated in the mineral medium described by Schraa et al. (31), except that yeast extract was not added. Ethanol (50 mM) was used as the sole carbon and energy source for all strains except strain P3, which was grown with 5 mM 3-chlorobenzoate. The other strains were cultivated either in nutrient broth (Difco) (8 g/liter of deionized water) (strain P2) or in brain heart infusion broth (Merck) (40 g/liter of deionized water) (coryneform bacteria other than the rhodococci). The bacterial cells were harvested in the late exponential phase by centrifugation for 10 min at $20,000 \times g$ at 4°C . Then the cells were washed three times by resuspension and centrifugation, using precooled PBS with the I required for each specific experiment. Finally, the cells were resuspended in an amount of PBS equal to 1% of the original culture volume and stored on ice until experiments were started (within 1 h).

Physicochemical and physical characterization of bacteria. The contact angles of drops of water (θ_w) placed on dried bacterial lawns were measured by using a microscope equipped with a goniometric eyepiece and the method of Van Loosdrecht et al. (42). The u values of bacterial cells in 0.010 M PBS were determined by using a laser-Doppler velocimetric device (Zetasizer 3; Malvern Instruments, Ltd., Worcestershire, Great Britain). The values given below for θ_w and u are the averages of the values from at least three independently grown cultures. The effective radii (R_e) (in meters) of the cells of the different bacterial strains were determined in the following two ways: (i) from the average geometric mean of the cell width (w) and length (l) determined for 50 cells by using a light microscope [$R_e = 0.5(wl)^{1/2}$], and (ii) with the Stokes-Einstein equation ($D_e = kT/6\pi\eta R_e$, where k is the Boltzmann constant [in joules per kelvin], T is the absolute temperature [in Kelvin], and η is the dynamic viscosity [in kilograms per meter per second]) by using effective diffusion coefficients (D_e) (in square meters per second) obtained from dynamic light-scattering (26) measurements and by using the Contin multiexponential fit of the autocorrelation function (24, 25).

Electron micrographs were obtained for negatively stained strain C2 and C3 cells. Prewashed cells from 1 drop of a suspension were allowed to attach to Formvar-coated grids, after which the specimens were washed in deionized water

and air dried. The cellular proteins and lipids were stained by incubating the preparations in a 1% uranyl acetate solution (pH 4.7, adjusted with 0.1 M KOH) for 0.5 to 1 min. Finally, the specimens were washed with deionized water, air dried, and placed in an electron microscope for observation. Suspended strain C4 cells were examined with a light microscope (Diaplan 2000; Leitz, Wetzlar, Germany) and were tested for capsular material by negatively staining them with India ink.

Solid surfaces. Surfaces of PFA-Teflon (also registered as Teflon 350; a copolymer of perfluoroalkoxyheptafluoropropylene and polytetrafluoroethylene) were obtained from Fluorplast, Raamsdonksveer, The Netherlands. Transparent 0.1-mm-thick film and granules (type 9738) with diameters ranging from 250 to 500 μm (average, 375 μm) were used. Glass microscope coverslips (Rofa-Mavi, Beverwijk, The Netherlands) and Teflon film were cut to a size of 9 by 18 mm. Glass beads with a diameter of 450 ± 50 μm were used (Boom, Meppel, The Netherlands). The surfaces were cleaned by submerging them in concentrated chromosulfuric acid for 24 h at 60°C , after which they were well rinsed, first with a 0.5 M KCl solution and then with deionized water. Finally, they were air dried and stored in glass containers until they were used.

Physicochemical characterization of surfaces. Specific outer surface areas (A_{out}) of 49 and 73 $\text{cm}^2 \text{g}^{-1}$ were calculated from the average radii of the glass and Teflon beads, respectively, assuming that the glass beads were nonporous. N_2 gas adsorption on the Teflon granules was determined and analyzed by using the Brunauer-Emmett-Teller method (13), which yielded a specific surface area of 1.2 $\text{m}^2 \text{g}^{-1}$ (much larger than A_{out}) and an internal porosity value of 0.5% resulting from pores with diameters ranging from 20 to 200 nm. Electron micrographs of gold-coated beads also revealed pores with diameters of <300 nm. Bacterial cells cannot penetrate these pores.

Three measurements of θ_w for two samples of each solid were obtained by using a microscope equipped with a goniometric eyepiece (42). The electrokinetic potentials of the surfaces were determined by measuring streaming potentials in a parallel plate flow cell (21), using 0.010 M PBS as the electrolyte. A 17-g portion of Teflon beads submerged in 50 cm^3 of a degassed 0.01 M KNO_3 solution was titrated with acid (HNO_3) and base (KOH) as described by Fokkink et al. (11); this procedure revealed the presence of unidentified, negatively charged groups with a pK_a of approximately 7 at an apparent surface charge density of 2.5 C/m^2 of surface available for N_2 adsorption as determined by the Brunauer-Emmett-Teller method (data not shown). Such high surface charges are never found (14, 37), and considering the hydrophobicity of the samples, we concluded that the majority of the charged groups are located inside the Teflon matrix and are accessible for protons but not for N_2 molecules.

The presence of surface-active compounds excreted by cells during adhesion was determined by measuring θ_w on the surfaces. To do this, we incubated suspensions of prewashed cells (cell concentration $[c]$, 1×10^8 cells cm^{-3}) for 4 h at room temperature. After centrifugation two pieces of each type of substratum were incubated for 2 h in 9- cm^3 samples of the supernatants. The surfaces were air dried, and θ_w values were determined.

Batch adhesion experiments. Three batch adhesion methods were used for the batch adhesion experiments.

(i) **Method 1.** Glass vials (volume, 9 cm^3) with rubber stoppers were cleaned with a nonionic detergent solution, rinsed well with deionized water, boiled twice in large

TABLE 1. Physicochemical properties of the bacteria used in this study

Strain	Other designation	ρ_c (g ³) ^a	$\mu(10^{-6} \text{ m}^2 \text{ V}^{-1} \text{ s}^{-1})$ ^b	Cell length (µm)	Cell width (µm)	R_c (GM) ^c (µm) ²	$D_c(DLS)$ (10 ⁻¹⁵ m ² s ⁻¹) ^d	$R_c(DLS)$ (µm) ²	Other properties ^e
Corynebacterium bacteria									
C1	<i>Arthrobacter</i> sp. strain DSM 6687	15 (1) ^f	-2.91	ND ^g	ND	ND	2.69 (0.10)	0.80 (0.03)	CNT, NA
C2	Coryneform strain DSM 6685	29 (1)	-2.18	1.0 (0.2)	0.7 (0.0)	0.41 (0.10)	5.90 (0.30)	0.36 (0.02)	Capsules, NA
C3	<i>Rhodococcus</i> sp. strain C125 ^h	70 (5)	-3.34	2.9 (0.8)	1.9 (0.5)	1.17 (0.37)	1.74 (0.03)	1.24 (0.27)	No capsules, NA
C4	<i>Rhodococcus erythropolis</i> A177 ^h	87 (5)	-3.15	3.2 (0.2)	1.2 (0.3)	0.97 (0.15)	1.95 (0.01)	1.10 (0.15)	No capsules, NA
C5	<i>Corynebacterium</i> sp. strain DSM 6688	89 (1)	-2.12	2.0 (0.8)	0.6 (0.2)	0.56 (0.21)	ND	ND	CNT, NA
C6	<i>Corynebacterium</i> sp. strain DSM 44016	103 (6)	-2.38	1.1 (0.5)	0.8 (0.3)	0.47 (0.19)	3.78 (0.13)	0.57 (0.02)	CNT, NA
C7	<i>Gordonia</i> sp. strain 1779/15 ⁱ	115 (5)	-2.47	ND	ND	ND	ND	ND	CNT, aggregates
C8	<i>Gordonia</i> sp. strain DSM 44015	117 (4)	-2.89	2.0 (0.7)	0.9 (0.5)	0.66 (0.32)	2.61 (0.12)	0.82 (0.04) ^j	CNT, aggregates
Pseudomonads									
P1	<i>Pseudomonas oleovorans</i> ATCC 29347	17 (1)	-1.86	3.4 (2.6)	0.90 (0.05)	0.89 (0.37)	ND	ND	CNT, NA, long cells
P2	<i>Pseudomonas fluorescens</i> p62 ^k	25 (1)	-1.03	1.3 (0.1)	1.1 (0.1)	0.59 (0.08)	3.75 (0.06)	0.57 (0.02)	CNT, NA
P3	<i>Pseudomonas</i> sp. strain B13 ^l	32 (1)	-2.11	ND	ND	ND	4.33 (0.01)	0.49 (0.01)	CNT, NA
P4	<i>Pseudomonas putida</i> m2 ^m	40 (4)	-1.08	1.3 (0.1)	1.1 (0.1)	0.59 (0.07)	3.65 (0.05)	0.59 (0.01)	CNT, NA

^a Results of at least three independent measurements.
^b The standard deviation in all cases was less than 14%.
^c Cell length and width were determined with a light microscope and were used to calculate R_c by using the geometric mean approach [R_c (GM)]. Cellular particles of strains C1, C3, and C4 were predominantly composed of two to four associated cells; only single cells were observed for all of the other nonaggregating strains.
^d D_c and R_c values were obtained from dynamic light-scattering measurements [D_c (DLS) and R_c (DLS), respectively].
^e The presence of capsules was determined either by electron microscopy (cells were negatively stained with uranyl acetate) (strains C3 and C5) or by light microscopy (cells were stained with India ink) (strain C9). CNT, presence of capsules not tested. Aggregation was tested at I values of 0.1 and 1 M. NA, aggregation not observed.
^f The values in parentheses are standard deviations.
^g ND, not determined.
^h *Rhodococcus* sp. strain C125 and *R. erythropolis* A177 were reclassified; they were formerly named *Corynebacterium* sp. strain C125 and *Arthrobacter* sp. strain A177, respectively (30).
ⁱ See references 2 and 4.
^j Dynamic light-scattering measurements were determined after cell aggregates had settled.
^k See reference 44.
^l See reference 9.
^m See reference 46.

volumes of deionized water, rinsed again, and air dried. For each adhesion measurement sealed vials were prepared in triplicate as follows. A piece of either glass or Teflon film was placed into each vial, and the vials were then filled to the top with degassed PBS and sealed without a headspace by using the rubber stoppers. Aliquots (between 60 and 170 μ l) of concentrated cell suspensions were gently injected into the vials in order to attain the appropriate initial suspended c . Values of c were determined by measuring optical density at either 280 or 660 nm (standard error, 2%), which was calibrated by determining direct counts with a light microscope and a counting chamber (standard error, 15%). The vials were immediately placed on a vertically positioned rotating wheel (8 rpm; amplitude, 10 cm) and incubated at room temperature ($20 \pm 3^\circ\text{C}$). The surfaces periodically moved slowly up and down at a maximum velocity of 6 mm s^{-1} . After incubation, 45 cm^3 of cell-free PBS was added to each vial, and the excess fluid was allowed to flow out freely. The flow inlet (internal diameter, 2 mm) was placed a few millimeters above the bottom of the flask, and the flow was not aimed directly at the solid support. The replacing fluid was added at a flow rate (Q) of either 15 or 100 $\text{cm}^3 \text{min}^{-1}$. The two Q values were used to test the effect of shear. Because the fluid in the batches was mixed completely by adding PBS to the vials, the c was reduced by a factor of $1/\exp(-45/Q)$ (approximately 150) for a Q of 100 $\text{cm}^3 \text{min}^{-1}$. The dilution factor was much greater than 150 at a Q of 15 $\text{cm}^3 \text{min}^{-1}$ because suspended cells were removed by plug flow wash-out. The glass and Teflon sheets were removed from the vials, placed on microscope slides (during which the glass remained wet but the Teflon dewetted at least partially), covered with coverslips, and examined with a microscope (magnification, $\times 250$; Diaplan 2000; Leitz) that had a video camera (magnification, $\times 2$; model LDK 12; Philips, Eindhoven, The Netherlands) mounted on top. The numbers of adhered cells were determined at six randomly chosen locations; these locations were not closer than 3 mm from the edges of the surfaces. This was because the diffusion layer was very narrow at the edges and did not provide local static conditions; hence, the levels of deposition at locations close to the edges were likely to be influenced by artifacts, whereas static conditions were maintained at the more central parts of the surfaces. The observed area was adjusted so that the number of cells counted per location ranged from 20 to 60. Levels of adhesion (Γ) (number of cells per square centimeter) were determined by averaging the values obtained for the three vials which, in turn, were determined from the mean for the six adhesion values obtained per vial.

The width (δ) of the diffusion boundary layer adjacent to the surfaces was defined as follows (17):

$$\delta = D_e^{1/3} (\eta/\rho)^{1/6} (x/v)^{1/2} \quad (1)$$

where ρ is the density of water (in kilograms per cubic meter), η is the viscosity of water (in kilograms per meter per second), x is the distance from the front or rear surface edge (in meters), and v is the velocity of the surface (in meters per second). The width of the diffusion boundary layer was calculated by using the D_e values obtained from dynamic light-scattering or geometric mean procedures (Table 1), the range of positions at which adhesion was determined (3 mm $\leq x \leq 9$ mm), and a value of 6 mm s^{-1} for the velocity of the surface.

(ii) **Method 2.** Method 2 differed slightly from method 1; its objective was to detect the effects of transfer of substrata

through the air-liquid interface in the presence of suspended cells. After incubation the surfaces were removed directly from the suspension. Nonattached cells were removed by transferring the substrata into 100 cm^3 of cell-free 0.1 M PBS, after which the substrate were moved gently forward and backward 10 times. The numbers of adhered cells were determined as described above for method 1.

(iii) **Method 3.** Sealed vials (see method 1) containing 5 g of degassed beads and 7 cm^3 of PBS were prepared in triplicate to assay adhesion to Teflon beads. The other procedures were similar to the method 1 procedures, except that levels of adhesion were determined from depletion data.

The methods and conditions used in the different adhesion experiments are summarized in Table 2. Adhesion to Teflon was studied as a function of time (t) at a c of 1×10^8 cells cm^{-3} and as a function of c after incubation for 2 h for strain P2 by using method 1 and for coryneform strains C3 and C4 by using methods 1 and 2 (Table 2, experiments 2 and 4). All of the other batch results were obtained after incubation for 4 h at a c of 5×10^8 cells cm^{-3} . Levels of adhesion were determined for all strain-surface combinations by using method 1 with a Q of 15 $\text{cm}^3 \text{min}^{-1}$ (Table 2, experiment 1). The effect of fluid velocity during washing was tested by comparing levels of adhesion at Q values of 100 and 15 $\text{cm}^3 \text{min}^{-1}$ for strains P1, P2, P4, and C1 on glass and for strains P1, P4, C5, and C8 on Teflon (Table 2, experiment 3). Levels of adhesion to Teflon beads (method 3) were determined for strains C3, C4, and P4 (Table 2, experiment 5). Desorption of strain C4 attached to Teflon film as determined by method 2 was studied in batch preparations in the presence and absence of 5 g of initially cell-free Teflon beads (Table 2, experiment 6).

Column experiments. Glass columns with an internal diameter of 1.0 cm and a length of 10 cm were used. Porous glass frits (thickness, 3 mm; pore size, 0.15 mm) separated the internal column space from the inlet and outlet parts. Any air between Teflon beads submerged in PBS was removed by decompression (-3.3 kPa for 10 min). Submerged glass or Teflon beads were transferred with a pipet to columns which were already filled with PBS, thus avoiding exposure of the beads to air. The columns were agitated during packing, which resulted in a reproducible length (9.0 ± 0.3 cm) and overall porosity (0.33 ± 0.03) of the granular bed. Total porosity values were estimated from breakthrough curves by using chloride as the conservative tracer. Chloride concentrations were measured with a microchloro-counter (Marius, Utrecht, The Netherlands). The influent was supplied to the vertical downflow columns by a peristaltic pump. The flow rate was kept constant (within 2%) for each column but varied between 16 and 21 $\text{cm}^3 \text{h}^{-1}$ for different columns. Samples of the concentrated stock suspensions were diluted in 0.1 M PBS to an optical density at 280 nm of 0.60 ± 0.05 (10^7 cells $\text{cm}^{-3} < c < 10^8$ cells cm^{-3}). These suspensions were applied to the columns for 1 h, during which their optical densities at 280 nm remained constant. The influent was then changed to cell-free 0.1 M PBS, which was added to the columns for 45 min. The effluent of a single column was collected in one flask in which the c was determined at the end of the experiment. Adhesion was studied for all strain-surface combinations (except aggregating strain C7) (Table 2, experiment 7). Detachment from Teflon as a result of passing through the air-liquid interface was tested for the same strains by using the same set of columns containing Teflon as described above and a second set of similarly treated columns which were flushed with deionized water (I , $< 0.0001\text{M}$) after flushing with

cell-free PBS (Table 2, experiment 8). The fluids from high-*I* and low-*I* columns were drained and collected in separate flasks. The level of adhesion (Γ) (in number of cells per square centimeter) and the fraction of cells desorbed as a result of passing through the air-liquid interface (f_{aH}) (expressed as a percentage) were calculated as follows:

$$\Gamma = (V_i c_i - V_e c_e)/(m A_{out}) \quad (2)$$

$$f_{aH} = (V_e c_e)/(V_i c_i - V_e c_e) \times 100\% \quad (3)$$

where the subscripts *i*, *e*, and *d* indicate influent, effluent, and drainage fluid, respectively, *V* is the suspension volume (in cubic centimeters), and *m* is the mass of the beads in the column (in grams). All results presented below were obtained from duplicate columns.

RESULTS

Characteristics of bacterial cells. The properties of the bacterial strains are shown in Table 1. The values for θ_w and *u* ranged from 15 to 117° and from -1.03×10^{-8} to $-3.34 \times 10^{-8} \text{ m}^2 \text{ V}^{-1} \text{ s}^{-1}$, respectively, indicating that there was wide variation in the levels of cell surface hydrophobicity and electrokinetic charges. The R_e values estimated by light microscopy did not differ much from those obtained from dynamic light scattering. Some microbial particles were found to be agglomerates (strains C1, C3, and C4) (Table 1). Capsular polymers were detected on the surface of strain C2 by electron microscopy. In an aqueous environment, these capsule polymers are likely to extend much farther than the approximately 2 μm observed when a dehydrated specimen was used. Electron micrographs of strain C3 and negative staining of C4 cells with India ink revealed no capsular material on either of the cell surfaces (Table 1). Strains C7 and C8 aggregated at *I* values of $\geq 0.1 \text{ M}$, which is consistent with their high levels of hydrophobicity.

Solid surface characteristics. The θ_w values are consistent with known properties; i.e., glass is hydrophilic ($\theta_w, 12 \pm 2^\circ$), and Teflon is hydrophobic ($\theta_w, 105 \pm 1^\circ$). The electrokinetic potentials were -44.8 ± 1.8 and $-43.6 \pm 1.7 \text{ mV}$ for glass and Teflon, respectively. Although the fact that there is a negative charge on Teflon is well established, its origin is not known. Perhaps the negative charge is related to the presence of the ether oxygens in the alkoxy groups. The hydrophilicity of glass and the hydrophobicity of Teflon are not substantially altered by adsorption of compounds excreted by cells into a medium; θ_w increased by less than 6° on glass, and on Teflon θ_w was reduced by 7 and 10° for strains C3 and C8, respectively, and by less than 4° for all of the other organisms. Since dried adsorbed biopolymer films lead to surface-water contact angles between 20 and 40° (45), we concluded that the amounts of excreted products that may have adsorbed on the test substrata were very small and probably did not influenced adhesion.

Diffusion-controlled adhesion in batch experiments. Γ increased linearly with the square root of time ($t^{1/2}$) (Fig. 1A) and *c* (Fig. 1B) for strains C3 and P2 when batch method 1 was used (Table 2, experiment 2). This is consistent with the hypothesis that the rate of attachment is controlled by the diffusion of particles from bulk liquid toward the surface (18).

Effect of transfer through the air-liquid interface. The low level of adhesion of strain C4 compared with strain C3 as determined by method 1 (Table 2, experiment 2, and Fig. 1) was unexpected since these two strains had similar θ_w and *u* values (Table 1). The level of adhesion of strain C4 when

TABLE 2. Methods, conditions, and strain-surface combinations used for the adhesion experiments

Expt	Phenomenon investigated	Method	Conditions				Strain-substratum combination(s) tested
			Q (cm ³ min ⁻¹)	t_{wash} (h)	<i>c</i> (cells cm ⁻³)	t_{column} (h)	
1	Deposition under static conditions	Batch method 1	15	4	5×10^8	0.1	All
2	Concn and time dependency of static deposition	Batch method 1	15	Various	Various	0.1	P2-Teflon, C3-Teflon, C4-Teflon
3	Effect of shear during washing	Batch method 1	15 or 100	4	5×10^8	0.1	P1-glass, P2-glass, P4-glass, C1-glass, P1-Teflon, P4-Teflon, C5-Teflon, C8-Teflon, C3-Teflon, C4-Teflon
4	Effect of passing through an air-liquid interface in the presence of suspended cells	Batch method 2		Various	Various	0.1	C3-Teflon, C4-Teflon
5	Deposition on colliding beads	Batch method 3		4	$10^7 < c < 10^8$	0.1	P4-Teflon, C3-Teflon, C4-Teflon
6	Detachment induced by colliding beads	Batch method 2 with beads added		0.5	5×10^8	0.1	C4-Teflon
7	Deposition under dynamic conditions	Column method			$10^7 < c < 10^8$	1	All except C7 combinations
8	Detachment upon passing through an air-liquid interface	Column method			approx 0	0.1 or <0.0001	All strains-Teflon except C7-Teflon and P3-Teflon at both <i>I</i> values and P4-Teflon at <i>I</i> of <0.0001 M

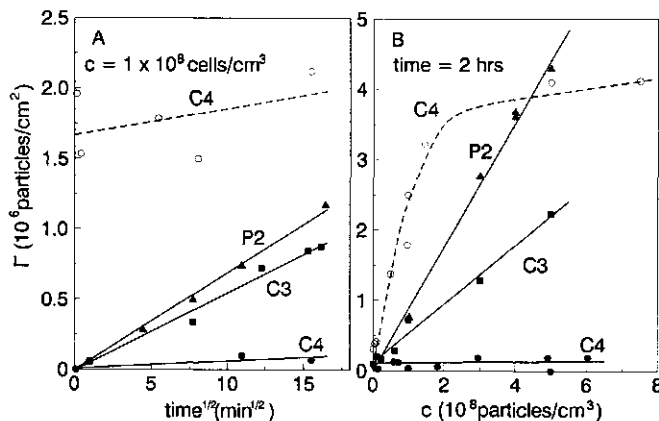


FIG. 1. Adhesion of strains C3 (■), C4 (●), and P2 (▲) to Teflon as determined by batch method 1 and adhesion of strain C4 as determined by method 2 (transfer of Teflon through the air-liquid interface in the presence of suspended cells) (○) as a function of time (A) and c (B).

batch method 2 was used (Table 2, experiment 4) was 20-fold higher than the level of adhesion when method 1 was used. The occurrence of a nondiffusive transport mechanism was demonstrated by the observation that adhesion instantaneously reached high levels and did not depend linearly on c . Similar results for strain C3 were observed when method 2 was used (data not shown). In additional tests in which a video camera mounted on a light microscope was used, it was demonstrated that strain C3 cells accumulated at the air-liquid interface (Fig. 2A) and preferentially attached to the solid surface at the three-phase boundary with contact times ranging from seconds (Fig. 2B) to minutes (Fig. 2A). Deposition without interference of the air-liquid interface was much slower (Fig. 2A) and resulted in a homogeneous distribution of adhered cells (Fig. 2C). Figure 3 shows detachment as a result of passing an air-liquid interface through columns (Table 2, experiment 8). At an I of 0.1 M the f_{att} (equation 3) was less than 3% for 9 of 11 strains studied. Higher levels of desorption were observed for C1 (22.5%) and P2 (7.5%). f_{att} values were higher for an I of <0.0001 M because of increased electrostatic repulsion, but most of the f_{att} values remained below 15%; the only exception was the strain C1 f_{att} (22.5%).

Effect of shear on adhesion in batch preparation. The effect of shear on adhesion in batch preparations was tested by adding 45 cm³ of cell-free PBS to vials at different Q values (100 or 15 cm³ min⁻¹) (method 1) (Table 2, experiment 3) and by studying adhesion in the presence of Teflon beads (Table 2, experiments 5 and 6). For hydrophilic strain P1 on both glass and Teflon and for the hydrophilic to intermediately hydrophobic organisms C1, P2, and P4 on glass, Γ was found to be reduced by the higher flow rate (Table 3). This indicates that weak adhesive bonds allowed shear forces to reduce adhesion. For Teflon and intermediately to highly hydrophobic bacteria (strains P4, C5, and C8) the opposite was found; Γ increased with Q . Apparently, the increased transport of particles from the bulk liquid to the surface was greater than the removal of adhered cells due to fluid shear. Shear forces induced by moving beads in mixed systems can also reduce adhesion. The experiments with the beads were

performed to test to what extent results obtained with mixed batch systems containing granular substrata can be used to predict deposition under more quiescent conditions. The levels of adhesion (Γ/c) on Teflon beads (Table 2, experiment 5) (method 3, strains C3, C4, and P4) (data not shown) were found to be 48 to 65% of the levels of adhesion on Teflon film (Table 2, experiment 1) (method 1). Cells of strain C4 attached irreversibly to Teflon film as determined by method 2 but desorbed completely when Teflon beads were added (Table 2, experiment 5, and Fig. 4).

Adhesion in batch preparations and columns compared. Adhesion data for all strain-surface combinations were obtained from both batch and column experiments (Table 2, experiments 1 and 2) at an I of 0.1 M (Table 4). Direct comparisons of the two sets of data are not possible since adhesion in batch experiments was assayed at a c of 5×10^8 cells cm⁻³ and adhesion in column experiments was determined at 1×10^7 cells cm⁻³ $\leq c \leq 1 \times 10^8$ cells cm⁻³. Therefore, Γ/c values were used for comparison (Fig. 5). The Γ/c values varied by more than 2 orders of magnitude for both systems. For 15 of the 22 strain-surface combinations studied, $\log(\Gamma/c)_{\text{column}}$ and $\log(\Gamma/c)_{\text{batch}}$ appeared to be related according to a linear regression line with a positive intercept and a slope that was not significantly different from unity ($P < 0.05$). Hence, $(\Gamma/c)_{\text{column}}/(\Gamma/c)_{\text{batch}}$ was nearly constant, and averaging the 15 ratios yielded:

$$(\Gamma/c)_{\text{column}} = (4.12 \pm 1.64) (\Gamma/c)_{\text{batch}} \quad (4)$$

Deviation of Γ/c values from the main trend was observed only when the bacterial cells aggregated (C8), were elongated (P1), produced capsules (C2), or displayed significant desorption from Teflon upon passing through an air-liquid interface (C1).

DISCUSSION

Adhesion in batch experiments under static conditions. Transport of bacteria from bulk liquid to surfaces was shown to be governed by diffusion for the batch systems studied by

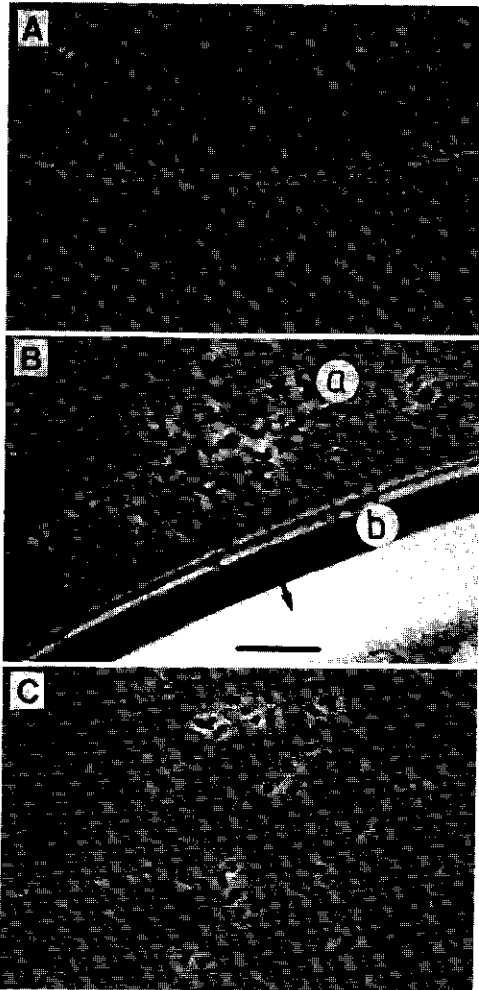


FIG. 2. Effects of the air-liquid interface on adhesion of strain C3 to Teflon. (A) On a surface placed in a suspension made with nondegassed PBS an air bubble developed, and the three-phase boundary moved through region a in the direction indicated by the arrows and stopped after 5 min at position b. Suspended cells were removed by washing ($Q, 15 \text{ cm}^3 \text{ min}^{-1}$), and the surface was placed under the microscope. Bar = $5 \mu\text{m}$. (B) Air-suspension interface. A microscope equipped with a video camera was used for direct observations. The air-liquid interface was first situated at position b, moved to position a after the system had been agitated, and receded in the direction indicated by the arrows. Cells were deposited mainly at position a, and the cells at the air-liquid interface (position b) moved very fast, indicating high fluid dynamics. Bar = $5 \mu\text{m}$. (C) Normal adhesion pattern of strain C3 observed with method 1 ($Q, 15 \text{ cm}^3 \text{ min}^{-1}$). Bar = $5 \mu\text{m}$.

using method 1 ($Q, 15 \text{ cm}^3 \text{ min}^{-1}$) (Fig. 1). By using equation 1 the diffusion boundary layer thickness was calculated to range from 5 to $8 \mu\text{m}$ and from 7 to $11 \mu\text{m}$ for the largest cells used (C3) and the smallest cells used (C2), respectively. Apparently, fluid motion in the bulk liquid did not penetrate these thin diffusion layers; hence, static conditions prevailed. The number of bacteria transported by diffusion (N_T) (in number of cells per square meter) was calculated by using the D_e values given in Table 1 and the following equation (18):

$$N_T = 2c(D_e t/m)^{1/2} \tag{5}$$

N_T values of 3.3×10^6 particles cm^{-2} and 4.75×10^6 cells cm^{-2} were obtained for strains C3 and P2, respectively; these values are not significantly different from the Γ values (Table 4) obtained for C3 ($3.16 \times 10^6 \pm 0.25 \times 10^6$ particles cm^{-2}) and P2 ($5.65 \times 10^6 \pm 1.46 \times 10^6$ particles cm^{-2}). Γ was either not significantly different from or smaller than N_T for all other strain-surface combinations tested (data not shown) except strain C2-surface combinations. These findings indicate that (i) in general equation 5 correctly describes particle transport in these batch systems, (ii) the net physicochemical interaction is attractive and deposition is not retarded by a repulsive barrier when Γ is approximately the same as N_T , and (iii) repulsive interactions prevent 100% efficient adhesion when Γ is less than N_T . For strain C2, Γ/N_T values of 1.33 and 5.85 were obtained for glass and Teflon, respectively, which indicates that equation 5 is not applicable to this strain. The specific behavior of strain C2 may be a result of the capsular polymers that extend several micrometers (probably more than $10 \mu\text{m}$) into the area surrounding the cells. The polymers may enhance deposition by penetrating the stagnant diffusion layer that separates the bulk liquid from the surface. The capsular polymers have a high affinity for both glass and Teflon; apparently, they do not impede adhesion by steric hindrance.

Comparison of adhesion in batch and column systems. Among the various combinations of strains and surfaces studied, the levels of adhesion (Γ/c) varied more than 2 orders of magnitude in both batch and column systems. The approximately similar ratios of level of adhesion in columns to level of adhesion in batch systems (equation 4) that were observed for 15 of 22 combinations of strains and surfaces indicate that the physicochemical origins of adhesion are the same for both systems. For a complete comparison of the batch and column results the solid-suspension contact times had to be taken into account; the solid-suspension contact time for columns (t_{column}) was 1 h, and the solid-suspension contact time for batch systems (t_{batch}) was 4 h. $(\Gamma/c)_{\text{batch}} \propto t^{1/2}$ (equation 5). For ideal deposition in columns, the effluent particle concentration and the rate of deposition are constant after the initial breakthrough (10); hence, $(\Gamma/c)_{\text{column}} \propto t$. Consequently, $[\Gamma/(c t)]_{\text{column}}$ and $[\Gamma/(c t^{1/2})]_{\text{batch}}$ are constants. From the slope of equation 4 and from the t_{batch} (4 h) and t_{column} (1 h), the following equation was derived:

$$(\Gamma/c)_{\text{column}} = (8.24 \pm 3.27)(t_{\text{column}}/t_{\text{batch}})^{1/2}(\Gamma/c)_{\text{batch}} \tag{6}$$

The factor $(8.24 \pm 3.27) \text{ h}^{-1/2}$ in equation 6 reveals that transport of microbial particles from bulk liquid to surfaces in columns (transport dominated by convection and diffusion) is more efficient than transport in batch systems (transport by diffusion only). This relationship may be extended to results obtained at various values of t_{batch} and t_{column} provided that additional tests confirm that ideal deposition occurs in columns.

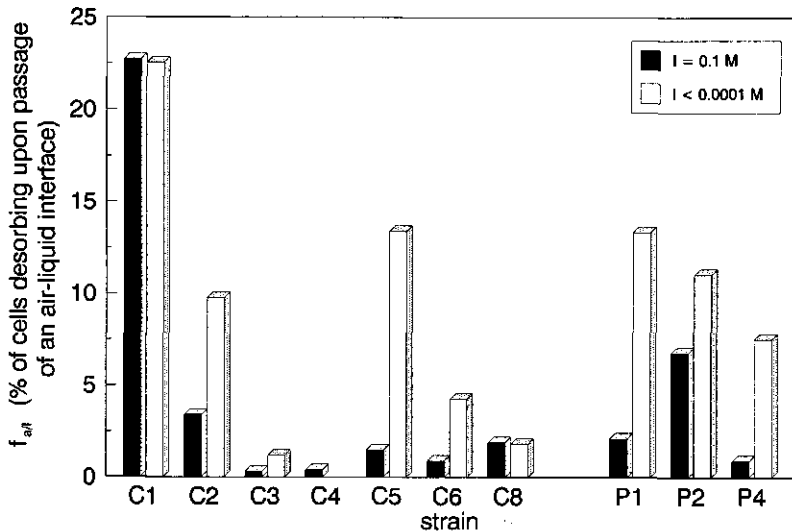


FIG. 3. Fraction of cells desorbing from Teflon beads in columns when an air-liquid interface was passed (f_{des}). The two aqueous media tested were 0.1 M PBS and deionized water ($I, < 0.0001$ M).

Deviations from equation 4 (Fig. 5) can be explained in all cases except the combination of strain C1 and Teflon. Cell aggregates of strain C8 and the elongated cells of strain P1 (Table 1) are most likely physically retained between the beads, leading to a high level of uptake of cells by columns. In addition, aggregation such as that observed for strains C7 and C8 reduces adhesion in batch systems (equation 5). For strain C2 in column systems, Γ/c did not exceed the Γ/c values found for the other bacterial species, which indicates that the surface polymers of strain C2 can increase the level of adhesion only under static conditions. The deviating behavior of strain C1 on Teflon may have been partly an effect of desorption in batch experiments after Teflon surfaces were transported through the air-liquid interface, but this behavior may also have been influenced by other (unknown) factors since the measured desorption value of 22.5% (Fig. 3) was not sufficient to account for the observed deviation. The correlation between column and batch results shown in Fig. 5 and equation 4 may be used in the future as

a reference to separate adhesion data directly suitable for further physicochemical analysis from results influenced by factors related to the method used.

Effect of shear on adhesion in batch experiments. High fluid velocities disturbed the static conditions of the batch system

TABLE 3. Γ in batch systems after washing with 45 cm³ of PBS at a Q of 100 cm³ min⁻¹ compared with Γ after washing at a Q of 15 cm³ min⁻¹, expressed as a ratio

Surface	Strain	$\Gamma_{100}/\Gamma_{15}^a$
Glass	P4	0.05
	P2	0.20
	P1	0.60
	C1	0.67
Teflon	P1	0.68
	C8	1.18
	P4	1.24
	C5	1.86

^a Γ_{100} , Γ after washing at a Q of 100 cm³ min⁻¹; Γ_{15} , Γ after washing at a Q of 15 cm³ min⁻¹.

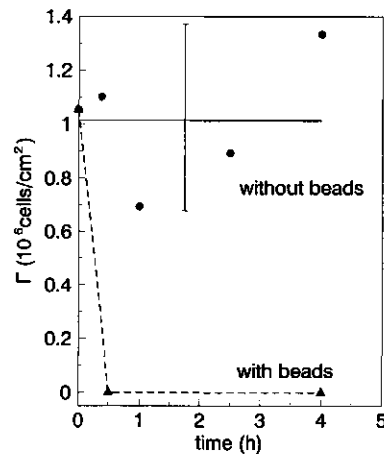


FIG. 4. Desorption of cells of strain C4 adhered to Teflon film as determined by batch method 2 in the presence (▲) and absence (●) of Teflon beads. The cells remained irreversibly attached in the absence of beads but desorbed completely after beads were added. The bar indicates the standard deviation for data obtained in the absence of beads.

TABLE 4. Γ in batch systems (method 1; Q , 15 $\text{cm}^3 \text{min}^{-1}$) and column systems

Strain	Γ (10^5 particles cm^{-2})			
	Batch system ^a		Column system ^b	
	Teflon	Glass	Teflon	Glass
C1	0.16 (0.02)	0.23 (0.03)	1.93	0.35
C2	35.49 (7.14)	8.05 (1.75)	15.50	5.94
C3	3.16 (0.25)	0.12 (0.04)	1.62	0.07
C4	0.34 (0.22)	0.06 (0.02)	0.20	0.05
C5	3.79 (0.09)	1.52 (0.18)	2.64	1.05
C6	4.44 (1.05)	2.02 (0.19)	3.25	2.32
C7	1.51 (0.60)	0.20 (0.08)	ND ^c	ND
C8	0.47 (0.07)	0.16 (0.03)	3.00	0.91
P1	0.22 (0.09)	0.050 (0.001)	8.03	1.59
P2	5.65 (1.46)	1.38 (0.31)	16.3	4.52
P3	0.17 (0.03)	0.113 (0.004)	0.50	0.50
P4	2.76 (0.52)	1.41 (0.16)	15.90	4.59

^a The values in parentheses are standard deviations. The average standard deviation was 19% (excluding the results for strain C4 on teflon).

^b The average standard deviation for duplicate column results was less than 2.5%.

^c ND, not determined.

and led to either higher or lower levels of adhesion (Table 3). The lower levels of adhesion for hydrophilic strain-surface combinations at higher washing Q values indicate that there were weak adhesive bonds which were disrupted by shear forces (33, 48). The greater resistance to shear found for the more hydrophobic strains on Teflon indicates that there was

strong attraction. High levels of adhesion and/or strong adhesion for more hydrophobic strain-surface combinations was also found in other studies (6, 22, 29, 42). The shear forces in batch systems with granular substrata were greater than the shear forces at high Q values since the levels of adhesion were also lower for combinations of hydrophobic surfaces and hydrophobic strains (method 3, strains C3, C4, and P4) (Fig. 4). One of the practical consequences of these findings is that the deposition of a bacterial species as measured in a mixed suspension of sediment grains cannot be used to predict its adhesion behavior in a natural sediment or in packed sediment columns, where shear forces are small or even absent. Not all investigators appear to be aware of these effects of ill-defined shear forces on adhesion on granular substrata in mixed batch systems (15, 36, 45).

Passing through the air-liquid interface. In general, the level of desorption when the air-liquid interface was passed (Fig. 3) was found to be lower than the standard deviations of 10 to 20% typical for most batch adhesion data (Table 4), which is at variance with the significant level of desorption predicted by Sjollem et al. (34). On the other hand, strong increases in the levels of adhesion of strains C3 and C4 to Teflon as a result of passing through the air-liquid interface were observed when method 2 was used (Fig. 1 and 2A and B). The low level of adhesion of strain C4 under submerged conditions in batch experiments (method 1) (Fig. 1A) and column experiments (Table 4 and Fig. 5) indicates that the high level of attachment of strain C4 determined by method 2 was a result of strong attraction triggered by the air-liquid interface. Neu and Poralla (20) identified a surface-active lipopolysaccharide on the cell surface of *Rhodococcus eryth-*

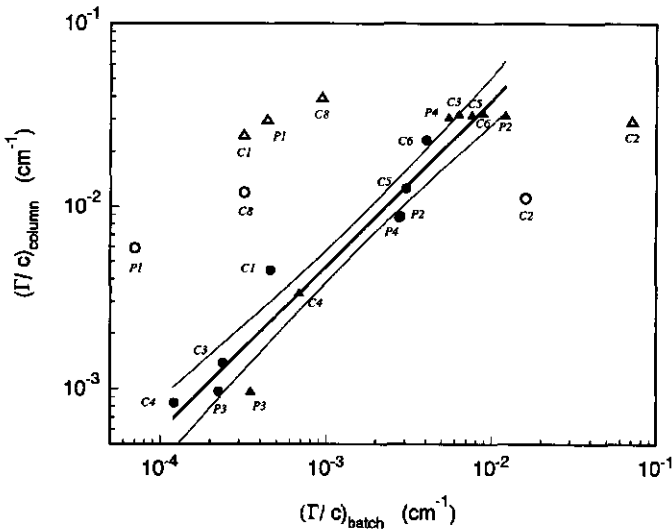


FIG. 5. Deposition in columns as a function of deposition in batch preparations for glass (circles) and Teflon (triangles). Deposition is expressed as Γ/c . The solid line corresponds to equation 4 and was obtained from linear regression analyses of the data (solid symbols) by excluding the results obtained for strains C1, C2, C8, and P1 on Teflon and for strains C2, C8, and P1 on glass (open symbols). These results were excluded for reasons explained in the text. The curves demarcate the confidence interval ($P < 0.05$). The slope close to unity indicates an approximately constant ratio of level of adhesion in columns to level of adhesion in batch preparations. The significant intercept shows that this ratio is greater than unity.

ropolis, and this compound may also be present on the exterior of *R. erythropolis* C4 cells. Such amphoteric polymers tend to orient their hydrophobic tails to the air side of the interface and their hydrophilic carbohydrate moieties into an aqueous environment. Steric hindrance between such hydrated polymers may prevent adhesion under submerged conditions. In addition, θ_w measured on dried bacterial lawns may not reflect the real hydrophobicity of the hydrated cell surface of strain C4, as has also been suggested for hydrophobic oral streptococci (40). The assumed hydrophilic outer polymer layer cannot be very thick since it could not be made visible by negative staining with India ink. Cells of C4 that adhered to the air-liquid interface may be able to contact the solid phase with the hydrophobic parts of their cell surface polymers, leading to the high level of adhesion observed when method 2 was used. Since the transfer of microorganisms with (partly) hydrophobic cell surface polymers from bulk liquid to the air-liquid interface is energetically favorable, these bacteria tend to accumulate at this interface (Fig. 2B). Moreover, the dynamics of the fluid near this interface facilitate the transport of cells to the substratum (Fig. 2A and B). Hence, a higher level of adhesion mediated by an air-liquid interface may result from (i) higher local cell concentration coupled with fast particle transport, and (ii) a change in the structure of the outer cell polymer layer. The increase in level of adhesion when the air-liquid interface is passed may be an important factor in the attachment and retention of bacteria in unsaturated soils (15, 38), aerated bioreactors, or waste gas biofilters (3).

Conclusions. The transport of microbial particles from bulk liquid to surfaces is a factor of 4.12 ± 1.63 more efficient in dynamic columns (transport dominated by convective diffusion) than in static batch systems (transport mediated by diffusion only) for the conditions used in this study. Our findings demonstrate that for any system used to study microbial deposition, the transport of cells from the bulk liquid to the substratum must be taken into account for a proper assessment of bacterial adhesion.

Comparing levels of bacterial deposition as measured by two independent hydrodynamically defined methods provides a way to distinguish between adhesion results that are suitable for further physicochemical analyses and adhesion results that are highly influenced by factors related to the method used. Selection of data is important since adhesion was influenced by system-dependent effects as a result of specific cell characteristics for 32% of the strain-surface combinations studied. Although these cases are regarded as less suitable for testing and developing general adhesion theories, the observed phenomena may have great importance for practical applications. For instance, aggregating and large cells are probably physically retained in porous media like soil, aquifers, and packed bed reactors and tend to clog the pores of such systems. Also, increased attachment as a result of passing through air-liquid interfaces may have great practical importance since this may be a dominant factor in the immobilization of hydrophobic microorganisms in unsaturated zones in soil and in aerated bioreactors.

The bacterium-subsurface combinations that appeared to be not influenced by effects related to the method used (68% of all cases tested) were used for a thorough analysis of the physical chemistry and reversibility of bacterial adhesion (29).

ACKNOWLEDGMENTS

This research was funded by grant C6/8939 from The Netherlands Integrated Soil Research Programme.

We thank Bernd Bendinger (Department of Microbiology, University of Osnabrück, Osnabrück, Germany) for providing six coryneform strains, and he and his colleague Stefan Klatt (Deutsche Sammlung von Mikroorganismen GmbH, Braunschweig, Germany) are kindly acknowledged for classifying the rhodococci used in this study. We thank Martien Cohen Stuart (Department of Physical and Colloid Chemistry, Wageningen Agricultural University, Wageningen, The Netherlands) for help with the dynamic light-scattering measurements and Francis Cottaar (Department of Microbiology, Wageningen Agricultural University) for the electron micrographs of strains C2 and C3.

REFERENCES

1. Absolom, D. R., F. V. Lamberti, Z. Policova, W. Zingg, C. J. Van Oss, and A. W. Neumann. 1983. Surface thermodynamics of bacterial adhesion. *Appl. Environ. Microbiol.* **46**:90-97.
2. Bendinger, B., R. M. Kroppenstedt, S. Klatt, and K. Altendorf. 1992. Chemotaxonomic differentiation of coryneform bacteria isolated from biofilters. *Int. J. Syst. Bacteriol.* **42**:474-486.
3. Bendinger, B., H. Rijnaarts, and K. Altendorf. 1991. Physicochemical surface properties of coryneform bacteria isolated from biofilters, p. 399-401. In H. Verachert and W. Verstraete (ed.), International Symposium on Environmental Biotechnology. Royal Flemish Society of Engineers, Antwerp, Belgium.
4. Bendinger, B., H. H. M. Rijnaarts, K. Altendorf, and A. J. B. Zehnder. Physicochemical cell surface and adhesive properties of coryneform bacteria related to the presence and chain length of mycolic acids. *Appl. Environ. Microbiol.*, in press.
5. Bryers, J. D. 1990. Biofilms in biotechnology, p. 733-773. In W. G. Characklis and K. C. Marshall (ed.), *Biofilms*. John Wiley and Sons, Inc., New York.
6. Busscher, H. J., M. H. M. J. C. Uyen, A. J. W. Pelt, A. H. Weerkamp, W. J. Postma, and J. Arends. 1986. Reversibility of adhesion of oral streptococci to solids. *FEMS Microbiol. Lett.* **35**:303-306.
7. Busscher, H. J., A. H. Weerkamp, H. C. van der Mei, A. J. W. Pelt, H. P. de Jong, and J. Arends. 1984. Measurement of the surface free energy of bacterial cell surfaces and its relevance for adhesion. *Appl. Environ. Microbiol.* **48**:980-983.
8. Characklis, W. G. 1990. Microbial fouling, p. 523-584. In W. G. Characklis and K. C. Marshall (ed.), *Biofilms*. John Wiley and Sons, Inc., New York.
9. Dorn, E., M. Hellwig, W. Reineke, and H. J. Knackmuss. 1974. Isolation and characterization of a 3-chlorobenzoate degrading pseudomonad. *Arch. Microbiol.* **99**:61-70.
10. Elimelech, M., and C. R. O'Melia. 1990. Kinetics of deposition of colloidal particles in porous media. *Environ. Sci. Technol.* **24**:1528-1536.
11. Fokkink, L. G. J., A. de Keizer, and J. Lyklema. 1989. Temperature dependence of the electrical double layer on oxides: rutile and hematite. *J. Colloid Interface Sci.* **127**:116-131.
12. Harvey, R. W. 1991. Parameters involved in modeling movement of bacteria in groundwater, p. 89-114. In C. J. Hurst (ed.), *Modeling the environmental fate of microorganisms*. American Society for Microbiology, Washington, D.C.
13. Hiemenz, P. C. 1986. Physical adsorption at the gas-solid interface, p. 489-544. In J. J. Lagowski (ed.), *Principles of colloid and surface chemistry*. Marcel Dekker, Inc., New York.
14. Hiemenz, P. C. 1986. The electrical double layer, p. 677-735. In J. J. Lagowski (ed.), *Principles of colloid and surface chemistry*. Marcel Dekker, Inc., New York.
15. Huysman, F., and W. Verstraete. 1993. Water-facilitated transport of bacteria in unsaturated soil columns: influence of cell surface hydrophobicity and soil properties. *Soil Biol. Biochem.* **25**:83-90.
16. Jang, L. K., P. W. Chang, J. E. Findley, and T. F. Yen. 1983. Selection of bacteria with favorable transport properties through porous rock for application of microbial enhanced oil recovery. *Appl. Environ. Microbiol.* **46**:1066-1072.
17. Levich, V. G. 1962. Convective diffusion in liquids, p. 39-138. In *Physicochemical hydrodynamics*. Prentice-Hall, Inc., Englewood Cliffs, N.J.
18. Lyklema, J. 1991. Transport phenomena in interface and colloid

- science, p. 6.1-6.97. In *Fundamentals of interface and colloid science*, vol. 1. Fundamentals. Academic Press, Ltd., London.
19. Martin, R. E., L. M. Hanna, and E. J. Bouwer. 1991. Determination of bacterial collision efficiencies in a rotating disk system. *Environ. Sci. Technol.* 25:2075-2082.
 20. Neu, T. R., and K. Poralla. 1988. An amphiphilic polysaccharide from an adhesive *Rhodococcus* strain. *FEMS Microbiol. Lett.* 49:389-392.
 21. Norde, W., and E. Rouwendal. 1990. Streaming potential measurements as a tool to study protein adsorption kinetics. *J. Colloid Interface Sci.* 139:169-176.
 22. Pelt, A. W. J., A. H. Weerkamp, M. H. M. J. C. Uyen, H. J. Busscher, H. P. de Jong, and J. Arends. 1985. Adhesion of *Streptococcus sanguis* CH3 to polymers with different surface free energies. *Appl. Environ. Microbiol.* 49:1270-1275.
 23. Pringle, J. H., and M. Fletcher. 1986. Influence of substratum wettability and adsorbed macromolecules on bacterial attachment to surfaces. *Appl. Environ. Microbiol.* 50:431-437.
 24. Provencher, S. W. 1982. A constrained regularization method for inverting data represented by linear algebraic or integral equations. *Comput. Phys. Commun.* 27:213-227.
 25. Provencher, S. W. 1982. Contin: a general purpose constrained regularization program for inverting noisy linear algebraic or integral equations. *Comput. Phys. Commun.* 27:228-242.
 26. Pusey, P. N., and R. J. A. Tough. 1985. Particle interactions, p. 85-102. In R. Pecora (ed.), *Dynamic light scattering: applications to photon correlation spectroscopy*. Plenum, New York.
 27. Quirynen, M., M. Marechal, D. van Steenberghe, H. J. Busscher, and H. C. van der Mei. 1991. The bacterial colonization of intra-oral hard surfaces *in vivo*: influence of surface free energy and surface roughness. *Biofouling* 4:187-198.
 28. Reid, G., H. S. Beg, C. A. K. Preston, and L. A. Hawthorn. 1991. Effect of bacterial, urine and substratum surface tension properties on bacterial adhesion to biomaterial. *Biofouling* 4:171-176.
 29. Rijnaarts, H. H. M., W. Norde, E. J. Bouwer, J. Lyklema, and A. J. B. Zehnder. Unpublished data.
 30. Schraa, G., B. M. Bethe, A. R. W. Van Neerven, W. J. Van den Tweel, E. Van der Wende, and A. J. B. Zehnder. 1987. Degradation of 1,2-dimethylbenzene by *Corynebacterium* strain C125. *Antonie van Leeuwenhoek* 53:159-170.
 31. Schraa, G., M. L. Boone, M. S. Jetten, A. R. W. van Neerven, P. J. Goldberg, and A. J. B. Zehnder. 1986. Degradation of 1,4-dichlorobenzene by *Alcaligenes* sp. strain A175. *Appl. Environ. Microbiol.* 52:1374-1381.
 32. Sikkema, J. S., and J. A. M. de Bont. 1991. Isolation and initial characterization of bacteria growing on tetralin. *Biodegradation* 2:15-23.
 33. Sjollema, J., H. J. Busscher, and A. H. Weerkamp. 1989. Deposition of polystyrene latex particles on polyacrylate in a parallel plate flow cell. *J. Colloid Interface Sci.* 132:382-394.
 34. Sjollema, J., H. J. Busscher, and A. H. Weerkamp. 1989. Experimental systems for studying adhesion of microorganisms to solid surfaces. *J. Microbiol. Methods* 9:79-90.
 35. Sjollema, J., H. J. Busscher, and A. H. Weerkamp. 1990. Deposition of oral streptococci and polystyrene latices onto glass in a parallel plate flow cell. *Biofouling* 1:101-112.
 36. Solari, J. A., G. Huerta, B. Escobar, T. Vargas, R. Badilla-Ohlbaum, and J. Rubio. 1992. Interfacial phenomena affecting the adhesion of *Thiobacillus ferrooxidans* to sulphide mineral surfaces. *Colloids Surf.* 69:159-166.
 37. Stumm, W., and J. J. Morgan. 1981. The solid-solution interface, p. 599-684. In *Aquatic chemistry: an introduction emphasizing chemical equilibria in natural waters*, 2nd ed. John Wiley & Sons, New York.
 38. Trevors, J. T., J. D. van Elsas, L. S. van Overbeek, and M. Starodub. 1990. Transport of a genetically engineered *Pseudomonas fluorescens* strain through a soil microcosm. *Appl. Environ. Microbiol.* 56:401-408.
 39. Updegraff, D. M. 1991. Background and practical applications of microbial ecology, p. 1-20. In C. J. Hurst (ed.), *Modeling the environmental fate of microorganisms*. American Society for Microbiology, Washington, D.C.
 40. Van der Mei, H. C. 1989. Ph. D. thesis. *Materia Technica*, University of Groningen, Groningen, The Netherlands.
 41. Van de Ven, T. G. M. 1989. Particle-wall interactions in colloidal systems, p. 435-505. In R. H. Ottewill and R. L. Rowell (ed.), *Colloidal hydrodynamics*. Academic Press, London.
 42. Van Loosdrecht, M. C. M., J. Lyklema, W. Norde, G. Schraa, and A. J. B. Zehnder. 1987. The role of bacterial cell wall hydrophobicity in adhesion. *Appl. Environ. Microbiol.* 53:1893-1897.
 43. Van Loosdrecht, M. C. M., J. Lyklema, W. Norde, G. Schraa, and A. J. B. Zehnder. 1987. Electrophoretic mobility and hydrophobicity as a measure to predict the initial steps of bacterial adhesion. *Appl. Environ. Microbiol.* 53:1898-1901.
 44. Van Loosdrecht, M. C. M., J. Lyklema, W. Norde, and A. J. B. Zehnder. 1989. Bacterial adhesion: a physicochemical approach. *Microb. Ecol.* 17:1-15.
 45. Van Loosdrecht, M. C. M., W. Norde, J. Lyklema, and A. J. B. Zehnder. 1990. Hydrophobic and electrostatic parameters in bacterial adhesion. *Aquat. Sci.* 52:103-114.
 46. Williams, P. A., and M. J. Worsey. 1976. Ubiquity of plasmids in coding for toluene and xylene metabolism in soil bacteria: evidence for the existence of a new TOL plasmid. *J. Bacteriol.* 125:818-828.
 47. Witholt, B., M. J. de Smet, J. Kingma, J. B. van Beilen, M. Kok, R. G. Lageveen, and G. Eggink. 1990. Bioconversions of aliphatic compounds by *Pseudomonas oleovorans* in multiphase bioreactors: background and economic potential. *Trends Biotechnol.* 8:46-52.
 48. Xia, Z., L. Woo, and T. G. M. van de Ven. 1989. Micro-rheological aspects of adhesion of *Escherichia coli* on glass. *Biorheology* 26:359-375.

Chapter 3

Reversibility and Mechanism of Bacterial Adhesion

Huub H.M. Rijnaarts, Willem Norde, Edward J. Bouwer, Johannes Lyklema and
Alexander J.B. Zehnder

Submitted to Colloids and Surfaces B: Biointerfaces

The reversibility and mechanism of adhesion of various pseudomonads and coryneform bacteria having different hydrophobicities and negative cell surface charges on negatively charged teflon and glass were studied. Adhesion at an ionic strength (I) of 0.1 M was irreversible and corresponded to activation Gibbs energies for detachment ($\Delta_D G^\ddagger$) higher than $5 kT$ for 19 out of 20 combinations of bacterial strains and surfaces. Calculations with the DLVO model revealed the presence of (i) electrostatic barriers too high to be overcome by whole bacterial cells, and (ii) Van der Waals attractions to be negligible for teflon but strong for glass. Two hydrophobic strains adhere irreversibly on glass by strong Van der Waals attraction in a secondary DLVO minimum but detach when the ionic strength is reduced to <0.0001 M. The irreversible adhesion of seven intermediately hydrophobic to hydrophobic strains on teflon appears to be accomplished by cell surface polymers bridging cells and solid. This adhesion persisted after a decrease of I to <0.0001 M. Experiments with one hydrophobic coryneform bacterium on teflon demonstrated that repulsive barriers diminish deposition at lower ionic strength but that $\Delta_D G^\ddagger$ remains $>5 kT$, thus keeping the adhered cells bound. The highest resilience against detachment ($\Delta_D G^\ddagger$) was observed for combinations of hydrophobic cells and hydrophobic surfaces. Deposition and $\Delta_D G^\ddagger$ were influenced by non-hydrophobic binding mechanisms and steric hindrance between the outer cell polymers for more hydrophilic combinations of surfaces and bacteria. The practical implications of these findings are discussed.

Introduction

Many current environmental and technological issues demand a better understanding of the factors controlling the immobilization of microorganisms at

List of frequently used symbols.

A	adhesion in columns (% of applied cells retained)
$A_{bs(w)}$	Hamaker constant for hetero-Van der Waals interaction between bacterium and solid surface across water (J or kT)
c_A	bulk cell concentration during adhesion period (cells m^{-3})
c_b	bulk cell concentration (cells m^{-3})
c_e	cell concentration in effluent from columns (cells m^{-3})
c_o	cell concentration in influent applied to columns (cells m^{-3})
D_e	effective diffusion constant ($m^2 s^{-1}$)
f_{RLI}	fraction of adhered cells resisting desorption at ionic strength <0.0001 M
$G(h)$	Interaction energy between cells and surfaces according to the power law equation B6 (J or kT)
G_m	Energy minimum for interaction between cells and surfaces according to the power law equation B6 (J or kT)
h	separation between cell and solid surface (m)
i	exponent in the power law equation B6
I	ionic strength (M)
I_A, I_D	ionic strength during adhesion and desorption period, respectively (M)
J	flux (cells $m^{-2} s^{-1}$)
J_A, J_D	flux towards and from surface, respectively (cells $m^{-2} s^{-1}$)
$J_{A,o}, J_{D,o}$	uninhibited flux towards ($J_{A,o}$) and from surface ($J_{D,o}$) (cells $m^{-2} s^{-1}$)
n	exponent in the power law equation B6
m_b	mass of the bacterial particle
R_e	effective particle radius (m)
R_{irr}	Irreversibility ratio = Γ_D/Γ_A (-)
t_A, t_D	duration of adhesion and desorption period (s)
u	electrophoretic mobility of bacterial cells ($10^{-8} m^2 V^{-1} s^{-1}$)
Θ_w	contact angle of a drop of water on bacterial lawns or on solid substrata ($^\circ$).
$\Delta G^\circ(h)$	Gibbs free energy of interaction as a function of h (J m^{-2} or kT per particle)
ΔG^\ddagger	activation Gibbs energy (J m^{-2} or kT per particle) for adhesion ($\Delta_A G^\ddagger$) and for detachment ($\Delta_D G^\ddagger$)
Γ	adhesion (cells m^{-2}): adhesion at $t = 0$ (Γ_o) and after fixed adhesion (Γ_A) and desorption (Γ_D) periods
σ	thickness of the compressed cell surface polymer coating (m) where further compression leads to strong steric repulsion according to eq. B1.
ζ	electrokinetic potential (zeta-potential) (V)

solid/liquid interfaces (4, 20, 28, 34, 41). Irreversible adhesion is assumed to be the most significant factor promoting retention and limiting transport of bacteria in natural and man-made environments (18). Despite the importance of adhesion, its reversibility and mechanism are still in dispute. The aim of the present paper is to help to resolve this problem by a systematic analysis of the adhesion reversibility and the interactions between bacteria and solid surfaces.

Definition of reversibility. Basically, the reversibility of any process should be assessed by studying departure and return to equilibrium (23). However, equilibrium often cannot be reached in adhesion experiments: detachment may be slow (38, 48) and long term reversibility tests are generally not suitable since bacteria are biologically active and change their cell-surface properties after longer times (2, 5, 6, 25, 48). Hence, an evaluation of reversibility in terms of the rates of adhesion (J_A) and detachment (J_D), as determined in short term experiments, is more appropriate. In the present study, adhesion is defined as reversible when $J_D \approx J_A$ and as irreversible when $J_D < J_A$.

Interactions in adhesion: activation Gibbs energies for adhesion and detachment. The fluxes J_A and J_D are related to activation Gibbs energies, i.e., $\Delta_A G^\ddagger$ and $\Delta_D G^\ddagger$ for adhesion and detachment, respectively:

$$J_A = J_{A,0} \exp(-\Delta_A G^\ddagger/kT) \quad (1A)$$

$$J_D = J_{D,0} \exp(-\Delta_D G^\ddagger/kT) \quad (1B)$$

(1 $kT = 4 \times 10^{-21}$ J at room temperature).

The activation energies $\Delta_A G^\ddagger$ and $\Delta_D G^\ddagger$ depend on the interactions between the bacterium and the substratum. At any distance h the Gibbs energy due to interactions between cells and surfaces is defined by the balance of the interfacial Gibbs energies (45):

$$\Delta G^\sigma(h) = G_{BS}^\sigma(h) - G_{BL}^\sigma(\infty) - G_{SL}^\sigma(\infty) \quad (2)$$

G^σ is the excess Gibbs energy (in either $J m^{-2}$ or kT per microbial particle) and (∞) indicates infinite separation; the subscript B stands for bacterium, S for

substratum and L for liquid. If the curve $\Delta G^{\circ}(h)$ has a maximum, this maximum leads to activation energies for adhesion ($\Delta_A G^{\ddagger}$) and detachment ($\Delta_D G^{\ddagger}$).

Two important interactions are the Van der Waals attraction and the electrostatic interaction as described by the DLVO (Derjaguin, Landau, Verwey and Overbeek) theory of colloid stability (37, 43, 45, 46). Bacterial cells and most natural and man-made surfaces are negatively charged at neutral pH. Hence, the electrostatic interactions are generally repulsive and increase with increasing negative charge on the bacterial cells and with decreasing ionic strength of the medium (10, 16, 17, 46). On the other hand, non-DLVO interactions influenced by the hydrophobicities of cells and solids have been reported to also contribute to adhesion (5, 6, 13, 14, 25, 26, 32, 42). Moreover, cell-surface macromolecules also play a role. The relative contributions of DLVO and non-DLVO interactions are not yet clear.

Approach. The basic factors that determine the reversibility and mechanism of bacterial adhesion were assessed by investigating various bacteria with varying negative electrokinetic potentials and hydrophobicities. Levels of $\Delta_A G^{\ddagger}$ were determined by measuring deposition in static batch systems where diffusion controls the transport of cells to the substratum (34). The activation energy for detachment ($\Delta_D G^{\ddagger}$) was assessed by studying detachment in batch and column systems under different conditions namely, upon (i) lowering suspended cell concentration c under absence of shear, (ii) lowering c and the ionic strength of the medium under absence of shear, and (iii) lowering c and applying shear. We refer to these as the reversibilities with respect to lowering c (WRC), with respect to lowering I (WRI), and with respect to applying shear (WRS), respectively.

Experimental

Aqueous media, substrata, and bacteria. The following materials were described previously in reference (34): (i) deionized water (MilliQ) and Phosphate Buffered Saline solutions (PBS) with various ionic strengths (I), (ii) the sources and cleaning procedures of the transparent pieces of PFA teflon and glass (9

TABLE 1. Contact angles and electrophoretic mobilities at various ionic strengths (μ) for the bacteria studied.

design- nation	Bacterial strain ^a	Θ_w^b (°)	μ^c (10^{-8} m ² V ⁻¹ s ⁻¹)		
			$I = 0.1$ M	$I = 0.01$ M	$I = 0.001$ M
Coryneform bacteria:					
C1	<i>Arthrobacter</i> sp. DSM 6687	15 (1)	-1.93	-2.91	-3.97
C2	coryneform DSM 6685	29 (1)	-2.01	-2.18	-2.61
C3	<i>Rhodococcus</i> sp. C125	70 (5)	-2.52	-3.34	-3.39
C4	<i>Rhodococcus erythropolis</i> A177	87 (5)	-1.95	-3.15	-3.59
C5	<i>Corynebacterium</i> sp. DSM 6688	89 (1)	-1.39	-2.12	-1.98
C6	<i>Corynebacterium</i> sp. DSM 44016	103 (6)	-2.08	-2.58	-2.51
C7	<i>Gordona</i> sp. 1775/15	115 (5)	-1.23	-2.47	-2.37
C8	<i>Gordona</i> sp. DSM 44015	117 (4)	-1.00	-2.89	-3.09
Pseudomonads:					
P1	<i>Pseudomonas oleovorans</i> ATCC 29347	17 (1)	-1.27	-1.86	-2.11
P2	<i>Pseudomonas fluorescence</i> p62	25 (1)	-0.54	-1.03	-2.25
P3	<i>Pseudomonas</i> sp. strain B13	32 (1)	-0.97	-2.11	-2.31
P4	<i>Pseudomonas putida</i> mt2	40 (4)	-0.59	-1.08	-2.32

^aThe sources of other than DSM or ATCC strains are described by Rijnaarts et al. (34). ^bStandard deviation in Θ_w determined by at least three independent measurements presented in parenthesis. ^cCoefficient of variation in electrophoretic mobility (μ) data obtained from independent duplicate measurements is smaller than 15%.

TABLE 2. Zetapotentials (ζ) of glass and teflon in 0.1, 0.01, and 0.001 M PBS.

Surface	I (M)	ζ (mV) ^a		
		0.1	0.01	0.001
Teflon		-21.3	-42.8	-63.0
Glass		-24.9	-44.8	-78.8

^aCoefficients of variation are less than 5%

mm x 18 mm x 0.1 mm) used for the batch experiments, (iii) the beads, used for column experiments which had radius of $190 \pm 60 \mu\text{m}$ for teflon and $225 \pm 25 \mu\text{m}$ for glass, and (iv) the bacterial strains (Table 1), their sources, cultivation, and preparation.

Physicochemical characterization of bacteria and surfaces. Cell surface hydrophobicity as determined from contact angles of drops of water (Θ_w) placed on dried bacterial lawns and electrophoretic mobilities (u) at values for I of 0.1, 0.01, and 0.001 M were measured according to Rijnaarts et al. (34) and listed in Table 1. Glass is hydrophilic $\Theta_w = 12^\circ \pm 2^\circ$ (mean \pm standard deviation) and teflon is hydrophobic ($\Theta_w = 105^\circ \pm 1^\circ$). The zeta-potentials of these surfaces in 0.1, 0.010, and 0.001 M PBS (Table 2) were calculated from measured streaming potentials (34).

Adhesion and reversibility assays. Adhesion and the reversibilities WRC and WRI were tested employing batch and/or column systems for various combinations of bacteria and surfaces under conditions listed in Table 3. The details of the batch and column experiments are given below.

Batch experiments. Adhesion was assayed in triplicate according to method 1 described in reference (34). Sealed vials with a volume of 9 cm^3 containing a flat piece of either teflon or glass submerged in PBS with the appropriate initial cell concentration were incubated. Subsequently, washing fluid was applied at a flow rate Q of $15 \text{ cm}^3 \text{ min}^{-1}$, that reduced suspended cell

concentration by at least a factor of 150 and at which shear forces are virtually absent. Subsequently, the surfaces were removed from the vial directly and the attached cells enumerated by light microscopy.

Adhesion was studied (i) as a function of adhesion time (t_A) at $c = 1 \times 10^8$ cells cm^{-3} for strains P2 and C4 on teflon (exp. 1, Table 3) and (ii) after $t_A = 4$ h at $c = 5 \times 10^8$ cells cm^{-3} for all bacterium/substratum combinations (exp 2, Table 3)

Adhesion at $I = 0.1$ M and detachment at $I = 0.1$ M (reversibility WRC) and $I = 0.001$ M (reversibility WRI) were investigated as a function of time for strain C3 and teflon in experiment 3 (Table 3). Adhesion from a suspension with $c_b = 6.2 \times 10^7$ cells cm^{-3} and $I = 0.1$ M was monitored for seven hours.

TABLE 3. Experimental systems, combinations of strains and surfaces and conditions applied for the different adhesion and reversibility experiments*

Exp	adhesion or reversibility*	System	Strain/Surface combinations ^b	Ionic Strength ^c	
				I_A (M)	I_D (M)
1	adhesion	batch	P2/T, C4/T	0.1	
2	adhesion	batch	all ^d	0.1	
3	rev. WRC	batch	C3/T	0.1	0.1
3	rev. WRI	batch	C3/T	0.1	0.001
4	rev. WRC	batch	all ^e	0.1	0.1
5	rev. WRI	column	all ^f	0.1	<0.0001
6	rev. WRI	column	C3/T	0.1-0.001	<0.0001

*Reversibility tested with respect to lowering c (WRC) and lowering ionic strength (WRI).

^bThe strain code (Table 1) is separated by "/" from the surface designations G and T for glass and teflon, respectively.

^c I_A and I_D are the ionic strengths applied during adhesion and detachment periods, respectively.

^dAll combinations were tested except the heavily capsulated strain C2 and aggregating strain C7 (34).

^eAll combinations except P4/G and C4/G were tested.

^fThe strains P1 and C7 were excluded since they are mechanically entrapped between the beads in the columns (34).

Detachment was studied after an adhesion period of 1 min at $c_b = 1.0 \times 10^9$ cells cm^{-3} (incubation plus washing spanned 5 min) and after incubation during two hours at $c_b = 6.2 \times 10^7$ cells cm^{-3} . After the adhesion period, the liquid phase was replaced by PBS with an ionic strength of either 0.1 M or 0.001 M. Then, the number of adhered cells was followed as a function of time.

Activation Gibbs energies for adhesion ($\Delta_A G^\ddagger$) were determined by applying eqns. A3 and A4 (appendix A) to the static batch adhesion results using estimates of effective diffusion coefficients (D_e) and radii (R_e) of the cells published previously (34).

The reversibilities WRC (exp. 4, Table 3) were determined for all bacterium/substratum combinations. Two sets of vials, prepared in triplicate, were incubated for four hours at $c_b = 5.0 \times 10^8$ cells cm^{-3} . In one set adhesion was determined immediately after the adhesion period; in the other after an additional four hours of incubation after reducing c_b by at least a factor of 150. The reversibility WRC was quantified in terms of an irreversibility ratio (R_{irr}):

$$R_{irr} = \Gamma_D / \Gamma_A \quad (3)$$

with Γ_A and Γ_D the number of attached cells per cm^2 after the adhesion period and after the detachment period following the adhesion period, respectively. If adhesion of the cells is completely reversible then $R_{irr} = 0$, whereas for $R_{irr} = 1.0$ adhesion is completely irreversible.

Column experiments. Glass columns (diameter, 1.0 cm; length, 10 cm) were packed with beads of teflon or glass and operated as described before (34). Bacterial suspensions in PBS with $l = l_A$ with an OD_{280} value of 0.6 were prepared by diluting samples of the concentrated stock suspensions. The OD_{280} was at least a factor 8 more sensitive to c than the optical density at 550 to 660 nm, which is normally measured. This provided a means to accurately measure c and to keep the fraction of the surface covered with cells $< 15\%$. The resulting suspensions with cell concentration c_0 were applied to the columns. The level of c_0 as measured by OD_{280} was found to be constant throughout the experimental time in all cases. After a fluid volume of 7 to 9

pore volumes had passed through the columns, the influent was switched to cell-free PBS with ionic strength I_A . After flushing with three pore volumes the influent was changed to MilliQ water ($I_D < 0.0001$ M) which was fed for at least three additional pore volumes. In the effluent c_e (OD_{280}) was monitored throughout the application of the different fluids. The adhesion A was defined as a fraction (%) of the applied cells retained on the column matrix,

$$A = (N_i - N_e) / N_i \times 100\% \quad (4)$$

and the reversibility WRI was quantified in terms of the fraction of the adhered cells resisting desorption at an ionic strength < 0.0001 M, f_{RLI} (%):

$$f_{RLI} = \left(1 - \frac{N_{MQ}}{N_i - N_e} \right) \times 100\% \quad (5)$$

Here, N_i , N_e , and N_{MQ} are the numbers of cells fed to the column, not retained by the column, and removed by MilliQ, respectively. Further, N_i is equal to c_0 times the volume of the applied influent suspension. Values of N_e and N_{MQ} were obtained from the areas under the two parts of the breakthrough curves, i.e. the first peak in c corresponding to the application of cell suspension and cell-free PBS (N_e) and the peak after applying MilliQ (N_{MQ}).

The reversibility WRI was tested at $I_A = 0.1$ M for most of the strain/substratum combinations (exp. 5, Table 3). The reversibility WRI was tested at I_A varying between 0.1 M and 0.001 M, for strain C3 and teflon (exp. 6, Table 3).

Reversibility WRS. The reversibility WRS data were taken from previously published work (34). Although shear was applied under standardized conditions, the shear force could not be quantified.

Results

Adhesion and reversibility in batch systems. The adhesion results of exp. 1 are shown in Fig. 1A. The adhesion of strains P2 on teflon increased linearly with $t_A^{1/2}$ and differed insignificantly from purely diffusion-controlled deposition

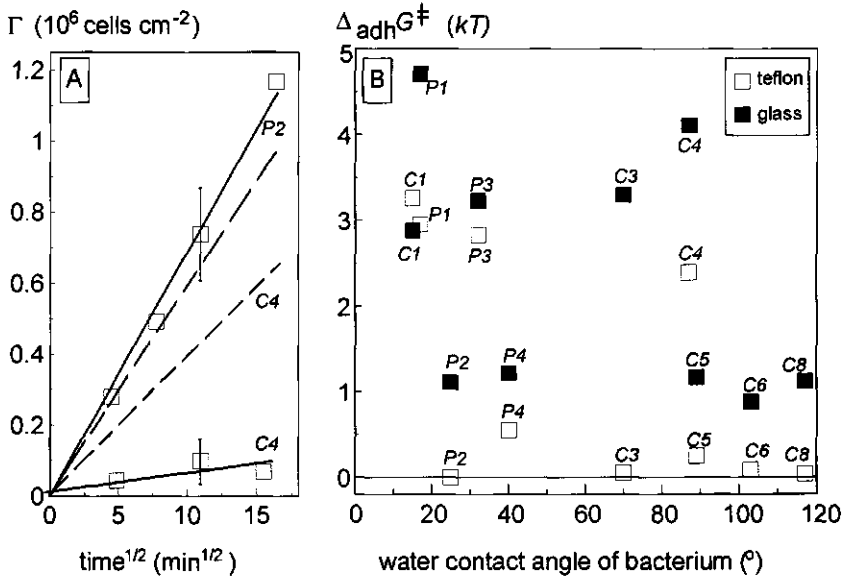


FIG. 1. A. Adhesion Γ of *Ps. fluorescence* p62 (strain P2) and *R. erythropolis* A177 (strain C4) onto teflon as a function of the square root of time (points, solid lines). Adhesion as would occur for deposition purely controlled by diffusion (eqn. A2) is indicated by the dashed lines. Error bars represent standard deviations. B. Activation energy for adhesion ($\Delta_A G^\ddagger$) onto glass and onto teflon derived from adhesion Γ determined in static batch systems. The coefficient of variation in the $\Delta_A G^\ddagger$ -values is $< 15\%$. The designations of the bacterial strains correspond to Table 1.

(eqn. A2). Hence, $\Delta_A G^\ddagger = 0$ (eqns. A3 and A4). The adhesion of strain C4 on teflon is much lower than the number of cells transported, indicating an inhibition of adhesion by cell-solid interactions, i.e., $\Delta_A G^\ddagger > 0$. The deposition results obtained at $I = 0.1$ M for all bacterium/substratum combinations tested (exp. 2) were converted to $\Delta_A G^\ddagger$ values with eq. A3 and plotted as a function of the water contact angle of the bacterial surface (Fig. 1B). The levels of $\Delta_A G^\ddagger$ varied between 0 and 5 kT . They were smaller (higher adhesion) on teflon than on glass, for all but one (C1) strains. Four out of five hydrophobic strains (the exception is strain C4) exhibited $\Delta_A G^\ddagger \approx 0$ with teflon, whereas both high and low $\Delta_A G^\ddagger$ values were observed for less hydrophobic organisms. No obvious relation between cell surface water contact angle and $\Delta_A G^\ddagger$ existed for glass.

Adhesion and the reversibilities WRC and WRI were studied in detail

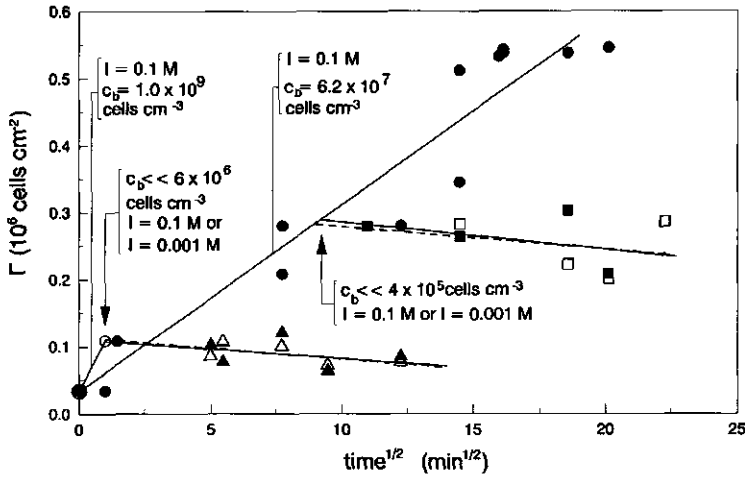


FIG. 2. Kinetics of adhesion and detachment of *Rhodococcus* strain C125 (C3) on PFA-teflon. Adhesion at $I = 0.1$ M (solid lines) at $c_b = 1.0 \times 10^9$ cells cm^{-3} (open circles) and at 6.2×10^7 cells cm^{-3} (filled circles). The desorption periods were started by a reduction in c_b by a factor of at least 150 and indicated by the arrows. Adhesion during the detachment period after initial adhesion periods at 0.1 M of five min (triangles) and two hours (squares) at 0.1 M (closed markers, solid lines) and 0.001 M (open markers, dashed lines).

performing time series batch experiments for strain C3 and teflon. The adhesion at $I = 0.1$ M increased with the square root of time (Fig. 2), and differed insignificantly from diffusion-controlled deposition according to eqn. A2 (not shown), i.e., $\Delta_A G^\ddagger \approx 0$. Detachment after the shorter (1 min, 5 min including washing procedures) and the longer (2 h) initial adhesion period was observed to be insignificant after replacing with medium of high (0.1 M) or low (0.001 M) ionic strength. Almost complete irreversibility WRC and WRI was observed within a few minutes which is strong evidence against a reversible step prior to irreversible attachment.

Reversibility WRC was tested in static batch systems for all strains and both surfaces at an ionic strength of 0.1 M (Fig. 3). Except for the very hydrophilic strain P1 on teflon, values of R_{ir} are insignificantly different from unity as indicated by the standard deviations for the individual values (error bars

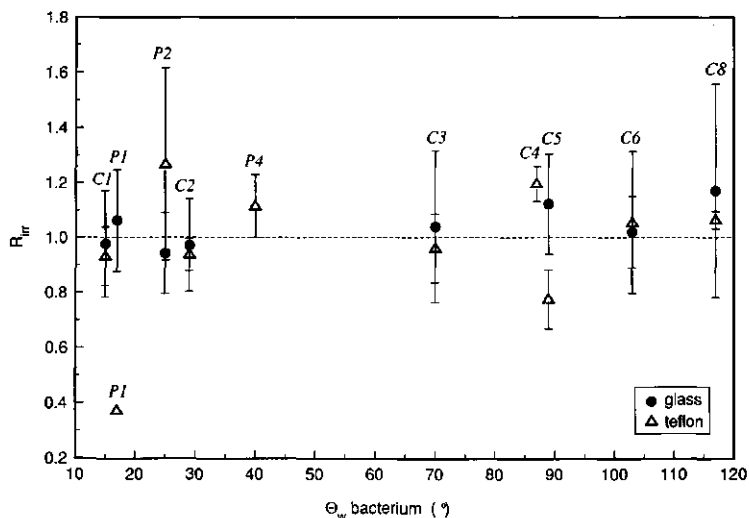


FIG. 3. The irreversibility ratio R_{irr} as a function of cell-surface water contact angle (Θ_w). Error bars indicate standard deviation in single values. The average of R_{irr} for all data is 1.00 (dashed line) (standard deviation = 0.20) and indicates fully irreversible adhesion for all but one case. Labels refer to bacterial strains listed in Table 1.

in Fig. 3) and the mean \pm standard deviation (1.00 ± 0.20) obtained for all data. Hence, adhesion was irreversible WRC in all cases except one. For strain C4 on glass and strain P3 on both glass and teflon, adhesion numbers were very low and the high coefficients of variation in R_{irr} ($> 50\%$) prevented any conclusion with respect to reversibility.

Adhesion and reversibility in column systems. Typical examples of column results (exp. 5) are Figs. 4A and 4B where breakthrough curves obtained for strain C6 on glass and teflon at $I_A = 0.1$ M are shown. The effluent cell concentrations (c_e) are normalized with respect to the initial influent concentration (c_0), i.e. they are given as c_e/c_0 . The irreversibility of adhesion WRC at $I = 0.1$ M was demonstrated by the following observations: (i) the breakthrough of cell suspension and cell-free buffer fronts was not retarded with respect to the average pore fluid velocity, and (ii) the cell concentrations decreased till close to the detection limit upon flushing with cell-free PBS, indicating insignificant desorption. A high reversibility WRI was observed for

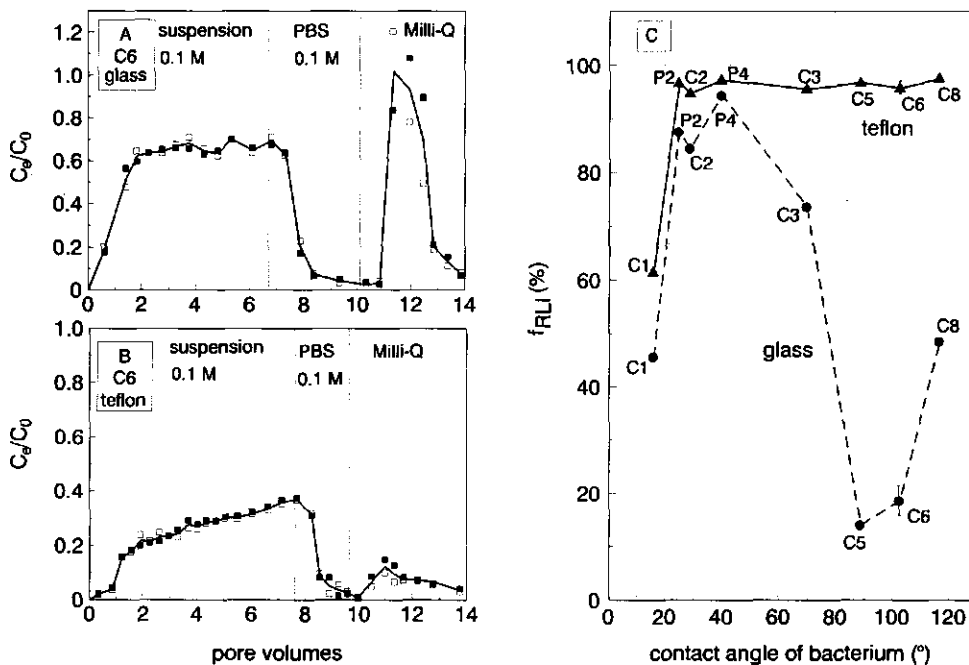


FIG. 4. A. Breakthrough curves for *Corynebacterium* sp. DSM 44016 (strain C6) and columns with glass beads, resulting from sequentially applying bacterial suspensions (0.1 M), cell-free PBS (0.1 M), and MilliQ to the columns. Open and filled markers represent results obtained from duplicate columns. B. Breakthrough curves for strain C6 and columns with tefflon beads. C. Reversibility with respect to lowering f (WRI) for all strain/substratum combinations tested, as a function of cell surface-water contact angle (Θ_w). Reversibility WRI is expressed in terms f_{RLI} , the fraction of the adhered cells that resist desorption at low f . Error bars indicate typical standard deviations for f_{RLI} .

strain C6 on glass: most adhered cells detached upon flushing with MilliQ (Fig. 4A). In contrast, reversibility WRI was very small for tefflon (Fig. 4B). The reversibility WRI (f_{RLI}) is presented as a function of Θ_w in Fig. 4C (exp. 5). For 10 out of the 16 combinations of bacteria and surfaces studied, high values of f_{RLI} (>80 %) indicate irreversibility WRI. For tefflon no significant detachment was found except for the hydrophilic strain C1 for which the fraction desorbed was almost 40%. On glass, reversibility WRI was relatively high for the strains

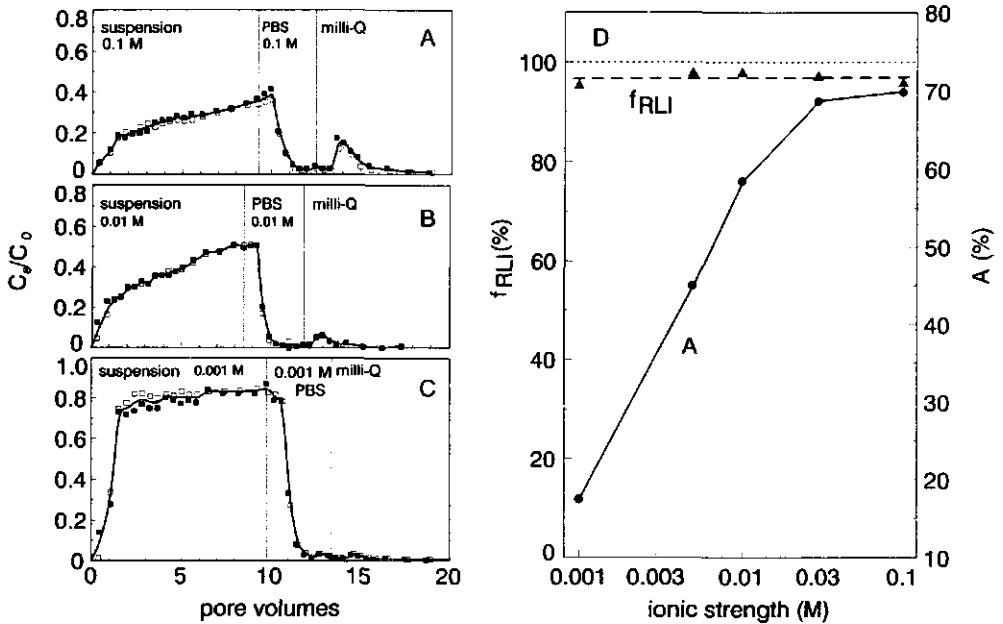


FIG. 5. A to C. Breakthrough curves for *Rhodococcus* strain C125 (C3) and columns with teflon beads, resulting from sequentially applying bacterial suspensions with either an I_A of 0.1 M (A), 0.01 M (B), or 0.001 M (C), cell-free PBS with $I = I_A$, and MilliQ to the columns. Open and filled markers represent results obtained from duplicate columns. D. Column results converted to attachment (A) and resilience of adhered cells against desorption upon lowering ionic strength (f_{RLI}), both plotted as a function of the ionic strength I_A .

C1, C5, C6 and C8 and low for the strains C2, C3, P2 and P4. The adhesion of strains P3 and C4 on glass and teflon is too low for accurate column desorption measurements (results not shown).

For strain C3 and teflon, adhesion and detachment was investigated under increasing electrostatic repulsion by letting I_A range from 0.1 to 0.001 M. Adhesion, as indicated by the levels of c_e/c_0 after breakthrough of the cells (Figs. 5A, 5B, and 5C) and values of A (Fig. 5D), decreased with decreasing values of I . The adhesion was irreversible WRC even in 0.001 M PBS, as was demonstrated by the absence of retardation of cell suspension and cell-free

buffer fronts and the insignificant desorption observed during flushing with cell-free PBS (Figs. 5A, 5B, and 5C). Unlike A , the reversibility WRI (f_{RLI}), remained approximately constant upon reducing I (Fig. 5D).

Discussion

Reversibility WRC. Adhesion appears to be generally irreversible WRC (Figs. 2 and 3). This finding is consistent with the observations of some other authors who also found adhesion to be irreversible when only weak shear forces are applied (5, 25, 32, 36, 38, 48). Furthermore, the results of strain C3 on teflon demonstrated that irreversibility was achieved within a few minutes (Fig. 2). This short time interval excludes the involvement of a rapid *de novo* production of bridging polymers as has been hypothesized to be an important mechanism contributing to irreversibility (2, 5, 6, 25). The strain C3 result is in agreement with direct observation studies on various types of streptococci (38). A cell-substratum contact time of 3 to 10 seconds was sufficient to attain a strong resilience against desorption. After the initial adhesion step, newly produced bridging polymers may strengthen the adhesive bond, but this takes several hours (48).

Reversibility WRC versus reversibility WRS. Van Loosdrecht et al. (44, 45) and others (1, 12) reported adhesion to be predominantly reversible. The discrepancy between our findings and results obtained formerly in our laboratory by van Loosdrecht et al. (45) was further investigated. We performed an additional experiment to compare the method used before (45) with our new procedures with the same materials namely, polystyrene film, strain P2 and PBS with $I = 0.1$ M. Using the former method we obtained $R_{irr} = 0.54 \pm 0.18$ which is similar to the result obtained before, namely $R_{irr} = 0.40$. Using our new method we obtained $R_{irr} = 1.09 \pm 0.14$ which is consistent with the other findings of irreversible adhesion reported here. Hence, the different results obtained by the two procedures has a methodical origin. In the former method, the substrata pass the air-liquid interface several times during washing and upon introducing the substrata in the incubation fluids. This induces shear forces at

close proximity of the air-solid-liquid boundary (34). Strain P2 and other organisms detach under the influence of shear forces (34). Such effects were precluded in our new method (34). Hence, the former data and other results obtained under dynamic washing conditions (1, 12, 19, 21, 25) predominantly reflect the reversibility WRS and not the reversibility WRC. The reversible attachment as found in end-over-end mixed batch systems containing granular solids (46) is also caused by strong shear forces (34).

Assessment of DLVO interactions in adhesion. The mechanism and reversibility of adhesion can only be analyzed by determining the interactions contributing to adhesion. The DLVO contribution to $\Delta G^{\circ}(h)$, which is the sum of the Van der Waals and electrostatic interactions, was calculated for each bacterium-solid-ionic strength combination using equations described elsewhere (31), and previously published values of the particle radius R_0 (34). The required values of the Hamaker constants and zeta-potentials were determined as described below.

The Van der Waals attraction is proportional to the Hamaker constant for interaction between bacterium (b) and surface (s) across water (w) $A_{bs(w)}$, which in turn is determined by the Hamaker constants of the individual materials (22, 46):

$$A_{bs(w)} = (A_s^{1/2} - A_w^{1/2}) (A_b^{1/2} - A_w^{1/2}) \quad (6)$$

Hamaker constants for glass, teflon, polystyrene and water were obtained from Lyklema (22). The range of the Hamaker constant for bacteria (A_b) was deduced from values presented by Nir (29) for interaction across water between vesicles coated with different saccharide-protein mixtures (Table 4). For glass, $A_{bs(w)}$ values are 40 to 50 fold higher than for teflon. The boundary values of the ranges over which $A_{bs(w)}$ varies were used for the DLVO calculations.

Zeta-potentials (ζ) of the cell surface were calculated from the values of u (Table 1) using the Debye-Hückel formula, i.e., $\zeta = f(\kappa a) \eta u / \epsilon E$, where $f(\kappa a)$ is a function of the product of the reciprocal Debye length κ (nm^{-1}) and the radius of the colloidal particle a (nm), η the viscosity of water (N s m^{-2}), ϵ the

TABLE 4. Hamaker constants (in kT)^a for individual materials (A_i) and for hetero-interaction across water ($A_{bs(w)}$).

material	A_i ^b			$A_{bs(w)}$ ^d		
	min	max	average	min	max	average
surface (s): glass	24.1	24.6	24.3	0.86	2.21	1.54
			16.2	0.45	1.12	0.79
			9.33	0.01	0.051	0.035
water (w)	9.09	9.58	9.34	8		
bacteria (b)	12.0 ^c	18.6 ^c	15.3			

^a1 $kT = 4.0 \times 10^{-21}$ J.

^bValues of A_i from Lyklema (22) except for

^cthe Hamaker constants of the bacteria which were determined from data reported by Nir (29); min. and max. denote minimum and maximum value, respectively.

^dValues $A_{bs(w)}$ were calculated from values of A_i using eq. 3.

dielectric permittivity of water ($C V^{-1} m^{-1}$), and E the electric field ($V m^{-1}$). Recently, it has been demonstrated that lines of the applied electric field travel through bacterial cell envelopes (Van der Wal, A., W. Norde, A. J. B. Zehnder, and J. Lyklema. Unpublished data) which implies that $\kappa a \gg 1$ and $f(\kappa a) = 1.5$. The values of ζ for the solid surfaces were listed in Table 2.

With the DLVO model, Gibbs energy barriers of hundreds of kT ($I = 0.1$ M) or more ($I \leq 0.01$ M) separating bacterial cells and substrata were calculated. A bacterial cell as a whole cannot cross such a high repulsive barrier. Hence, the deep minimum, the so called primary minimum, at the substratum-side of the maximum in $\Delta G^{\sigma}(h)$ cannot be reached if the adhesion would proceed according to the DLVO mechanism. At the solution-side of the maximum in $\Delta G^{\sigma}(h)$ there is another minimum, the secondary minimum. At $I = 0.1$ M, the depth of this minimum was calculated to range from -7 to $-70 kT$ and from -0.05 to $-2 kT$ for glass and teflon, respectively. Its depth was smaller than $|0.05| kT$ at $I \leq 0.001$ M for both materials. A secondary minimum must be at least, say, $3 kT$ deep to support adhesion, i.e., to provide

a resilience to detachment high enough to withstand the cell's thermal energy. Hence, according to the DLVO model, only secondary minimum adhesion is possible, and only so for the combination of glass surfaces and high ionic strengths.

DLVO and non-DLVO interactions. Our observations that adhesion on hydrophobic surfaces (teflon) is higher than on glass (Fig. 1B) is similar to the findings of Van Loosdrecht et al. (46) who used polystyrene ($\Theta_w \approx 70^\circ$) as the hydrophobic surface. These authors stated that the effects of hydrophobicity resulted in stronger Van der Waals attraction between bacteria and polystyrene. However, a more detailed analyses reveals that the Van der Waals attraction with polystyrene is weaker than with glass (Table 4). The Hamaker constant $A_{bs(w)}$, and hence the Van der Waals interaction at given distance, decrease in the order glass > polystyrene > teflon. Increasing and stronger adhesion with increasing surface hydrophobicity as found in the present and other studies (5, 34, 43, 46) indicates that non-DLVO interactions must be operating, increasing in strength in the order glass < polystyrene < teflon.

If only DLVO forces would operate, adhesion would not be possible on teflon. Hence, the high adhesion (Fig. 1) and irreversibility WRC (Figs. 2 and 3) observed for teflon is a second evidence for non-DLVO interactions.

Adhesion in the secondary DLVO minimum has two typical characteristics: (i) $\Delta_A G^\ddagger \approx 0$, since the cells arrive in the minimum without passing a barrier, and (ii) reversibility WRI is complete, because the depth of the minimum at low I is insufficient to support adhesion. These conditions are only met for the combinations of strains C5 and C6 with glass where $\Delta_A G^\ddagger$ is very low (Fig. 1B) and reversibility WRI is almost complete (Fig. 4C). Hence, at $I = 0.1$ M, adhesion of strains C5 and C6 on glass occurs in the secondary DLVO minimum, whereas non-DLVO interactions control adhesion for all other bacterium/substratum combinations .

The deposition rate of strain C3 on teflon (Fig. 5D) is greatly diminished ($\Delta_A G^\ddagger$ is increased) upon decreasing the I , which means that here DLVO interactions do inhibit deposition. However, the irreversibility WRI is high and

independent on l , i.e., non-DLVO interactions control detachment even at low l .

Nature of the non-DLVO contribution: steric interactions. Non-DLVO interactions causing irreversible attachment are generally associated with cell-surface macromolecules that penetrate the electrostatic barrier between cells and solids (5, 6, 13, 14, 25, 26, 32, 42). Cell surface macromolecular structures are often found to extend into the surroundings of bacterial cells over distances of up to 100 nm or more (3, 9, 34, 35, 39). Even when these polymer tails are negatively charged they are likely to span the separation between cell and substratum because they are confronted with relatively small electrostatic repulsive barriers (45). Macromolecular-substratum interactions are generally called steric interactions (11). When the macromolecules have a high affinity for the solid they cause strong attractive bridging. On the other hand, a strong steric repulsion may be induced when such macromolecules have a high affinity for water. In practice these two types of steric interactions may both operate and, as they will depend differently on h , the net result may be attractive at some distances and repulsive at other separations.

The relationships between steric interactions and the hydrophobicities of the cells and solids were assessed in terms of the activation energies $\Delta_A G^\ddagger$ and $\Delta_D G^\ddagger$. This approach is superior to the interfacial tension method (1, 7, 47) which is not a viable alternative, primarily because it is an equilibrium-model and therefore does not allow for a kinetic interpretation of adhesion. Furthermore, it ignores the distance dependence of $\Delta G^\sigma(h)$ and contains inappropriate theoretical assumptions as pointed out by others (33, 44).

Activation Gibbs energy for adhesion ($\Delta_A G^\ddagger$) related to cell surface and substratum hydrophobicity. The low $\Delta_A G^\ddagger$ values observed for hydrophobic strains (C5, C6 and C8) indicate bridging on teflon and low steric hindrance on glass. The high barriers retarding deposition of strain C4 on glass and teflon and of strain C3 on glass confirm earlier observations indicating the presence of amphiphilic cell surface polymers diminishing deposition by steric hindrance (34). Steric hindrance is completely outweighed ($\Delta_A G^\ddagger \approx 0$) by bridging for strain C3 on teflon. The strain C3 and C4 results show that in addition to Θ_w

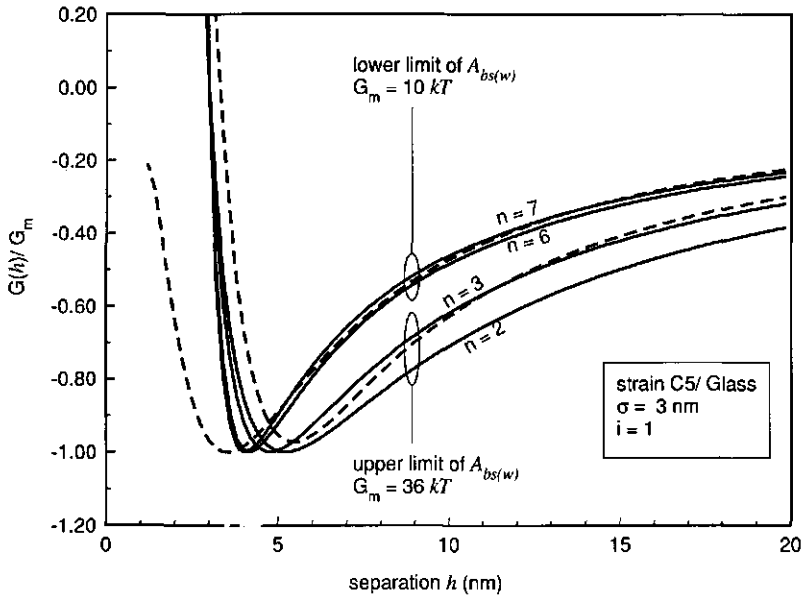


FIG. 6. Example of fitting the power-law equation B6 (solid lines) to the outer part of the DLVO interaction curves (dashed lines) for *Corynebacterium* sp. DSM 6688 (strain C5) on glass at an ionic strength of 0.1 M. The two DLVO curves correspond to the limiting values of the range of the Hamaker constant (Table 4). σ was set at 3 nm, i.e. one half of the length over which the outer polymers protrude from the cell surface. A best match between the power-law and DLVO curves were obtained for $i = 1$ (results for $i \geq 2$ not shown) and $n = 3$ and $n = 6$ for the highest and lowest Hamaker constant (Table 5), respectively. For given values of i and n , the energy minimum is entirely determined by the attractive part of the interaction curve and the value of σ .

other parameters are required to assess the steric interactions between cells and solids. This is further demonstrated by the results of the bacteria with $\Theta_w < 50^\circ$, where $\Delta_A G^\ddagger$ ranges between 0 and 5 kT .

Determination of the activation energy for detachment ($\Delta_D G^\ddagger$). Unlike for other cases, the outer regions of the profiles of interaction between C5 and C6 cells and glass at $I = 0.1$ are well described by the DLVO theory. This makes it possible to derive $\Delta_D G^\ddagger$ from R_{irr} values and estimates of the oscillation frequency of adhered cells k_0 (eq. B5), according to the theory and calculation procedures outlined in appendix B. Values for σ were (arbitrarily) defined as

50% of the distance over which cell surface polymers are extended in the surroundings of the cells. This distance is 6 nm ($\sigma = 3$ nm) and 28 nm ($\sigma = 14$ nm) for strain C5 and C6, respectively (Chapter 5). The power-law curve was calculated with these σ -values and eq. B6 for different values of n and i . These curves were compared with the outer region of $\Delta G^{\ddagger}(h)$ as calculated from DLVO theory. Some of the results obtained for strain C5 are shown as an example in Fig. 6. The best match between the power-law curves and the DLVO profile occurred with $i = 1$ and $n \geq 3$ for both strain C5 and C6 (Fig. 6; Table 5). The values of k_0 are in the order of 10^{-2} to 10^{-3} s $^{-1}$ and combining these with the lower limits (mean value - standard deviation) of the R_{irr} estimates (Fig. 3) yields $\Delta_D G^{\ddagger} \approx 5 kT$ (calculated values range between 4.4 and 6.0 kT , Table 5) as a borderline beyond which adhesion starts to become irreversible. This is consistent with the findings of Xia et al. (48) who estimated $\Delta_D G^{\ddagger}$ to range from 11 to 15 kT for the irreversible adhesion of an *E. coli* strain on glass. Relaxation

TABLE 5. The adhered particle oscillation frequency (k_0) and activation Gibbs energy for detachment ($\Delta_D G^{\ddagger}$) derived from results of fitting the power-law equation B6 to the outer region of the DLVO curves for glass and the strains C5 and C6 for an ionic strength of 0.1 M.

Strain	Hamaker ^a constant (kT)	σ ^b (nm)	Fit results			k_0 (ms $^{-1}$)	$\Delta_D G^{\ddagger}$ ^c (kT)
			$-G_m$ (kT)	i	n		
C5	0.86	3	10	1	3	2.0	4.8
	2.21	3	36	1	6	6.7	6.0
C6	0.86	8	5	1	12	1.4	4.4
	2.21	8	16	1	12	2.8	5.1

^a Calculations were performed for the two limiting values of the range of the Hamaker constant (Table 3).

^b σ was set at 50% of the length over which polymers protrude from the cell surface (Chapter 5).

^c $\Delta_D G^{\ddagger}$ was calculated with eq. B5 using the values of R_{irr} given in Fig. 3.

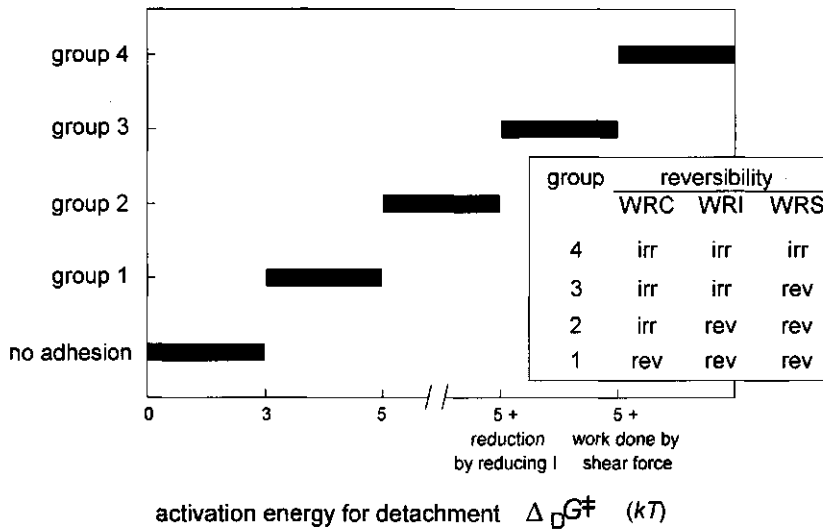


Fig. 7. Classification of the various combinations of bacteria and surfaces into four groups with different $\Delta_D G^\ddagger$ -levels according to their reversibilities WRC, WRI and WRS (insert): irr = irreversible; rev = reversible.

times for detachment of 10 to 30 h were calculated with $(k_0 \exp(-\Delta_D G^\ddagger/kT))^{-1}$ and the results presented in Table 5: the real relaxation times are probably much higher. Hence, equilibrium cannot be reached within an experimental time of a few hours which again shows that assessing the adhesion reversibility requires a kinetic approach.

Significant adhesion will occur when $\Delta_D G^\ddagger > 3 kT$. Consequently, $3 kT < \Delta_D G^\ddagger < 5 kT$ for reversible adhesion WRC such as for strain P1 on teflon (Group 1). Generally, the detachment rate increases when $\Delta_D G^\ddagger$ is reduced. Under our experimental conditions, the increase in the detachment rate becomes significant when $\Delta_D G^\ddagger$ is reduced to a level $< 5 kT$. This occurs upon lowering the ionic strength as a result of the increased electrostatic repulsion for the cases that exhibit reversibility WRI. Adhesion is reversible WRS when the sum of the work that can be done by the shear force and $\Delta_D G^\ddagger$ is smaller than $5 kT$.

TABLE 6. Ranking of relative activation Gibbs energies for detachment ($\Delta_D G^\ddagger$) for the different combinations of bacteria and surfaces with various hydrophobicities, deduced from the reversibilities WRC, WRI and WRS.

surface/strain combinations ranked in the order of increasing $\Delta_D G^\ddagger$			hydrophobicity ^a		reversibility ^b		
group	surface	strain	surface	cells	WRC	WRI	WRS
1	teflon	P1	+	-	R	n.t.	R
2	glass	C1	-	-	I	R	R
	glass	P1	-	-	I	n.t.	R
	teflon	C1	+	-	I	R	R
	glass	C3, C5, C6, C8	-	+	I	R	n.t.
3	glass	C2	-	-/+	I	I	n.t.
	glass	P2	-	-/+	I	I	R
	glass	P4	-	-/+	n.t.	I	R
4	teflon	P2, C2	+	-/+	I	I	n.t.
	teflon	P4	+	-/+	I	I	I
	teflon	C3, C6	+	+	I	I	n.t.
	teflon	C5, C8	+	+	I	I	I

^aHydrophobicity is divided in classes according to values of Θ_w : $\Theta_w < 20^\circ$, (-); $20^\circ \leq \Theta_w \leq 50^\circ$, (-/+); $50^\circ > \Theta_w$, (+).

^b reversibility, (R); irreversibility, (I); n.t. means reversibility not tested.

The various combinations of bacteria and surfaces could be classified into four groups with different $\Delta_D G^\ddagger$ -levels according to their reversibilities WRC, WRI and WRS (Fig. 7). For group 1, all the changes in the system induced desorption. Lowering c , lowering l and shear forces become step-wise ineffective when changing to group 2, group 3 and group 4, respectively.

Hence, $\Delta_p G^\ddagger$ also increases in this order.

Activation Gibbs energy for detachment ($\Delta_p G^\ddagger$) related to cell surface and substratum hydrophobicity. The relative level of $\Delta_p G^\ddagger$ is compared with the hydrophobicity of cells and solids in Table 6. The highest resilience to detachment was found for combinations of hydrophobic cells and hydrophobic substrata (group 4); desorption was never observed, confirming the trend that was reported by others ((5, 43, 46). We infer that adsorption of cell surface polymers by a hydrophobic dehydration mechanism (30) can make the strongest initial adhesive bonds. No clear relation between the resilience against desorption and cell surface and solid hydrophobicity exists among the bacterium/substratum combinations in group 1, 2 and 3 (Table 6). This shows that factors other than hydrophobicity dominate the adhesion for more hydrophilic bacterium/surface combinations. These factors are steric hindrance, strong Van der Waals attraction, and non-hydrophobic polymer adsorption mechanisms (possibly H-bonding or ion-pair interactions (11, 40)).

Implications of the results for control of bacterial adhesion. The results presented in this study show that the reversibility of adhesion can be controlled by varying the surface chemical properties of cells and solid supports and by choosing appropriate hydrodynamic conditions. In mixed bioreactors initial biofilm formation can be enhanced by selecting substrata with a rough surface to obtain local quiescent hydrodynamic conditions as suggested before (8, 34, 45). Employing extremely hydrophilic strains or coupling hydrophobic organisms and hydrophilic substrata provides a means to subsequently immobilize and remobilize bacteria by changing the ionic strength of the medium as was already demonstrated to be possible for non-living colloids (27). In addition, varying the ionic strength of the bulk liquid offers a possibility for further control of bacterial deposition as shown in this study (Figs. 4A, 4C, 5A, 5B, 5C, and 5D) and by others (15, 45). For example, during introduction of bacteria into the subsurface to facilitate bioremediation, a low ionic strength may be advantageous to prevent retention of microorganisms and to allow transport over relatively long distances. At the location of the contamination the cells can be deposited by

increasing I. By using strains with appropriate cell surface properties, adhered cells may be remobilized again upon reducing I. Similar techniques may be used for separation of different microorganisms from microbial samples or for the control of adhesion in biotechnological processes.

Conclusion

The work presented here demonstrates that both steric and DLVO-type interactions are important for the adhesive behaviour of microorganisms in man-made and natural environments. The rate of adhesion is dominated by steric interactions in aqueous media with high ionic strength while at lower ionic strengths the effects of DLVO interactions do enter. Establishment of the relative importance of these two types of interactions under various ionic strength conditions emerges as a major subject for further bacterial adhesion research.

Appendix A

Derivation of the activation energy for adhesion

The flux of adhesion is related to its activation energy:

$$J_A = J_{A,0} \exp(-\Delta_A G^\ddagger/kT) \tag{A1}$$

The initial diffusion rate of cells during adhesion under static conditions is given by ((24, 34):

$$J_{A,0} = c_b (D_c/\pi t)^{1/2} \tag{A2}$$

Substituting eq. A2 into A1 yields upon integration for initial adhesion ($c_b = c_A \approx \text{constant}$; surface coverage < 15%):

$$\Gamma_A = 2 c_b (t_A D_e / \pi)^{1/2} \exp(-\Delta_A G^\ddagger / kT) \quad (\text{A3})$$

Differentiating Γ_A (eq. A4) with respect to $t_A^{1/2}$ yields:

$$\Delta_A G^\ddagger / kT = -\ln \left[\frac{(\pi / D_e)^{1/2}}{2 c_b} \left(\frac{d\Gamma}{dt^{1/2}} \right) \right] \quad (\text{A4})$$

Appendix B

Deduction of the activation energy for detachment

The flux of detachment is related to its activation energy:

$$J_D = J_{D,0} \exp(-\Delta_D G^\ddagger / kT) \quad (\text{B1})$$

Detachment is a first order reaction:

$$J_{D,0} = k_0 \Gamma \quad (\text{B2})$$

with k_0 (s^{-1}) the frequency at which the adhered particles oscillate in the energy minimum. Substituting eq. B2 into B1 yields for detachment at $c_b \approx 0$:

$$J_D = \frac{d\Gamma}{dt_D} = -k_0 \Gamma \exp(-\Delta_D G^\ddagger / kT) \quad (\text{B3})$$

Desorption is preceded by adhesion at $c_b = c_A$, i.e. $\Gamma(t_D = 0) = \Gamma_A$, it follows that

$$\ln \left(\frac{\Gamma(t_D)}{\Gamma_A} \right) = \ln(R_{irr}) = -k_0 t_D \exp(-\Delta_D G^\ddagger / kT) \quad (\text{B4})$$

$$\Delta_D G^\ddagger / kT = \ln \left(\frac{k_0 t_D}{-\ln(R_{irr})} \right) \quad (\text{B5})$$

The oscillation frequency k_0 can be estimated when the cell-solid interactions are known. Adhesion in a minimum implies attraction at greater separation and repulsion at smaller separation. Detailed knowledge of the chemical and physical properties of the coating polymers, required for an exact

determination of the repulsive part, are not (yet) available. However, it is known that repulsion due to compression of the outer polymer layer strongly increases with decreasing distance (11). As a first approximation, we applied an empirical power law accounting for an $r^{-(i+n)}$ steric repulsion and an r^{-i} attraction in a similar way as done for Lennard-Jones type molecular pair-interactions (22):

$$G(h) = f(i, n) \left[\left(\frac{\sigma}{h} \right)^{i+n} + \left(\frac{\sigma}{h} \right)^i \right] \quad (\text{B6})$$

The corresponding curve has a minimum $G(h = h_m) = -G_m$. Strong repulsion results from polymer layer compression at $h \leq \sigma$. Setting $dG(h_m)/dh = 0$ it can be deduced that

$$h_m = \sigma(1 + n/i)^{1/n} \quad (\text{B7})$$

and

$$f(i, n) = G_m \left[\left(\frac{i}{i+n} \right)^{\frac{i+n}{n}} - \left(\frac{i}{i+n} \right)^{\frac{i}{n}} \right]^{-1} \quad (\text{B8})$$

An adhered bacterial particle vibrates around $h = h_m$ with a frequency k_0 depending on the shape of the interaction curve at the minimum (22). For a harmonic oscillation,

$$k_0 = (f/m_b)^{1/2} \quad (\text{B9})$$

The force constant f , defining the force pulling the particle back to position h_m (22), is equivalent to the value of the second derivative of $G(h)$ at the minimum:

$$f = \left(\frac{\partial^2 G}{\partial h^2} \right)_{h=h_m} \quad (\text{B10})$$

Hence,

$$f = f(i,n) \left[\frac{(i+n)(i+n+1)}{\sigma^2} \left(\frac{i}{i+n} \right)^{\frac{i+n+2}{n}} - \frac{i(i+1)}{\sigma^2} \left(\frac{i}{i+n} \right)^{\frac{i+2}{n}} \right] \quad (\text{B11})$$

When σ is known and the attractive part of the interaction can be described by a model, h_m (eq. B7) and f (eq. B11) can be estimated from values of n and i obtained by fitting the power law equation B6 to the outer part of $\Delta G^\sigma(h)$, taking $-G_m = \Delta G^\sigma(h = h_m)$. Substituting f in eq. B9 yields the level of k_0 . Thus, $\Delta_p G^\ddagger$ can be calculated with eq. B5, the experimental values of R_{arr} , and the estimates of k_0 .

References

1. Absolom, D. R., F. V. Lamberti, Z. Policova, W. Zingg, C. J. Van Oss and A. W. Neumann. 1983. Surface thermodynamics of bacterial adhesion. *Appl. Environ. Microbiol.* **46**:90-97.
2. Allison, D. and I. W. Sutherland. 1987. The role of exopolysaccharides in adhesion of freshwater. *J. Gen. Microbiol.* **133**:1319-1327.
3. Beveridge, T. J. and L. L. Graham. 1991. Surface layers of bacteria. *Microbiol. Rev.* **55**:684-705.
4. Bryers, J. D. 1990. Biofilms in biotechnology, p. 733-773. *In* W. G. Characklis and K. C. Marshall (ed.), *Biofilms*, John Wiley & Sons Inc., New York.
5. Busscher, H. J., M. H. M. J. C. Uyen, A. J. W. Pelt, A. H. Weerkamp and J. Arends. 1986. Kinetics of adhesion of the oral bacterium *Streptococcus sanguis* CH# to polymers with different surface energies. *Appl. Environ. Microbiol.* **51**:910-914.
6. Busscher, H. J. and A. H. Weerkamp. 1987. Specific and non-specific interactions in bacterial. *FEMS Microbiol. Rev.* **46**:165-173.
7. Busscher, H. J., A. H. Weerkamp, H. C. van der Mei, A. J. W. Pelt, H. P. de Jong and J. Arends. 1984. Measurement of the surface free energy of bacterial cell surfaces and its relevance for adhesion. *Appl. Environ. Microbiol.* **48**:980-983.
8. Characklis, W. G. 1990. Biofilm processes, p. 193-232. *In* W. G. Characklis and K. C. Marshall (ed.), *Biofilms*, John Wiley and Sons, Inc., New York.
9. De Graaf, F. K. and F. R. Mooi. 1986. The fimbrial adhesins of *E. Coli*. *Advances in Microbial Physiology* **28**:65-145.
10. Dickson, J. R. and K. Koochmaraie. 1989. Cell surface charge characteristics and their relationship to bacterial attachment to meat surfaces. *Appl. Environ. Microbiol.* **55**:832-836.
11. Fler, G. J. and J. M. H. M. Scheutjens. 1993. Modeling Polymer adsorption, steric stabilization and flocculation, p. 209-263. *In* B. Dobias (ed.), *Coagulation and Flocculation*, Marcel Dekker Inc., New York.
12. Fletcher, M. 1977. The effects of culture concentration and age, time and temperature on

- the bacterial attachment to polystyrene. *Can. J. Microbiol.* 23:1-6.
13. Fletcher, M. 1988. Attachment of *Pseudomonas fluorescens* to glass and influence of electrolytes on bacterium-substratum separation distance. *J. Bacteriol.* 170:2027-2030.
 14. Fletcher, M., I. Lessmann and J. M. Loeb. 1991. Bacterial surface adhesives and biofilm matrix polymers of Marine and Freshwater bacteria. *Biofouling* 4:129-140.
 15. Gannon, J., Y. Tan, P. Baveye and M. Alexander. 1991. Effect of sodium chloride on transport of bacteria in saturated aquifer material. *Appl. Environ. Microbiol.* 57:2497-2501.
 16. Gilbert, P., D. J. Evans, E. Evans and I. G. Duguid. 1991. Surface characteristics and adhesion of *Escherichia coli* and *staphylococcus epidermidis*. *J. Appl. Bacteriol.* 71:72-77.
 17. Gordon, A. S. and F. Millero. 1984. Electrolyte effects on attachment of an estuarine bacterium. *Appl. Environ. Microbiol.* 47:495-499.
 18. Harvey, R. W. 1991. Parameters involved in modeling movement of bacteria in groundwater, p. 89-114. *In* C. J. Hurst (ed.), *Modeling the Environmental Fate of Microorganisms*, American Society for Microbiology, Washington D. C.
 19. Hermansson, M. and M. K. C. 1985. Utilization of surface localized substrate by non-adhesive marine bacteria. *Microb. Ecol.* 11:91-105.
 20. Jang, L. K., P. W. Chang, J. E. Findley and T. F. Yen. 1983. Selection of bacteria with favourable transport properties through porous rock for application of microbial enhanced oil recovery. *Appl. Environ. Microbiol.* 46:1066-1072.
 21. Kjelleberg, S. and M. Hermansson. 1984. Starvation induced effects on bacterial surface characteristics. *Appl. Environ. Microbiol.* 48:497-503.
 22. Lyklema, J. 1991. Interactions in interface and colloid science, p. 4.1-4.87. *In* *Fundamentals of Interface and Colloid Science*, Academic Press Ltd., London.
 23. Lyklema, J. 1991. Thermodynamic foundations of interface and colloid science, p. 2.1-2.104. *In* *Fundamentals of Interface and Colloid Science*, Academic Press Ltd., London.
 24. Lyklema, J. 1991. Transport phenomena in interface and colloid science, p. 6.1-6.97. *In* *Interactions in Interface and Colloid Science*, Academic Press Ltd., London.
 25. Marshall, K. C., R. Stout and R. Mitchell. 1971. Mechanisms of the initial events in the sorption of marine bacteria to surfaces. *J. Gen. Microbiol.* 68:337-348.
 26. Marshall, P. A., G. I. Loeb, M. M. Cowan and M. Fletcher. 1989. Response of microbial adhesives and biofilm matrix polymers. *Appl. Environ. Microbiol.* 55:2827-2831.
 27. McDowell-Boyer, L. M. 1992. Chemical mobilization of micron-sized particles in saturated porous media under steady flow conditions. *Environ. Sci. Technol.* 26:586-593.
 28. McDowell-Boyer, L. M., J. R. Hunt and N. Sitar. 1986. Particle transport through porous media. *Water Resources Research* 22:1901-1921.
 29. Nir, S. 1976. Van der Waals interactions between surfaces of biological. *Progr. Surf. Sci.* 8:1-58.
 30. Norde, W., T. Arai and H. Shirahama. 1991. Protein adsorption in model systems. *Biofouling* 4:37-51.
 31. Norde, W. and J. Lyklema. 1989. Protein adsorption and bacterial adhesion to solid surfaces: a colloid chemical approach. *Colloids Surf.* 38:1-13.
 32. Pelt, A. W. J., A. H. Weerkamp, M. H. M. J. C. Uyen, H. J. Busscher, H. P. de Jong and J. Arends. 1985. Adhesion of *Streptococcus sanguis* CH3 to polymers with different surface free energies. *Appl. Environ. Microbiol.* 49:1270-1275.

33. Pethica, B. A. 1980. Microbial and cell adhesion, p. 19-45. *In* J. M. Berkeley , J. M. Lynch, J. Melling , P. R. Rutter and B. Vincent (eds.), Microbial adhesion to surfaces, Ellis Horwood Lim., Chisester, England.
34. Rijnaarts, H. H. M., W. Norde, E. J. Bouwer, J. Lyklema and A. J. B. Zehnder. 1993. Bacterial adhesion under static and dynamic conditions. *Appl. Environ. Microbiol.* **59**:3255-3265.
35. Rosenberg, M., E. A. Bayer, J. Delarea and E. Rosenberg. 1982. Role of thin fimbriae in adherence and growth of *Acinetobacter calcoaceticus* RAG-1 on hexadecane. *Appl. Environ. Microbiol.* **44**:929-937.
36. Rutter, P. R. and R. Leech. 1980. The deposition of *Streptococcus sanguis* NCTC 7868 from flowing suspension. *J. Gen. Microbiol.* **120**:301-307.
37. Rutter, P. R. and B. Vincent. 1984. Physicochemical interactions of the substratum, microorganisms, and the fluid phase, p. 21-38. *In* K. C. Marshall (ed.), Microbial Adhesion and Aggregation, Springer-verlag, Berlin.
38. Sjollema, J., A. H. Weerkamp and H. J. Busscher. 1990. Deposition of oral streptococci and polystyrene latices onto glass in a parallel plate flow cell. *Biofouling* **1**:101-112.
39. Stenström, T. A. and S. Kjelleberg. 1985. Fimbriae mediated non-specific adhesion of *Salmonella typhimurium* to mineral particles. *Arch. Microbiol.* **143**:6-10.
40. Stumm, W. and J. J. Morgan. 1981. The solid-solution interface, p. 599-684. *In* Aquatic chemistry: an introduction emphasizing chemical equilibria in natural waters, John Wiley & Sons, New York.
41. Updegraff, D. M. 1991. Background and practical applications of microbial ecology, p. 1-20. *In* C. J. Hurst (ed.), Modeling the Environmental Fate of Microorganisms, American Society of Microbiology, Washington DC.
42. Uyen, H. M., H. C. van der Mei, A. H. Weerkamp and H. J. Busscher. 1988. Comparison between the adhesion to solid substrata of *Streptococcus mitis* and that of polystyrene particles. *Appl. Environ. Microbiol.* **54**:837-838.
43. Van Loosdrecht, M. C. M., J. Lyklema, W. Norde, G. Schraa and A. J. B. Zehnder. 1987. Electrophoretic mobility and hydrophobicity as a measure to predict the initial steps of bacterial adhesion. *Appl. Environ. Microbiol.* **53**:1898-1901.
44. Van Loosdrecht, M. C. M., J. Lyklema, W. Norde, G. Schraa and A. J. B. Zehnder. 1987. The role of bacterial cell wall hydrophobicity in adhesion. *Appl. Environ. Microbiol.* **53**:1893-1897.
45. Van Loosdrecht, M. C. M., J. Lyklema, W. Norde and A. J. B. Zehnder. 1989. Bacterial adhesion: a physicochemical approach. *Microb. Ecol.* **17**:1-15.
46. Van Loosdrecht, M. C. M., W. Norde, J. Lyklema and A. J. B. Zehnder. 1990. Hydrophobic and electrostatic parameters in bacterial adhesion. *Aquat. Sci.* **52**:103-114.
47. Van Oss, C. J. 1991. The forces involved in bioadhesion to flat surfaces and particles-their determination and relative roles. *Biofouling* **4**:25-35.
48. Xia, Z., L. Woo and T. G. M. Van de Ven. 1989. Microrheological aspects of adhesion of *Escherichia coli* on glass. *Biorheology* **26**:359-375.

Chapter 4

The Isoelectric Point of Bacteria as an Indicator for the Presence of Cell Surface Polymers that Inhibit Adhesion

Huib H.M. Rijnaarts, Willem Norde, Johannes Lyklema and
Alexander J.B. Zehnder

Submitted for publication to Colloids and Surfaces B: Biointerfaces

The use of the isoelectric point (*iep*) of a bacterium as a measure of the ability of bacterial surface polymers to inhibit adhesion was tested. Values of *iep* were compared with literature data on cell wall composition and with adhesion results, obtained at pH 7 and an ionic strength of 0.1 M. The literature data demonstrate that an $iep \leq 2.8$ indicates the presence of significant amounts of cell surface polysaccharides containing negatively charged phosphate and/or carboxyl groups. The experimental results showed that these polymers inhibit adhesion onto both hydrophilic (glass) and hydrophobic (teflon) surfaces. The coryneform *Rhodococcus* strain C125 with an *iep* of 3.0 possesses amphiphilic cell surface components which inhibit adhesion onto glass and promote deposition onto teflon. Bacteria with an $iep \geq 3.2$ appear to be free from polymer coatings that inhibit adhesion. They adhere in high numbers on teflon and in slightly lower amounts onto glass. Our findings therefore indicate that the *iep* is a suitable parameter complementary to hydrophobicity in predicting the affinity of bacterial surface polymers for substrata with different hydrophobicities.

Introduction

Bacterial adhesion at high ionic strength (0.1 M) is mainly determined by steric interactions between the outer cell surface polymers and the substratum (8, 14, 15, 25, 30, 32, 34, 36, 37). Steric interactions can be repulsive thereby

inhibiting the deposition of the bacterium on the substratum or attractive thereby promoting adhesion by cell-substratum bridging (30). The ability of cell surface polymers to inhibit or to promote adhesion is determined by their affinities for the substratum and the aqueous solvent. Although the cell surface hydrophobicity is a major parameter indicating these affinities, other properties are also of importance (10, 16, 17, 30, 31, 40, 41, 42). Van Loosdrecht et al. (40, 42) observed a decrease of adhesion at $I = 0.1$ M (pH = 7) with decreasing (more negative) electrophoretic mobility u of the cells measured at $I = 0.0075$ M and pH = 7. They and others (10, 16, 17) reasoned that this was probably caused by a DLVO-type electrostatic repulsion. However, our previous studies demonstrated that steric interactions rather than DLVO interactions control adhesion at such a high ionic strength (30). Hence, the observed correlation with electrophoretic mobility must ultimately also have a steric origin. In this paper we demonstrate that, in addition to hydrophobicity (as measured by the water contact angle on dried bacterial lawns), the isoelectric point (i_{ep}) of the bacterium is a more appropriate parameter than the electrophoretic mobility u in predicting the steric properties of cell surface polymers and their consequences for cell adhesion.

The i_{ep} of a bacterium is determined by the balance between charging of anionic and cationic acid/base groups in the cell surface, together with some specific adsorption of some ions. It is much more sensitive to the chemical composition of the bacterial surface than u at pH 7 (6, 27). Sulfate groups are rarely reported to occur in bacterial cell surfaces, which leaves the following acid/base couples as the most probable ones to be involved in the charging of microbial surfaces (21): phosphate either in phosphodiester bridges (R-O-HPO₂-O-R\|R-O-PO₂⁻-O-R) as in teichoic acids or at the end of a polymer (R-H₂PO₄\|R-HPO₄⁻) as in phospholipids ($pK_a = 2.1$ (23)), protein-associated COOH/COO⁻ ($2.1 \leq pK_a \leq 2.4$), peptidoglycan-associated COOH/COO⁻ ($pK_a = 2.1$, which is the value for alanine), polysaccharide-associated COOH/COO⁻ ($pK_a = 2.8$, (21)), protonated phosphate (R-HPO₄\|R-PO₄²⁻) ($pK_a = 7.2$), and peptidoglycan or protein-associated ammonium (R-NH₃⁺/R-NH₂) ($9.0 \leq pK_a \leq$

9.8). The interaction between the charged moieties within a polyelectrolyte can result in a pK_a different from that of the isolated group: the pK_a of an anion is increased by anionic-anionic interactions, and reduced by anionic-cationic interactions.

The negative charge of polysaccharides is determined by phosphate and/or carboxyl groups which give these molecules an $iep \leq 2.8$ (18, 21, 23, 29). Peptidoglycan and proteins contain both $COOH/COO^-$ and $-NH_3^+/-NH_2$ groups. Peptidoglycan contains at least one $-NH_3^+/-NH_2$ moiety per three $COOH/COO^-$ groups (4, 33) and should therefore have an iep of >4.0 . However, the interaction between the carboxyl and ammonium groups may reduce its iep below this value. On the other hand, the amount of $-COO^-$ groups may be partially or completely amidated (4, 33) which may strongly increase the iep . Hence, the iep of different types of peptidoglycan may vary over a wide range exceeding 3.0. The iep of proteins is well documented and in general >4.0 .

Values of iep of bacterial cells >3.0 are difficult to interpret. They may reflect mixed contributions of protein- or peptidoglycan-associated COO^- or $-NH_3^+$ and may in principle even result from a combination of NH_3^+ -containing polymers and low pK_a anionic polysaccharides containing phosphate and/or carboxyl groups. Hence, indications for the predominance of a specific chemical cell surface polymer cannot be deduced solely on the basis of iep values greater than about 3.0. In contrast, an $iep \leq 2.8$ does indicate the predominance of a specific type of polymers, namely anionic polysaccharides containing phosphate and/or carboxylic acid groups which have a $pK_a \leq 2.8$. Such anionic polysaccharides can be classified as strong polyelectrolytes; they are known to be able to induce strong steric hindrance (13). Hence, it may well be that the adhesion of bacteria with an $iep \leq 2.8$ is impeded by steric hindrance induced by anionic polysaccharides on their surface. This hypothesis was tested and confirmed in the present study.

Materials and Methods

Aqueous media, solid surfaces, and bacteria. All aqueous media were made with deionized water (MilliQ). Phosphate Buffered Saline solutions (PBS) with various ionic strengths (I) were prepared as described previously (31). Solutions of 0.01 M $\text{HNO}_3/\text{KNO}_3$ with a pH varying between 2 and 4 were prepared by mixing appropriate volumina of 0.01 M HNO_3 and 0.01 M KNO_3 .

Thin transparent pieces of PFA teflon and glass of a size of 9 mm x 18 mm served as solid surfaces. The strains and their denomination used in this paper are listed in Table 1. Sources and preparation procedures are described elsewhere (31).

Hydrophobicity of bacteria and surfaces. Cell surface hydrophobicity was determined from contact angles of drops of water (Θ_w) placed on dried bacterial lawns (31). Values of Θ_w ranged from 15° to 117° . The cell surface hydrophobicity was classified as hydrophilic for $\Theta_w < 20^\circ$, intermediately hydrophobic for $20^\circ \leq \Theta_w \leq 50^\circ$, and hydrophobic for $50^\circ > \Theta_w$. According to this classification, glass is hydrophilic ($\Theta_w = 12^\circ \pm 2^\circ$) and teflon is hydrophobic ($\Theta_w = 105^\circ \pm 1^\circ$).

Electrokinetic characterization of bacteria. Electrophoretic mobilities (u) of the bacteria were measured at an ionic strength of 0.01 M using the method described by Rijnaarts et al. (31). Values of u ranged from -1.03 to $-3.34 \cdot 10^{-8} \text{ m}^2 \text{ V}^{-1} \text{ s}^{-1}$. The isoelectric point (iep) of the bacteria was determined from u -pH plots obtained by measuring u in 0.01 M $\text{HNO}_3/\text{KNO}_3$ solutions of a pH varying between 2 and 4.

Adhesion was studied in static batch systems at an ionic strength of 0.1 M following the method 1 procedures described in ref. (31). For each adhesion data point, sealed vials with a volume of 9 cm^3 containing a piece of surface submerged in PBS were prepared in triplicate and incubated for four hours at room temperature. The initial cell concentration was $5 \times 10^8 \text{ cells cm}^{-3}$. After incubation, a washing procedure was performed to reduce the suspended cell concentration to negligible levels. This procedure was executed in such a way that shear forces were insignificant and adhered cells were kept bound on the

surface in all but one case (P1 on teflon) (30, 31). Subsequently, the surfaces were removed from the vial directly. Attached cells were enumerated by light microscopy. The deposition in these systems is controlled by a diffusive transport mechanism and physicochemical interactions determining the degree of steric inhibition at close proximity of the surface (30). Adhesion data of the

TABLE I. Water contact angles, electrophoretic mobilities ($I = 0.01$ M, $pH = 7$), and isoelectric points ($I = 0.01$ M) for the bacteria studied.

Denomination	Bacterial strain	Θ_w ($^\circ$)	u (10^{-8} $m^2 \cdot V^{-1} \cdot s^{-1}$)	i_{ep}
Coryneform bacteria:				
C1	<i>Arthrobacter</i> sp. DSM 6687	15 (1)	-2.91	1.7
C2	coryneform DSM 6685	29 (1)	-2.18	2.6
C3	<i>Rhodococcus</i> sp. C125	70 (5)	-3.34	3.0
C4	<i>Rhodococcus erythropolis</i> A177	87 (5)	-3.15	2.8
C5	<i>Corynebacterium</i> sp. DSM 6688	89 (1)	-2.12	3.2
C6	<i>Corynebacterium</i> sp. DSM 44016	103 (6)	-2.58	3.8
C7	<i>Gordona</i> sp. 1775/15	115 (5)	-2.47	3.3
C8	<i>Gordona</i> sp. DSM 44015	117 (4)	-2.89	3.4
Pseudomonads:				
P1	<i>Pseudomonas oleovorans</i> ATCC 29347	17 (1)	-1.86	1.7
P2	<i>Pseudomonas fluorescens</i> p62	25 (1)	-1.03	3.6
P3	<i>Pseudomonas</i> sp. strain B13	32 (1)	-2.11	2.2
P4	<i>Pseudomonas putida</i> mt2	40 (4)	-1.08	3.2

The sources of other than DSM or ATCC strains are described by Rijnaarts et al. (31). The standard deviation in Θ_w determined by at least three independent measurements is presented in parenthesis. The coefficient of variation in the electrophoretic mobility (u) data obtained from independent duplicate measurements is smaller than 15%. i_{ep} was measured as explained in Materials and Methods; the possible error made by interpolation ($i_{ep} > 2$) and extrapolation ($i_{ep} < 2$) of the u -pH plots is estimated to be < 0.2 .

strains C2, C7 and C8 were excluded from comparison with iep because the deposition of these strains is affected by either capsular material protruding the hydrodynamic stagnant layer near the surface (C2) or by aggregation (C7 and C8) (31). Hence, their deposition results are affected by factors difficult to quantify and do not reflect the steric inhibition of adhesion.

Results

The values of Θ_w , u (at $I = 0.01$ M and $pH = 7$), and the iep are shown in Table I. There appears to be a genus-specific relation between cell surface hydrophobicity (Θ_w) and iep (Fig. 1) but there is no correlation between u and iep (not shown). Θ_w depends linearly on iep for the coryneform strains but is

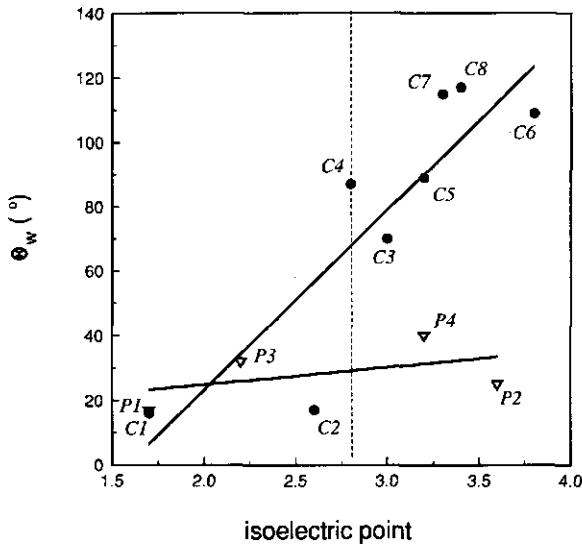


FIG. 1. Correlation between the isoelectric point (iep) and the water contact angle (Θ_w) for coryneform bacteria (closed symbols) and pseudomonads (open symbols). The dashed line indicates the iep value below which anionic polysaccharides appear to occur on a bacterial surface.

adhesion (cells cm^{-2}) at $I = 0.1 \text{ M}$

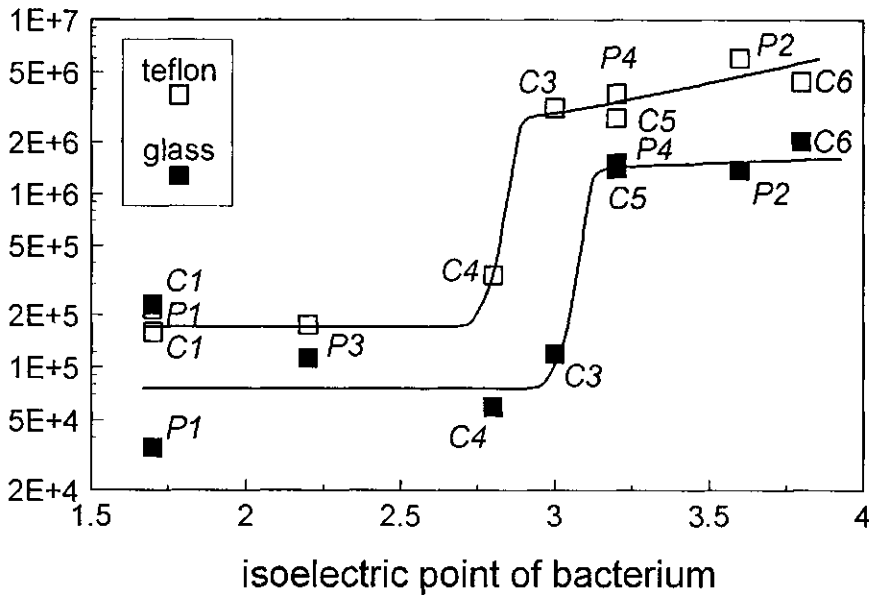


FIG. 2. Adhesion on glass (closed symbols) and on teflon (open symbols) as a function of the isoelectric point (iep). Adhesion was measured in medium with a pH of 7 and an ionic strength of 0.1 M. The deposition of strains with an $iep > 3.1$ on teflon is diffusion controlled and not impeded by steric hindrance (30, 31).

less dependent on iep for the pseudomonads (Fig. 1). The correlation between iep of bacteria and adhesion from medium with $I = 0.1 \text{ M}$ and pH 7 is shown in Fig. 2. Adhesion was low on glass when the $iep \leq 3.0$ and on teflon when the $iep \leq 2.8$. An iep below these values suggests the presence of cell surface polymers that inhibit adhesion by steric hindrance. Strain C3 has an iep of 3.0 which is in the range where transition from low to high adhesion occurs. The deposition of this strain was low on glass but high on teflon. Strains with an $iep \geq 3.2$ deposited in high numbers and therefore seem not to have much polymers on their surface that induced steric hindrance.

Discussion

An $iep \leq 2$ can only result from the presence of phosphate-groups. Among the coryneform strains studied, strain C1 must therefore have significant amounts of phosphate moieties in its cell exterior. This is consistent with the observation that *Arthrobacters* of the nicotianae group, to which the hydrophilic strain C1 belongs (4), possess high amounts of teichoic acids in their cell wall (12). In contrast, mycolic-acid containing strains, like the strains C3 to C8 (4) with a high iep , were never reported to have such compounds (3, 7, 12). A similar relation between a low iep and the presence of teichoic acids was demonstrated by Van der Mei et al. for oral streptococci (38, 39). Phosphate groups, other than those associated to teichoic acids, are found in coryneform or mycobacterial cell walls. They may be associated to lipopolysaccharides (19) or occur in the form of phosphodiester bridges that covalently bind the mycolic acid-arabinogalactan molecules to peptidoglycan muramic acid (22, 24, 26). The contribution of these groups to the iep (and u) of the cells may be much less pronounced as for teichoic acids: the phosphate content in these polymers is much lower than in teichoic acids, and these phosphate moieties are situated deeper in the cell wall because they either bind the lipoarabinomannan to the cell membrane (depth > 10 nm = the minimum cell wall thickness of Gram positive organisms) or the mycoloylarabinogalactan to the peptidoglycan matrix (depth > 2 nm = the approximate minimum length of a mycolic acid associated with arabinogalactan). Strain P1 appears also to have a hydrophilic phosphate-containing outer polymer layer. This is likely due to the sugar chain of the outer membrane lipopolysaccharide, which is hydrophilic and negatively charged by carboxylated and/or phosphorylated sugar units (18, 29).

Our findings are consistent with observations showing that increasing concentrations of phosphate in the microbial cell surface, as deduced from XPS measurements, is paralleled by a decrease (becoming more negative) of u at pH 4 (1, 2, 27) or iep (38, 39). It should be noted that a decrease of u at pH = 4 coincides with a decrease of the iep in most cases.

An iep between 2.0 and 2.8 has been shown to result from a

predominance of cell wall glucuronic acids or other polysaccharide-associated carboxyl groups (21) although contributions of phosphate groups cannot be excluded. The outer part of the several μm thick capsular layer on the surface of strain C2 (31) probably contains carboxylated and/or phosphorylated polysaccharides that lead to an *iep* value of 2.6. Such compounds appear also to occur on the surfaces of strains P3 and C4. This may be caused by the polysaccharide parts of outer membrane-associated lipopolysaccharides for the Gram negative strain P3 (18, 29). For strain C4, the surface polymer may be a lipopolysaccharide: such a compound was found on the surface of a *Rhodococcus erythropolis* strain similar to strain C4 (28). The presence of amphiphilic polymers on the surface of strain C4 is further evidenced by the combination of a high Θ_w value (Table I) and the strongly reduced adhesion on teflon (Fig. 2), and by the tendency of this organism to accumulate at the air-water interface (31).

Strain C3 also appears to have an amphiphilic polymer on its exterior, as shown by previous findings (31) and by the different adhesion behaviour of this organism for glass and teflon: on glass adhesion is sterically impeded while on teflon adhesion is promoted by bridging (30). These cell surface polymers cause an *iep* in the range at which the transition occurs from low to high deposition.

The organisms with an *iep* \geq 3.2 do not seem to be coated with anionic polysaccharides or other compounds that inhibit adhesion. They adhered in high numbers on teflon and slightly lower numbers on glass. Their deposition on teflon is closely related to the number of cells transported to the substratum by diffusion, indicating a complete absence of steric hindrance (30, 31). The peptidoglycan matrix of the exteriors of strain C5 to C8 is partially coated by the non-charged long hydrocarbon tails of mycolic acids (5, 6) and have high *iep* values. The high *iep* of strain P2 and P4 indicates that the outer membrane LPS is covered with a non-polysaccharide layer. Such LPS covering polymers are often found to be proteins for these type of organisms (5, 6, 9, 11, 20, 29, 35).

The prediction of adhesion of cells to substrata at high ionic strengths in

terms of cell surface hydrophobicity (Θ_w) can be greatly improved by also considering the *iep* as a parameter. Levels of Θ_w hardly indicate a difference between the *Pseudomonads* displaying low (P1 and P3) and high (P2 and P4) deposition while the *iep* values give a clear distinction (Figs. 1 and 2). The Θ_w -value is smaller for strain C3 than that for strain C4, and u is more negative for strain C3 than for C4. According to this, strain C4 should adhere better on both glass and teflon than strain C3. However, the opposite was observed (Fig. 2). Moreover, the low adhesion of strain C4 on both test surfaces and strain C3 on glass compared to the other hydrophobic strains C5 and C6, can also not be explained in terms of Θ_w . Hence, the adhesion of the coryneforms C3 and C4 cannot be predicted solely on the basis of Θ_w or u . The use of the *iep* as an additional property of the cell surface appears to resolve these problems. The *iep* is measured on suspended cells and detects polymers on the surface of strain C3 and C4 that are presumably in part hydrophilic (Table I, Fig. 1). The hydrophobicity as measured by Θ_w does not reflect such cell wall constituents, probably as a result of changes in the orientation of the cell surface polymers during dehydration of the bacterial lawn before measuring Θ_w (31). Hence, the *iep* can be used to correct for some of the deviations in Θ_w that result from sample dehydration. In general, the *iep* is an appropriate parameter complementary to cell surface hydrophobicity in predicting the affinity of bacteria to adhere on different substrata. An *iep* \leq 2.8 indicates the presence of significant amounts of anionic-polysaccharides containing negatively charged phosphate and/or carboxylic groups. These polymers sterically inhibit adhesion. In contrast, an *iep* \geq 3.2 indicates the absence of such polymers, and adhesion is not limited by steric interactions.

Disregarding the results of strain C3 and C4, the combination $\Theta_w - u$ predicts adhesion equally well as the combination $\Theta_w - iep$. This explains the correlations between $\Theta_w - u$ and adhesion reported in the literature (10, 16, 40, 42). However, we prefer the combination of $\Theta_w - iep$ because it accounts for all our adhesion results and the *iep* is a more natural parameter to characterize the polymeric chemistry of bacterial cell surfaces than u .

Acknowledgements

Bernd Bendinger is kindly acknowledged for furnishing part of the literature concerning the cell wall composition of coryneform bacteria.

References

1. Amory, D. E., N. Mozes, M. P. Hermesse, A. J. Leonard and P. G. Rouxhet. 1988. Chemical analysis of the surface of microorganisms by X-ray photoelectron spectroscopy. *FEMS Microbiol. Lett.* **49**:107-110.
2. Amory, D. E. and P. G. Rouxhet. 1988. Surface properties of *Saccharomyces cerevisiae* and *Saccharomyces carlsbergensis*: chemical composition, electrostatic charge and hydrophobicity. *Biochim. Biophys. Acta* **938**:61-70.
3. Barksdale, L. and K. S. Kim. 1977. Mycobacterium. *Bacteriological Reviews* **41**:217-372.
4. Bendinger, B., R. M. Kroppenstedt, S. Klatt and K. Altendorf. 1992. Chemotaxonomic differentiation of coryneform bacteria isolated from biofilters. *International Journal of Systematic Bacteriology* **42**:474-486.
5. Bendinger, B., H. Rijnaarts and K. Altendorf. 1991. Physicochemical surface properties of coryneform bacteria isolated from biofilters, p. 399-401. *In* H. Verachtert and W. Verstraete (ed.), *Int. Symp. Environmental Biotechnology*, Royal Flemish Society of Engineers., Antwerpen, Belgium.
6. Bendinger, B., H. H. M. Rijnaarts, K. Altendorf and A. J. B. Zehnder. 1993. Physicochemical cell surface and adhesive properties of coryneform bacteria related to the presence and chain length of mycolic acids. *Appl. Environ. Microbiol.* **59**:3973-3977.
7. Brennan, P. J. 1988. Mycobacterium and other actinomycetes, p. 203-298. *In* C. Ratledge and W. G. Wilkinson (ed.), *Microbial lipids*, Academic Press, London.
8. Busscher, H. J. and A. H. Weerkamp. 1987. Specific and non-specific interactions in bacterial adhesion to solid substrata. *FEMS Microbiol. Rev.* **46**:165-173.
9. DeFlaun, M. F., A. S. Tanzer, A. L. McAteer, B. Marshall and S. B. Levy. 1990. Development of an adhesion assay and characterization of an adhesion deficient mutant of *Pseudomonas fluorescens*. *Appl. Environ. Microbiol.* **56**:112-119.
10. Dickson, J. R. and K. Koohmaraie. 1989. Cell surface charge characteristics and their relationship to bacterial attachment to meat surfaces. *Appl. Environ. Microbiol.* **55**:832-836.
11. Doyle, R. J. and E. M. Sonnenfeld. 1989. Properties of the cell surfaces of pathogenic bacteria. *International Reviews of Cytology* **18**:33-92.
12. Fiedler, F. and M. J. Schäffler. 1988. Teichoic acids in cell walls of strains of the "nicotianae" group of *Arthrobacter*: a chemotaxonomic marker. *Syst. Appl. Microbiol.* **9**:828-836.
13. Fleer, G. J. and J. M. H. M. Scheutjens. 1993. Modeling Polymer adsorption, steric stabilization and flocculation, p. 209-263. *In* B. Dobias (ed.), *Coagulation and Flocculation*, Marcel Dekker Inc., New York.
14. Fletcher, M. 1988. Attachment of *Pseudomonas fluorescens* to glass and influence of electrolytes on bacterium-substratum separation distance. *J. Bacteriol.* **170**:2027-2030.
15. Fletcher, M., I. Lessmann G and J. M. Loeb. 1991. Bacterial surface adhesives and biofilm

- matrix polymers of Marine and Freshwater bacteria. *Biofouling* 4:129-140.
16. Gilbert, P., D. J. Evans, E. Evans and I. G. Duguid. 1991. Surface characteristics and adhesion of *Escherichia coli* and *Staphylococcus epidermidis*. *J. Appl. Bacteriol.* 71:72-77.
 17. Gordon, A. S. and F. Millero. 1984. Electrolyte effects on attachment of an estuarine bacterium. *Appl. Environ. Microbiol.* 47:495-499.
 18. Hancock, I. C. 1991. Microbial cell surface architecture, p. 21-59. *In* N. Mozes, P. S. Handley, H. J. Busscher and P. G. Rouxhet (ed.), *Microbial Cell Surface Analyses: structural and physicochemical methods*, VCH Publishers, Inc., New York.
 19. Hunter, S. W., H. Gaylord and P. J. Brennan. 1986. Structure and antigenicity of the phosphorylated lipopolysaccharide antigens from leprosy and tubercle bacilli. *J. Biol. Chem.* 261:12345-12351.
 20. Irvin, R. T. 1990. Hydrophobic proteins and bacterial fimbriae, p. 137-177. *In* R. J. Doyle and M. Rosenberg (ed.), *Microbial cell surface hydrophobicity*, American Society of Microbiology, Washington DC.
 21. James, A. M. 1991. Charge properties of microbial cell surfaces, p. 223-262. *In* N. Mozes, P. S. Handley, H. J. Busscher and P. G. Rouxhet (ed.), *Microbial cell surface analyses*, VCH Publishers, Inc., New York.
 22. Kanetsuna, F. and G. San Blas. 1970. Chemical analysis of a mycolic acid-arabinogalactan-mucopeptide complex of mycobacterial cell wall. *Biochim. Biophys. Acta* 208:434-443.
 23. Lambert, P. A., I. C. Hancock and J. Baddiley. 1975. The interaction of magnesium ions with teichoic acid. *J. Biochem.* 149:519-524.
 24. Liu, T. H. and E. C. Gotschlich. 1967. Muramic acid phosphate as a component of the mucopeptide of Gram-positive bacteria. *J. Biol. Chem.* 242:471-476.
 25. Marshall, P. A., G. I. Loeb, M. M. Cowan and M. Fletcher. 1989. Response of microbial adhesives and biofilm matrix polymers to chemical treatments as determined by interference reflection microscopy and light section microscopy. *Appl. Environ. Microbiol.* 55:2827-2831.
 26. McNeil, M., M. Daffe and P. J. Brennan. 1990. Evidence for the nature of the link between the arabinogalactan and peptidoglycan of mycobacterial cell walls. *J. Biol. Chem.* 265:18200-18206.
 27. Mozes, N. 1988. On the relation between elemental surface composition of yeasts and bacteria and their charge and hydrophobicity. *Biochim. Biophys. Acta* 745:324-334.
 28. Neu, T. R. and K. Poralla. 1988. An amphiphilic polysaccharide from an adhesive *Rhodococcus* strain. *Fems Microbiol. Letters* 49:389-392.
 29. Nikaido, H. and M. Vaara. 1985. Molecular basis of Bacterial Outer Membrane Permeability. *Microbiol. Rev.* 49:1-24.
 30. Rijnaarts, H. H. M., W. Norde, E. J. Bouwer, J. Lyklema and A. J. B. Zehnder. Reversibility and mechanism of bacterial adhesion. *Colloids Surf. B: Biointerf.*: submitted for publication.
 31. Rijnaarts, H. H. M., W. Norde, E. J. Bouwer, J. Lyklema and A. J. B. Zehnder. 1993. Bacterial adhesion under static and dynamic conditions. *Appl. Environ. Microbiol.* 59:3255-3265.
 32. Rutter, P. R. and B. Vincent. 1988. Attachment mechanisms in the surface growth of microorganisms, p. 87-107. *In* J. M. Bazin and J. I. Prosser (ed.), *CRC Series in Mathematical Models for Microbiology*, CRC Press, Inc., Boca Raton, Florida.

33. Schleifer, K. H. and O. Kandler. 1972. Peptidoglycan types of bacterial cell walls and their taxonomic implications. *Bacteriological Reviews* 36:402-477.
34. Sjollem, J., A. H. Weerkamp and H. J. Busscher. 1990. Deposition of oral streptococci and polystyrene latices onto glass in a parallel plate flow cell. *Biofouling* 1:101-112.
35. Sleytr, U. B. and P. Messner. 1988. Crystalline surface layers on bacteria, p. 160-186. In U. B. Sleytr, P. Messner, D. Pum and M. Sara (ed.), *Crystalline Bacterial Cell Surface Layers*, Springer-Verlag KG, Berlin.
36. Stenström, T. A. and S. Kjelleberg. 1985. Fimbriae mediated non-specific adhesion of *Salmonella typhimurium* to mineral particles. *Arch. Microbiol.* 143:6-10.
37. Uyen, H. M., H. C. van der Mei, A. H. Weerkamp and H. J. Busscher. 1988. Comparison between the adhesion to solid substrata of *Streptococcus mitis* and that of polystyrene particles. *Appl. Environ. Microbiol.* 54:837-838.
38. Van der Mei, H. C., A. J. Leonard, A. H. Weerkamp, P. G. Rouxhet and H. J. Busscher. 1988. Properties of oral streptococci relevant for adherence: zeta potential, surface free energy and elemental composition. *Colloids Surf.* 32:297-305.
39. Van der Mei, H. C., A. J. Leonard, A. H. Weerkamp, P. G. Rouxhet and H. J. Busscher. 1988. Surface properties of streptococcus salivarius HB and non-fibrillar mutants: measurements of zetapotential and elemental composition with x-ray photoelectron spectroscopy. *J. Bacteriol.* 170:2462-2466.
40. Van Loosdrecht, M. C. M., J. Lyklema, W. Norde, G. Schraa and A. J. B. Zehnder. 1987. Electrophoretic mobility and hydrophobicity as a measure to predict the initial steps of bacterial adhesion. *Appl. Environ. Microbiol.* 53:1898-1901.
41. Van Loosdrecht, M. C. M., J. Lyklema, W. Norde and A. J. B. Zehnder. 1989. Bacterial adhesion: a physicochemical approach. *Microb. Ecol.* 17:1-15.
42. Van Loosdrecht, M. C. M., W. Norde, J. Lyklema and A. J. B. Zehnder. 1990. Hydrophobic and electrostatic parameters in bacterial adhesion. *Aquat. Sci.* 52:103-114.

Erratum Chapter 4

Page 58, Line 27-29:

for "protein-associated COOH/COO⁻ ($2.1 \leq pK_a \leq 2.4$), peptidoglycan-associated COOH/COO⁻ ($pK_a = 2.1$, which is the value for alanine)"

read "protein- or peptidoglycan-associated COOH/COO⁻ ($4.0 \leq pK_a \leq 5.0$)".

Page 59, Line 9:

for ">4.0" read ">3.8".

Chapter 5

DLVO and Steric Contributions to Bacterial Deposition in Different Ionic Strength Environments

Huub H.M. Rijnaarts, Willem Norde, Johannes Lyklema and Alexander J.B. Zehnder

Submitted for publication to Environmental Science & Technology

The interactions of eight bacterial strains with teflon and glass in aqueous media with ionic strengths (I) varying between 0.0001 and 1 M were investigated. Two types were considered: (i) those described by the DLVO theory, which comprise Van der Waals attraction and the electrostatic repulsion (bacteria and surfaces are both negatively charged), and (ii) steric interactions between the outer cell surface macromolecules and the substrata. At low ionic strength (<0.001 M), deposition is inhibited by DLVO-type electrostatic repulsion, but at high ionic strength (≥ 0.1 M) it is dominated by steric interactions. The ionic strength at which the transition occurs, is determined by the effective extension of the macromolecules into the solution, which varied between 5 and 100 nm among the bacterial strains studied. The steric interactions either promote deposition by bridging or inhibit adhesion by steric hindrance. Between teflon and hydrophobic bacteria, bridging is generally observed. One bacterial strain has amphiphilic macromolecules on its surface that form bridges with teflon but induce steric hindrance on glass. The presence of hydrophilic anionic polysaccharide coatings on the cells impedes attachment on both glass and teflon substrata. The general conclusion is that the deposition of most bacteria is (i) strongly inhibited by DLVO-type electrostatic repulsion in systems of low ionic strength such as streams and lakes, (ii) controlled by DLVO and/or steric interactions in groundwater and domestic waste waters, and (iii) determined by steric interactions only in saline ecosystems.

Introduction

Control of bacterial adhesion is an important issue in current environmental biotechnology (18, 29, 36). Despite this fact, the relative importance of the various interactions determining the mechanism of adhesion has not been fully resolved yet (28). It is generally accepted that adhesion is determined by the sum of (i) interactions described by the DLVO theory of colloid stability, and (ii) those between the outer cell surface macromolecules reaching into the liquid medium and the substratum (steric interactions) (8, 28, 31, 32, 40, 41). All these interactions contribute to the total Gibbs energy of interaction ΔG° which is a function of the separation h between the cell and the substratum (28). The relative contribution of DLVO and steric interactions to $\Delta G^\circ(h)$ and the ensuing adhesion has not yet been investigated systematically. The present paper contributes to the elucidation of this problem by studying the influence of the ionic strength which affects the electrostatic contributions but not the other.

DLVO interactions. The DLVO contribution is the sum of the Van der Waals attraction and the electrostatic interaction, the latter being almost exclusively repulsive because bacteria and most man-made and natural surfaces are negatively charged at pH 7 (27, 28, 29, 31, 32, 38, 40, 41). The DLVO contribution to $\Delta G^\circ(h)$ can be estimated rather exact, given the electrostatic properties, Hamaker constants, and cell geometry (28). The long range DLVO-type electrostatic repulsion dominates over the Van der Waals attraction at $I \leq 0.001$ M but is outweighed by the Van der Waals attraction at high ionic strength (28).

Steric interactions may be repulsive (steric hindrance) or attractive (bridging) (13, 28). Steric hindrance occurs when the cell-surface macromolecules are hydrophilic and have a low affinity for the substratum, whereas macromolecules with a low solvent- and/or high substratum affinity promote bridging (13). Bridging and/or high adhesion numbers are generally observed for solids and microorganisms that are both relatively hydrophobic (1, 9, 29, 39, 41).

Depending on the ionic strength I of the medium (5, 7, 37),

macromolecular polyelectrolytes may act through electrical and non-electrical interactions on adhesion. Increasing I will reduce all electrostatic (including electrosteric) forces on adhesion but will not influence non-electrical interactions. An ionic strength of at least 0.5 M is needed to suppress all electrostatic interactions (4, 5, 37).

The complexity of steric interactions in bacterial adhesion is illustrated by the observation that they can first inhibit deposition and subsequently cause irreversible binding (28). Furthermore, the steric contribution to $\Delta G^{\circ}(h)$ is difficult to quantify because this requires detailed information on the length, the charge and the chemical nature of the cell surface macromolecules. However, this chemical nature can, to some extent, be inferred from the isoelectric point (i_{ep}) of the bacterium (30), and from the water contact angle Θ_w on dried bacterial lawns (2, 29, 39, 41). These parameters help to distinguish between cell coatings of negatively charged polysaccharides, amphiphilic macromolecules, and non-polysaccharide macromolecules, like lipids and proteins (30). The effective extension of the macromolecules is one of the topics discussed in the present paper.

Experimental establishment of interactions. The interactions in adhesion are usually determined by measuring the activation energy of adhesion ΔG^{\ddagger} , which is related to the adhesion efficiency α according to $\alpha = \exp(-\Delta G^{\ddagger}/kT)$. The adhesion efficiency α is the probability for a (bacterial) particle to adhere upon arrival at close proximity of a substratum which may be a macroscopic solid surface (23, 24, 28, 33), another suspended particle during flocculation (35), or a grain of a porous medium (12, 22).

Relative importance of DLVO and steric interactions at various ionic strengths. At high ionic strength (≥ 0.1 M), the rate of bacterial deposition is dominated by steric interactions whereas at lower ionic strength electrostatic repulsion inhibits deposition (11, 15, 16, 22, 23, 28, 34). The ionic strength at which the transition occurs is determined by the range and magnitude of the steric interaction. The main objective of the present paper is to determine these two steric properties and in this way to assess the relative importance of steric

and DLVO contributions in different ionic strength environments.

Experimental

Aqueous media, solid surfaces and bacteria. Sources and preparative procedures of the following materials were described before (29): Phosphate Buffered Saline solutions (PBS) with various ionic strengths (I), thin transparent pieces of PFA teflon and glass of a size of 9 mm x 18 mm, and the bacterial strains listed in Table 1.

Cell surface polymer composition. The isoelectric points (iep) of the cells and their hydrophobicities as measured by contact angles of drops of water (Θ_w) placed on dried bacterial lawns, and the polymer composition tentatively inferred from these parameters, were taken from a previous report (30) and summarized in Table 1.

Transmission electron micrographs of cross-sections of cells of strains C5 and C6 were made to examine their cell surface polymer structure. The specimen were prepared and negatively stained with ruthenium red and uranyl acetate according to the method of Handley (17).

Hydrophobicity of the substrata. Glass is hydrophilic ($\Theta_w = 12^\circ \pm 2^\circ$) and teflon is hydrophobic ($\Theta_w = 105^\circ \pm 1^\circ$) (29).

Electrokinetic characterization of bacteria and surfaces. Electrophoretic mobilities (u) of the bacteria and streaming potentials of the surfaces were measured according to Rijnaarts et al. (29) in PBS with ionic strengths varying between 0.1 and 0.001 M. Values of u at $I = 0.01$ M ranged from -1.03 to $-3.34 \cdot 10^{-8} \text{ m}^2 \text{ V}^{-1} \text{ s}^{-1}$. The ζ -potential for the bacterial surface (ζ_b) was calculated using the Debye-Hückel formula (28) and for the substratum (ζ_s) from streaming potential measurements using equations described elsewhere (29). The electrokinetic data were analyzed with the capacitor model described in the Appendix. The purpose of this was to reliably extrapolate to ionic strengths of 1 M and/or 0.0001 M where electrokinetic measurements are practically not feasible.

Activation Gibbs energies for adhesion (ΔG^\ddagger) were obtained from static

TABLE 1. Designation, water contact angle Θ_w , isoelectric point *iep* (*I* = 0.01 M), and the proposed type of cell surface polymer, for the bacteria studied.

Strain	Other designation ^a	Θ_w ^b (°)	<i>iep</i> ^c	type of polymer ^d
Coryneform bacteria:				
C1	<i>Arthrobacter</i> sp. DSM 6687	15 (1)	1.7	AP
C2	coryneform DSM 6685	29 (1)	2.6	AP
C3	<i>Rhodococcus</i> sp. C125	70 (5)	3.0	AMPH
C4	<i>Rhodococcus erythropolis</i> A177	87 (5)	2.8	AMPH
C5	<i>Corynebacterium</i> sp. DSM 6688	89 (1)	3.2	NP
C6	<i>Corynebacterium</i> sp. DSM 44016	103 (6)	3.8	NP
C7	<i>Gordona</i> sp. 1775/15	115 (5)	3.3	NP
C8	<i>Gordona</i> sp. DSM 44015	117 (4)	3.4	NP
Pseudomonads:				
P1	<i>Pseudomonas oleovorans</i> ATCC 29347	17 (1)	1.7	AP
P2	<i>Pseudomonas fluorescens</i> p62	25 (1)	3.6	NP
P3	<i>Pseudomonas</i> sp. strain B13	32 (1)	2.2	AP
P4	<i>Pseudomonas putida</i> mt2	40 (4)	3.2	NP

^aThe sources of organisms other than DSM or ATCC strains are described by Rijnaarts et al. (29).

^bStandard deviation in Θ_w determined by at least three independent measurements presented in parenthesis.

^cStandard error in values of *iep* is 0.2.

^d The types of cell surface polymer were deduced from *iep* and Θ_w values, and literature data on cell wall composition, in a previous study (30). These macromolecules and the corresponding *iep* and Θ_w ranges are: anionic polysaccharides (AP), with *iep* \leq 2.8 and $\Theta_w \leq 32^\circ$; amphiphilic compounds (AMPH), most likely hydrophobic polysaccharides, with $2.8 \leq iep \leq 3.0$ and $70^\circ \leq \Theta_w \leq 87^\circ$; non-polysaccharide compounds (NP), which are probably proteins ($25^\circ \leq \Theta_w \leq 40^\circ$) or lipids ($89^\circ \leq \Theta_w \leq 117^\circ$) having an *iep* ≥ 3.2 .

deposition experiments at ionic strengths varying between 0.0001 M and 1 M following the method 1 tested and described in reference (29). For each adhesion data point, sealed vials with a volume of 9 cm³ containing a piece of surface submerged in PBS were prepared in triplicate and incubated for four hours at room temperature. The initial concentration c_b was 5×10^8 cells cm⁻³. After incubation, washing procedures were performed which reduced the suspended cell concentration by at least a factor of 150 and at which shear forces are virtually avoided. These procedures also kept adhered cells for all but one (strain P1/teflon) cases irreversibly bound on the surfaces (28, 29). Subsequently, the surfaces were removed from the vial directly. Adhesion Γ (cells m⁻²) was determined by counting attached cells under a light microscope. ΔG^\ddagger can be calculated from Γ and previously published values of the effective diffusion constant D_e of the cells (29), according to (28):

$$\Delta G^\ddagger/kT = \ln[2c_b(tD_e/m)^{1/2}/\Gamma] \quad (1)$$

where k (J K⁻¹) is Boltzmann's constant, T (K) is the absolute temperature and t (s) is the incubation time.

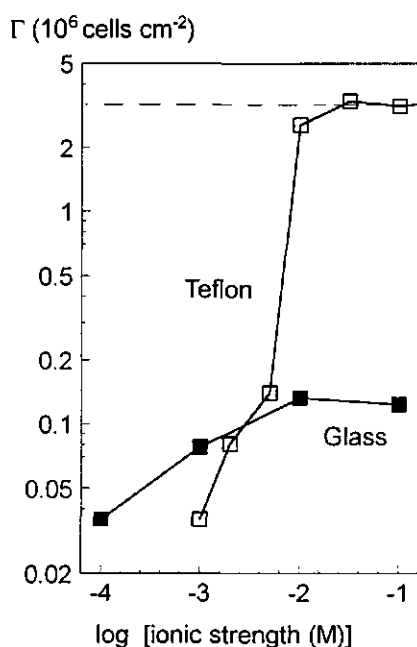


FIG. 1. The deposition of strain C3 (*Rhodococcus* C125) onto Teflon and glass as a function of the ionic strength I of the medium. The long-dashed line indicates the deposition level expected for purely diffusive transport of cells to the substratum.

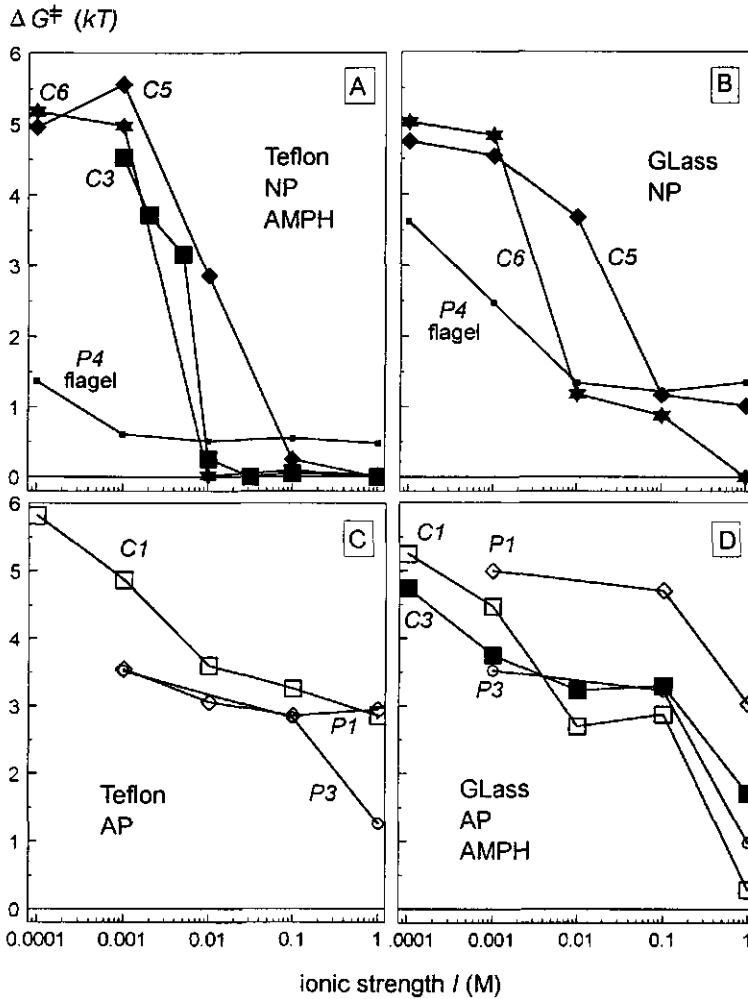
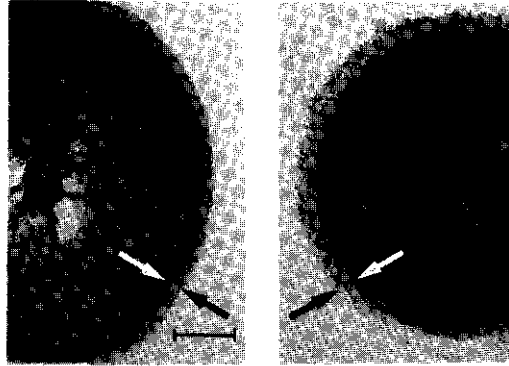


FIG. 2. Activation energy of adhesion ΔG^\ddagger , derived from deposition experiments for the various bacteria (Table 1) on teflon and glass, as a function of the ionic strength I of the medium. The abbreviations indicate the following types of cell coatings (Table 1): AP, anionic polysaccharides; AMPH, amphiphilic compounds, most likely amphiphilic polysaccharides in combination with lipids; NP, non-polysaccharide compounds such as proteins or lipids.

Results

Activation energy for adhesion ΔG^\ddagger as a function of the ionic strength
 Adhesion of strain C3 on the two test substrata is shown as a function of I in Fig. 1. The deposition on teflon at $I > 0.01$ M was diffusion-limited and not

FIG. 3. Transmission electron micrographs of thin sections of the strains C5 (left) and C6 (right), negatively stained with uranyl acetate and ruthenium red: bar = 150 nm; white arrow indicates cytoplasmic membrane; black arrow indicates cell exterior. The macromolecular matrix outside the cytoplasmic membrane is about 30 nm for strain C5 and approximately 50 nm for strain C6.



inhibited by any repulsion (Fig. 1). Reducing I to values < 0.01 M resulted in a strongly diminished adhesion. The deposition of this organism on glass levels off at $I > 0.01$ M. The inhibition of adhesion increased with decreasing I at $I < 0.01$ M.

The adhesion data for the strains C1, C3, C5, C6, P1, P3, and P4 with teflon and glass, were converted to activation energies ΔG^\ddagger . These indicate the degree of inhibition and makes the results of different species comparable. There was a great variation in the $\Delta G^\ddagger/I$ dependency among the different strain/substratum combinations tested (Figs. 2A to 2D). The activation energy ΔG^\ddagger varied between 0 and 5 kT at $I = 0.1$ M, and increased for the various cell-coating/substratum combinations in the following order: NP or AMPH/teflon $<$ NP/glass $<$ AP/teflon $<$ AP or AMPH/glass (explanation of abbreviations in Table 1). The ionic strength below which ΔG^\ddagger further increased varied between 0.1 M and 0.001 M among the different strain/substratum combinations studied (Figs. 2A to 2D). The pseudomonad P4 possesses a non-polysaccharide surface and a flagellum. For this organism and teflon, a rather low ionic strength (< 0.001 M) was needed to attain an increase in ΔG^\ddagger (Fig. 2A). Under a microscope it was observed that, at low ionic strength, some of the attached cells of this strain on both test substrata made fierce rotating movements. Apparently, some of the cells attached by their flagella. Attached and suspended cells

displayed no motility at higher ionic strength.

The level of ΔG^\ddagger significantly decreases upon increasing I from 0.1 to 1 M for cells coated with anionic polysaccharides (C1, P1, P3) in combination with glass or teflon (Figs. 2C and 2D), and for amphiphilic (C3) or hydrophobic (C6) cell surface layers in combination with glass (Figs. 2B and 2D).

Electron microscopy results. The EM micrographs (Figs. 3A and 3B) indicate a difference in the extension of cell surface macromolecules between strain C5 and C6. The thickness of the polymer matrix outside the cytoplasmic membrane is 30 nm for strain C5 and 50 nm for strain C6.

Electrokinetic results. These are presented and discussed in the Appendix.

Discussion

Establishment of the DLVO contribution to $\Delta G^\ddagger(h)$. The DLVO contribution to $\Delta G^\ddagger(h)$ was calculated for each bacterium-solid-ionic strength

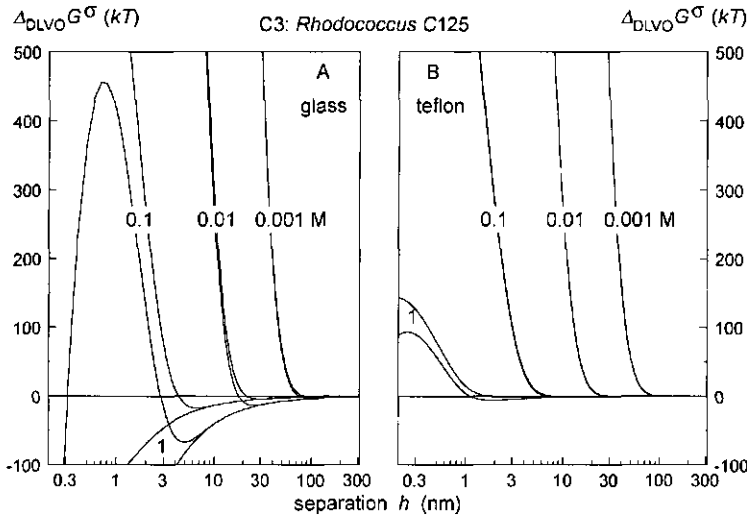
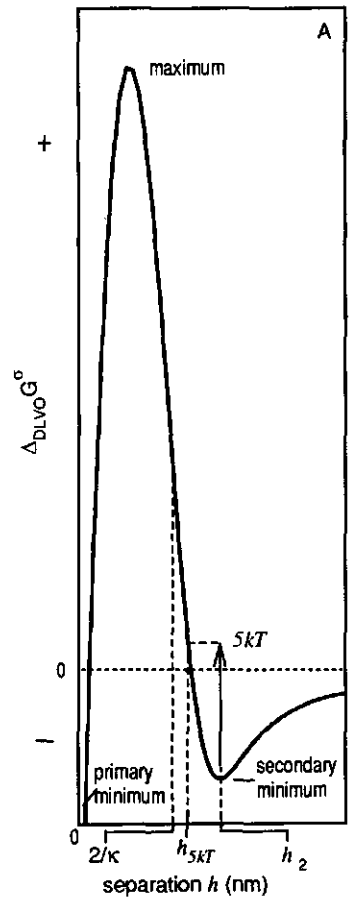
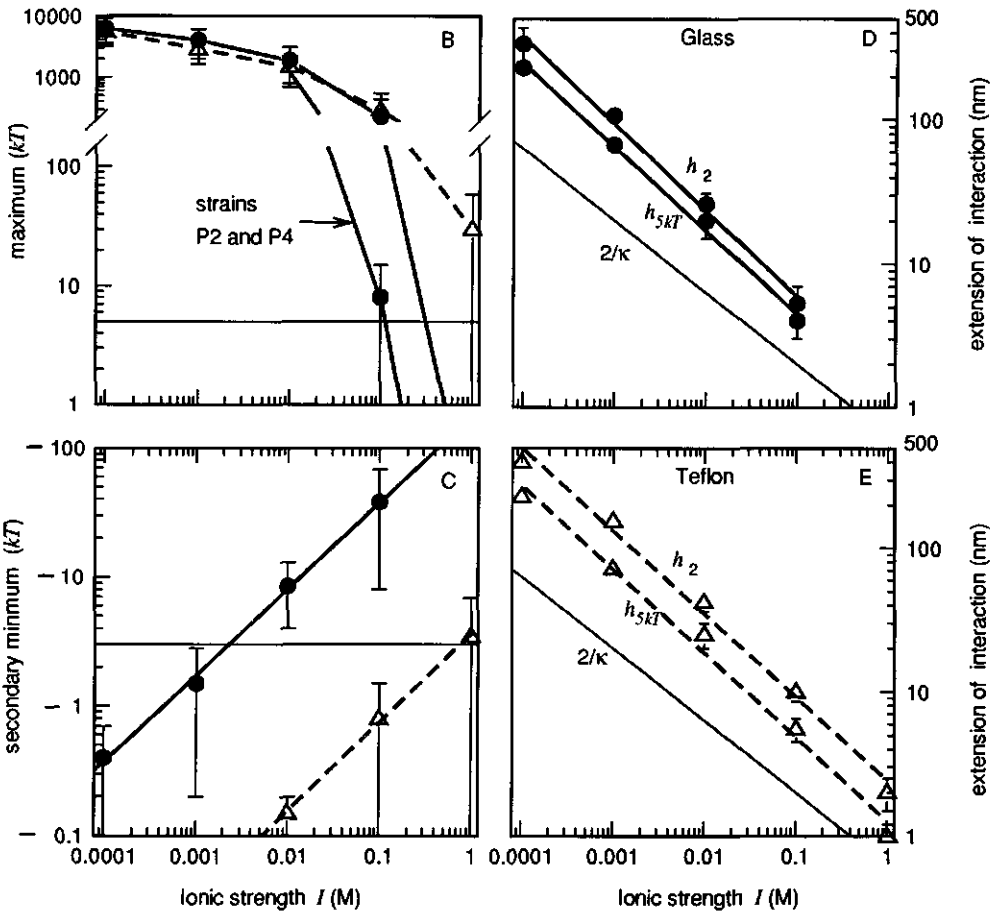


FIG. 4. The DLVO contribution to $\Delta G^\ddagger(h)$ calculated for the combination of *Rhodococcus* strain C125 (strain C3, Table 1) with glass (A) and teflon (B) at different ionic strengths using the extremes of the range for the Hamaker constant (28): $3.4 \times 10^{-21} \text{ J} \leq A_{bs(w)} \leq 8.8 \times 10^{-21} \text{ J}$ for glass and $7.2 \times 10^{-23} \text{ J} \leq A_{bs(w)} \leq 2.0 \times 10^{-22} \text{ J}$ for teflon. The lower, most negative, set of curves corresponds to the highest value of $A_{bs(w)}$ in both figures A and B. The maxima of the curves at $I \leq 0.1 \text{ M}$ (not shown) are hundreds to thousands of kT high.

FIG. 5. Summary of the results of the DLVO contribution to $\Delta G^{\circ}(h)$ for combinations of various bacterial strains with glass (closed circles, solid lines) and teflon (open triangles, dashed lines) as a function of the ionic strength. The error bars indicate the summed variation between the different bacteria and the uncertainty in the Hamaker constant $A_{bs(w)}$. **A. A typical DLVO-curve.** Maximum, minima and extension (h_2 , h_{5kT} and $2/\kappa$; see text) of the DLVO interaction. **B. The height of the DLVO maximum.** The results of the strains P2 and P4 at $I \geq 0.01$ M, are plotted separately because of extremely low ζ values. The horizontal line demarcates the critical barrier height ($5 kT$, (28)) below which, according to the DLVO model, significant primary minimum deposition will occur. **C. The depth of the secondary minimum.** The horizontal line at $3 kT$ separates the cases for which adhesion will not be possible according to the DLVO model (below the line), from cases that allow secondary minimum adhesion (above the line) (28). **D and E.** Extension of the DLVO contribution. The level of h_2 , h_{5kT} and $2/\kappa$ as a function of I for glass (D) and teflon (E).



combination studied, using the measured or extrapolated values of the ζ -potentials for the bacterial (ζ_b) and solid (ζ_s) surface (Appendix A), the boundaries of the interval over which the Hamaker constant $A_{bs(w)}$ varies (28), and estimates of the effective radius R_e of the cells (29). Typical examples of the DLVO modeling results are the curves of strain C3 (Figs. 4A and 4B). The differences found between glass and teflon reflect the influence of the Hamaker constant which is approximately 45 fold higher on glass than on teflon (28). According to the DLVO-contribution (Fig. 5A), the ionic strengths above which



adhesion becomes possible, either by suppression of repulsive electrostatic Gibbs energy barriers allowing primary minimum adhesion, or by the formation of a secondary minimum, are different between glass and teflon. Primary minimum adhesion can occur for glass at $I > 0.1$ M while for most bacteria and teflon this is still not possible at $I = 1$ M (Fig. 5B). A significant secondary DLVO minimum (i.e. deeper than $3 kT$ (28)) exists for combinations of most bacteria, glass and ionic strengths > 0.002 M and for most bacteria combined with teflon and levels of $I \geq 0.8$ M (Fig. 5C). Such a minimum does in no case

exist for glass at $I < 0.001$ M and for teflon at $I < 0.3$ M. Hence, if interaction would only be of the DLVO-type, the ionic strength below which adhesion would generally not be possible because of a too high level of ΔG^\ddagger , is 0.001 M for glass and 0.3 M for teflon.

DLVO versus steric interactions at low ionic strength. At low ionic strength, say < 0.001 M, the DLVO interactions are strongly repulsive (Figs. 4A, 4B, and 5B). However, the inhibition of deposition (Figs. 2A to 2D) is not as strong as predicted by the high DLVO barriers of thousands of kT (Fig. 5B); instead ΔG^\ddagger values of about $5 kT$ are measured (Figs. 2A to 2D). This is probably caused by steric interactions. The effective range of the DLVO interactions falls between h_2 , the position of the secondary minimum, and h_{5kT} , the position where $\Delta_{DLVO}G^\circ - \Delta G^\circ(h_2)$ equals $5kT$, the maximum observed ΔG^\ddagger -value (Figs. 5D and 5E). At $I < 0.001$ M, this range is greater than 100 nm in all cases. Very long polymer tails are needed to bridge these separations and cause irreversible attachment (28). Only strain P4 on teflon (Fig. 5B) is able to bridge such long cell-substratum separations rather efficiently, probably by its flagellum. These results lead to the conclusion that in general DLVO-type electrostatic repulsion is the dominant interaction at low I and that cell surface macromolecules may have a secondary influence on adhesion.

It should be noted that the effective range of the DLVO interactions as characterized by h_{5kT} is about the same order but three to five fold higher than $2/\kappa$ (nm) which is usually taken as a first estimate of the separation at which a significant double-layer overlap occurs (Figs. 5D and 5E).

Transition from DLVO to steric interactions: range (λ) and magnitude ($\Delta_s G^\ddagger$) of steric interactions. The dependency of ΔG^\ddagger at $I = 0.1$ M on the type of cell coating (Figs. 2A-D) confirmed previously reported observations (28) that steric interactions control adhesion at this ionic strength. The activation energy $\Delta_s G^\ddagger$ for adhesion due to steric interaction is insensitive to I at ionic strengths ≤ 0.1 M, even in case of electrosteric contributions (4, 5, 6). On the other hand, a decrease of $\Delta_s G^\ddagger$ when exceeding $I = 0.5$ M indicates a suppression of electrosteric effects. The value of $\Delta_s G^\ddagger$ is the resultant of steric and Van der

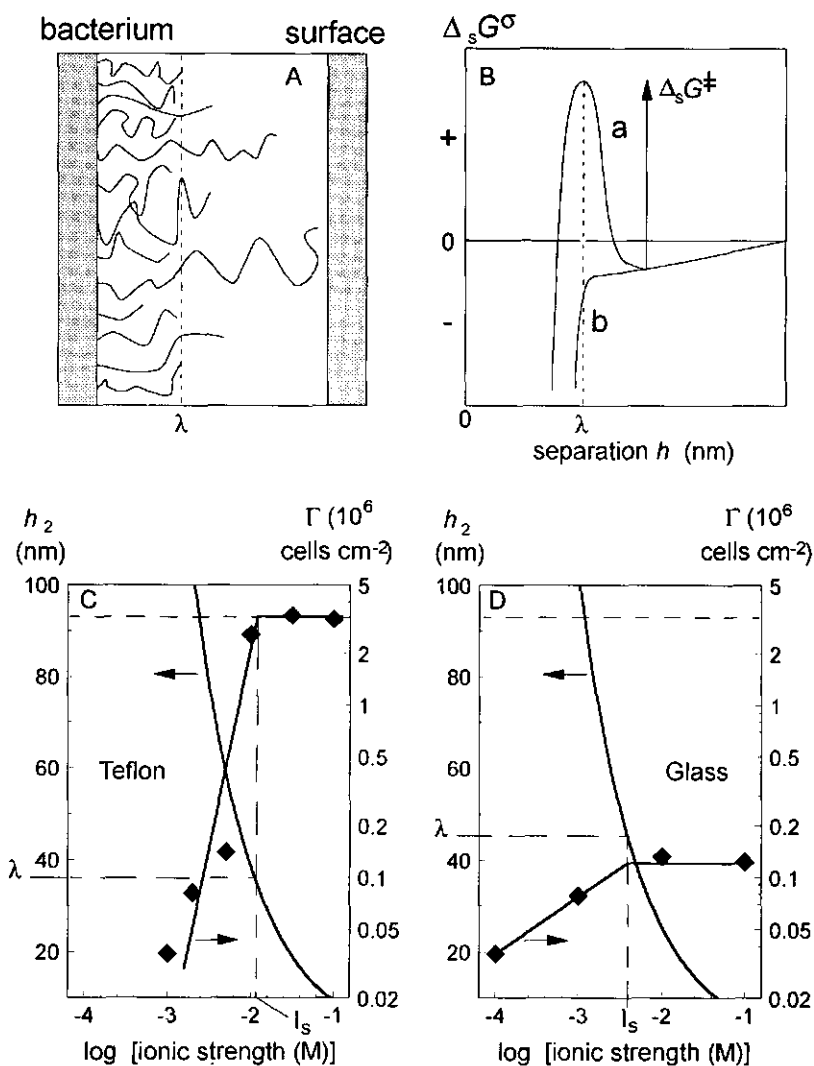


FIG. 6. A and B. Illustration of the magnitude and the effective extension λ of steric interactions. Two types of steric contributions $\Delta_s G^\sigma(h)$ to the Gibbs energy of interaction $\Delta G^\sigma(h)$ can occur: the shorter macromolecules either induce steric hindrance (a) ($\Delta_s G^\sigma > 0$) or cause bridging (b) ($\Delta_s G^\sigma = 0$). In practice, the longer macromolecules always cause an attraction at large separations. C and D. Deposition and the extensions of DLVO (h_2) and steric (λ) interactions. The deposition of strain C3 (*Rhodococcus* C125) onto Teflon (C) and glass (D) and the calculated extension of the DLVO interaction as a function of the ionic strength I of the medium. The short-dashed lines indicate the deposition level expected for purely diffusive transport of cells to the substratum. The long-dashed lines indicate how λ can be derived from the h_2 - I curve and the level of I_s obtained from adhesion experiments.

ΔG^\ddagger (kT)

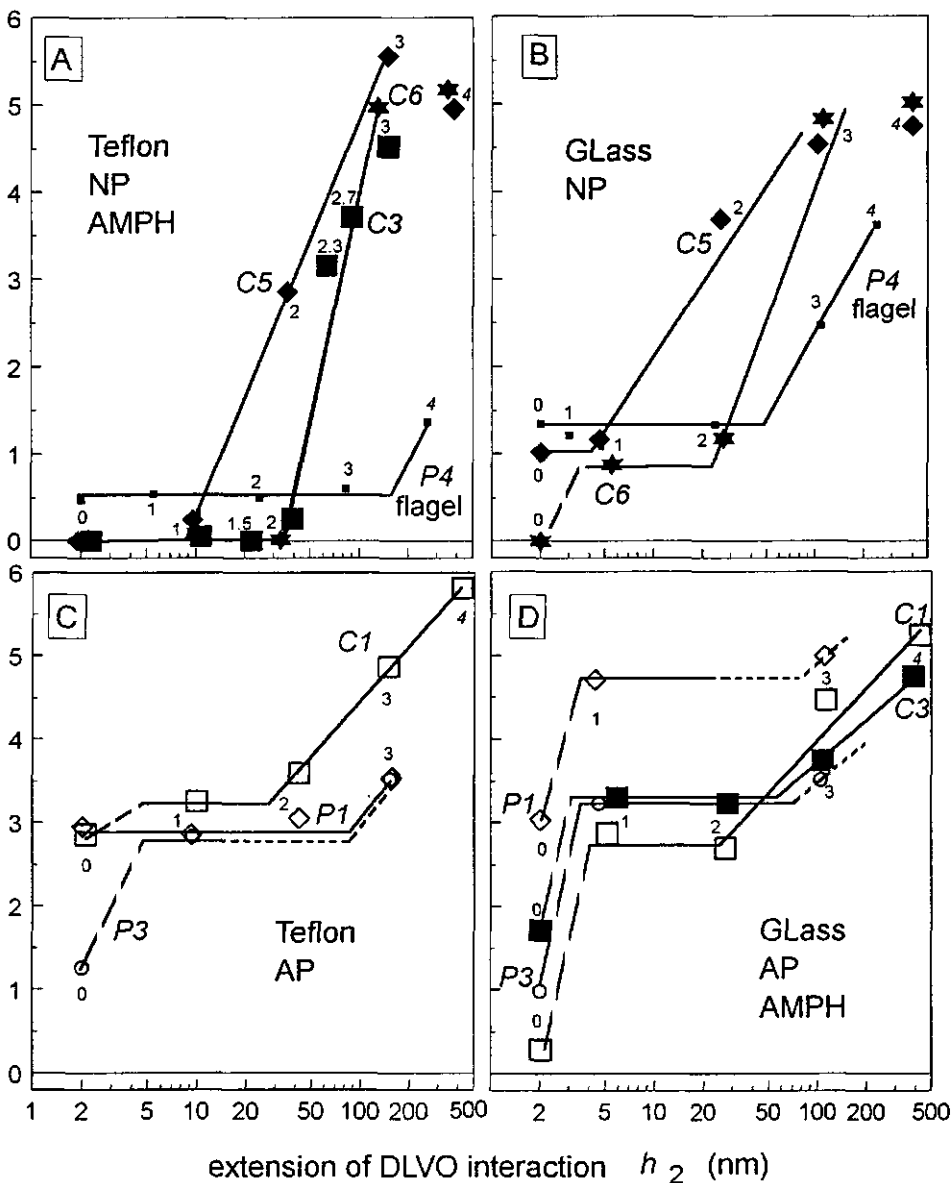


FIG. 7. Experimental activation energies of adhesion ΔG^\ddagger as a function of the calculated extension h_2 of the DLVO contribution to $\Delta G^\ddagger(h)$. Small numbers indicate the ionic strength at which the different data were obtained as $-\log(I)$ values. Dotted lines are likely but not completely certain. Dashed lines indicate a reduction of steric hindrance at high ionic strengths, most probably as a result of a suppression of electrosteric interactions.

Waals contributions.

The results of *Rhodococcus* strain C125 (C3) (Figs. 6C and 6D) exemplify the two possible cases of steric interactions as illustrated in Figs. 6A and 6B Fig. 6B. For teflon, $\Delta_s G^\ddagger = 0$, which indicates bridging (Fig. 6B; curve b). For glass, $\Delta_s G^\ddagger > 0$, namely $3.3 kT$ (Fig. 6D), which proves an occurrence of steric hindrance (Fig. 6B; curve a). This repulsion is greater than the relatively strong Van der Waals attraction (Figs. 4A, 5C).

A transition from adhesion purely controlled by steric interactions to deposition influenced by DLVO interactions occurred upon reducing the ionic strength below a certain value I_s . Levels for I_s of 0.013 M for teflon and 0.004 M for glass were obtained for strain C3 (Fig. 6C and 6D). The I_s -values correspond to the situation that the extension λ (nm) of the steric interactions, i.e., the extension of the majority of the cell surface macromolecules (Fig. 6A and 6B), just exceeds the range of the DLVO-contribution as indicated by the position of the secondary minimum h_2 (Figs. 5D and 5E). Values of λ were determined using the h_2 - I dependency and the adhesion results (Figs. 6C and 6D). For strain C3, λ is 38 nm for teflon and 46 nm for glass. The level of λ for bridging with teflon was slightly smaller than that for steric hindrance on glass.

Steric effects related to the type of predominant cell surface polymer. All adhesion data were converted to values of ΔG^\ddagger and plotted as a function of h_2 (Figs. 7A to 7D). The λ values are summarized in Table 2. The height of the repulsive steric barrier $\Delta_s G^\ddagger$ for the different cell polymer coatings increases in the following order: non-polysaccharide (lipids or proteins) or amphiphilic compounds with teflon < non-polysaccharide compounds like lipids or proteins with glass < anionic polysaccharides with teflon < anionic polysaccharides or amphiphilic compounds with glass (Figs. 7A - 7D; Table 2). Bridging ($\Delta_s G^\ddagger = 0$) occurs between combinations of teflon and bacterial surfaces coated with non-polysaccharide macromolecules or amphiphilic compounds.

Anionic polysaccharide cell coatings. Anionic polysaccharide is a hydrophilic polyelectrolyte which will induce a strong steric hindrance for any surface in water (5, 13, 37). This is confirmed by the high steric barriers

observed for combinations of the strains P1, P3, and C1 with glass and teflon (Figs. 7C and 7D; Table 2). These surface polyelectrolytes protrude over considerable distance into the surroundings of the cell, as indicated by λ -values up to approximately 100 nm (Figs. 7B and 7D; Table 2).

Amphiphilic cell coatings. Evidence for the amphiphilic character of the surface of strains C3 and C4 was found in previous studies (29, 30). The hydrophilic part seems to dominate the steric interactions of strain C4 inducing a repulsion on both glass and teflon (30). The adhesion results at $I = 1$ M for strain C3 on glass (Fig. 7D) confirmed the hypothesis of the presence of highly charged polyelectrolytes on the surface of this strain. The hydrophilic moieties on this bacterial surface impede adhesion on glass while the lipophilic parts cause bridging with teflon. Adhesion of bacteria by different types of polymer moieties on surfaces differing in hydrophobicity has also been observed by others (14).

Non-polysaccharide cell coatings. The hydrophobic long chain mycolic acids on the surface of C6 cells (2) are probably not the sole cause of the bridging on teflon and the low steric repulsion on glass as observed for this strain. Their hydrophobic tails would condense to a thin layer to minimize contact with water and would not be able to span separations of 25 to 33 nm as indicated by the λ -values (Table 2). Hence, there must be one or more compounds that either help to keep these aliphatic chains extended into the aqueous phase or contribute to adhesion by themselves. The adhesion results at $I = 1$ M on glass (Fig. 7B) indicate that this additional compound is a polyelectrolyte. The high i_{ep} of 3.8, the absence of strong steric hindrance on glass, and the high contact angle, point into the direction of macromolecules other than polysaccharides (30). Possible candidates are carboxylated lipids or peptidolipids, which are known to exist on surfaces of mycobacteria (20, 26) which are closely related to coryneform bacteria. The adhesion of strain C5 is similar to that of strain C6, except for the steric extensions, which are much smaller (6 - 8 nm) (Figs. 7A and 7B, Table 2). Possibly, these cells have a bare peptidoglycan-mycolic acid cell wall matrix (2, 30).

TABLE 2. The type of cell coating and the steric properties towards glass and teflon for the various bacteria studied. The properties listed are the height of the steric barrier $\Delta_s G^\ddagger$ and the effective extension λ of the steric interactions.

cell-coating	strain	Steric barrier $\Delta_s G^\ddagger$ (kT)		Effective steric length λ (nm)	
		Glass	Teflon	Glass	Teflon
Anionic polysaccharides:	P1	4.8	3.2	>30	80
	P3	3.2	2.8	>50	>50
	C1	2.8	3.1	25	25
Amphiphilic macromolecules (hydrophobic polysaccharides)	C4	4.1	2.4	n.d. ^c	n.d.
	C3	3.3	0	45	38
Non-polysaccharide macromolecules (lipids and proteins)	C5	1.0	0	8	6
	C6	0.8	0	25	33
	P2	1.1	0	n.d.	n.d.
	P4	1.2	0.6	50 ^b	165 ^b

^aThe most probable type of polymer present on the cell surface was deduced from Θ_w and iep values, and literature data on cell wall composition (29).

^bIt is very likely that these bridging distances are partially determined by the flagellum of this organism.

^cn.d. = not determined.

The difference in steric extension between the strains C5 and C6 was confirmed by the EM micrographs (Figs. 3A and 3B) although a complete match of the steric range and the EM results is not to be expected for the following reasons: (i) the EM specimen preparation used here involves sample dehydration, which is known to cause a (partial) collapse of outer polymer structures (3); (ii) the location in the cell envelope at which the firm peptidoglycan fabric changes into a more loosely steric structure is unknown; (iii) the effective steric extension is smaller than the actual length of the cell surface macromolecules (Fig. 6A; (3)). Assuming a peptidoglycan layer of 20

nm thick, which is a reasonable estimate for Gram-positive organisms (3), the loosely organized outer polymer structure appears to be about 10 nm for strain C5 and 30 nm for strain C6. This follows the same trend as found for λ which have values of 7 ± 1 nm for strain C5 and 29 ± 4 nm for strain C6 (Table 2).

The adhesion behaviour of strain P4 may partially be determined by its flagellum. Bridging separations were relatively large, namely 165 nm for teflon and 50 nm for glass (Figs. 7A and 7B). However, the flagellum did not make adhesion 100% efficient as indicated by barriers of $0.6 kT$ on teflon and $1.2 kT$ on glass. In addition, this organism has a non-polysaccharide (possibly protein) coating on its outer membrane LPS structure (30). DeFlaun et al. (10) showed that an adhesion deficient *Pseudomonas* mutant strain had lost its ability to form flagella as well as its ability to synthesize the predominant outer membrane protein of the parent strain. Hence, the contribution of flagella relative to other cell surface structures in the adhesion of these type of organisms remains to be resolved.

Suppression of electrosteric effects at an ionic strength of 1 M. Attachment is predominantly under the control of steric interactions at $I \geq 0.1$ M, although Van der Waals interactions may also be of influence. The decrease in $\Delta_s G^\ddagger$, as observed for strains C1, C3, C6, P1, and P3 when changing the ionic strength from 0.1 M to 1 M (Figs. 7B, 7C, and 7D), is to be expected since these cells are coated with polyelectrolytes. At such high values of I , the electrosteric repulsion is suppressed (4, 5, 13, 37). This also leads to a shrinking of the polyelectrolyte coating and allows the cell to approach the surface more closely which results in a stronger contribution of the Van der Waals attraction (Figs. 4A, and 4B). The Van der Waals attraction is greater for glass than for teflon (28) (Figs. 4A, 4B and 5C). This is probably the cause that the reductions in $\Delta_s G^\ddagger$ upon increasing I to 1 M are more pronounced for glass (Figs. 7B and 7D) than for teflon (Fig. 7C).

Implications for the adhesive behaviour of microorganisms in different aqueous environments. Among the strains studied, the variation in the range of the DLVO-interactions at ionic strengths between 0.1 M and 0.001 M (Figs. 5D

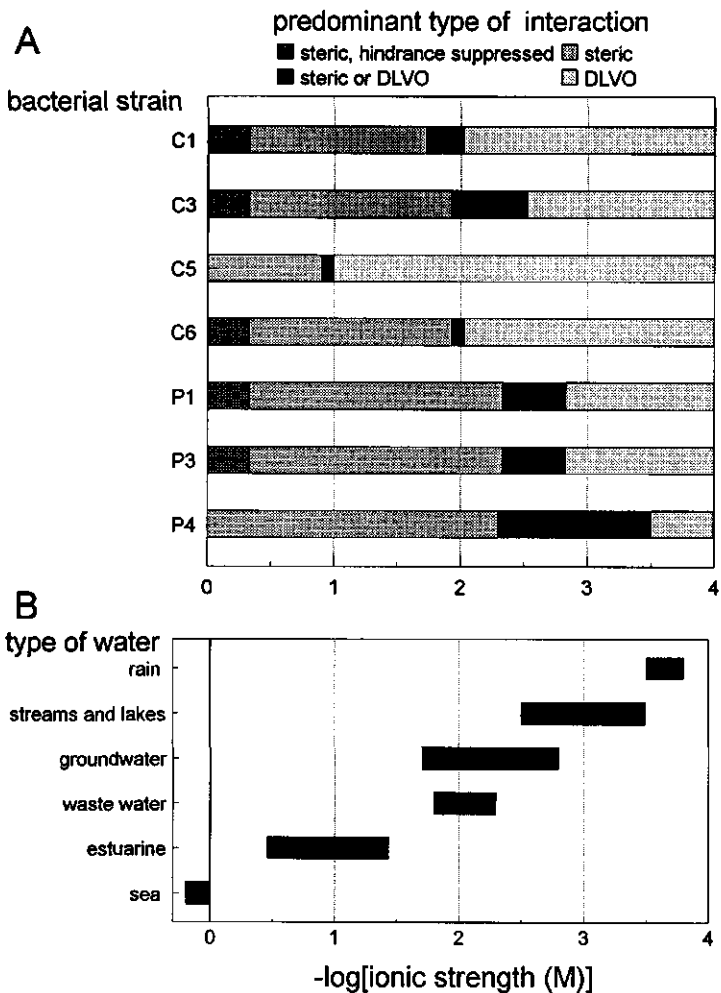


FIG. 8. The relative importance of DLVO and steric interactions at different ionic strength intervals for the bacteria studied (A) compared with the ionic strength of various natural or technical environments (B)

and 5E) is similar to the variation in the steric extension (Figs. 7A to 7D, and Table 2), namely between a few nm and, say, 100 nm. As a consequence, I_s values vary over this same I -range. Hence, the adhesion behaviour of a specific

bacterial species in a specific environment requires an assessment of both steric and DLVO contributions for each case. Nevertheless, some general implications for bacterial deposition in various ionic strength systems can be deduced from the results presented in this paper.

Teflon is hydrophobic which is favourable for bridging and has a relatively low Hamaker constant which is unfavourable for DLVO promoted adhesion (Figs. 4B, 5B, and 5C). In contrast, glass is hydrophilic which is unfavourable for bridging. On the other hand, this may partly be compensated by the stronger Van der Waals attraction (Figs. 4A and 5C). The properties of these two test substrata can be considered to represent the extremes of the macroscopic properties of negatively charged substrata encountered in natural and technical environments. Hence, the ionic strengths at which the DLVO/steric interaction transition occurs for teflon and for glass demarcate the ionic strength interval where this will probably occur for any other negatively charged clean surface. These I -intervals are shown in Fig. 8A for the bacteria studied and compared with the ionic strengths of various aqueous environments (Fig. 8B). The ionic strength ranges of natural waters were taken from Stumm and Morgan (35) and that for typical domestic waste waters was calculated using waste water composition data tabulated by Metcalf & Eddy, Inc. (25).

In low ionic strength environments like rain water, streams and lakes, the adhesion of most bacteria is controlled by DLVO type electrostatic repulsion. Only flagellated organisms (like strain P4) are able to efficiently bridge cell-substratum separations in these systems. In groundwater and most domestic waste waters, deposition may either be dominated by steric or DLVO interactions and both types of interactions have to be addressed for an assessment of bacterial deposition. Adhesion is dominated by steric interactions in more saline systems, like estuary and sea water. In sea water, electrosteric effects are also suppressed and microorganisms have only one option to prevent their immobilization, namely to form a hydrophilic coating that induces a non-electrostatic steric repulsion.

The steric effects demonstrated in the present study resulted from

interactions between bacterial and clean solid surfaces. Natural surfaces are in general coated with negatively charged macromolecules which are known to inhibit colloidal (35) and bacterial (14, 41) deposition. Hence, the steric effects as predicted above, may be even more pronounced in natural environments.

Conclusion.

Combining results of deposition experiments at various ionic strength with DLVO model predictions is a successful procedure to estimate the extension and magnitude of both DLVO- and steric contributions to microbial adhesion. The data show that the development of a quantitative bacterial deposition model that unifies DLVO and macromolecular adsorption concepts is a major challenge for future research.

Appendix

Electrokinetic analyses of cells and solid surfaces.

The main purpose of this analysis was to obtain reliable extrapolations of ζ to $I = 1$ M and/or $I = 0.0001$ M where electrokinetic measurements are not feasible. For this we used the Stern-layer capacitor concept of the electrical double layer:

$$\psi_0 - \psi_d = \sigma_0 / C \quad (\text{A1})$$

where ψ_0 and ψ_d are the potentials (V) at the surface and at the fluid-side of the Stern-layer, σ_0 the surface charge density (C m^{-2}), and C is the Stern-layer capacitance ($\text{C V}^{-1} \text{m}^{-2}$). For smooth and non-conducting interfaces one can estimate the thickness of the Stern-layer δ_s from C (21). However, for bacterial cell surfaces the situation is more complex. Macromolecules may extend into the solution and may shift the plane of shear outwards or place surface-associated charge beyond this plane. Surface conductance, and specific adsorption of the counter-ions may also complicate interpretation. Despite its limitations, the Stern-layer model provides more accurate estimates of ζ for I -

ranges where ζ cannot be measured than a linear ζ - I extrapolation.

Applying the Gouy-Chapman theory with $\zeta \approx \psi_d$, it follows that

$$\sigma_d = - (2\kappa\epsilon RT/F) \sinh\left(\frac{zF\zeta}{2RT}\right) \quad (\text{A2})$$

where the reciprocal Debye-length κ (nm^{-1}) is defined as

$$\kappa^2 = 2F^2 I / \epsilon RT \quad (\text{A3})$$

and where R is the gas constant (J K^{-1}), ϵ the dielectric constant for water ($\text{C}^2 \text{J}^{-1} \text{m}^{-3}$), F the Faraday constant (C mol^{-1}), and z the valency of the symmetrical electrolyte. ζ cannot be explicitated as a function of I . Therefore, for computational purposes we used:

$$I = \frac{z^2}{8\epsilon RT} \left(\frac{-C(\psi_0 - \zeta)}{\sinh(zF\zeta/2RT)} \right)^2 \quad (\text{A4})$$

The values of ψ_0 and C were estimated by fitting eq. A4 to experimental ζ and I values.

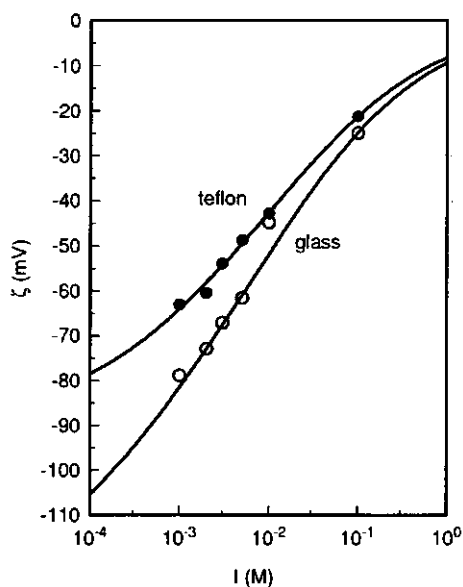


Fig. A1. The zeta-potential ζ for glass (open symbols) and teflon (filled symbols) as a function of the ionic strength I of the medium. The curves represent the result of fitting the capacitor model (eq. A4) to the experimental data (points).

Solids. The model fits the experimental data well for glass and teflon (Fig. A1). The C -values are $-17 \pm 2 \mu\text{F cm}^{-2}$ for glass and $-23 \pm 2 \mu\text{F cm}^{-2}$ for teflon. Assuming that $C = \epsilon_s/\delta_s$ and $\epsilon_s \approx 0.1 \epsilon$ (the subscript s stands for Stern-layer) (21), these values correspond to a thickness of the Stern-layer δ_s of 0.40 and 0.28 nm, for glass and teflon, respectively. These values are close to the radius of 0.36 nm of the hydrated Na^+ (19), which was the main counterion in the systems studied.

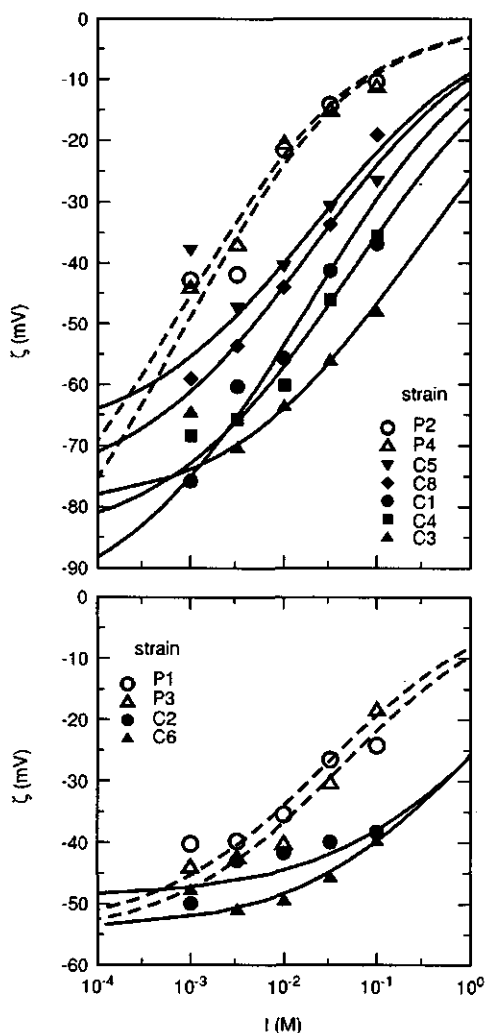


FIG. A2. The zeta-potential ζ for the bacteria listed in Table 1 as a function of the ionic strength I of the medium. The curves resulted from fitting the capacitor model (eq. A4) to experimental data (points): solid curves, coryneform bacteria; dashed curves, pseudomonads.

Bacteria. The results for the bacteria are shown in Fig. A2. The experimental results of C1, C2, C5, and C8 at $I = 0.1$ M and C3, C4, C5, and C6 at $I = 0.001$ M were excluded from the fit procedure, to keep coefficients of variation in the parameter estimates $< 15\%$. One exception was the coefficient of variation of 50% for strain C2. This demonstrates the limited applicability of the Stern-model to bacteria. Non-ideal electrokinetic behaviour was quantified by the extent to which C depended on I . Basically, C should be a constant. This is approximately so for $10^{-2.5}$ M $\leq I \leq 10^{-1.5}$ M, in all but one (C2) cases. Outside this interval, the macromolecular structure interferes. At $I = 0.0001$ M and $I = 1$ M, ζ was estimated with eq A4 and the fitted ψ_0 value, accounting for this non-ideality by using values of C obtained from extrapolating $C = f(I)$.

The most reliable capacitance, i.e., that for the intermediate I -range, may be related to the type of cell-coating. For most bacterial strains (C1, C5, C8, P1 and P3) $20 \mu\text{F cm}^{-2} \leq C \leq 50 \mu\text{F cm}^{-2}$. The low level for C of $6.6 \pm 0.2 \mu\text{F cm}^{-2}$, observed for the pseudomonads P2 and P4, may be caused by a low charged non-polysaccharide (possibly proteineous) cell-coating (10, 30). The strains C4 and C3 have a higher value of C possibly as a result of the amphiphilic macromolecules that extend from these cell surfaces into the solution. The capsule of strain C2 (29) and the surface macromolecules of strain C6 cause extremely high values of C ($> 200 \mu\text{F cm}^{-2}$). Future research is required to elucidate the possible effects of the chemical nature and the structure of the outer cell surface on the electrokinetic behaviour of bacteria.

Acknowledgements

We thank Dr. Henk Busscher of the Laboratory for Materia Technica of the University of Groningen, Groningen, The Netherlands, for making the electron micrographs of strain C5 and C6.

References

1. Absolom, D. R., F. V. Lamberti, Z. Policova, W. Zingg, C. J. Van Oss and A. W. Neumann. 1983. Surface thermodynamics of bacterial adhesion. *Appl. Environ. Microbiol.* **46**:90-97.
2. Bendinger, B., H. H. M. Rijnaarts, K. Altendorf and A. J. B. Zehnder. 1993. Physicochemical cell surface and adhesive properties of coryneform bacteria related to the presence and chain length of mycolic acids. *Appl. Environ. Microbiol.* **59**:3973-3977.
3. Beveridge, T. J. and L. L. Graham. 1991. Surface layers of bacteria. *Microbiol. Rev.* **55**:684-705.
4. Blaakmeer, J., M. R. Böhmer, M. A. Cohen Stuart and G. J. Fleer. 1990. Adsorption of weak polyelectrolytes on highly charged surfaces. Poly(acrylic acid) on polystyrene latex with strong cationic groups. *Macromolecules* **23**:2301-2309.
5. Böhmer, M. R., O. A. Evers and L. M. H. M. Scheutjens. 1990. Weak Polyelectrolytes between two surfaces: adsorption and stabilization. *Macromolecules* **23**:2288-2301.
6. Bonekamp, B. C. 1989. Conformational properties and adsorbed layer structure of adsorbed poly-L-lysine and poly-DL-lysine as inferred from adsorption measurements and proton titrations. *Colloids Surf.* **41**:267-286.
7. Bonekamp, B. C. and J. Lyklema. 1985. Conductometric and potentiometric monitoring of the polyelectrolyte adsorption on charged surfaces. *J. Colloid Interf. Sci.* **113**:67-75.
8. Busscher, H. J., M. H. M. J. C. Uyen, A. J. W. Pelt, H. J. Busscher and A. H. Weerkamp. 1987. Specific and non-specific interactions in bacterial. *FEMS Microbiol. Rev.* **46**:165-173.
9. Busscher, H. J., A. H. Weerkamp, H. C. van der Mei, A. J. W. Pelt, H. P. de Jong and J. Arends. 1984. Measurement of the surface free energy of bacterial cell surfaces and its relevance for adhesion. *Appl. Environ. Microbiol.* **48**:980-983.
10. DeFlaun, M. F., A. S. Tanzer, A. L. McAteer, B. Marshall and S. B. Levy. 1990. Development of an adhesion assay and characterization of an adhesion deficient Mutant of *Pseudomonas fluorescens*. *Appl. Environ. Microbiol.* **56**:112-119.
11. Dickson, J. R. and K. Koohmaraie. 1989. Cell surface charge characteristics and their relationship to bacterial attachment to meat surfaces. *Appl. Environ. Microbiol.* **55**:832-836.
12. Elimelech, M. and C. R. O'Melia. 1990. Kinetics of deposition of colloidal particles in porous media. *Environ. Sci. Technol.* **24**:1528-1536.
13. Fleer, G. J. and J. M. H. M. Scheutjens. 1993. Modeling Polymer adsorption, steric stabilization and flocculation, p. 209-263. *In* B. Dobias (ed.), *Coagulation and flocculation*, Marcel Dekker Inc., New York.
14. Fletcher, M. and K. C. Marshall. 1982. Bubble contact angle method for evaluating substratum interfacial characteristics and its relevance to bacterial attachment. *Appl. Environ. Microbiol.* **44**:184-192.
15. Gannon, J., Y. Tan, p. Baveye and M. Alexander. 1991. Effect of sodium chloride on transport of bacteria in saturated aquifer material. *Appl. Environ. Microbiol.* **57**:2497-2501.
16. Gordon, A. S. and F. Millero. 1984. Electrolyte effects on attachment of an estuarine bacterium. *Appl. Environ. Microbiol.* **47**:495-499.
17. Handley, P. S. 1991. Detection of cell surface carbohydrate components, p. 87-107. *In* N. Mozes, P. S. Handley, H. J. Busscher and P. G. Rouxhet (ed.), *Microbial cell surface analyses: structural and physicochemical methods*, VCH Publishers, Inc., New York.

18. Harvey, R. W. 1991. Parameters involved in modeling movement of bacteria in groundwater, *In* C. J. Hurst (ed.), *Modelling the Environmental Fate of Microorganisms*, American Society for Microbiology, Washington D. C.
19. Israelachvili, J. N. 1989. Interactions involving polar molecules, p. 36-49. *In* *Intermolecular and surface forces, with applications to colloidal and biological systems*, Academic Press Ltd., London.
20. Krasil'nikov, N. A. and T. V. Koronelli. 1971. Nature of polar lipids from a paraffin-oxidizing culture of *Mycobacterium rubrum*. *Microbiology* **40**:196-200.
21. Lyklema, J. 1991. Electrochemistry and its applications to colloids and interfaces, p. 5.1-5.114. *In* *Fundamentals of interface and colloid science*, Academic Press Ltd., London.
22. Martin, R. E., E. J. Bouwer and L. M. Hanna. 1992. Application of clean-bed filtration theory to bacterial deposition in porous media. *Environ. Sci. Technol.* **26**:1053-1058.
23. Martin, R. E., L. M. Hanna and E. J. Bouwer. 1991. Determination of bacterial collision efficiencies in a rotating disk system. *Environ. Sci. Technol.* **25**:2075-2082.
24. Meinders, J. M. and H. J. Busscher. *In press*. Influence of ionic strength and shear rate on the desorption of polystyrene particles from a glass collector as studied in a parallel plate flow chamber. *Colloid Polym. Sci.*
25. Metcalf & Eddy, I. and G. Tchobanoglous. 1984. *Wastewater engineering: treatment, disposal, and reuse*, 4th ed., Tata McGraw-Hill Publishing Company Ltd., New-Delhi.
26. Minikin, D. E. 1982. Lipids: Complex lipids, their chemistry, biosynthesis and roles, p. 95-184. *In* C. Ratledge and J. Stanford (ed.), *The biology of mycobacteria: Physiology, identification and classification.*, Academic Press, London.
27. Norde, W. and J. Lyklema. 1989. Protein adsorption and bacterial adhesion to solid surfaces: a colloid chemical approach. *Colloids Surf.* **38**:1-13.
28. Rijnaarts, H. H. M., W. Norde, E. J. Bouwer, J. Lyklema and A. J. B. Zehnder. *Mechanism and reversibility of bacterial adhesion.* submitted to *Colloids and Surfaces B: Biointerfaces*.
29. Rijnaarts, H. H. M., W. Norde, E. J. Bouwer, J. Lyklema and A. J. B. Zehnder. 1993. Bacterial adhesion under static and dynamic conditions. *Appl. Environ. Microbiol.* **59**:3255-3265.
30. Rijnaarts, H. H. M., W. Norde, J. Lyklema and A. J. B. Zehnder. The isoelectric point of bacteria as an indicator for the presence of cell surface polymers that inhibit adhesion. submitted to *Colloids and Surfaces B: Biointerfaces*.
31. Rutter, P. R. and B. Vincent. 1984. Physicochemical interactions of the substratum, microorganisms, and the fluid phase, *In* K. C. Marshall (ed.), *Microbial adhesion and aggregation*, Springer-verlag, Berlin.
32. Rutter, P. R. and B. Vincent. 1988. Attachment mechanisms in the surface growth of microorganisms, p. 87-107. *In* J. I. Bazin and J. M. Prosser (eds.), *CRC Series in Mathematical models for microbiology*, CRC Press, Inc., Boca Raton, Florida.
33. Sjollem, J., H. J. Weerkamp and A. H. Busscher. 1990. Deposition of oral streptococci and polystyrene latices onto glass in a parallel plate flow cell. *Biofouling* **1**:101-112.
34. Solari, J. A., G. Huerta, B. Escobar, T. Vargas, R. Badilla-Ohlbaum and J. Rubio. 1992. Interfacial phenomena affecting the adhesion of *Thiobacillus ferrooxidans* to sulphide mineral surfaces. *Colloids and Surf* **69**:159-166.
35. Stumm, W. and J. J. Morgan. 1981. The solid-solution interface, p. 599-684. *In* *Aquatic chemistry: an introduction emphasizing chemical equilibria in natural waters*, John Wiley &

Sons, New York.

36. Van der Meer, J. R., T. N. P. Bosma, W. P. de Bruin, H. Harms, C. Holliger, H. H. M. Rijnaarts, M. E. Tros, G. Schraa and A. J. B. Zehnder. 1992. Versatility of soil column experiments to study biodegradation of halogenated compounds under environmental conditions. *Biodegradation* 3:265-284.
37. Van der Schee, H. A. and J. Lyklema. 1984. A lattice theory of polyelectrolyte adsorption. *J. Phys. Chem.* 88:6661-6667.
38. Van Loosdrecht, M. C. M., J. Lyklema, W. Norde, G. Schraa and A. J. B. Zehnder. 1987. Electrophoretic mobility and hydrophobicity as a measure to predict the initial steps of bacterial adhesion. *Appl. Environ. Microbiol.* 53:1898-1901.
39. Van Loosdrecht, M. C. M., J. Lyklema, W. Norde, G. Schraa and A. J. B. Zehnder. 1987. The role of bacterial cell wall hydrophobicity in adhesion. *Appl. Environ. Microbiol.* 53:1893-1897.
40. Van Loosdrecht, M. C. M., J. Lyklema, W. Norde and A. J. B. Zehnder. 1989. Bacterial adhesion: a physicochemical approach. *Microb. Ecol.* 17:1-15.
41. Van Loosdrecht, M. C. M., W. Norde, J. Lyklema and A. J. B. Zehnder. 1990. Hydrophobic and electrostatic parameters in bacterial adhesion. *Aquat. Sci.* 52:103-114.

Chapter 6

Bacterial Deposition in Porous Media Related to the Clean Bed Collision Efficiency and to Substratum-Blocking by Attached Cells

Huub H.M. Rijnaarts, Willem Norde, Edward J. Bouwer, Johannes Lyklema and Alexander J.B. Zehnder

Submitted for publication to Environmental Science and Technology

Deposition of *Pseudomonas putida* mt2 and *Rhodococcus* strain C125 during transport through columns packed with teflon grains was investigated. Deposition was analyzed in terms of the clean bed collision efficiency α_0 (the probability of a cell to attach upon reaching a cell-free substratum), and the surface area blocked by attached cells. Blocking was quantified by a blocking factor B , the ratio of the blocked area per cell to the geometric area of a cell. At an average interstitial fluid velocity of $200 \mu\text{m s}^{-1}$, α_0 was close to unity (0.83 ± 0.01) for both strains indicating that cell-solid interactions were favourable for deposition. Values of B were 1.6 ± 0.1 for *Ps. putida* and 12.0 ± 0.8 for *Rhodococcus* strain C125, which correspond to maximum fractional surface coverages (Θ_{max}) for single layer adhesion of $52 \pm 2\%$ and $8.3 \pm 0.6\%$, respectively. The difference in blocking behaviour is consistent with differences in cell size and cell-cell repulsion, which were both smaller for *Ps. putida* than for *Rhodococcus* strain C125. Multilayer adhesion and/or pore clogging occurred at high coverages ($>0.5 \Theta_{\text{max}}$) for the weakly blocking *Pseudomonas* cells but not for the strongly blocking *Rhodococcus* cells. An analysis of literature data (Lindqvist and Enfield) on dispersal of *Bacillus* cells in columns packed with coarse sand demonstrated that the collision-blocking model applies to this system at all surface coverages. Here $\alpha_0 = 0.098 \pm 0.008$ which indicates inhibition by cell-solid interactions, and $B = 5.8 \pm 0.8$ which demonstrates relatively strong blocking. The general conclusion is that deposition of microbes during their transport through coarse grain media is adequately described by the collision-blocking model in cases of strongly blocking cells or weakly blocking cells at low coverage conditions.

Introduction

Bacterial deposition in porous media is an important issue in current environmental microbiology (32). For example, preventing transport of pathogenic bacteria to aquifers is vital for maintaining high quality drinking water resources (18, 19). On the other hand, stimulating the activity of indigenous bacteria (6, 33) or introducing specialized bacteria into the subsurface, may be used for clean-up of groundwater polluted by organic chemicals. However, an uncontrolled increase in number and migration of bacteria in groundwater may have undesired effects, such as the reduction in the microbial quality of groundwater and/or spreading of chemicals by colloidal facilitated transport (19). Hence, successful groundwater and soil bioremediation must rely on control and appropriate modelling of microbial transport in porous media.

Many researchers have attempted to describe the transport of microbial colloids in porous media with advection-dispersion models extended with rate terms to account for one or more of the following processes: (i) deposition, (ii) detachment, (iii) particle capture by straining (mechanical filtering) which leads to pore-clogging, and (iv) particle release from clogged pores (3, 4, 5, 7, 8, 14, 15). However, in most studies, the relative contributions of these different mechanisms were not measured independently which has prevented appropriate model calibration and validation (11).

The present study identified and quantified some of the principal mechanisms of bacterial transport and retention in porous media. We limited our investigation to coarse grain media, where the bacterial radius a_b (m) is much less than the grain radius a_s (m), so that straining is excluded ($N_R = a_b/a_s \ll 0.05$) (22, 23). Furthermore, previous studies demonstrated that bacterial deposition is generally irreversible, which excludes detachment as a significant process (26, 30). Hence, deposition is the only process initially controlling cell removal from the fluid phase during transport in these systems.

Deposition is determined by two processes: (i) the transfer of particles from bulk water to the grain (collector) surface, and (ii) adhesion. Colloid

filtration theory was used to quantify these two processes in terms of the single collector mass transfer efficiency η (the probability of a particle approaching a collector to reach its surface), and the adhesion or collision efficiency α (the probability of a particle to attach upon reaching the surface) (12, 17, 22, 23). The level of α is controlled by cell-solid interactions (25, 26, 28) and by the amount of previously attached bacteria. An attached (bacterial) particle can prevent further deposition by blocking a part of the collector surface thus reducing the overall deposition rate (1, 9, 10, 20, 29, 30). The effect of blocking may be substantial: the blocked area may vary between 1.5 to more than 20 times the geometrical cross-section of a particle or cell depending on the hydrodynamic and colloid-chemical conditions of the system (9, 29).

After a continued application of (bacterial) particle suspensions to a porous medium, straining may occur. This generally leads to an enhanced particle removal which is known as "filter ripening" (21).

The present study separated cell-solid interactions from effects of cell-cell interactions (blocking) in order to provide an appropriate formulation of the deposition rate which can be used in modeling bacterial transport. Column experiments were performed with previously defined materials (25): teflon spherical collectors, two bacterial strains, and an aqueous phase with an ionic strength of 0.1 M. The influence of flow rate and column length were also tested. Finally, the applicability of the collision-blocking approach to natural porous media was tested with some literature data on bacterial dispersal in coarse sand media.

Theory

The following expression was used to calculate η (16, 22, 23):

$$\eta = 4A_s^{1/3} N_{Pe}^{-2/3} + A_s N_{vdw}^{1/8} N_R^{15/8} + 0.00338 A_s N_G^{1.2} N_R^{-0.4} \quad (1)$$

Here, $A_s = 2(1 - \rho^5)/(2 - 3\rho + 3\rho^5 - 2\rho^6)$, $\rho = (1 - \epsilon)^{1/3}$, and ϵ is the porosity of the column to account for the effect of neighbouring collectors. The dimensionless numbers N are indicative of the various contributions to η : the

Peclet-number $N_{Pe} = 2Ua_s/D_b$ for the sum of convection and diffusion, $N_R = a_b/a_s$ for interception (particles collide with the surface because of their size) and hydrodynamic retardation due to viscous drag at close proximity of the collector surface, $N_G = 2a_b^2(\rho_p - \rho)g/[9\mu U]$ for sedimentation, and $N_{vdw} = A_{bs(w)}/[9\pi a_b^2 U]$ for acceleration of mass-transfer as a result of Van der Waals attraction. The parameters in these formulations of N are defined as follows: U (m s^{-1}) is the velocity of the fluid phase which enters the column, D_b ($\text{m}^2 \text{s}^{-1}$) is the diffusion coefficient of the bacterium, ρ_b and ρ (kg m^{-3}) are the densities of the bacterium and fluid phase, respectively, μ ($\text{kg m}^{-1} \text{s}^{-1}$) is the dynamic viscosity of the fluid phase, and $A_{bs(w)}$ (J) is the Hamaker constant for Van der Waals interaction between a bacterium (b) and the solid phase (s) across the medium water (w). The first term on the right hand side of eq. 1 describes the contribution of convection and diffusion to η while the other terms account for direct interception and deviation from trajectories due to the other influences. For a detailed description of eq. 1, the reader is referred to ref. (16, 22, 23).

An expression for the influence of cell-solid interactions and cell-cell interactions (blocking) on α becomes (9, 20):

$$\alpha = \alpha_0(1 - B\Theta) \quad (2)$$

where α_0 is the clean bed collision efficiency, B the blocking factor, and Θ the fraction of surface covered with cells, i.e., $\Theta = (\text{number of deposited cells}) \times \pi a_b^2 / A_{col}$, with A_{col} the surface area present in the porous medium column. Initially, $\Theta = 0$ and α is solely determined by cell-solid interactions ($\alpha = \alpha_0$); $\alpha_0 = 1$ when these interactions do not inhibit the adhesion step. The blocking factor B accounts for screening of a part of the solid surface by attached cells, i.e., it is the ratio of the area blocked by an attached cell to the geometric area of that cell. It is related to the maximum fractional surface coverage Θ_{max} for single layer adhesion: $\Theta_{max} = 1/B$. The B -factor is a complex function of the geometric/hydrodynamic parameters a_b and N_{Pe} , the ratio of diffusion to convection (10). Furthermore, repulsive particle-particle interactions may significantly enhance blocking (1, 10).

Under steady-state conditions, the deposition of dispersed particles from water flowing through a porous medium results in a decline of the suspended particle concentration c with porous medium depth L according to (2)

$$c = c_0 e^{-\lambda L} \quad (3)$$

where c_0 is the influent cell concentration and λ (m^{-1}) is the filter coefficient. Deposition in terms of $\eta\alpha$ is coupled to λ via the factor $G_1 = 3/4 (1 - \epsilon)/a_s$ in m^{-1} :

$$\lambda = G_1 \eta\alpha = G_1 \eta\alpha_0 (1 - B\Theta) \quad (4)$$

The deposition rate at any position in the porous bed can be expressed as change in either c or Θ :

$$-\frac{dc}{dt} = G_2 \frac{d\Theta}{dt} = kc\alpha_0(1 - B\Theta) \quad (5)$$

where the factor G_2 (m^{-3}) and mass transfer coefficient k (s^{-1}) are given by $G_2 = 3(1/\epsilon - 1)/(\pi a_s a_b^2)$ and $k = 3/4 (1/\epsilon - 1)U\eta/a_s$, respectively.

Materials and methods

Aqueous media. Phosphate Buffered Saline solution (PBS) with an ionic strength of 0.1 M (25) was used for all experiments.

Bacteria. Sources, procedures for cultivation and preparation, and cell surface properties of *Pseudomonas putida* mt2 and *Rhodococcus* strain C125 were described elsewhere (25). The geometric mean radius a_b and diffusion coefficient D_b are $0.59 \pm 0.07 \mu m$ and $(3.65 \pm 0.05) \times 10^{-13} m^2 s^{-1}$, respectively, for *Ps. putida*, and $1.17 \pm 0.37 \mu m$ and $(1.74 \pm 0.03) \times 10^{-13} m^2 s^{-1}$, respectively, for *Rhodococcus* C125. The bacteria differ in electrostatic properties; at an ionic strength of 0.1 M, the ζ -potentials are -50 mV and -10 mV for *Rhodococcus* C125 and *Ps. putida*, respectively (26).

Collectors and columns. Spherical collectors of PFA-tesflon, previously described (25) and PTFE (Fluorplast, Raamsdonksveer, The Netherlands) were

Table I. Dimensions of collectors and columns

Collector		column		
type of teflon	radius a_c , μm	diameter, cm	porosity ϵ^a	length L , cm
PFA	190 \pm 50	1.00	0.34 \pm 0.03	2.5 - 13.6
PTFE	1600 \pm 25	2.05	0.43 \pm 0.02	25.2

^aaverage value \pm standard deviation in data obtained with chloride tracer experiments and gravimetry.

used. Procedures for cleaning the collectors and packing of the columns are described elsewhere (25). The dimensions of collectors and the glass columns are given in Table I. Total porosity values of PFA-packed columns were estimated from breakthrough curves using chloride as the conservative tracer. Chloride concentrations were measured with a micro-chlorocounter (Marius, Utrecht, The Netherlands). In addition, the pore volumes and porosities of all columns were estimated by gravimetry.

Experiments. Experiments were done with vertical down-flow columns. Bacterial suspensions in PBS with an OD_{280} value of 0.6 were prepared by diluting samples of concentrated stock suspensions. The resulting suspensions with cell concentration c_0 of 5.3×10^8 cells cm^{-3} for *Ps. putida* and 3.6×10^7 cells cm^{-3} for *Rhodococcus* C125, were applied to the columns by means of a peristaltic pump. The effluent cell concentration c , as measured by OD_{280} , was monitored with time. c_0 (OD_{280}) was found to be constant throughout the experimental time in all cases. The columns were operated for two hours to four hours.

The different experiments and specific conditions are listed in Table II. Experiment 1 and 2 were performed with duplicate columns, using independently grown and prepared cells for each column. The other experiments were conducted with a single column for each condition (flow rate and/or column length) studied. An experiment with a column packed with *Rhodococcus* C125 and the larger PTFE beads (Exp. 5) was performed as an additional control

Table II. List of experiments, flow rates Q at which suspensions were applied, column lengths L , and the hydraulic retention times t_{HR} (V_{col}/Q) of the columns used.

experiment	bacterium/collector	Q , $\text{cm}^3 \text{h}^{-1}$	L , cm	t_{HR} , min	
1. Reproducibility test	<i>Ps. putida</i> /PFA	19.0 ± 0.5	7.5	6.3	
2. Reproducibility test	<i>Rhodococcus</i> C125/PFA	14.9 ± 0.3	8.9	12.2	
3. Effect of column length	<i>Ps. putida</i> /PFA	20.0 ± 0.5	2.5	2.0	
			4.8	3.8	
			7.5	6.3	
			12.0	9.8	
4. Effect of column length and flow rate	4A	<i>Rhodococcus</i> C125/PFA	21.6 ± 0.5	3.3	2.4
				5.0	3.7
				7.5	5.6
				13.6	10.0
	4B	<i>Rhodococcus</i> C125/PFA	12.2 ± 0.6	4.3	6.0
				9.8	12.3
				13.0	17.0
	4C	<i>Rhodococcus</i> C125/PFA	4.2 ± 0.3	2.9	10.3
				4.5	16.6
				7.5	31.5
				13.6	52.0
5. Large collectors	<i>Rhodococcus</i> C125/PTFE	74.6 ± 1.5	25.2	29.8	

to demonstrate absence of straining and pore-clogging.

Determination of λ , α , and Θ . λ and α were experimentally determined in two ways. **Method 1.** The filter coefficient λ was estimated by linear regression analysis of the $\ln(c/c_0)$ - L data (eq. 3) obtained from columns with different lengths L (exp 3 and 4). This calculation was performed for c -levels taken just after the initial breakthrough and at the end of the experiment. Values of α were calculated with eq. 4, the measured values of λ and the calculated levels of η (eq. 1). The Hamaker constant $A_{bs(w)}$ for the teflon-water-bacterium was set to 2×10^{-22} J (26) for calculating N_{VdW} (eq. 1).

Method 2. The λ was measured as a function of time for every single column studied, by calculating $\ln(c/c_0)/L$ for each measured c -value. The collision efficiency α was calculated following method 1. In addition, the average surface

coverage $\Theta_{col}(t)$ attained in the columns was estimated by integrating the breakthrough curve. After a number of V pore volumes ($V = t \times Q/V_{col}$, Q is the flow rate ($\text{m}^3 \text{s}^{-1}$), t is time (s) and V_{col} is the column pore volume (m^3)) have passed through the column, Θ_{col} is:

$$\Theta_{col}(t) = V_{col} \left(-c_0 + \int_0^{V_m} (c_0 - c) dV + \int_{V_m}^{V(t)} (c_0 - c) dV \right) \pi a_b^2 / A_{col} \quad (6)$$

where

$$V_{col} \left(-c_0 + \int_0^{V_m} (c_0 - c) dV \right)$$

equals the number of cells deposited during the initial non-steady state phase, and A_{col} (m^2) is the total surface area present in the column. V_{ss} is the number of pore volumes beyond which a semi-steady state exists, i.e., initial breakthrough has occurred and tailing effects due to hydrodynamic dispersion have died away. Finally, α_0 and B were estimated by fitting eq. 2 to the α - Θ_{col} data by a standard linear regression procedure.

In some cases, $\Theta(L,t)$ was estimated from λ_i -values, determined from c -levels measured at different time intervals Δt_i (method 2) according to,

$$\Theta(L,t) = \frac{c_0 U}{G_2} \sum_{i=1}^n (\lambda_i e^{-\lambda_i L} \Delta t_i) \quad (7)$$

where $\Delta t_1 = t_1 - t_{L,0}$, $\Delta t_2 = t_2 - t_1, \dots, \Delta t_n = t_n - t_{n-1}$, and $t_{L,0} = L\epsilon/U < t_1 < t_2, \dots < t_n$.

Analysis of literature data on bacterial transport in sand columns. The applicability of the approach presented here to natural porous media was tested by an analysis of data on the dispersal of *Bacillus* strain CB2 in columns with coarse (Texas) sand reported by Lindqvist and Enfield (15). The system properties and parameters used for the calculations, in part given by these authors, were as follows: $\epsilon = 0.34$, $Q = 34.3 \text{ cm}^3 \text{ h}^{-1}$, column diameter = 5 cm, $L = 5 \text{ cm}$, $V_{col} = 33.6 \text{ cm}^3$, the geometric mean estimate of the bacterial

Table III. Interstitial fluid velocity (U/ϵ), values of the dimensionless numbers N of the mass-transfer equation 1, the dimensionless flux η , and the fractional contribution (η_{conv}/η) of the sum of convection and diffusion to η

strain/collector	exp	U/ϵ , $\mu\text{m s}^{-1}$	N_{Rv} , x 10^{-3}	N_{Pev} , x 10^4	N_G , x 10^{-3}	N_{VdW} , x 10^{-5}	η , x 10^{-2}	η_{conv}/η
<i>Ps. putida</i> /PFA	1 + 3	206	3.1	7.2	1.0	28.4	0.76	0.97
<i>Rhodococcus</i> C125/PFA	4A	225	6.1	15.7	3.5	6.8	0.51	0.85
<i>Rhodococcus</i> C125/PFA	2	155	6.1	10.9	4.9	9.6	0.64	0.87
<i>Rhodococcus</i> C125/PFA	4B	127	6.1	9.9	6.3	12.4	0.71	0.87
<i>Rhodococcus</i> C125/PFA	4C	44	6.1	3.3	16.5	32.7	1.39	0.90
<i>Rhodococcus</i> C125/PTEF	5	221	0.73	104	4.4	8.7	0.15	0.80
<i>Bacillus</i> CB1/sand	ref. (15)	14	3.1	0.5	13.6	13300	54.4	0.96

radius (25) $a_b = \frac{1}{2}(1.9 \mu\text{m} \times 0.7 \mu\text{m})^{1/2} = 0.58 \mu\text{m}$, $a_s = 550 \pm 50 \mu\text{m}$, a specific area for the sand of $21 \text{ cm}^2 \text{ g}^{-1}$, i.e., $A_{\text{col}} = 0.36 \text{ m}^2$, and $A_{\text{bs}(w)} = 6.2 \times 10^{-21} \text{ J}$ which is appropriate for glass and silica surfaces (26).

Results

Dimensionless transport flux η . The different dimensionless numbers and η as calculated for the various experiments are listed in Table III.

Replicate column experiments (Exp. 1 and 2) resulted in very similar breakthrough profiles, for the chloride tracer (Fig. 1A) as well as for the bacteria (Figs. 1A and 2A). The chloride results indicated that effects of hydrodynamic dispersion were absent at $V > 2$. Therefore V_{ss} in eq. 6 was set to a value of 2.

Initially, 18 to 20% of the cells of both strains travelled with the same velocity as the interstitial fluid and appeared in the effluent after approximately one pore volume (Figs. 1A and 2A), whereas 80% deposited. The deposition

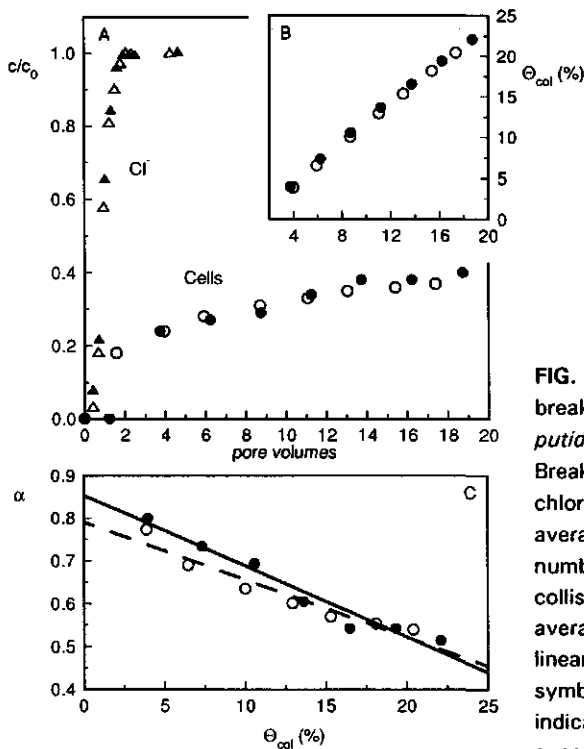


FIG. 1. Check of reproducibility of breakthrough; results for *Pseudomonas putida* mt2 and PFA collectors. A. Breakthrough of cells (circles) and chloride (triangles). B. The increase of the average surface coverage Θ_{col} with number of pore volumes fed. C. The collision efficiency α as a function of average surface coverage; lines represent linear regression results. Open and filled symbols, and solid and dashed lines indicate results of independent duplicate experiments.

decreased after the initial breakthrough as indicated by (i) the increase of c/c_0 from 0.2 to 0.4, (ii) a decrease of the slope of the Θ_{col} - V plots with increasing Θ_{col} (Fig. 1B and 2B), and (iii) the decrease of α from initial (α_0) levels of 0.82 and 0.83 (Table IV) to values between 0.4 and 0.6 at $\Theta_{col} = 20\%$ for *Ps. putida* mt2 (Fig. 1C) and at Θ_{col} -levels of about 4% for *Rhodococcus* C125 (Fig. 2C). The values of B indicate a great difference in blocking between the two strains, and correspond to maximum coverages of 54% for *Ps. putida* and 9% for *Rhodococcus* C125 (Table IV). The good experimental reproducibility permitted the use of a single column for each subsequent condition investigated.

Effect of column length. Methods 1 and 2 were both used for the determination of λ and α . The results obtained with *Ps. putida* (exp. 3) are

Table IV. Experimental values of the clean bed collision efficiency α_0 , the blocking factor B and the maximum coverage Θ_{\max} , determined according to method 2.

exp	strain/collector	α_0	B	Θ_{\max} , %
1	<i>Ps. putida</i> /PFA	0.82 ± 0.03	1.84 ± 0.22	54.3
3	<i>Ps. putida</i> /PFA	0.82 ± 0.03	2.00 ± 0.02	50.0
2	<i>Rhodococcus</i> C125/PFA	0.83 ± 0.01	10.61 ± 0.96	9.4
4A	<i>Rhodococcus</i> C125/PFA	0.81 ± 0.06	11.98 ± 0.72	8.3
4B	<i>Rhodococcus</i> C125/PFA	0.62 ± 0.04	10.03 ± 2.34	10.0
4C	<i>Rhodococcus</i> C125/PFA	0.55 ± 0.04	8.36 ± 5.25	12.0
5	<i>Rhodococcus</i> C125/PTFE	1.07 ± 0.10	11 ± 7	8
ref. (15)	<i>Bacillus</i> CB1/sand	0.098 ± 0.008	5.8 ± 0.8	17

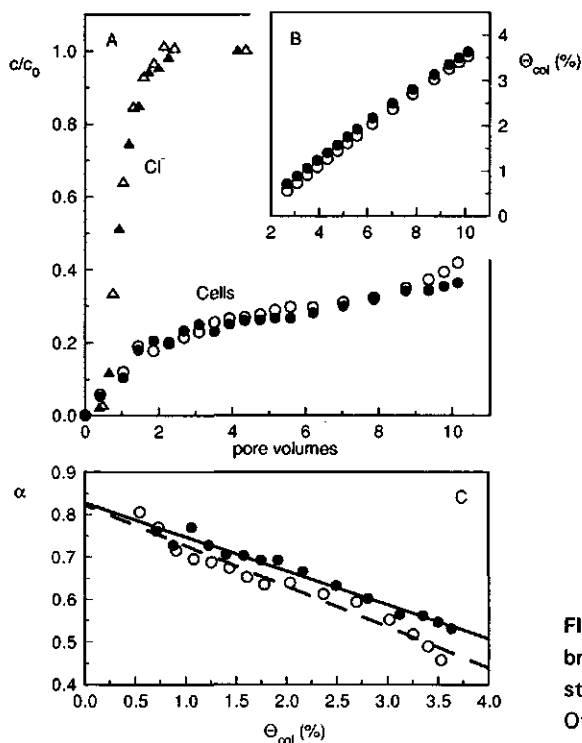


FIG. 2. Check of reproducibility of breakthrough; results for *Rhodococcus* strain C125 and PFA collectors. Otherwise as in Figure 1.

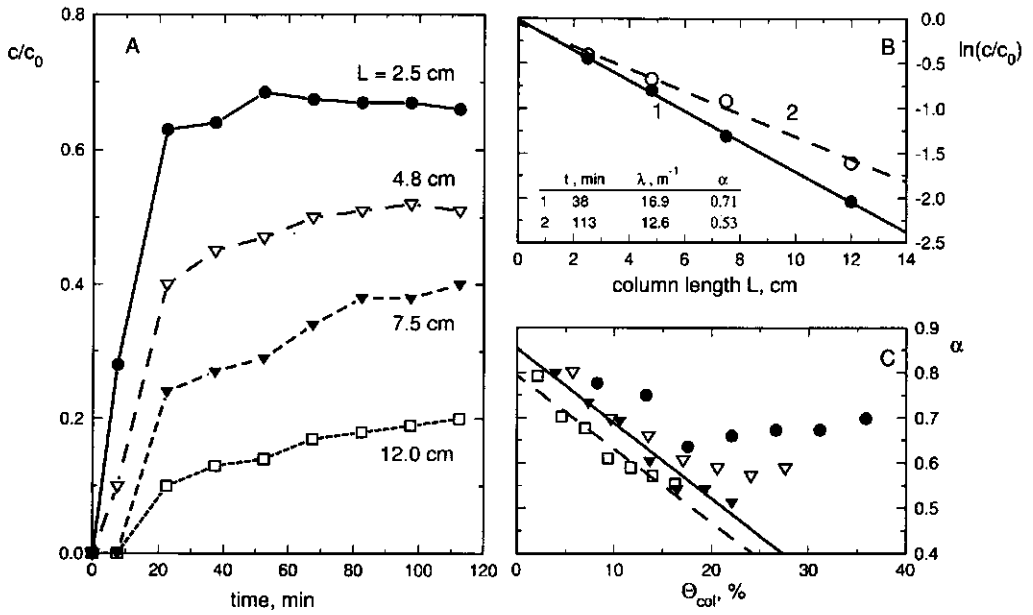


FIG. 3. Results for *Pseudomonas putida* mt2 and PFA-packed columns with various lengths L . A. Breakthrough profiles of the cells. B. Plot of $\ln(c/c_0)$ as a function of column length at two times; lines indicate linear regression results. C. The collision efficiency α as a function of average surface coverage Θ_{col} ; lines represent linear regression results of the two longest columns.

Table V. Filter coefficient λ , and collision efficiency α derived from λ according to method 1.

exp	strain/collector	λ, m^{-1}		α from $\lambda(t_i)^a$
		t_1^a	t_2^a	
3	<i>Ps. putida</i> /PFA	16.9 ± 0.4	12.6 ± 1.0	0.71 ± 0.01
4A	<i>Rhodococcus</i> C125/PFA	12.8 ± 0.7	9.8 ± 0.5	0.74 ± 0.04
4B	<i>Rhodococcus</i> C125/PFA	11.2 ± 0.2	6.8 ± 2.4	0.47 ± 0.01
4C	<i>Rhodococcus</i> C125/PFA	23.9 ± 1.2	26.6 ± 1.3	0.52 ± 0.02

^a $t_1 = 38$ min and $t_2 = 113$ min for exp. 3 and 4A; $t_1 = 105$ min and $t_2 = 360$ min for exp. 4B and 4C.

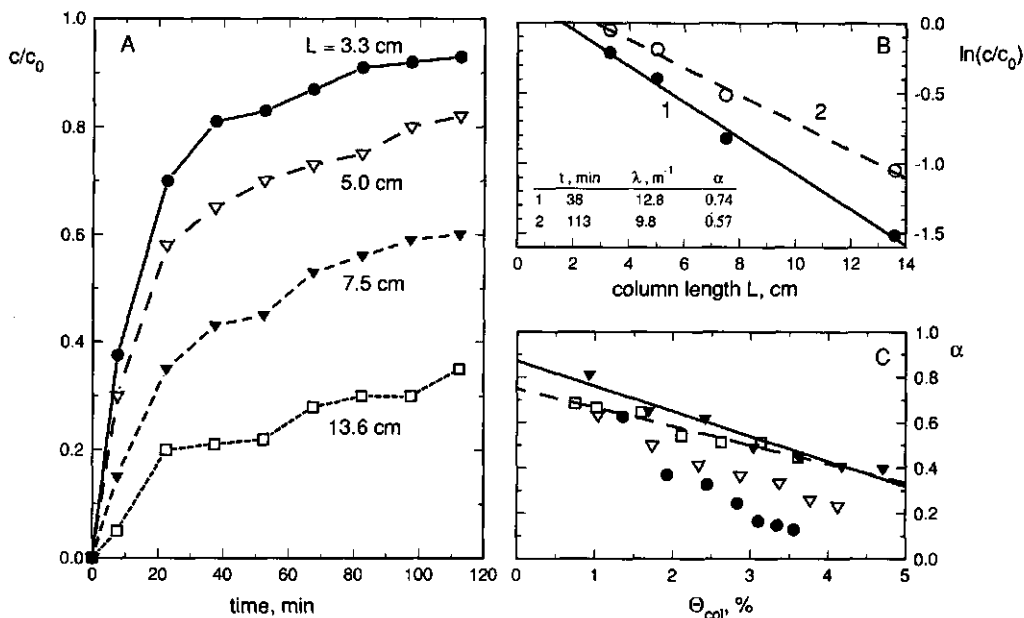


FIG. 4. Results for *Rhodococcus* strain C125 and PFA-packed columns with various lengths L . Otherwise as in Figure 3.

shown in Fig. 3. The fraction of cells removed from the fluid phase increases with column length (Fig. 3A). At $t = 38$ min, c/c_0 decreased exponentially with bed length according to eq. 3 (Fig. 3B). However, λ as determined by method 1, decreased by 25% over the period $t = 38$ min to $t = 113$ min (Fig. 3B; Table V). The dependency of α on Θ_{col} (method 2) is shown in Fig. 3C. Here, α is initially about 0.8, then decreases with Θ_{col} for all columns and finally levels off or slightly increases with Θ_{col} . For the two longest columns, the initial decrease was most pronounced and approximately linear with Θ . The average value of B of these columns is similar as for exp. 1 (Table IV). The results of the two shortest columns were not analyzed with eq. 3 because α increased with Θ at higher coverages, i.e. at $\Theta_{col} > 18\%$ ($t > 53$ min) for the 2.5 cm column, and at $\Theta_{col} > 24\%$ ($t > 97$ min) for the 4.8 cm column. The estimated variation of Θ (eq. 7) between the column outlet and inlet was $14\% < \Theta(L) < 33\%$ at $t =$

53 min for the first column and $16\% < \Theta(L) < 47\%$ at $t = 97$ min for the second column. Apparently, an effect opposite to blocking, i.e., an increase of cell removal from the fluid phase (filter ripening), occurred at coverages exceeding about half Θ_{\max} valid for single layer attachment.

The number of deposited *Rhodococcus* C125 cells also increased with porous bed length (exp 4A; Figs. 4A to C). Effluent concentration c decreased exponentially with L in the lower parts of the columns (Fig. 4B): the regression lines of the $\ln(c/c_0)$ - L plots intersected the L -axis at a value >0 . Apparently, after 38 min, there was low or no deposition in the upper few cm of the columns. These low deposition zones became longer with time. Values of λ and α , obtained with method 1, decreased with time (Fig. 4B; Table V), indicating blocking. The α -values (method 2) obtained from the shortest columns were much smaller than those for the two longest columns (Fig. 4C). The value of α determined by method 1 ($t = 38$ min; Table V) is somewhat smaller than the α_0 -value derived with method 2 for the two longest columns (Fig. 4C; Table IV). The average of the levels of B obtained with these columns is similar to that of exp. 2 (Table IV) and indicates that each cell blocks about 12 times its own geometric area. The coverage at the top of the columns $\Theta(L = 0)$, estimated with eq. 7 and the breakthrough data of the four columns, was $(4.9 \pm 0.3)\%$ at $t = 38$ min and $(8.1 \pm 1)\%$ at $t = 113$ min. Considering $\Theta_{\max} \approx 9\%$, the low deposition in the top layers of the columns may have resulted from surface saturation by the strongly blocking attached cells.

Although straining was not likely in the system used ($N_R = 0.006$), a column-test with the larger PTFE beads (exp. 5) was performed to confirm this hypothesis. The pores between the PTFE-beads are much too large to permit straining ($N_R = 0.0007 \ll 0.05$). Except for a difference in α_0 , α decreased with Θ_{col} (Fig. 5) in a similar way as in the two longest columns packed with PFA grains (Fig. 4), as indicated by insignificant differences in B (Table IV). Therefore, blocking caused the decrease of α with increasing Θ_{col} for both types of teflon collectors as well as the low deposition in the top of the PFA packed columns.

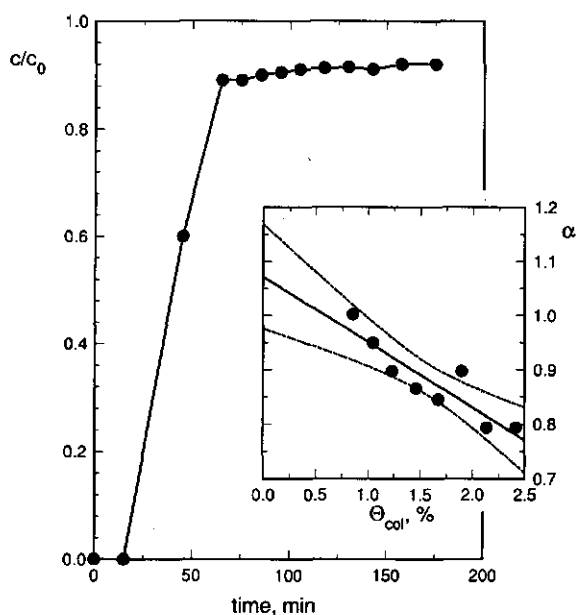


FIG. 5. Dispersal of *Rhodococcus* strain C125 in columns packed with PTFE beads. Insert: the collision efficiency α as a function of average surface coverage Θ_{col} ; the drawn line represents the linear regression result and the curves the confidence interval ($P = 0.05$).

Effect of fluid velocity on the deposition of *Rhodococcus* C125. The level of c/c_0 increases much slower with t and V for the lowest flow rate $Q = 4.3 \text{ cm}^3 \text{ h}^{-1}$ (exp. 4C) in comparison to the highest flow rate $Q = 21.6 \text{ cm}^3 \text{ h}^{-1}$ (Fig. 4A). Values of λ and α determined according to method 1 are summarized in Table V, whereas the method 2 results, α_0 and B , are given in Table IV. In all cases α , according to method 1 is smaller than α_0 . Both parameters decrease with average interstitial fluid velocity U/ϵ whereas the opposite is observed for B .

The collision-blocking concept applied to a natural porous system. Part of the data reported by Lindqvist et al. (Fig. 9 in ref. (15)) are replotted in Fig. 6A.

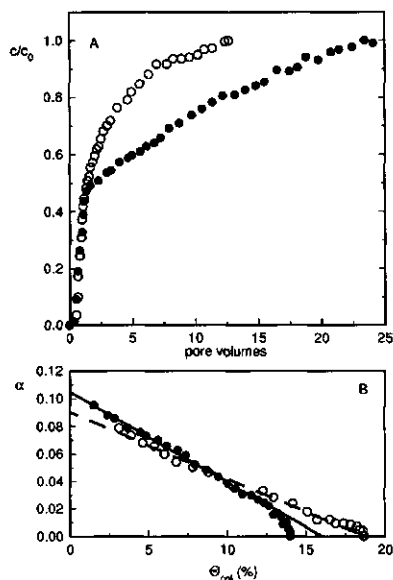


FIG. 6. The breakthrough of *Bacillus* strain CB1 through columns packed with coarse Texas sand for two different levels of c_0 : 3×10^8 cells cm^{-3} (filled symbols) and 1.2×10^9 cells cm^{-3} (open symbols). A. Breakthrough results as reported by Lindqvist and Enfield (part of Fig. 9 in ref. (15)). B. The collision efficiency α is given as a function of average surface coverage Θ_{col} ; the lines represents the linear regression results; the data with $\Theta_{col} > 13\%$ were excluded from the regression analysis.

The α - Θ_{col} plots are linear and very similar for the two different levels of c (Fig. 6B) which indicates that the collision-blocking model applies to this system. The average values of α_0 and B are given in Table IV.

Discussion

Mass transfer efficiency η and dimensionless numbers N . The mass transfer efficiency and the fraction of η determined by convection and diffusion increased with decreasing N_{pe} , i.e. with decreasing U (exp 2 and 4), decreasing cell size and decreasing collector size (exp. 4A versus exp. 5) (Table III). The fraction of η determined by convection and diffusion varied between 80 to 90% for the largest organism (*Rhodococcus* C125) and was 97% for the relatively small cells of *Ps. putida*. Compared to *Ps. putida*, the larger size of *Rhodococcus* C125 cells results in greater N_R and N_G values, which leads to greater relative contributions of sedimentation and Van der Waals attraction

(22, 23). The condition $N_{vdw} > 10^{-8}$ necessary for Van der Waals interactions to counterbalance hydrodynamic retardation (23) is met in all cases, but is irrelevant for these bacterial cells since attractive interactions between cell surface macromolecules and teflon, not included in eq. 1, dominate attachment (26, 28). The *Bacillus* CB1/sand system studied by Lindqvist and Enfield (15) deviated from our experiments by its low interstitial fluid velocity. Thus, η was high and dominated by convection and diffusion, and N_{pe} was relatively low.

Method of determining λ and α . The procedure of coupling α , determined as a function of t or V (method 2), to surface coverage data (Θ_{col}) is superior to estimation of λ and α from $\ln(c/c_0)$ - L plots obtained with different columns (method 1). The α - Θ_{col} analyses provide much more information than the other method, namely estimates of the clean bed collision efficiency α_0 and blocking factor B . Moreover, α obtained with the $\ln(c/c_0)$ - L method is in all cases lower than α_0 (Tables IV and V), and does therefore, at these c -levels, not provide a good estimate of α_0 . The α - Θ_{col} method requires a minimum column length $L > 7.5$ cm for systems with a high initial deposition as the teflon-grain columns used in this study (Figs. 3C and 4C). In this way, surface saturation that may be reached in the top of the columns does not significantly influence the total column result, and allows interpretation of the α - Θ_{col} plot.

Clean bed collision efficiency α_0 and blocking factor B . Values for α_0 of 0.82 to 0.83 observed for both bacterial species indicate close to favourable cell-solid interactions ($\alpha_0 = 1$) which confirmed previous findings obtained with hydrodynamically less defined batch systems (25, 26). For strain *Rhodococcus* C125, the increase of α_0 with N_{pe} indicates that shear forces help these cells to surmount a small energy barrier during deposition on teflon. This barrier appears to be completely counter-balanced in the PTFE/*Rhodococcus* C125 system ($\alpha_0 \approx 1$) for which N_{pe} is relatively high (Table III). A stimulation of deposition of *Rhodococcus* C125 and other cells by shear forces was also observed in previous studies (25, 26).

The blocking factor B differs strongly between the two bacterial strains at comparable interstitial fluid velocities (exp. 1, 3, and 4A; Table IV)). They

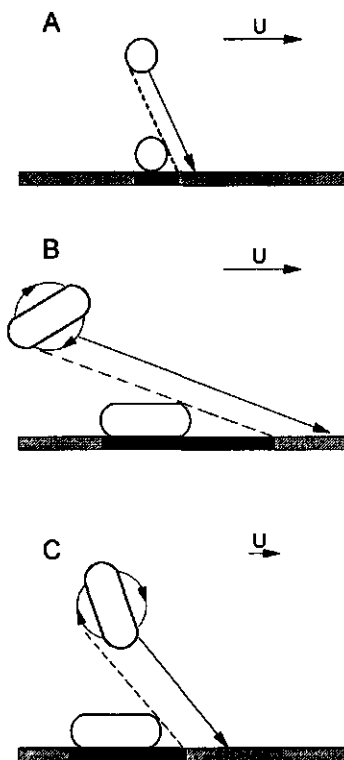


FIG. 7. Illustration of Hydrodynamic effects on blocking illustrated for *Ps. putida* (A) and *Rhodococcus* strain C125 (B) at comparable flow rates and for *Rhodococcus* strain C125 at lower flow rate (C). The blocked area is indicated by a black "shadow".

correspond to values for Θ_{\max} often reported in the particle deposition literature: 54%, as observed for *Ps. putida*, is the theoretical upper limit for random coating (1), whereas 8.3% (*Rhodococcus* C125) ($B \approx 12$) is not an exceptional value (9, 20, 29, 30). This contrast can at least partially be explained by the difference in the hydrodynamic/geometric properties a_b and N_{pe} . The *Ps. putida* cells are smaller than those of *Rhodococcus* C125 and exhibit a smaller N_{pe} value at the same flow rate (Table III). As a consequence, they diffuse faster, approach the collector surface in steeper trajectories, and are less hindered by the attached cells than *Rhodococcus* C125 (they have a smaller hydrodynamic "shadow" and consequently a smaller blocking factor (Fig. 7A and 7B)). For *Rhodococcus* C125, B depends on the hydrodynamic condition of the system: B increases with N_{pe} (Tables III and IV). N_{pe} is increased by reduction in U/ϵ (exp.

4A-C) or by choosing a larger collector (exp. 5). This phenomenon was well studied with polystyrene particles (10) and can also be qualitatively understood in terms of the shadow effect (Figs. 7B and 7C). A lower N_{pe} value gives steeper trajectories and a reduced blocking.

Factors having a non-hydrodynamic/geometric origin must also contribute to blocking, especially for the *Rhodococcus* C125 cells: for *Rhodococcus* C125 at $N_{pe} = 3.3 \times 10^{-4}$ (exp. 4c), B is more than a factor 4 higher than for *Ps. putida* at $N_{pe} = 7.2 \times 10^{-4}$ (exp 1 and 3) (Table IV). One of these factors may be a different extent in cell-cell electrostatic repulsion. At an ionic strength of 0.1 M, double layer repulsion is screened and (electro)steric interactions dominate (26, 27, 28). These are likely to be much more repulsive for *Rhodococcus* C125 than for *Ps. putida* since *Rhodococcus* C125 is coated with highly charged amphiphilic macromolecules ($\zeta = -50$ mV, at an ionic strength of 0.1 M) whereas *Ps. putida* has a non-polysaccharide cell surface with much less charge ($\zeta = -10$ mV) (27, 28). Increased blocking by particle-particle repulsion (1, 10) should therefore be much more pronounced for *Rhodococcus* C125 than for *Ps. putida*, which is consistent with our observations.

The different degree in cell-cell repulsion is probably also caused the dissimilar deposition behaviour of the two strains at coverages close to saturation. The deposition of *Rhodococcus* C125 was completely blocked (Fig. 4B), whereas multilayer attachment and possibly pore-clogging occurred for *Ps. putida*, as indicated by the increase in α with Θ at high coverage (Figs. 3A and 3C).

Both geometric and colloidal factors are consistent with the observation that *Rhodococcus* C125 is an extremely strong and *Ps. putida* is an extremely weak blocking strain. Blocking phenomena have important consequences for bacterial transport in porous media. The initial dispersal of different bacterial strains with identical α_0 and contrasting B is expected to be similar at low applied bulk cell concentrations and low surface coverages. However, great discrepancies will occur when higher surface coverages are reached, namely after a prolonged feeding with suspensions low in c or already after a short time

when high cell concentrations are applied. At coverages close to saturation, strong blocking cells will be freely transported and the hydraulic properties of the porous medium will hardly change. In contrast, weak blocking cells may start the forming multilayered biofilms which eventually will lead to significant hydraulic head loss and a pore-clogging/declogging mechanism governing the retention and migration of the bacteria (8, 11).

Applicability of the collision-blocking approach to natural porous media. The α_0 and B values (Fig. 6A and 6B) obtained from the literature data on *Bacillus*/sand breakthrough data (15) are similar for different levels of c , which demonstrates that collision and blocking also control the deposition in this system. Differences in breakthrough at different values of c is a phenomenon that is often observed but not accounted for in conventional microbial transport models (11, 13, 14, 15). The occurrence of blocking is further confirmed by the data of Lindqvist and Enfield (15). After injection with cell-free groundwater, a repeated feeding of a cell suspension to pre-saturated columns did not result in any further deposition. Since collision-blocking appear to be the deposition mechanism, eq. 5 applies to this system, i.e., $k = -7.0 \times 10^{-4} \text{ s}^{-1}$ and $dc/dt = -6.86 \times 10^{-5} (1 - 5.8 \Theta) c$.

The α_0 value of 0.098 for the experiment of Lindqvist and Enfield (15) is in the range reported for other (bio)colloids in systems with a low ionic strength like groundwater ($<0.01 \text{ M}$, (31)), in which electrostatic repulsion inhibits deposition and consequently keeps α_0 low (12, 16, 17, 19, 27). The value for N_{pe} is rather low, (Table III) and the blocking results can at best be compared with the *Rhodococcus* C125/PFA system with the lowest flow rate and N_{pe} -value (exp. 4C; Table III). The levels of B (Table IV) indicate that strain *Bacillus* CB1 is a strongly blocking organism, a feature that is confirmed by the unhindered transport through the sand columns after surface saturation as observed by Lindqvist and Enfield (15). It is likely that electrostatic cell-cell repulsion promoted the blocking in this low ionic strength system.

Conclusion. The collision-blocking concept applies to transport of microbes through coarse grain porous media in cases of strongly blocking cells

and weakly blocking cells under low-coverage conditions. Hence, an advection-dispersion equation extended with the deposition rate equation 5 should be used to model microbial transport for these systems. The collision-blocking concept provides an accurate mechanistic basis to describe bacterial transport by coupling it to colloid chemistry and particle deposition theory. In another paper we show that α_0 and B can be related to properties of the cell and solid surface and the ionic strength of the aqueous medium (24). Hence, bacteria can be considered as well characterizable biocolloids of which the mobility in subsurface and other environments can be reliably described and predicted.

References

1. Adamczyk, Z., B. Siwek and M. Zembala. 1992. Reversible and irreversible adsorption of particles on homogeneous surfaces. *Colloids Surf.* **62**:119-130.
2. Awasaki, T. 1937. Some notes on sand filtration. *J. Amer. Water. Works Assoc.* **29**:1591-1602.
3. Bales, R. C., S. R. Hinkle, T. W. Kroeger and K. Stocking. 1991. Bacteriophage adsorption during transport through porous media: chemical perturbations and reversibility. *Environ. Sci. Technol.* **25**:2088-2095.
4. Bosma, T. N. P., R. Kockelkoren, R. Kolhuis-Tanke, H. de Wilde, G. Schraa and A. J. B. Zehnder. in prep. Transport of introduced bacteria and biotransformation of organic compounds in saturated columns. .
5. Bouwer, E. J. and B. Rittmann. 1992. Comment on "use of colloid filtration theory in modeling movement of bacteria through a contaminated aquifer". *Environ. Sci Technol.* **26**:400-401.
6. Bouwer, E. J. and A. J. B. Zehnder. 1993. Bioremediation of organic compounds - putting microbial metabolism to work. *Trends in Biotechnology* **11**:360-367.
7. Corapcioglu, M. Y. and A. Haridas. 1984. Transport and fate of microorganisms in porous media: a theoretical investigation. *J. Hydrology* **72**:149-169.
8. Corapcioglu, M. Y. and A. Haridas. 1985. Microbial Transport in porous media: a numerical model. *Adv. Water Res.* **8**:188-200.
9. Dabros, T. and T. G. M. Van de Ven. 1983. A direct method for studying particle deposition onto solid surfaces. *Colloid Polym. Sci.* **261**:694-707.
10. Dabros, T. and T. G. M. Van de Ven. 1993. Particle deposition on partially coated surfaces. *Colloids and Surfaces A: Physicochemical and Engineering Aspects* **75**:95-104.
11. Dickinson, R. A. 1991. Problems with using existing transport models to describe microbial transport in porous media, p. 21-47. *In* C. J. Hurst (ed.), *Modeling the environmental fate of Microorganisms*, American Society of Microbiology, Washington DC.
12. Elimelech, M. and C. R. O'Melia. 1990. Kinetics of Deposition of Colloidal particles in porous media. *Environ. Sci. Technol.* **24**:1528-1536.
13. Gannon, J., Y. Tan, P. Baveye and M. Alexander. 1991. Effect of sodium chloride on

- transport of bacteria in saturated aquifer material. *Appl. Environ. Microbiol.* **57**:2497-2501.
14. Harvey, R. W. and S. P. Garabedian. 1991. Use of colloid filtration theory in modeling movement of bacteria through a contaminated aquifer. *Environ. Sci. Technol.* **25**:178-185.
 15. Lindqvist, R. and C. G. Enfield. 1992. Cell Density and Non-equilibrium sorption effects on bacterial dispersal in groundwater microcosms. *Microb. Ecol.* **24**:25-41.
 16. Martin, R. E., E. J. Bouwer and L. M. Hanna. 1992. Application of clean-bed filtration theory to bacterial deposition in porous media. *Environ. Sci. Technol.* **26**:1053-1058.
 17. Martin, R. E., L. M. Hanna and E. J. Bouwer. 1991. Determination of bacterial collision efficiencies in a rotating disk system. *Environ. Sci. Technol.* **25**:2075-2082.
 18. Matthess, G., A. Pekdeger and J. Schroeter. 1988. Persistence and transport of bacteria and viruses in groundwater- a conceptual evaluation. *J. Contam. Hydrol.* **2**:171-188.
 19. McDowell-Boyer, L. M., J. R. Hunt and N. Sitar. 1986. Particle transport through porous media. *Water Resources Research* **22**:1901-1921.
 20. Meinders, J. M., J. Noordmans and H. J. Busscher. 1992. Simultaneous monitoring of the adsorption and desorption of colloidal particles during deposition in a parallel plate flow chamber. *J. Colloid Interf. Sci.* **152**:265-280.
 21. Moran, D. C., M. C. Moran, R. S. Cushing and D. F. Lawler. 1993. Particle behaviour in deep-bed filtration: part 1-Ripening and Breakthrough. *J. Am. Water Works Assoc.* **85**:69-93.
 22. Rajagopalan, R. and C. Tien. 1976. Trajectory analysis of deep bed filtration with the sphere-in-cell porous media model. *J. Am. Inst. Chem. Eng.* **22**:523-533.
 23. Rajagopalan, R. and C. Tien. 1979. The theory of deep bed filtration, p. 169-268. *In* R. J. Wakeman (ed.), *Progress in Filtration and Separation Science*, Elsevier, Amsterdam.
 24. Rijnaarts, H. H. M., E. J. Bouwer, W. Norde, J. Lyklema and A. J. B. Zehnder. in prep. Bacterial deposition in porous media: effect of cell-solid and cell-cell interactions at different ionic strengths. *ES&T or Coll. Surf.*:B.
 25. Rijnaarts, H. H. M., W. Norde, E. J. Bouwer, J. Lyklema and A. J. B. Zehnder. 1993. Bacterial adhesion under static and dynamic conditions. *Appl. Environ. Microbiol.* **59**:3255-3265.
 26. Rijnaarts, H. H. M., W. Norde, E. J. Bouwer, J. Lyklema and A. J. B. Zehnder. submitted. Mechanism and reversibility of bacterial adhesion. *Colloids Surf. B: Biointerf.*
 27. Rijnaarts, H. H. M., W. Norde, J. Lyklema and A. J. B. Zehnder. in prep. Steric and DLVO interactions in bacterial adhesion. *ES&T or Coll. Surf.*:B.
 28. Rijnaarts, H. H. M., W. Norde, J. Lyklema and A. J. B. Zehnder. submitted. The isoelectric point of bacteria as an indicator for the presence of cell surface polymers that inhibit adhesion. *Biochim. Biophys. Acta.*
 29. Sjollem, J. and H. J. Busscher. 1990. Deposition of polystyrene particles in a parallel plate flow cell. 2. pair distribution functions between deposited particles. *Colloids Surf.* **47**:337-352.
 30. Sjollem, J., A. H. Weerkamp and H. J. Busscher. 1990. Deposition of oral streptococci and polystyrene latices onto glass in a parallel plate flow cell. *Biofouling* **1**:101-112.
 31. Stumm, W. and J. J. Morgan. 1981. The solid-solution interface, p. 599-684. *In* *Aquatic Chemistry: an Introduction Emphasizing Chemical Equilibria in Natural Waters*, John Wiley & Sons, New York.
 32. Updegraff, D. M. 1991. Background and practical applications of microbial ecology, p.

- 1-20. In C. J. Hurst (ed.), Modeling the environmental fate of Microorganisms, American Society of Microbiology, Washington DC.
33. Van der Meer, J. R., T. N. P. Bosma, W. P. De Bruin, H. Harms, C. Holliger, H. H. M. Rijnaarts, M. E. Tros, G. Schraa and A. J. B. Zehnder. 1992. Versatility of soil column experiments to study biotransformation of halogenated compounds under environmental conditions. *Biodegradation* 3:265-284.

Chapter 7

Bacterial Deposition in Porous Media: Effects of Cell-Coating, Substratum Hydrophobicity, and Electrolyte Concentration

Huub H.M. Rijnaarts, Willem Norde, Edward J. Bouwer, Johannes Lyklema and
Alexander J.B. Zehnder

Submitted for publication to Environmental Science & Technology

Deposition of seven bacterial strains on spherical glass and teflon collectors was studied in vertical down flow columns at an ionic strength (I) of 0.1 M. The various bacteria had either one of the following types of major cell-surface constituents: non-polysaccharide (NP), amphiphilic (AMPH), or anionic polysaccharide (AP) macromolecules. Deposition was analyzed in terms of the clean bed collision efficiency α_0 (the probability of a cell to attach upon reaching a substratum free of cells), and a blocking factor B (the ratio of the area blocked by an attached cell to the geometric area of a cell). The value of α_0 decreased from 1.0 to about 0.01 in the following order of cell-surface constituents/collector combinations: NP/teflon and AMPH/teflon > NP/glass > AMPH/glass, AP/teflon, and AP/glass. The value for B , at a Peclet-number of 1×10^6 , increased from about 3 to 18 in the order NP/low cell charge < NP or AMPH/high cell charge < AP/high cell charge. This indicates that cell-cell repulsion enhances blocking. Blocking is higher on teflon than on glass. Most likely cell-surface macromolecules adsorb in the surroundings of the attached cells and enhance blocking on teflon. The deposition of four bacterial strains was investigated at $0.0001 \text{ M} \leq I \leq 0.1 \text{ M}$. For I -values smaller than a critical level, α_0 decreased with decreasing I . The critical I is determined by the range over which cell-surface macromolecules can penetrate the repulsive Gibbs-energy barrier between cell and solid. The value for B increases about one order of magnitude upon changing I from 0.1 M to 0.001 M. Maximal control of microbial mobility in porous media can be reached in systems for which B and α_0 are high at high I (0.1 M): the high B -value minimizes the occurrence of pore-clogging whereas the dependencies of α_0 and B on I allow manipulation of deposition by varying the ionic strength.

Introduction

Control of microbial transport and retention in porous media is required for (i) successfully applying techniques for groundwater bioremediation (5, 28, 37, 38), (ii) for protection of subsurface drinking water resources against contamination by pathogens (23), and (iii) for assessing the risk of dispersing chemicals by biocolloid facilitated transport upon introducing bacteria in aquifers (24). Research previously performed in our laboratories revealed the basic mechanisms of bacterial deposition in non-porous (22, 29, 30, 31, 32) and porous media systems (21, 28). The primary aim of the present study is to link these mechanisms into a comprehensive quantitative expression of the rate of bacterial deposition in porous media.

This investigation is limited to coarse grain media, where the bacterial radius a_b (m) is much smaller than the grain radius a_s (m), i.e., $N_R = a_b/a_s \ll 0.05$. Under this condition, mechanical entrapment (straining) of bacteria does not occur and deposition controls initial cell removal from the fluid phase during transport (26, 27, 28).

Bacterial deposition is determined by two processes: (i) the transfer of particles from bulk water to the grain (collector) surface, and (ii) adhesion. Colloid filtration theory was used to quantify these two processes in terms of the single collector mass transfer efficiency η (the probability of an approaching particle to reach the collector surface), and the adhesion or collision efficiency α (the probability of a particle to attach upon reaching the surface) (13, 22, 26, 27, 28). The adhesion efficiency α is a function of the fractional surface coverage Θ ($\Theta = (\text{number of deposited cells}) \times \pi a_b^2 / A_{col}$, with A_{col} the total surface area present in the porous medium column) (28):

$$\alpha = \alpha_0(1 - B\Theta) \quad (1)$$

Here, α_0 is the clean bed collision efficiency ($\Theta = 0$) and B the blocking factor. The initial collision efficiency α_0 is determined by cell-solid interactions which are determined by the following factors: (i) the type of cell-coating and the substratum hydrophobicity (1, 3, 6, 7, 12, 15, 17, 19, 29, 30, 31, 41, 42), (ii)

the amount of negative charge on the solid and the bacterial surface and the ionic strength (I) of the medium (13, 16, 17, 18, 19, 22, 25, 29, 32, 33, 34, 36, 40, 42), and (iii) the range over which cell-surface macromolecules can penetrate the Gibbs energy barrier that exists between bacterium and solid phase (32). When these interactions do not inhibit deposition, $\alpha_0 = 1$.

The blocking factor B accounts for the screening of a part of the solid surface by attached cells. It is defined as the ratio of the area blocked by an attached cell to the geometric area of that cell (11, 28). It is related to the maximum surface coverage Θ_{\max} for single layer adhesion: $\Theta_{\max} = 1/B$. Blocking is primarily controlled by hydrodynamic factors and by cell-cell interactions (11, 28). Repulsive cell-cell interactions may significantly enhance blocking (2, 11, 28, 36). These interactions may be of an electrostatic or non-electrostatic nature (28, 32) and depend on the type of cell-coating and the ionic strength of the medium. Blocking may be substantial: B may vary between values of 1.5 to more than 20, depending on the hydrodynamic condition and colloid-chemical properties of the system (10, 28, 36).

Bacterial transport in systems without clogging can be quantitatively described by the advective-dispersion equation and the following deposition rate term (28):

$$-\frac{dc}{dt} = G \frac{d\Theta}{dt} = kc\alpha_0(1 - B\Theta) \quad (2)$$

where geometry factor G (m^{-3}) and mass transfer coefficient k (s^{-1}) are defined as $G = 3(1/\epsilon - 1)/(\pi n_s a_b^2)$ and $k = 3/4 (1/\epsilon - 1)U\eta/a_s$, respectively. Here, ϵ is the porosity, U ($m s^{-1}$) is the velocity of the fluid phase which enters the column and η ($kg m^{-1} s^{-1}$) is the dynamic viscosity of the fluid phase. In the present study, column experiments were performed with teflon and glass spherical collectors and seven bacterial strains possessing a range of cell-surface constituents (30). The primary aim is to determine the dependencies of α_0 and B on three important factors influencing adhesion: (i) the type and structure of the cell-coating, (ii) the hydrophobicity of the substratum, and (iii) the ionic strength of the aqueous phase.

Materials and methods

Aqueous media. Phosphate Buffered Saline solutions (PBS) (pH = 7.2) with *I* varying between 0.0001 and 0.1 M were previously described (30).

Bacteria. The microorganisms used are listed in Table I, and their following characteristics have been described in other papers: (i) the origins of the strains and the procedures for cultivation and preparation (30), (ii) the effective cell radii, diffusion constants, and cell surface hydrophobicities (30), (iii) the negative zeta-potential at pH 7 at various *I* (32), (iii) the isoelectric points and type of macromolecular cell-coating (31), and (iv) the range over which the cell-surface macromolecules can penetrate electrostatic barriers (32).

TABLE I. Designations and types of macromolecular cell-coating for the bacteria studied.

Strain	Other designation ^a	type of cell-coating ^d
Coryneform bacteria:		
C1	<i>Arthrobacter</i> sp. strain DSM 6687	AP
C3	<i>Rhodococcus</i> sp. strain C125	AMPH-II
C4	<i>Rhodococcus erythropolis</i> A177	AMPH-I
C5	<i>Corynebacterium</i> sp. strain DSM 6688	NP
C6	<i>Corynebacterium</i> sp. strain DSM 44016	NP
Pseudomonads:		
P3	<i>Pseudomonas</i> sp. strain B13	AP
P4	<i>Pseudomonas putida</i> mt2	NP

^aThe sources of organisms other than DSM or ATCC strains are described by Rijnaarts et al. (30).

^bThe types of macromolecular cell-coating were deduced in a previous study (31). The following types can be discriminated: AP, anionic polysaccharide; AMPH-I, amphiphilic macromolecules of which the hydrophilic parts dominate interactions with all solid surfaces; AMPH-II, amphiphilic macromolecules of which the hydrophilic parts dominate interactions with hydrophilic surfaces and the hydrophobic parts control the interactions with hydrophobic surfaces; NP, non-polysaccharide cell-coating.

Collectors and columns. Spherical collectors of PFA-teflon and glass and procedures for cleaning the collectors and packing of the columns are described elsewhere (30). The collector radii were $190 \pm 50 \mu\text{m}$ for teflon and 225 ± 25 for glass. The columns had an internal diameter of 1.00 cm, the porous bed length L was 9 ± 0.3 cm and the porosity ϵ was 0.34 ± 0.02 (28).

Experiments. Experiments were conducted in duplicate with vertical down-flow columns. Bacterial suspensions in PBS with an OD_{280} value of 0.6 were prepared by diluting samples of concentrated stock suspensions. The resulting suspensions varied in cell concentration c_0 between 3×10^7 cells cm^{-3} and 5×10^8 cells cm^{-3} , depending on the strain used. These were applied to the columns by a peristaltic pump. The flow rate was kept constant for each column but varied between 16 and 21 cm^3 for different columns. The effluent cell concentration c , as measured by OD_{280} , was monitored with time. The level of c_0 (OD_{280}) was found to be constant throughout each experiment. The columns were operated for two hours.

Two types of experiments were performed with both glass and teflon collectors: (i) experiments at $I = 0.1$ M with all bacterial strains listed in Table I, and (ii) experiments with strains C3, C6, P3 and P4, at ionic strengths varying between 0.0001 M and 0.1 M.

Determination of α and Θ . The collision efficiency α and the average coverage Θ were experimentally determined from the breakthrough response of bacterial cells. The computational procedures were described in a preceding paper (28).

Parameters for the calculations. The Hamaker constant $A_{bs(w)}$ for the solid-water-bacterium system was assigned a value of 2×10^{-22} J for teflon and 6.2×10^{-21} J for glass (29). The radii and diffusion coefficients of the bacteria were determined in previous research (30).

Results

The breakthrough curves of strains C1, C5, and C6, at $I = 0.1$ M are shown in Fig. 1A. The corresponding α_0 -values (Fig. 1B) were higher for teflon than for

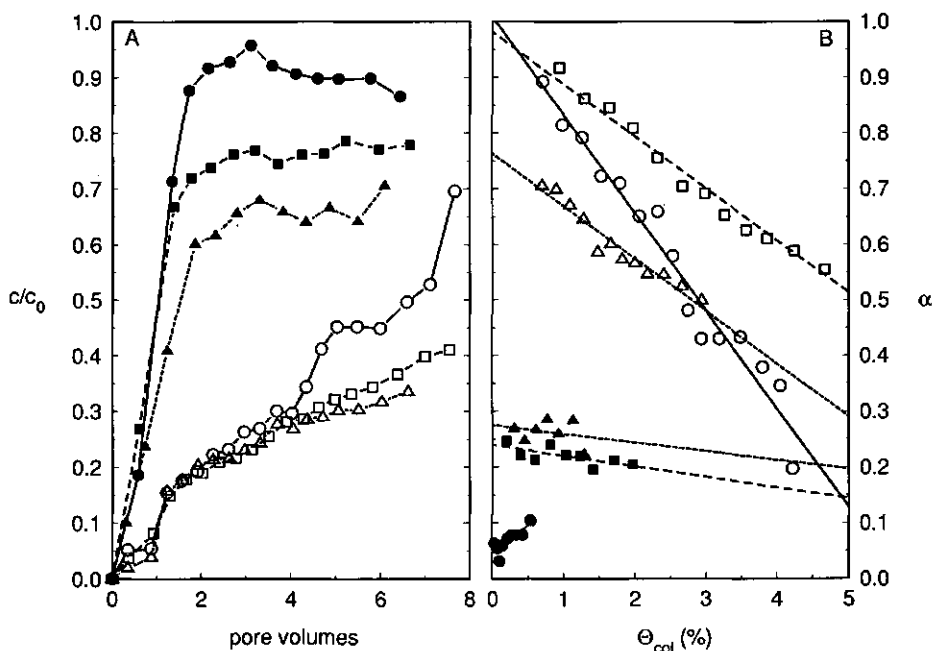


FIG. 1. Breakthrough curves (A) and α - Θ plots (B) for the strains C1 (circles), C5 (squares), and C6 (triangles) for columns with glass (filled symbols) and teflon (open symbols) collectors and $I = 0.1$ M.

Table II. Experimental values of the clean bed collision efficiency α_0 , and the blocking factor B at an ionic strength of 0.1 M, listed in the order of increasing α_0 and decreasing B .

Cell-coating ^a	strain	Glass		Teflon	
		α_0	B	α_0	B
AP	P3	0.02 ± 0.01	ND ^b	0.013 ± 0.006	ND
AP	C1	0.05 ± 0.02	NEG ^c	1.00 ± 0.04	17.4 ± 1.0
AMPH-I	C4	0.012 ± 0.005	ND	0.09 ± 0.02	ND
AMPH-II	C3	0.021 ± 0.010	ND	0.83 ± 0.01	10.7 ± 1.0
NP	C6	0.28 ± 0.01	8.2 ± 0.7	0.77 ± 0.02	12.5 ± 0.3
NP	C5	0.24 ± 0.01	8.1 ± 1.4	0.98 ± 0.03	9.5 ± 0.1
NP	P4	0.12 ± 0.01	2.9 ± 2.9	0.83 ± 0.02	2.5 ± 0.9

^a Abbreviations for the types of cell-coatings as in Table I. ^bND, could not be determined because of data scatter and c/c_0 -values close to unity. ^cNEG, a negative B -value was obtained as a result of an effect opposite to blocking, i.e. α increases with increasing Θ .

glass. The adhesion efficiency α decreased with Θ except for strain C1 on glass where α increased with Θ . Values of α_0 and B were deduced from the α - Θ plots by linear regression analysis for all bacterium/solid combinations tested at $I = 0.1$ M (Table II). No reliable estimates of B could be obtained for the low deposition cases ($\alpha_0 < 0.1$), since α is very sensitive to c/c_0 at c/c_0 -levels close to unity.

Typical examples of results of deposition experiments at various ionic strengths are Figs. 2A and 2B, where breakthrough curves and α - Θ plots of strain C3 and teflon are shown. Initial deposition (α_0) decreased and the slope of the α - Θ plots varied with I . The variation between the duplicates gives a good impression of the reproducibility, which is generally satisfactory. An exception is

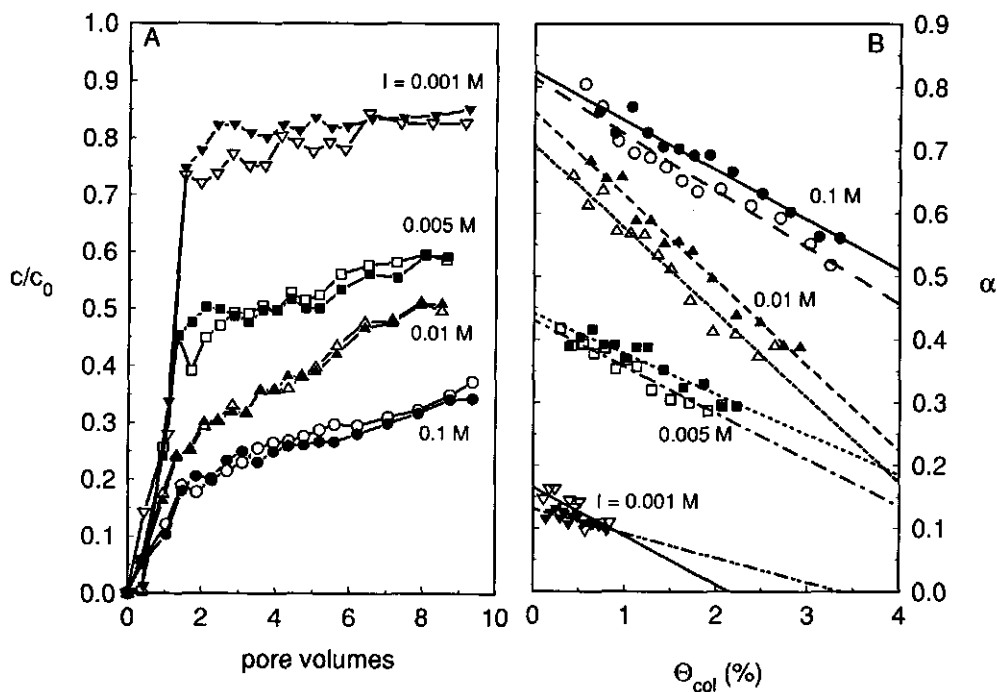


FIG. 2. Breakthrough curves (A) and α - Θ plots (B) for strain C3 and columns with teflon collectors at various ionic strengths I . Filled and open symbols indicate duplicate results.

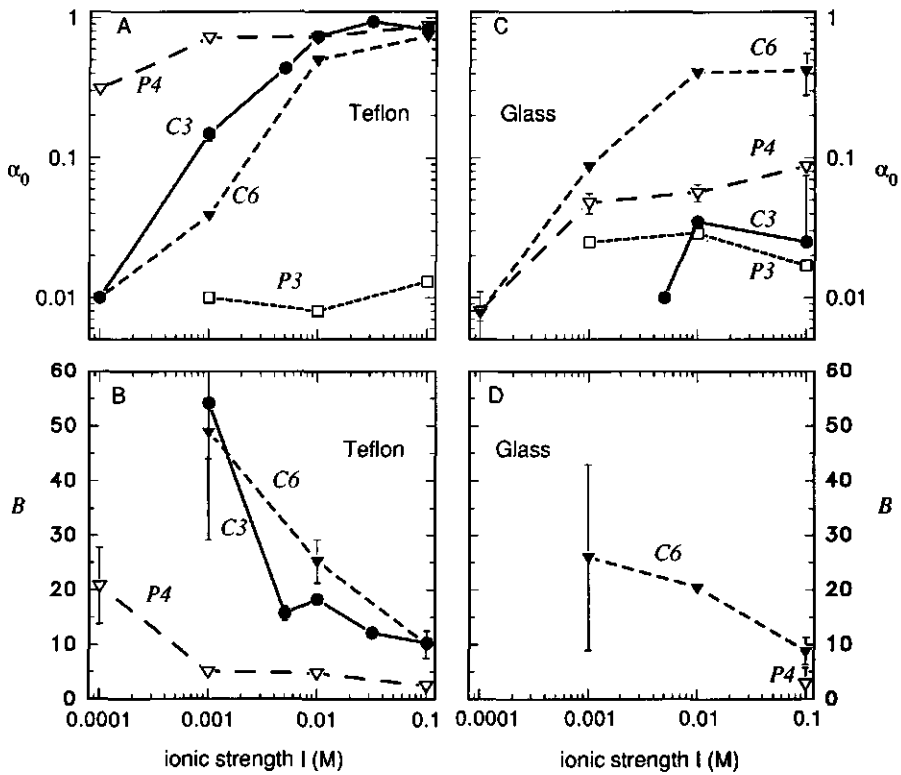


FIG. 3. The clean bed collision efficiency α_0 (A and B) and blocking factor B (C and D) as a function of the ionic strength I for strains C3, C6, P3, and P4 in columns with glass and teflon collectors.

the low deposition case at $I = 0.001$ M where the uncertainty in B exceeds 50% of the average value.

The dependencies of α_0 and B on I are shown in Fig. 3A to 3D for all the cases tested. The α_0 -values of strains C3 and C6 on teflon decreased in a similar way with decreasing I (Fig. 3A), whereas for strain P4 and P3 the values were hardly influenced by I . The deposition efficiencies of strain P3 were much lower than those of the other strains. The blocking factor B of strains P4, C3, and C4, displayed an I -dependency opposite to that of α_0 (Fig. 3B): B increased

with decreasing I . The low deposition of strain P3 prevented an estimation of B .

The initial collision efficiency α_0 was smaller on glass (Fig. 3C) than on teflon, except for strain P3. The difference between glass and teflon was most pronounced for the P4 and C3 cells. Values of B on glass could only be estimated for strain C6 at $I \geq 0.001$ M and for strain P4 at $I = 0.1$ M (Fig. 3D); B increased with decreasing I for strain C6.

Discussion

Effect of type of cell-coating and substratum hydrophobicity on the clean bed collision efficiency α_0 at $I = 0.1$ M. The α_0 -value corresponds to a Gibbs energy barrier or activation energy for adhesion ΔG^\ddagger_0 (J) (29), i.e., $\Delta G^\ddagger_0/kT = -\ln(\alpha_0)$ (k (J K⁻¹) is the Boltzmann constant, T (K) is the absolute temperature). This parameter is completely determined by steric interactions between the cell-surface macromolecules and the substratum at $I = 0.1$ M (32). The steric hindrance, as indicated by ΔG^\ddagger_0 , is clearly related to the composition of the cell-coating, see Fig. 4. It decreases (ΔG^\ddagger_0 increases) upon changing from coatings of the anionic polysaccharide (AP) type via AMPH to NP. Quantitatively, these

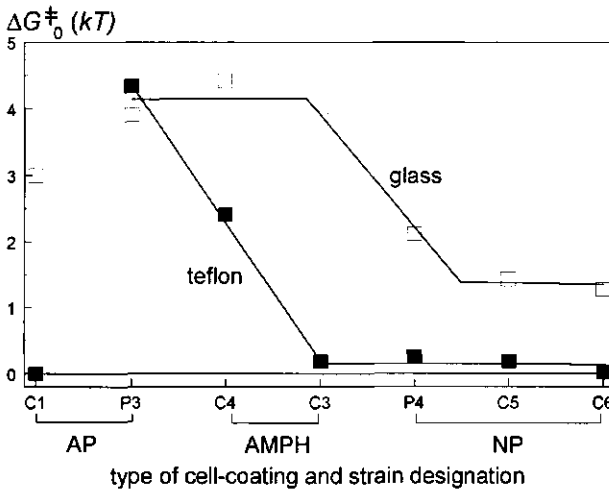


FIG. 4. The activation energy (ΔG^\ddagger_0) for initial deposition at $I = 0.1$ M, derived from α_0 -values (29), as a function of type of cell-coating, for columns with glass (open symbols) or teflon (filled symbols) collectors. Strain designations refer to Table I.

Table III. The normalized blocking factor B^* on glass and teflon at an ionic strength of 0.1 M, for some of the organisms tested. The type of cell-coating, and the zeta-potential ζ of the bacteria at an ionic strength of 0.1 M, are also listed.

Strain	cell-coating ^a	ζ , mV ^b	B^* ^c	
			glass	teflon
C1	AP	38	NEG ^d	17.8 ± 1.0
C3	AMPH-II	50	ND ^e	10.4 ± 1.0
C6	NP	42	8.1 ± 0.7	14.0 ± 0.3
C5	NP	28	7.0 ± 1.3	9.5 ± 0.1
P4	NP	11	3.0 ± 3.0	2.7 ± 1.0

^a Abbreviations for types of cell-coatings as in Table I.

^b The values of ζ were collected from reference (32).

^c Blocking was normalized to a Peclet-number of 1×10^6 .

^d ND, could not be determined because of data scatter and c/c_0 -values close to unity.

^e NEG, a negative B -value was obtained as a result of an effect opposite to blocking, i.e. α increases with increasing Θ .

trends also depend on the substratum hydrophobicity (Fig. 4) for all but one bacterium/collector combination. Low or absent steric hindrance is observed for non-polysaccharide cell-coatings combined with a hydrophobic substratum (Fig. 4). Strain C1 on teflon is an exception. In contrast to other anionic polysaccharide cell-coatings like that of P3, the anionic cell surface polyelectrolytes of C1 adsorb readily on teflon and make initial adhesion on this substratum 100% efficient.

Effect of type of cell-coating and substratum hydrophobicity on the blocking factor B at $I = 0.1$ M. Blocking is determined by hydrodynamic factors and by cell-cell interactions (11, 28). The Peclet-number N_{pe} , which is the ratio of convection to diffusion, defines the hydrodynamic condition during deposition (28):

$$N_{pe} = 2 U a_s / D_b \quad (3)$$

where D_b ($m^2 s^{-1}$) is the diffusion coefficient of the bacterium. Blocking

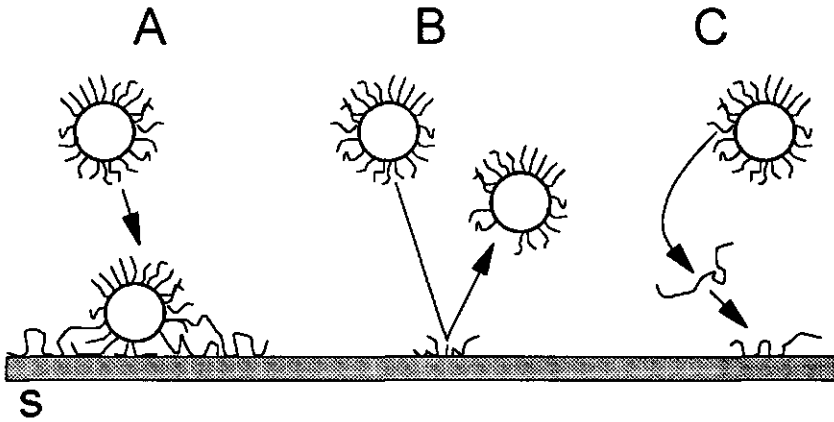


FIG. 5. Different mechanisms of transfer of bacterial surface macromolecules to solid substrata. A: adsorption in the surroundings of an attached cell. B: transfer by a collision of the cell with the substratum. C: excretion and adsorption without cell-solid contact.

increases with increasing N_{pe} (11, 28). The Peclet-number varied between 6×10^4 and 1.8×10^5 among the different column tests due to small differences in collector radius, bacterial radius, and interstitial fluid velocity U . The blocking data were made comparable by normalizing them to $N_{pe} = 10^5$ according to:

$$B^* = \frac{a + b}{a 10^{-5} N_{pe} + b} B \quad (4)$$

where B^* is the normalized blocking factor. The constants a and b can be derived experimentally when the $B-N_{pe}$ dependency is linear over the N_{pe} range studied as was demonstrated for strain C3 on teflon (28) ($a = 2.9 \pm 0.2$ and $b = 7.3 \pm 0.2$). These values of a and b were used for normalizing all blocking results obtained at $I = 0.1$ M (Table III). The B^* -values for strains C5 and C6 show that blocking on glass is less pronounced than on teflon, suggesting that cell-solid interactions influence B^* in addition to cell-cell interactions. A likely explanation is that cell-surface macromolecules adsorb during adhesion (29). Their affinity for the solid phase and, as a consequence their tendency to stretch along the solid-liquid interface (Fig. 5A), increases with increasing

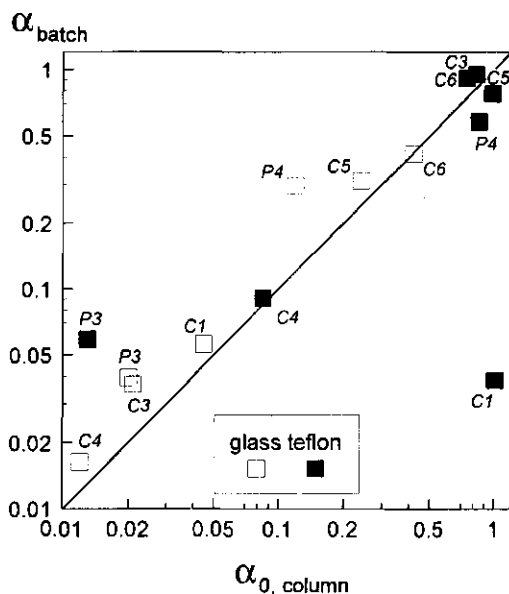


FIG. 6. Comparison of collision efficiencies in static batch systems, collected from reference (29), with that of column systems (α_0), at an ionic strength of 0.1 M. The solid line indicates $\alpha_{0, \text{column}} = \alpha_{\text{batch}}$. The strain designations refer to Table I.

substratum hydrophobicity (4, 14, 39). As a result, the adsorbed polymers cause greater blocked areas on teflon than on glass.

The magnitude of B' increased in the order of increasing cell-surface charge and decreasing cell hydrophobicity (Table III), namely: low charged non-polysaccharide coating (strain P4) < highly charged non-polysaccharide or amphiphilic coating (strains C3, C5 and C6) < highly charged cells covered with anionic polysaccharide (C1). This is consistent with increases in steric and electrosteric (cell-cell) repulsion as cell-surface charge increases and cell hydrophobicity decreases (31, 32).

Blocking is exceptional for strain C1 on glass and teflon (Figs. 1A and 1B; Tables II and III). On teflon, this strain displays the strongest blocking among all bacterium/collector combinations studied. The adsorbed anionic polysaccharide tails appear to form large blocked areas on teflon (Fig. 5A). On glass, the initial deposition is very low, but the deposition becomes more favourable during the

course of the experiment which is most likely due to the formation of a conditioning macromolecular layer according to mechanisms shown in Figs. 5A and 5B. Polymer excretion and adsorption without cell-solid contact (Fig. 5C) is not likely to play a role for the systems studied here (30).

Comparison of the adhesion efficiency in porous media and in static batch systems at $I = 0.1 \text{ M}$. The trend in Fig. 4 confirms previous observations on deposition of bacteria on flat sheet-collectors in batch systems (29). Comparison of the batch and column derived values of α (Fig. 6) shows good agreement (same order of magnitude) for all but one bacterial/collector combinations. The column results should be considered more reliable than the batch results because columns provide better defined hydrodynamic conditions and allow the determination of B . However, the reasonable correlation between α_{batch} and α_0 indicates that blocking was not a major factor influencing the batch results. This was the consequence of diffusion controlling particle transport in the batch system which is a random non-directional process which excludes blocking according to a "hydrodynamic shading" mechanism (28) (Fig. 7B).

A great discrepancy between batch and column results was only observed for strain C1 on teflon (Fig. 6). Possibly the adsorption of the surface polymers of this organism caused a substantial blocking under static batch conditions.

Effect of the ionic strength. Previous investigations with static batch systems demonstrated that cell-surface macromolecules can penetrate the repulsive double-layer barriers between cells and solids (32). Most bacterial surface polymers can reach the substratum at high I . For example, at an I of 0.1 M , α_0 is at its maximum and controlled by steric interactions (Fig. 7A). The separation between the bacterial and solid surface created by the electrostatic barrier becomes wider upon decreasing the ionic strength. Below a certain critical ionic strength level I_s , the number of the cell-surface macromolecules that are not long enough to reach the substratum increases with decreasing I . As a consequence, double layer repulsion reduces α_0 with decreasing I at $I < I_s$ (Fig. 7C).

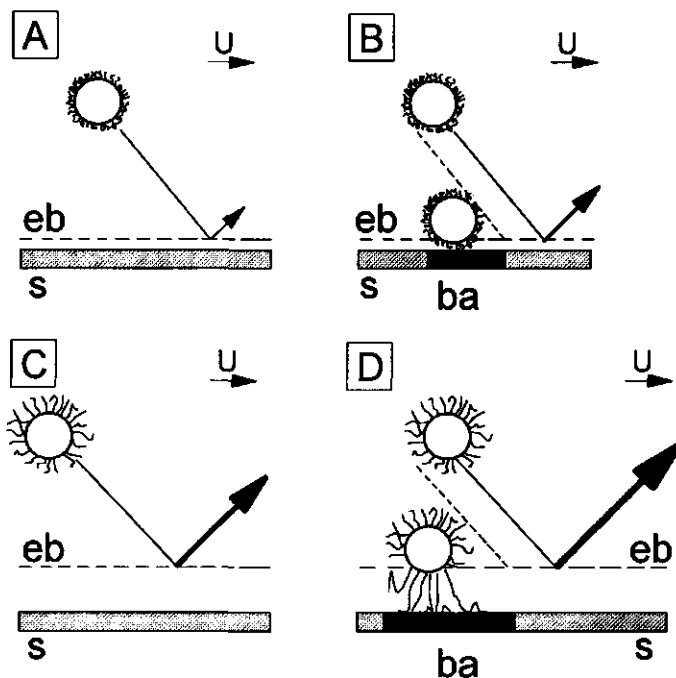


FIG. 7. Illustration summarizing the ionic strength effects on bacterial deposition. The escape probability is indicated by the arrows directed away from the substratum: a small arrow indicates a low escape probability (high collision efficiency α) whereas a thick and long arrow indicates a high escape probability (low α). **High ionic strength:** **A.** Cell-surface macromolecules can penetrate the electrostatic barrier (eb) and can easily reach the substratum (s) which results in a maximum α . **B.** Blocking is at minimum as a result of minimal cell-cell repulsion. Nevertheless, the blocked area (ba) reduces α . **Low ionic strength:** **C.** Most cell-surface macromolecules cannot reach the substratum (s) which results in a contribution of double layer repulsion; α_0 decreases (escape probability increases) with decreasing I . Some cells can still attach. **D.** Electrostatic cell-cell repulsion is increased, which causes an enhanced blocking and an additional reduction in α .

The initial collision efficiency (α_0) is shown as a function of I for the strains C3, C6, P3 and P4 in Figs. 3A and 3C. At high ionic strength, deposition depends on the type of cell-coating and substratum as discussed above (Fig. 4). Additional differences in deposition behaviour among these strains occur at lower ionic strengths due to differences in the structure of the cell surface.

The initial deposition of strain P3 is low and hardly influenced by the I (Figs. 3A and 3B). This is consistent with the anionic polysaccharides of this

strain capable of penetrating more than 50 nm into the electrostatic barrier region between cell and solid and thus inhibiting deposition even at an ionic strength as low as 0.001 M (32). The extension of the cell surface macromolecules of the strains C3 and C6 vary between 25 and 60 nm, depending on the type of substratum, and yield I_s -levels of about 0.01 M (32). Similar I_s -values were observed in the column porous media (Figs. 3A and 3C). The structures on the cell-surface of the pseudomonad P4 can bridge a teflon-cell separation of 165 nm (32). As a consequence, inhibition of deposition by double layer repulsion only occurs at $I < 0.001$ M. This was also observed in the columns (Fig. 3A). For strain P4 on glass, the I_s -value in columns is 0.001 M (Fig. 3B) and that in batch is 0.01 M (32). Disregarding the latter discrepancy, the results indicate that the extension and chemical nature of bacterial surface macromolecules exert a similar influence on the initial deposition in dynamic (columns) and static (batch) systems at ionic strengths between 0.1 M and 0.0001 M.

Blocking increases with decreasing ionic strength (Figs. 3B and 3D), i.e., with increasing electrostatic repulsion between adhered and depositing cells (Fig. 7D). The electrostatic effect is further demonstrated by the increase in B with decreasing I being more pronounced for the highly charged strains C3 and C6 than for the weakly charged P4 cells (Table III; Fig. 3A). These observations confirm predictions and findings of others (11, 28, 36).

In general, the ionic strength influenced bacterial deposition by affecting both the initial adhesion efficiency α_0 and the blocking factor B : α_0 decreases (Figs. 7A, 7C, 3A, and 3C) and B increases with decreasing I (Figs. 7B, 7D, 3B, and 3D). Both effects cause a reduction of α upon decreasing I (eq. 1).

Relevance for microbial mobility in porous media. The parameters α_0 and B characterize the first two steps of bacterial accumulation at solid-liquid interfaces: (i) the initial deposition (α_0) and (ii) the level of surface saturation that can be reached (B). Since B indicates the extent of cell-cell interactions it may also provide information on bacterial deposition at surface coverages close to or beyond saturation. Weakly blocking bacterial species will form multiple cell

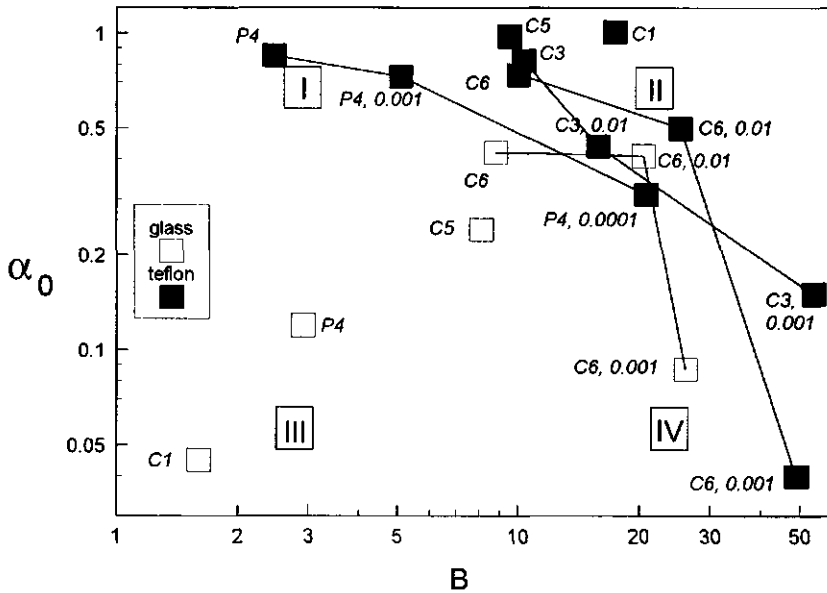


FIG. 8. Clean bed collision efficiency α_0 as a function of blocking factor B . This figure summarizes all deposition data. The bacterium/substratum/ionic strength combinations in sectors I to IV display a different deposition and transport behaviour as explained in the text. The number after the strain designation indicates the ionic strength. When no number is given $I = 0.1$ M.

layers at higher coverages and therefore tend to clog a porous medium after prolonged application of the cell-suspension (28). In contrast, the deposition of strongly blocking organisms stops after saturation of the surface. This prevents clogging and allows newly introduced cells to be transported down-gradient throughout the porous medium (20, 28).

An evaluation of the mobility of the different bacterial species in the model porous media can be illustrated using an α_0 - B plot (Fig. 8) that is divided into four regions. Region I comprises bacterium/collector combinations with a high α_0 - and a low B -value which cause fast deposition to a high coverage level. A continued feeding of a cell-suspension with region I characteristics would cause multiple cell-layers to form and eventually lead to pore-clogging. This was demonstrated to occur for strain P4 on teflon (28). Region II contains

bacterium/collector combinations with a fast initial deposition, but strong blocking will result in low final coverages, resulting in an absence of clogging and an unhindered microbial transport through the porous medium after surface saturation. This was observed with strain C3 and a *Bacillus* species in columns packed with teflon collectors (28) and sand-grains (20), respectively. Region III includes the bacteria with a slow deposition (low α_0 -value) that can reach high coverages because B is low; they may even cause pore-clogging after a prolonged input of a cell-suspension. Sector IV contains the cases for which deposition is highly unfavourable due low α_0 and high B .

Although the boundaries between the different sectors in Fig. 8 cannot be fully established with the data, it appears that most bacterium/collector combinations studied fall into regions II and IV which are considered to be non-clogging systems. Bacterial transport in such systems can be quantitatively described by an advective-dispersion equation extended with the deposition rate term (28) given by eqn 2. Variation of the ionic strength can be used to influence microbial mobility (i.e. cause a shift from sector II to IV). The bacterium/collector combinations in regions I and III may be considered as clogging systems. Microbial transport can only be quantitatively described with eq. 2 for low coverage conditions before the formation of multiple cell-layers. Reduction in I may shift the system to non-clogging where microbial mobility is increased. A shift to sector II or IV is therefore caused, as shown for strain P4 on teflon (Fig. 8).

Plots similar to Fig. 8 may be helpful to assess the mobility of pathogens, beneficial microorganisms and genetically engineered bacteria in natural and engineered systems. For instance, such a plot constructed with data obtained with aquifer and sediment grains in combination with a bacterial dispersal model that includes eq. 2 will greatly facilitate the selection of an appropriate organism and suitable ionic strength for seeding a contaminated aquifer with a bacterium specialized in degrading a specific pollutant.

The results presented here were obtained under non-growth conditions. In practice, growth will often occur after or simultaneously with deposition (9, 35).

Since the blocking factor is indicative for cell-cell interactions, B may be of relevance for ascertaining the ease at which deposited cells can grow into a stable biofilm. A first confirmation of this hypothesis is that *Pseudomonas* strains similar to the weakly blocking *Ps. putida* (P4) are known to colonize surfaces rapidly and to form stable biofilms (8).

Conclusion

Bacterial deposition in porous media can be adequately described with the clean bed adhesion efficiency α_0 and blocking factor B under low coverage conditions. The dependencies of these parameters on factors like the type and length of cell-surface macromolecules, substratum hydrophobicity, and ionic strength, provide ample possibilities to manipulate microbial mobility in soil, aquifers, and biofilm reactors. Furthermore, B appears to be a suitable characteristic to discriminate between microorganisms that are capable of pore clogging at higher attached cell-concentrations and those that can be transported freely after surface saturation. The relationship between B and the occurrence of pore clogging and formation of biofilms emerge as primary subjects for further research. The relationships between the deposition parameters α_0 and B and cell-coating, substratum hydrophobicity, and ionic strength hypothesized from the present study, should be further explored using a broader range of different bacteria and various natural and man-made materials. This would greatly facilitate and improve the assessment of the mobility and retention of bacteria in natural and porous media and engineered biofilm reactors.

References

1. Absolom, D. R., F. V. Lamberti, Z. Policova, W. Zingg, C. J. Van Oss and A. W. Neumann. 1983. Surface thermodynamics of bacterial adhesion. *Appl. Environ. Microbiol.* **46**:90-97.
2. Adamczyk, Z., B. Siwek and M. Zembala. 1992. Reversible and irreversible adsorption of particles on homogeneous surfaces. *Colloids Surf.* **62**:119-130.
3. Bendinger, B., H. H. M. Rijnaarts, K. Altendorf and A. J. B. Zehnder. 1993. Physicochemical cell surface and adhesive properties of coryneform bacteria related to the presence and chain length of mycolic acids. *Appl. Environ. Microbiol.* **59**:3973-3977.

4. Bonekamp, B. C. 1989. Conformational properties and adsorbed layer structure of adsorbed poly-L-lysine and poly-DL-lysine as inferred from adsorption measurements and proton titrations. *Colloids Surf.* 41:267-286.
5. Bouwer, E. J. and A. J. B. Zehnder. 1993. Bioremediation of organic compounds- putting microbial metabolism to work. *Trends in Biotechnology* 11:360-367.
6. Busscher, H. J., M. H. M. J. C. Uyen, A. J. W. Pelt, H. J. Busscher and A. H. Weerkamp. 1987. Specific and non-specific interactions in bacterial. *FEMS Microbiol. Rev.* 46:165-173.
7. Busscher, H. J., A. H. Weerkamp, H. C. van der Mei, A. J. W. Pelt, H. P. de Jong and J. Arends. 1984. Measurement of the surface free energy of bacterial cell surfaces and its relevance for adhesion. *Appl. Environ. Microbiol.* 48:980-983.
8. Caldwell, D. E. and J. R. Lawrence. 1986. Growth kinetics of *Pseudomonas fluorescens* microcolonies within the hydrodynamic boundary layers of surface microenvironments. *Microb. Ecol.* 12:299-312.
9. Cunningham, A. B., E. J. Bouwer and W. G. Characklis. 1990. Biofilms in porous media, p. 697-732. *In* W. G. Characklis and K. C. Marshall (ed.), *Biofilms*, John Wiley & Sons Inc., New York.
10. Dabros, T. and T. G. M. Van de Ven. 1983. A direct method for studying particle deposition onto solid surfaces. *Colloid Polym. Sci.* 261:694-707.
11. Dabros, T. and T. G. M. Van de Ven. 1993. Particle deposition on partially coated surfaces. *Colloids and Surfaces A: Physicochemical and Engineering Aspects* 75:95-104.
12. Dickson, J. R. and K. Koochmaraie. 1989. Cell surface charge characteristics and their relationship to bacterial attachment to meat surfaces. *Appl. Environ. Microbiol.* 55:832-836.
13. Elimelech, M. and C. R. O'Melia. 1990. Kinetics of deposition of colloidal particles in porous media. *Environ. Sci. Technol.* 24:1528-1536.
14. Fleer, G. J. and J. M. H. M. Scheutjens. 1993. Modeling Polymer adsorption, steric stabilization and flocculation, p. 209-263. *In* B. Dobias (ed.), *Coagulation and flocculation*, Marcel Dekker Inc., New York.
15. Fletcher, M. and G. L. Loeb. 1979. Influence of substratum Characteristics on the Attachment of a Marine Pseudomonad to Solid Surfaces. *Appl. Environ. Microbiol.* 37:67-72.
16. Gannon, J., Y. Tan, p. Baveye and M. Alexander. 1991. Effect of sodium chloride on transport of bacteria in saturated aquifer material. *Appl. Environ. Microbiol.* 57:2497-2501.
17. Gilbert, P., D. J. Evans, E. Evans and I. G. Duguid. 1991. Surface characteristics and adhesion of *Escherichia coli* and *staphylococcus epidermidis*. *J. Appl. Bacteriol.* 71:72-77.
18. Gordon, A. S. and F. Millero. 1984. Electrolytes effects on attachment of an estuarine bacterium. *Appl. Environ. Microbiol.* 47:495-499.
19. Harvey, R. W. 1991. Parameters involved in modeling movement of bacteria in groundwater, p. 89-114. *In* C. J. Hurts (ed.), *Modeling the environmental fate of microorganisms*, American Society for Microbiology, Washington, DC.
20. Lindqvist, R. and C. G. Enfield. 1992. Cell Density and Non-equilibrium sorption effects on bacterial dispersal in groundwater microcosms. *Microb. Ecol.* 24:25-41.
21. Martin, R. E., E. J. Bouwer and L. M. Hanna. 1992. Application of Clean-bed filtration theory to bacterial deposition in porous media. *Environ. Sci. Technol.* 26:1053-1058.

22. **Martin, R. E., L. M. Hanna and E. J. Bouwer.** 1991. Determination of bacterial collision efficiencies in a rotating disk system. *Environ. Sci. Technol.* **25**:2075-2082.
23. **Matthess, G., A. Pekdeger and J. Schroeter.** 1988. Persistence and transport of bacteria and viruses in groundwater- a conceptual evaluation. *J. Contam. Hydrol.* **2**:171-188.
24. **McDowell-Boyer, L. M., J. R. Hunt and N. Sitar.** 1986. Particle transport through porous media. *Water Resources Research* **22**:1901-1921.
25. **Meinders, J. M. and H. J. Busscher.** in press. Influence of ionic strength and shear rate on the desorption of polystyrene particles from a glass collector as studied in a parallel plate flow chamber. *Colloid Polym. Sci.*
26. **Rajagopalan, R. and C. Tien.** 1976. Trajectory analysis of deep bed filtration with the sphere-in-cell porous media model. *Journal of American Institute of Chemical Engineers* **22**:523-533.
27. **Rajagopalan, R. and C. Tien.** 1979. The theory of deep bed filtration, p. 169-268. *In* R. J. Wakeman (ed.), *Progress in Filtration and Separation*, Elsevier, Amsterdam.
28. **Rijnaarts, H. H. M., E. J. Bouwer, W. Norde, J. Lyklema and A. J. B. Zehnder.** Bacterial deposition in porous media related to the clean-bed collision efficiency and substratum-blocking by attached cells. *Environ. Sci. Technol.*: submitted for publication.
29. **Rijnaarts, H. H. M., W. Norde, E. J. Bouwer, J. Lyklema and A. J. B. Zehnder.** Reversibility and mechanism of bacterial adhesion. *Colloids Surf. B: Biointerf.*: submitted for publication.
30. **Rijnaarts, H. H. M., W. Norde, E. J. Bouwer, J. Lyklema and A. J. B. Zehnder.** 1993. Bacterial adhesion under static and dynamic conditions. *Appl. Environ. Microbiol.* **59**:3255-3265.
31. **Rijnaarts, H. H. M., W. Norde, J. Lyklema and A. J. B. Zehnder.** The isoelectric point of bacteria as an indicator for the presence of cell surface polymers that inhibit adhesion. *Colloids Surf. B: Biointerf.*: submitted for publication.
32. **Rijnaarts, H. H. M., W. Norde, J. Lyklema and A. J. B. Zehnder.** Steric and DLVO interactions in bacterial adhesion. *Environ. Sci. Technol.*: submitted for publication.
33. **Rutter, P. R. and B. Vincent.** 1984. Physicochemical interactions of the substratum, microorganisms, and the fluid phase, *In* K. C. Marshall (ed.), *Microbial adhesion and aggregation*, Springer-verlag, Berlin.
34. **Rutter, P. R. and B. Vincent.** 1988. Attachment mechanisms in the surface growth of microorganisms, p. 87-107. *In* J. M. a. J. I. P. Bazin J. M. (ed.), *CRC Series in Mathematical models for microbiology*, CRC Press, Inc., Boca Raton, Florida.
35. **Sharma, P. K., M. J. McInerney and R. M. Knapp.** 1993. In situ growth and activity and modes of penetration of *Escherichia coli* in unconsolidated porous materials. *Appl. Environ. Microbiol.* **59**:3686-3694.
36. **Sjollema, J., A. H. Weerkamp and H. J. Busscher.** 1990. Deposition of oral streptococci and polystyrene latices onto glass in a parallel plate flow cell. *Biofouling* **1**:101-112.
37. **Updegraff, D. M.** 1991. Background and practical applications of microbial ecology, p. 1-20. *In* C. J. Hurst (ed.), *Modeling the environmental fate of Microorganisms*, American Society of Microbiology, Washington DC.
38. **Van der Meer, J. R., T. N. P. Bosma, W. P. De Bruin, H. Harms, C. Holliger, H. H. M. Rijnaarts, M. E. Tros, G. Schraa and A. J. B. Zehnder.** 1992. Versatility of soil column experiments to study biotransformation of halogenated compounds under environmental conditions. *Biodegradation* **3**:265-284.

39. Van der Schee, H. A. and J. Lyklema. 1984. A lattice theory of polyelectrolyte adsorption. *J. Phys. Chem.* **88**:6661-6667.
40. Van Loosdrecht, M. C. M., J. Lyklema, W. Norde, G. Schraa and A. J. B. Zehnder. 1987. Electrophoretic mobility and hydrophobicity as a measure to predict the initial steps of bacterial adhesion. *Appl. Environ. Microbiol.* **53**:1898-1901.
41. Van Loosdrecht, M. C. M., J. Lyklema, W. Norde, G. Schraa and A. J. B. Zehnder. 1987. The role of bacterial cell wall hydrophobicity in adhesion. *Appl. Environ. Microbiol.* **53**:1893-1897.
42. Van Loosdrecht, M. C. M., W. Norde, J. Lyklema and A. J. B. Zehnder. 1990. Hydrophobic and electrostatic parameters in bacterial adhesion. *Aquat. Sci.* **52**:103-114.

Summary and concluding remarks

Interactions between bacteria and solid surfaces strongly influence the behaviour of bacteria in natural and engineered ecosystems. Many biofilm reactors and terrestrial environments are porous media. The purpose of the research presented in this thesis is to gain a better insight into the basic mechanisms of bacterial adhesion and transport in such systems. This knowledge is essential for bacterial adhesion science in general, and important for practical applications such as the bioremediation of contaminated soils, sediments and groundwaters and the treatment of industrial waste streams in fixed bed biofilm reactors.

Model systems

Assessment of cell-substratum interactions in bacterial adhesion require materials with defined properties and an experimental set-up that allows a reproducible quantification of the transport of bacterial cells from bulk liquid to substratum. We performed our studies with model systems and under well-defined conditions in which these prerequisites are met.

Characteristics of solids and bacteria. Negatively charged teflon and glass were used as the model substrata. Eight coryneform bacteria and four pseudomonads were selected. These organisms have different negative cell surface charges at pH 7 (chapter 2). The hydrophobicity of solids and bacteria were determined by measuring the contact angle of drops of water on flat pieces of solid and on dried bacterial lawns. Glass is hydrophilic and teflon extremely hydrophobic. The hydrophobicities of dried bacteria varied between strongly hydrophilic and extremely hydrophobic. However, evidence was found that the drying of the bacteria changes their surface properties, especially in the case of amphiphilic cell-coatings. Therefore, a further characterization of the bacterial cell-surfaces was performed under hydrated conditions by measuring

the isoelectric point of the bacterial strains (Chapter 4). An isoelectric point smaller than 2.8 correlated with the presence of anionic polysaccharides on the cell surface. On the basis of the isoelectric point, the water contact angle and adhesion data, three types of macromolecular cell-coatings were identified: (i) non-polysaccharide macromolecules, like lipids and/or proteins, (ii) amphiphilic macromolecules, i.e., combinations of hydrophilic polysaccharides with either lipids or hydrophobic polysaccharides, and (iii) anionic hydrophilic polysaccharides.

Experimental set-ups. Two types of experimental set-ups were used: (i) static batch systems containing bacterial suspension and flat pieces of surface and (ii) dynamic model porous media that consisted of water-saturated columns packed with spherical substrata to which the bacterial suspensions were applied. Transport of cells from bulk liquid to substratum is much more efficient in dynamic columns than in static systems: transport is controlled by convection and diffusion under dynamic conditions (chapters 2 and 3) but by diffusion only in static systems (chapter 2).

Discrimination between method-dependent and method-independent effects. A comparison of the static and dynamic deposition results demonstrated the absence of methodical influences on adhesion in 68 % of the cases tested. The deviating deposition behaviour of the other cases could be attributed to methodical effects resulting from specific cell characteristics, i.e., to the presence of capsular polymers, an ability to aggregate, large sizes, or a tendency to desorb after passing through an air-liquid interface. Interestingly, a strong stimulation of adhesion upon passing through an air-liquid interface occurred for bacteria coated with amphiphilic compounds. Although important for specific practical applications, all method-dependent cases were excluded from further studies. The cases for which such effects are absent were subjected to further studies in order to reveal generally occurring adhesion mechanisms.

Interactions between bacteria and solid surfaces.

Adhesion is generally irreversible with respect to lowering cell concentration (chapter 3). Hence, analyses of the interactions in adhesion requires a kinetic approach. We quantified the interactions in terms of activation Gibbs energies for adhesion and detachment as determined from experimental adhesion and detachment rates. The adhesion efficiency α , which is the probability of a cell to attach upon reaching a substratum, is related to this activation energy for adhesion: activation energy = $-\ln \alpha$.

Interactions at high ionic strength (0.1 M). The activation energies for adhesion varied between 0 and $5 kT$ (k ($J K^{-1}$) is the Boltzmann constant; $1 kT = 4 \times 10^{-21}$ J at room temperature) at an ionic strength of 0.1 M. A Gibbs energy barrier, located between cell and substratum and several hundreds of kT high, is created by the DLVO (Derjaguin, Landau, Verwey and Overbeek) interactions (chapters 2 and 3). This barrier cannot be surmounted by whole cells. However, bacterial cell surface macromolecules can penetrate this energy barrier and hence reach the substratum at high ionic strength. Therefore, the interactions between the cell surface macromolecules and the substratum, which are generally called steric interactions, determine adhesion at high ionic strength. The following two types of steric interactions generally occur: (i) bridging, that promotes adhesion and causes a lowering of the activation energy of adhesion, and (ii) steric hindrance that inhibits adhesion and therefore increases the activation energy of adhesion.

Mechanisms of adhesion at high ionic strength (0.1 M). The various mechanisms of adhesion (chapter 3) as deduced for the different combinations of types of cell-surface coatings and solid substrata (chapter 4) are summarized in Fig. 1 (the capitals given below refer to this figure). Long range electrostatic interactions as described by the DLVO theory (A and B) create strong repulsive barriers which cannot be passed by whole cells. In addition, deep secondary minima exist for glass but not for teflon. The secondary minima on glass result from strong Van der Waals attraction and are sufficiently deep for irreversible adhesion. Lipid or protein (non-polysaccharide) cell surface macromolecules

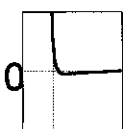
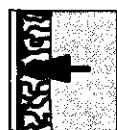
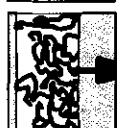
type of cell-coating	substratum			
	teflon		glass	
	interaction	mechanism	interaction	mechanism
	DLVO		DLVO	
	A		B	
	steric		steric	
non-poly-saccharides	C	 bridging	D	 secondary minimum adhesion
amphiphilic macromolecules	E	 bridging	F	 steric hindrance
anionic poly-saccharides	G	 steric hindrance	H	 steric hindrance

FIG. 1. Summary of the adhesion mechanisms that occur among different bacterium/substratum combinations. The arrows indicate attraction due to bridging (arrow points to the surface, i.e., to the left) or repulsion due to steric hindrance (arrow points away from the surface, i.e., to the right).

cause strong attractive bridging on the hydrophobic surface (teflon) (C). On glass they slightly inhibit adhesion and permit adhesion in the secondary DLVO minimum as was demonstrated to occur for two hydrophobic coryneforms (D). Bacteria with an amphiphilic cell surface may adhere by bridging on a hydrophobic surface (E) whereas strong steric hindrance prevents secondary minimum adhesion on glass (F). The adhesion of bacterial cells coated with anionic polysaccharides is strongly inhibited on both surfaces (G and H). The values of the activation energy for adhesion and the adhesion efficiency for the different adhesion mechanisms are summarized in Table 1.

Activation energy for detachment. This activation energy exceeds $5 kT$ for irreversible adhering bacteria (chapter 3). The greatest resilience against

Table 1. The level of the activation energy for adhesion and the adhesion efficiency α for different adhesion mechanisms.

Adhesion mechanism	activation energy for adhesion (kT)	adhesion efficiency α
bridging	0	1
secondary minimum adhesion	1	0.3
steric hindrance	2.5 - 5	0.01 - 0.05

detachment exists for hydrophobic bacteria on hydrophobic substrata. For hydrophobic/hydrophilic and hydrophilic/hydrophilic bacterium/substratum combinations, binding mechanisms not related to hydrophobicity inhibit the detachment.

Contribution of DLVO and steric interactions at various ionic strengths.

The effect of DLVO and steric interactions on adhesion as a function of the

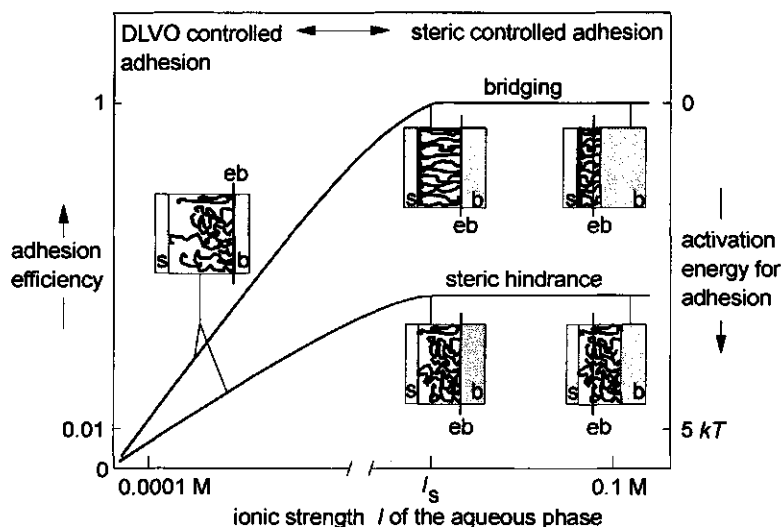


FIG. 2. Illustration of the effect of the ionic strength on bacterial adhesion. eb = electrostatic barrier; b = bacterium; S = substratum.

ionic strength (chapter 5) is illustrated in Fig. 2. Steric interactions dominate at high ionic strength (0.1 M): adhesion is at maximum and even 100% efficient ($\alpha = 1$) in the case of bridging. Long range electrostatic repulsion, as described by the DLVO model, starts to exert its influence when the ionic strength is reduced to below a critical value I_s (Fig. 2). These interactions dominate the adhesion at an ionic strength of 0.0001 M. The value of I_s is determined by the distance over which the cell-surface macromolecules penetrate the electrostatic barrier. Between the bacterial strains tested, the extension of cell surface macromolecules varies between 5 nm and 80 nm, which correspond to I_s -values varying between 0.1 and 0.001 M. A cell-substratum separation of 165 nm can even be bridged by a flagellated *Pseudomonas putida* strain. The practical consequence of these findings is that studying and controlling bacterial adhesion in groundwater and waste water should include the assessment of both DLVO and steric interactions since the ionic strength of these environments varies around 0.01 M.

Bacterial transport in porous media.

Bacterial deposition on spherical glass and teflon collectors was studied in vertical downflow columns (chapters 6 and 7). Deposition was analyzed in terms of the clean bed collision efficiency α_0 (the probability of a cell to attach upon reaching a cell-free substratum), and a blocking factor B (the ratio of the area blocked by an attached cell to the geometric area of a cell).

Deposition in porous media at high ionic strength (0.1 M). The influence of the bacterial cell coating and substratum type on the initial adhesion efficiency is similar as found for the static batch systems (Fig. 1; Table 1). However, the dynamic column system is superior to the static batch system, since it provides a means to also determine the influence of cell-cell interactions on bacterial deposition. Cell-cell repulsion, enhancing blocking, increases with decreasing (more negative) charge of the cell and with increasing hydrophilicity of the cell-surface macromolecules.

Deposition in porous media at varying ionic strengths. The initial efficiency (α_0) decreased with decreasing I , for I -values smaller than the critical level I_s in a similar way as found for the static batch systems. The level of B in-

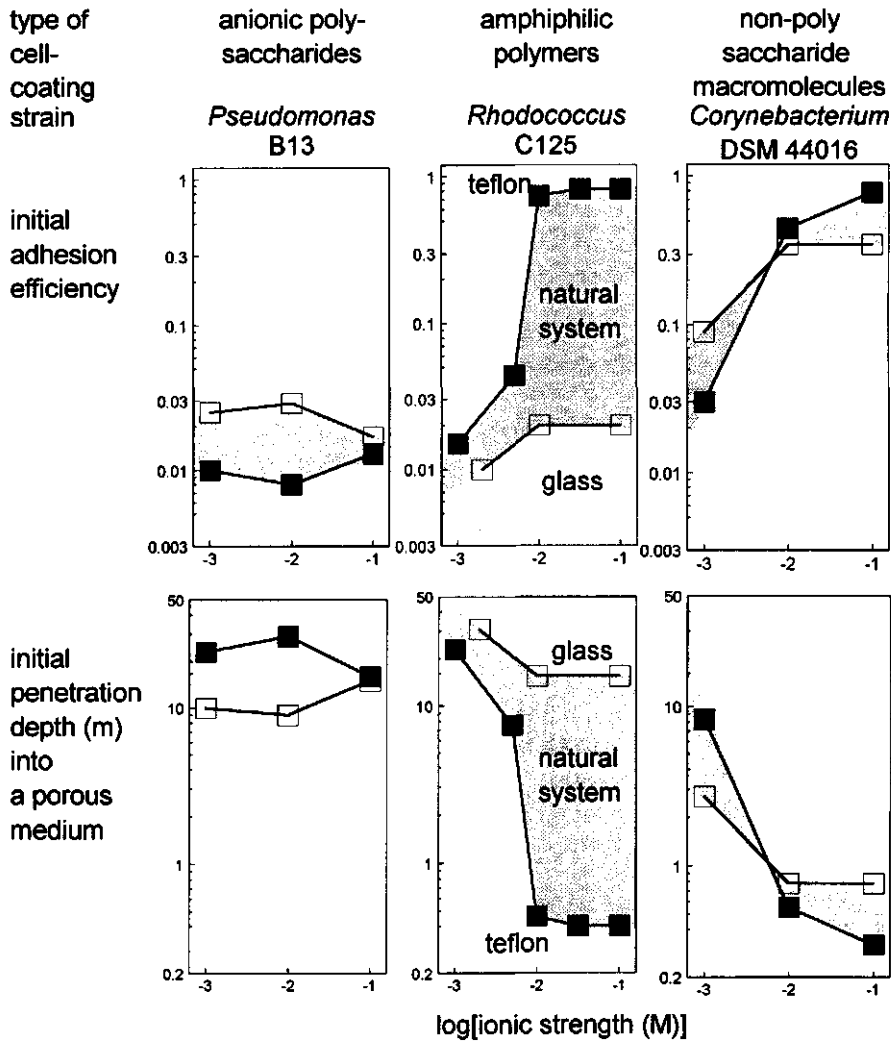


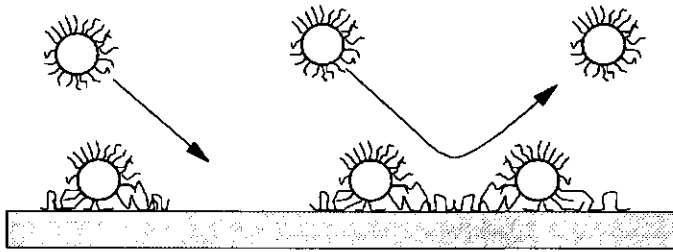
FIG. 3. Effect of the ionic strength on adhesion and transport of bacteria in porous media. Results of the following organisms are shown: *Pseudomonas* strain B13, *Rhodococcus* strain C125, and *Corynebacterium* strain DSM 44016. Adhesion and transport for natural porous media (shaded area) probably falls between the values for glass (open symbols) and for teflon (closed symbols). The penetration depth into the porous medium is the porous medium length required to reduce the influent cell concentration by a factor 100 at an interstitial fluid velocity 30 cm h⁻¹.

creases about one order of magnitude upon changing I from 0.1 M to 0.001 M.

Control of bacterial transport and the occurrence of pore-clogging. The effect of cell-solid interaction (as inferred from the initial adhesion efficiency) on bacterial transport in porous media is illustrated in Figure 3. Depths of penetration into a porous medium may be as high as 50 m at low ionic strength. At high ionic strength, this penetration depth varies between about 0.25 m and 20 m depending on the type of cell-coating.

Maximum control of microbial mobility in porous media can be reached in systems for which B and α_0 are high at high ionic strength: the high B -value

A . Strongly blocking cells; free transport of cells after surface saturation.



B. Weakly blocking cells; multilayer adhesion and pore-clogging

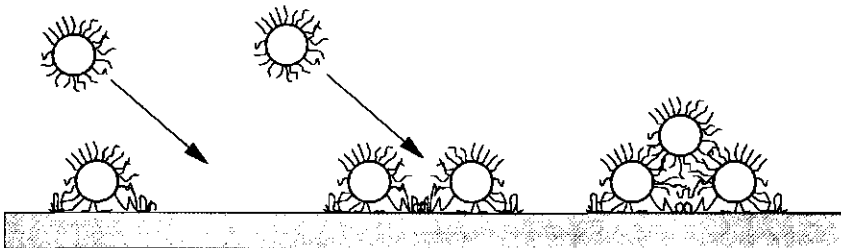


FIG. 4. Illustration of the performance of bacterial deposition for strongly (A) and weakly (B) blocking bacterial cells.

corresponds to strong cell-cell repulsion which minimizes the occurrence of multilayer adhesion and pore-clogging (Fig. 4). The dependencies of α_0 and B on the ionic strength allow manipulation of deposition by varying the ionic strength.

An analysis of literature data on dispersal of *Bacillus* cells in columns packed with coarse sand (chapter 6) demonstrated that the collision-blocking model also applies to natural systems. Hence, deposition of microbes during their transport through engineered or natural porous media is adequately described by the collision-blocking model for strongly blocking cells or weakly blocking cells at low coverage conditions.

Concluding remarks

In this study we have entered the interface between microbiology and physical chemistry. It was demonstrated that the interactions between, at first sight complex biological systems like bacteria, and solid surfaces can be well analyzed and understood in terms of basic physico-chemical principles. A major accomplishment of the research presented here is the quantification of the steric interactions between cell-surface macromolecules and solid surfaces. Combining these with the effects of long range Van der Waals and electrostatic interactions provided a complete classification of the generally occurring mechanisms of bacterial adhesion. A second important achievement is the quantitative formulation of bacterial deposition during transport in porous media. This makes it possible to describe and predict bacterial transport in natural and engineered porous media with basic particle deposition parameters, which in turn, are related to the properties of the bacterial cells.

Several challenges for further research emerged during our research. The analyses of the steric interactions in bacterial adhesion presented in this study are strictly empirical. A more fundamental approach could be the investigation of the adhesion of better defined organisms, like lipopolysaccharide mutants of *Salmonella typhimurium* and various *Rhizobium* species. These mutants are fully characterized and have cell-surface macromolecules varying in chain-length and chemical composition. In some cases, these cell-surface polymers are even

commercially available. Combining experimental studies with these defined materials with theoretical investigations by computer-simulation promises to provide further insights into the steric interactions in bacterial adhesion.

Another important topic for further research is the role of cell-cell interactions in the performance of bacterial deposition. This is of great practical relevance for the application of bacteria in porous media since it is a key-factor in the occurrence of pore-clogging. Furthermore, these interactions may also be of relevance for bacterial biofilm formation. Bacterial deposition techniques using isolated cells may serve as tools to characterize these cell-cell interactions which may then be related to the performance of the biofilm.

Revealing the fundamentals of bacterial deposition is a key step towards the application of these organisms in the bioremediation of contaminated soils and groundwaters. However, bacterial adhesion is not the only factor in a successful bioremediation procedure. The interactions between contaminants and the solid matrix are also important. In fact, many pollutants adsorb very strongly to the solid phase and become only slowly available for biodegradation. We also investigated this problem using the porous medium model systems presented in this study. That work is not included in this thesis and will be presented in separate papers to be published in the near future.

This research is a symbiosis between the disciplines of physical and colloid chemistry and microbiology that produced knowledge about the interactions between bacteria and solid surfaces which could not have been revealed without this cooperation. Hopefully, the highly interesting and economically important interface between microbiology and physical chemistry will be further explored in future.

Samenvatting

Hechting van bacteriën in poreuze media

Een basis voor de toepassing van bacteriën in de biologische reiniging van bodem en water

Dit promotie-onderzoek is uitgevoerd in het kader van het Speerpuntprogramma Bodemonderzoek. Het heeft kennis opgeleverd die onder andere nodig is voor de ontwikkeling van biologische reinigingstechnieken. Bij deze technieken worden bacteriën gebruikt om verontreinigd bodemmateriaal, grondwater en afvalwater schoon te maken. Bodem en grondwatersystemen zijn poreuze media: ze bestaan uit korrels waar tussen water stroomt. Bioreactoren voor reiniging van verontreinigd afval- en grondwater zijn ook vaak gevuld met korrels of andersoortig dragermateriaal. Hechting van bacteriën aan de vaste fase speelt een cruciale rol in het slagen van een biologische reinigingsmethode. Een aantal facetten van het hechtingsproces zijn nog onvoldoende belicht en daarom onderwerp van dit onderzoek. Na een korte uiteenzetting over bacteriën, hun functie en hun toepassing, volgt de samenvatting van de resultaten van dit onderzoek.

Bacteriën als gif- en afvalopruimers

Bacteriën zijn kleine eencellige organismen met een afmeting van ongeveer één-duizenste millimeter. Ofschoon enkele bacteriesoorten ziekteverwekkers zijn, zijn de meeste juist heel nuttig. Ze breken namelijk allerlei organische afvalstoffen af. Dit doen ze in de natuur maar ook in reactoren voor de zuivering van huishoudelijk en industrieel afvalwater. De meeste organische chemicaliën, inclusief zeer giftige stoffen, kunnen door bacteriën worden afgebroken als de omstandigheden gunstig zijn. Bacteriën zijn daarom bij uitstek geschikt als gif-

opruimers. En die zijn tegenwoordig hard nodig.

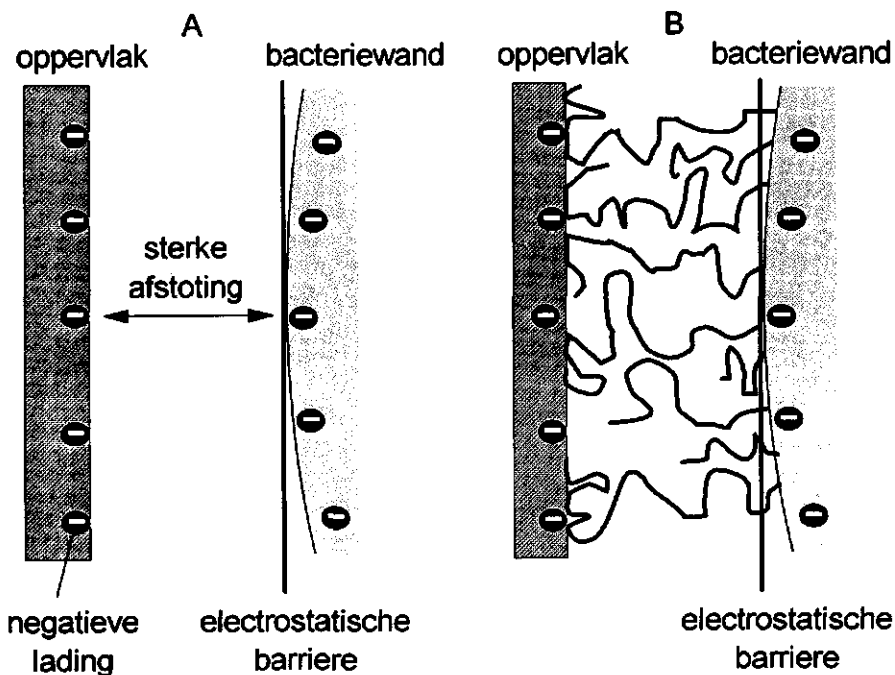
Vaak wordt vervuild grondwater of industrieel afvalwater biologisch behandeld in een zogenaamde bioreactor. Hierin zit een dragermateriaal, bijvoorbeeld zandkorrels. De reinigende bacteriën moeten enerzijds door het dragermateriaal worden vastgehouden, anderzijds moeten ze geen verstopping veroorzaken. Hechting van micro-organismen speelt daarom een belangrijke rol in het functioneren van dit soort systemen.

In Nederland, en daarbuiten, zijn talloze locaties bekend waar de bodem en het grondwater sterk vervuild zijn met organische gifstoffen. Op dit moment zijn verschillende, veelal niet-biologische technieken in gebruik om deze plekken te saneren. Echter, in veel gevallen is dat met die methoden onbetaalbaar of zelfs helemaal niet mogelijk. Het toepassen van bacteriën, die de bodem kunnen binnendringen en daar het gif onschadelijk kunnen maken, kan in een aantal gevallen een oplossing bieden. Het slagen van een biologische bodemreiniging hangt onder andere af van de hechting van bacteriën. Hechting moet bijvoorbeeld niet leiden tot verstopping van de poriën tussen de bodemdeeltjes want dit maakt verdere behandeling onmogelijk. Soms zit de vervuiling diep in de grond en moeten de micro-organismen naar die plek getransporteerd kunnen worden. Eenmaal daar aangekomen moeten ze weer vastgehouden worden om de reiniging efficiënt te laten verlopen.

Ondanks het belang van hechting, zijn het mechanisme hiervan en het effect op het transport van deze organismen in poreuze media nog onvoldoende bekend. Daarom zijn deze tot onderwerp van dit onderzoek gekozen.

Hechtingsmechanisme van bacteriën

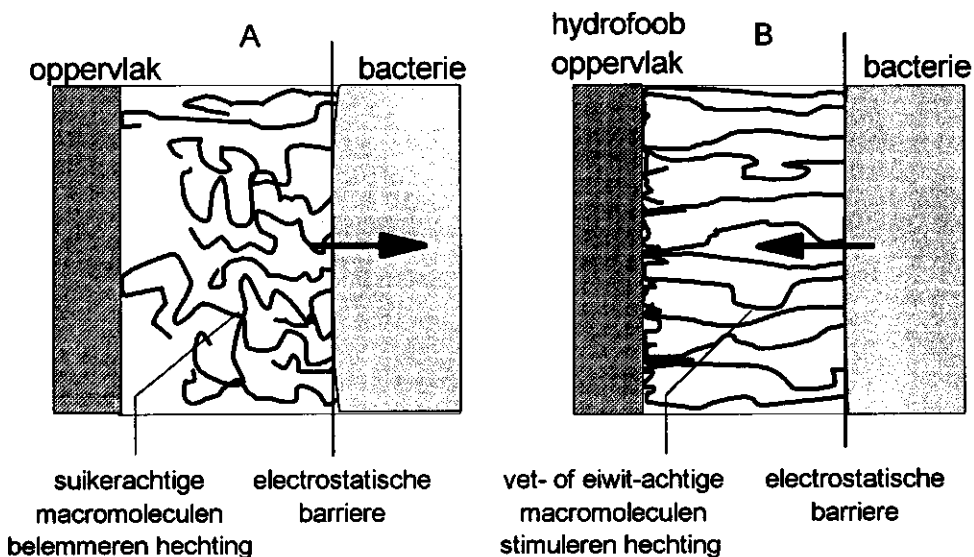
Karakterisering en methoden. In dit onderzoek zijn glas en teflon (een soort plastic) oppervlakken gebruikt. Natuurlijke oppervlakken, zoals bijvoorbeeld die van bodemdeeltjes, zijn minder geschikt om het mechanisme van hechting te bestuderen. Er is een reeks micro-organismen gekozen die in een aantal eigenschappen verschillen. Vervolgens werden de oppervlakken en bacteriën gekarakteriseerd en de omstandigheden onderzocht waarbij hechting het best



Figuur 1. A. Electrostatistische afstoting houdt bacteriën op afstand van een oppervlak. B. Bacteriën kunnen toch hechten omdat de draadvormige structuren (macromoleculen) die ze op hun buitenkant hebben door de electrostatistische barrière heen steken en contact maken met het oppervlak.

bestudeerd kan worden (hoofdstuk 2).

De electrostatistische barrière. Bacteriën en oppervlakken zijn negatief geladen hetgeen resulteert in een afstotende elektrische kracht. Wanneer een bacterie naar een oppervlak beweegt wordt op een bepaalde afstand die afstotende kracht zo groot dat het organisme het vaste materiaal niet dichter kan naderen (Figuur 1A). Op die afstand bevindt zich dus een electrostatistische barrière die het micro-organisme niet kan passeren. De ligging van deze barrière is afhankelijk van de zoutconcentratie in het water. Is het water zo zout als zeewater, dan ligt deze heel dicht bij het oppervlak, nl. op 1 tot 2 nanometer (1 nanometer is één-miljoenste millimeter. Ter vergelijking; de afmeting van een bacterie is ongeveer 1000 nanometer). Bevat het water weinig zout, zoals in



Figuur 2. De macromoleculen kunnen hechting belemmeren (A) of stimuleren (B).

kraanwater, dan bevindt de electrostatistische barrière zich op ongeveer 100 nanometer van het oppervlak.

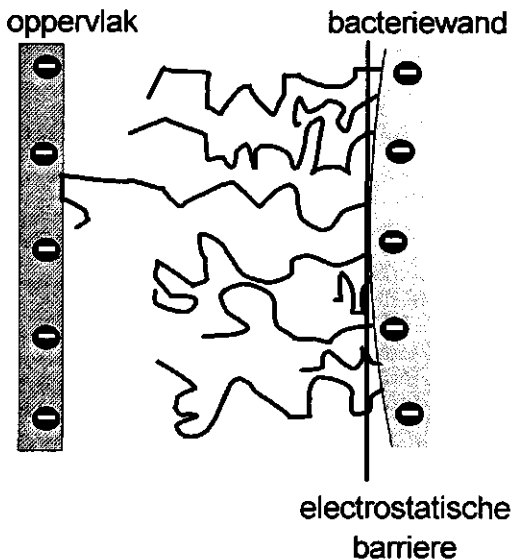
Macromoleculen op de buitenkant van de bacterie. Als je puur naar ladingseffecten kijkt kunnen bacteriën niet hechten: ze worden immers tegengehouden door een electrostatistische barrière. Toch blijken bacteriën te hechten. Dit doen ze door middel van draadvormige structuren die ze aan hun buitenkant hebben zitten (hoofdstuk 3 en 4). Deze structuren zijn aan-eengeschakelde moleculen, macromoleculen. Deze macromoleculen worden niet tegengehouden door de electrostatistische barrière en kunnen, onder bepaalde omstandigheden, contact maken met het oppervlak en hechting bewerkstelligen (Figuur 1B).

In systemen met veel zout wordt hechting bepaald door de macromoleculen. In systemen met veel zout staat de electrostatistische muur dicht bij het oppervlak. Voor alle bacteriën zijn de buitenste macromoleculen

lang genoeg om contact te maken met het oppervlak. Zij bepalen de hechting. Er zijn goed- en slecht-hechtende micro-organismen en het ene oppervlak is beter voor hechting dan het andere. Dit komt door verschillen in de interacties tussen de macromoleculen en het oppervlak. Deze interacties hangen af van de chemische samenstelling van de macromoleculen en van het type oppervlak.

De samenstelling van deze macromoleculen varieert enorm tussen de verschillende bacteriesoorten. Toch kunnen ze, qua effect op hechting, ruwweg in twee hoofdgroepen worden ingedeeld (hoofdstuk 4), namelijk in i) zure suikers en ii) andere macromoleculen, veelal eiwitten en vetachtige of andere hydrofobe (watervrezende) stoffen. De zure suikers zijn sterk negatief geladen en hydrofiel, d.w.z., ze zitten het liefst in water. Bacteriën die deze stoffen op hun celoppervlak hebben worden daarom sterk belemmerd in hun hechting (Figuur 2A). De hechting van bacteriën met de andere soort macromoleculen wordt slechts in geringe mate gehinderd. Op teflon wordt hun hechting zelfs sterk gestimuleerd (Figuur 2B); teflon is namelijk hydrofoob (houdt niet van water) en zal daarom liever bedekt zijn met de macromoleculen van de bacterie dan met water. Er zijn ook bacteriën die een mengsel van beide soorten macromoleculen op hun buitenkant hebben: die hechten goed op teflon maar slecht op glas.

Hechting in systemen met minder zout. In systemen met veel zout bevindt de electrostatische barrière zich zo dicht bij het oppervlak dat in alle gevallen de macromoleculen contact maken met het oppervlak (Figuur 1B). In systemen met minder zout staat de electrostatische barrière verder van het oppervlak (Figuur 3). Dit heeft grote consequenties voor de hechting van micro-organismen (hoofdstuk 5). Als de macromoleculen te kort zijn om de afstand tussen electrostatische barrière en het oppervlak te kunnen overbruggen wordt de hechting sterk belemmerd. De lengte van de macromoleculen varieert tussen 5 en 100 nanometer voor verschillende micro-organismen. De ligging van de electrostatische barrière in grond- en afvalwater ligt tussen de 25 en 50 nm. Er zijn dus micro-organismen waarvan de macromoleculen te kort zijn voor maximale hechting in dit type water. Er zijn er ook met macromoleculen die lang



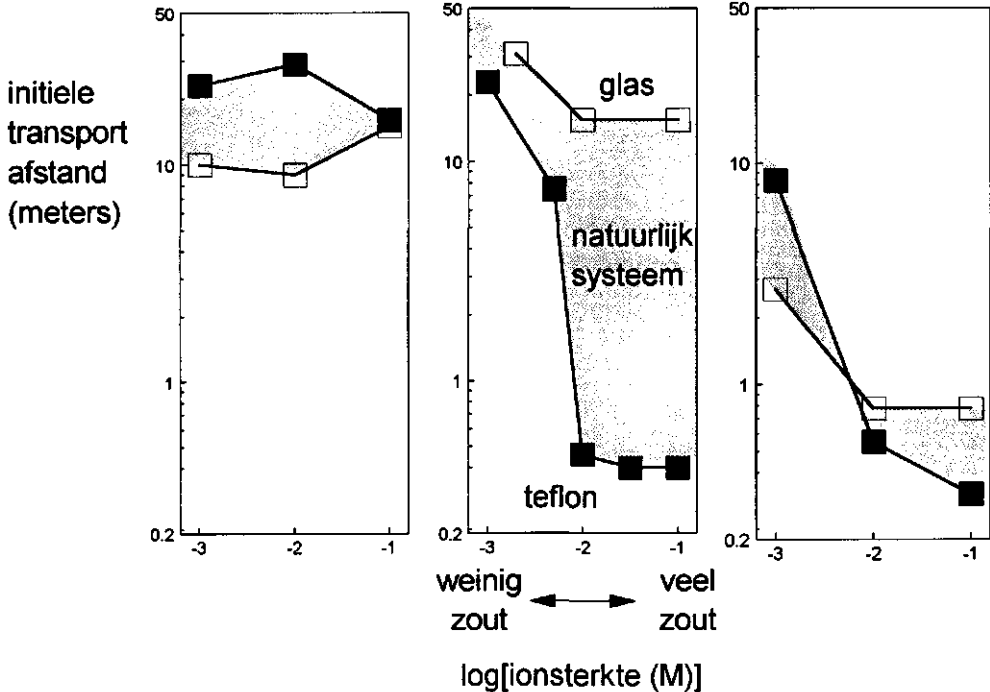
Figuur 3. In water met een lage zoutconcentratie staat de electrostatistische barrière verder van het oppervlak. Bacteriën waarvan de meeste macromoleculen te kort zijn om nog contact te maken met het oppervlak hechten dan minder goed.

genoeg zijn om iedere belemmering van de electrostatistische barrière te voorkomen. Voor een adequate beschrijving van hechting van bacteriën in dit type water moeten daarom naast de electrostatistische eigenschappen van micro-organismen en oppervlak ook de chemische samenstelling en de lengte van de macromoleculen bekend zijn. Aan de ene kant is dat vervelend, want het maakt hechting van bacteriën zo ingewikkeld. Aan de andere kant is het voordelig; er ligt een schat aan mogelijkheden om de hechting van bacteriën te sturen. En dat is gewenst voor toepassing van dit soort organismen in biologische reinigingstechnieken. Bij de selectie en ontwikkeling van bacteriesoorten voor dit soort toepassingen moet daarom rekening gehouden worden met de hechteigenschappen van de microorganismen.

Hechting en transport van bacteriën in poreuze media.

Het transport van bacteriën in poreuze media is bestudeerd met kolommen waarin bolletjes van glas of van teflon waren gebracht (hoofdstukken 6 en 7). Er werd onderscheid gemaakt tussen initiële hechting en tussen hechting op

bacterie	<i>Pseudomonas</i> B13	<i>Rhodococcus</i> C125	<i>Corynebacterium</i> DSM 44016
macro- moleculen	suikerachtige macromoleculen	mengsel van suikerachtige en andere macromoleculen	macromoleculen die geen suikers zijn



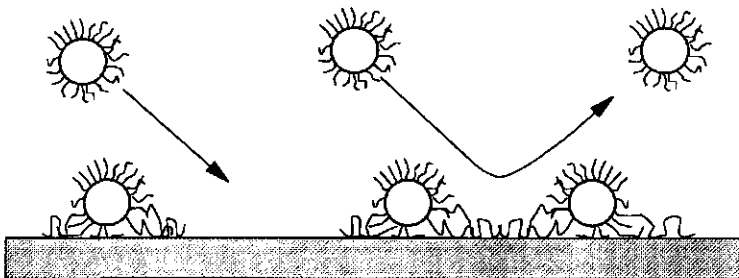
Figuur 4. De afstand waarover bacteriën in een poreus medium getransporteerd kunnen worden bij verschillende zoutconcentraties. Dit is uitgerekend op basis van hun initiële hechting. De transportafstand is die afstand waarbij 99% van de cellen die in het systeem zijn gebracht uit het water zijn verwijderd door hechting.

bolletjes die al voor een deel bedekt waren met bacteriën. Deze laatste situatie ontstaat namelijk als water met bacteriën gedurende langere tijd in het poreus systeem wordt gepompt.

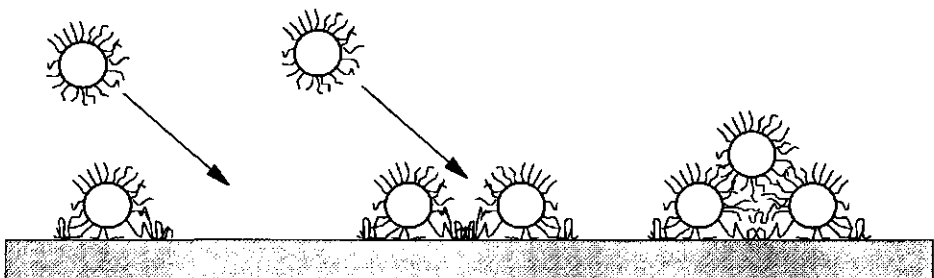
Initiële hechting en transport. De initiële hechting in deze poreuze systemen bleek te verlopen conform de gegevens die uit het mechanisme-onderzoek waren verkregen: de ligging van de electrostatische barrière

(afhankelijk van de zoutconcentratie), de lengte en de chemische samenstelling van de macromoleculen, en het type oppervlak bepalen de hechting van een bacterie. Het aanvankelijke effect van hechting op transport in een poreus medium is geïllustreerd in Figuur 4. Hierbij is aangenomen dat de eigenschappen van natuurlijke oppervlakken tussen die van glas en teflon in liggen. De bacterie bedekt met de suikerachtige stoffen (linker figuur) kan wel 10 tot 20 meter in een poreus medium doordringen. Zijn initiële hechting en transport wordt niet beïnvloed door zout omdat het organisme lange macromoleculen heeft die in alle gevallen de afstand tussen de electrostatische barrière en oppervlak kunnen

A . Bacterie-cellen die het oppervlak afschermen voor verdere hechting



B. Bacterie-cellen die op elkaar hechten



Figuur 5. Effect van gehechte cellen op het verdere verloop van hechting. **A.** Gehechte cellen schermen het oppervlak af voor verder hechting. Als het oppervlak vol zit vindt geen verdere hechting plaats en kunnen de bacteriën ongehinderd getransporteerd worden.

B. Bacteriecellen hechten op elkaar. In een poreus systeem zal dit al snel tot verstopping leiden.

overbruggen. Dit is anders bij de bacteriën getoond in de middelste en rechter figuur; deze hebben polymeren die te kort zijn om bij weinig zout het oppervlak te bereiken. Bij meer zout kunnen ze dat wel. Het transport van het organisme met een mengsel van beide typen macromoleculen op zijn buitenkant is bij hogere zoutconcentraties zeer gevoelig voor de aard van het oppervlak. Dit is niet het geval voor de bacterie met de niet-suiker polymeren (rechter figuur). Deze kan, bij veel zout, slechts over zeer geringe afstand getransporteerd worden.

Hechting en transport na langere tijd. Gehechte bacterie-cellen beïnvloeden de hechting van nieuwe bacteriën. Dit kan op twee manieren (Figuur 5). Ze kunnen het oppervlak ontoegankelijk maken voor verdere hechting (Figuur 5A). Dit blijkt vooral op te treden bij bacteriën die sterk negatief geladen zijn. Deze bacteriën kunnen ongehinderd getransporteerd worden nadat het oppervlak bedekt is met cellen. De tweede mogelijkheid is dat de cellen op elkaar hechten (Figuur 5B). Dit blijkt op te treden bij zwak geladen bacteriën. Deze micro-organismen zullen een poreus medium al snel volledig verstoppem. Voor toepassing in poreuze media zijn ze dus ongeschikt maar voor andere doeleinden kunnen ze weer precies de juiste micro-organismen zijn.

Tot slot

Dit onderzoek laat zien dat wisselwerkingen die zich afspelen over afstanden van enkele nanometers gevolgen kunnen hebben die zich uitstrekken over tientallen meters of meer. De verkregen kennis, die door sommigen als fundamenteel en door anderen als zeer toegepast beschouwd wordt, vormt een goede basis voor de ontwikkeling van nieuwe biologische methoden voor reiniging van bodem en water. Dit onderzoek kwam tot stand door samenwerking tussen de vakgroep Microbiologie en de vakgroep Fysische en Kolloïdchemie van de LandbouwUniversiteit te Wageningen. Deze interdisciplinaire aanpak heeft tot een duidelijke meerwaarde van de verkregen kennis geleid en verdient navolging in de toekomst.

Dankwoord

Een promotie-studie is te vergelijken met een schip op de grote vaart. Tal van factoren zijn van belang om het schip zijn eindbestemming, het proefschrift, te laten bereiken. De haven van vertrek is de eerste factor: Marc, zonder jouw pionierswerk was dit proefschrift nooit geschreven.

Vervolgens zijn de klimatologische omstandigheden onderweg heel belangrijk. Iedereen van de Vakgroep Microbiologie wil ik bedanken voor de gezellige en stimulerende sfeer. Ik heb bij jullie een fijne tijd gehad en zal daar met plezier naar terug blijven kijken. Sjaan en Ria, zonder de koffie en gezellige babbels van jullie was ik de vaak lange experimenteedagen nooit door gekomen. Alle leden van de "Xenobiotica-groep" wil ik extra bedanken voor de gezelligheid op het werk en daarbuiten. Daarnaast wil ik iedereen van de vakgroep Fysische en Kolloïdchemie bedanken. Jullie hadden altijd belangstelling voor mij en mijn onderzoek. De door jullie georganiseerde PhD Student Conference in Haamstede staat me nog altijd bij als een hoogstandje in het combineren van wetenschappelijke kwaliteit met gezelligheid.

Ondanks het gunstige klimaat was het zicht onderweg niet altijd even best. Alex, ik wil jouw bedanken voor jouw bijdrage als radar op mijn promotieschip. Zonder jouw vermogen om mijn hersenspinsels tot hun simpele en begrijpelijke essentie terug te brengen zaten we misschien nu nog op zee. Ondanks jouw drukke bestaan, de laatste jaren zelfs in Zwitserland, was je op de cruciale momenten beschikbaar om mij in mijn onderzoek te ondersteunen.

Onder water schuilt veel gevaar. Hans en Willem, jullie waren mijn sonar en hebben voor de nodige fysisch-chemische diepgang gezorgd. Vele riffen en ijsbergen zijn gesignaleerd en omzeild met jullie hulp. In de laatste, zeker niet gemakkelijke fase van mijn onderzoek hebben jullie de nodige uren met mij door gebracht om een adequate fysisch-chemische analyse van bacterie-hechting boven water te krijgen.

Tijdens stormachtig weer kreeg ik gelukkig een extra loods aan boord: Ed, I would like to thank you for all the help with the writing of several research papers which are also chapters of this thesis. This has been a great support for me in bringing this difficult PhD task to a successful end.

Gedurende enkele jaren heb ik in convooi gevaren. Hauke, jij bent gedurende twee jaar een gezellige compagnon geweest. Je was mijn klankbord op de werkvloer en door jouw slimme suggesties was ik in staat om met mijn experimenten "er uit te halen wat er in zat". Bert, ik wil jouw bedanken voor de

samenwerking van de afgelopen jaren. Zonder jouw kennis over de elektrische eigenschappen van bacteriën was mijn onderzoek nooit zover gekomen. Nu ben jij ook aan het schrijven: succes daarmee!

Bernd, I would like to thank you for your friendship and for the nice cooperation. Without your decision to come to Wageningen with your coryneforms, I would never had the opportunity to get the experimental results that now form an essential part of my thesis.

Mijn schip is bemand geweest met heel wat studenten. Caroline, Angelica, Yde, Sandra, Janneke, Arthur, Roy, Jan, Simon, en Gerty, jullie doctoraalwerk is niet in dit proefschrift terecht gekomen. Maar er zijn nog een paar extra publicaties over "afbraak van geadsorbeerde verbindingen door bodembacteriën" in voorbereiding. Dit zou zonder jullie inzet en kritische inbreng nooit mogelijk zijn geweest. De samenwerking met jullie heb ik altijd erg plezierig gevonden. Caroline, Angelica en Yde, jullie hebben wel aan hechting van bacteriën gewerkt, en wel in een fase waar dit proces nog volledig verkeerd begrepen werd. De ogenschijnlijke mislukkingen van toen stonden echter aan de wieg van dit proefschrift. Bedankt voor jullie doorzettingsvermogen.

Door adequate technische, administratieve en andere ondersteuning bleef alles in de machinekamer geïlied lopen. Frits, Wim, Nees, Loes en Ans, bedankt. Ab, Martien, en Erna, jullie hulp bij de fysisch-chemische karakterisatie van oppervlakken en cellen is heel belangrijk voor mijn onderzoek geweest. Wil, jij was mijn rots in de branding wat betreft computer-zaken.

Nora, zonder jou had ik dit werk niet kunnen doen. Samen met Timon en Iris heb jij voor vaste grond onder mijn voeten gezorgd. Bedankt voor al jouw steun en vertrouwen.

Curriculum Vitae

Huub (Hubertus Henricus Martinus) Rijnaarts werd op 5 mei 1957 geboren te Eindhoven en verhuisde in zijn tweede levensjaar naar Breda. Hij behaalde daar het MAVO-4 diploma in 1973. Daarna volgde hij gedurende enkele jaren een analistenopleiding en was achtereenvolgens enige tijd werkloos, kantoorklerk, produktiemedewerker en meter-opnemer bij het plaatselijke gas-, water-, en lichtbedrijf. In 1978 begon hij aan een schriftelijke opleiding HAVO die hij in mei 1979 afronde met een staatsexamen. Op eenzelfde wijze verwierf hij in oktober 1980 het VWO-diploma. In september 1981 begon hij zijn studie milieuhygiëne aan de toenmalige Landbouwhogeschool, nu LandbouwUniversiteit, te Wageningen (LUW). Na het doorlopen van de propaedeuse (augustus 1982) slaagde hij voor zijn kandidaatsexamen dat voldeed aan de normen van de oriëntaties bodemhygiëne en waterzuivering. In zijn doctoraalfase koos hij voor de richting bodemhygiëne met als specialisatie adsorptie en microbiologische omzetting van organische verontreinigingen in de bodem (Prof. F. A. M. de Haan en Prof. A. J. B. Zehnder). Hij bestudeerde onder andere de adsorptie en biologische omzetting van alpha-hexachloorcyclohexaan in bodemmateriaal. In maart 1988 verkreeg hij de titel Ingenieur in de Landbouw- en Milieuwetenschappen met de aanmerking "met lof". Vanaf 1 maart 1988 verrichte hij, binnen het kader van het Speerpuntprogramma Bodemonderzoek, wetenschappelijk onderzoek bij de vakgroep Microbiologie van de LUW in samenwerking met de vakgroep Fysische en Kolloïdchemie van diezelfde universiteit. Het resultaat hiervan is o.a. dit proefschrift. Hij en zijn vrouw Nora Stadhouders kregen twee kinderen: Timon (12-4-1989) en Iris (10-10-92). Vanwege een 80%-aanstelling kon hij bijdragen aan de zorg voor hen.